UC San Diego

UC San Diego Electronic Theses and Dissertations

Title

From Pain Relief to Mystical Experience: Predictive Brain-Body Mechanisms of Transformative States

Permalink

https://escholarship.org/uc/item/60x2b1vd

ISBN

9798193298472

Author

Jinich-Diamant, Alex

Publication Date

2026-10-15

Peer reviewed|Thesis/dissertation

eScholarship.org Powered by the California Digital Library
University of California

UNIVERSITY OF CALIFORNIA SAN DIEGO

From Pain Relief to Mystical Experience: Predictive Brain-Body Mechanisms of Transformative States

A Dissertation submitted in partial satisfaction of the requirements
for the degree Doctor of Philosophy

in

Cognitive Science

by

Alex Jinich-Diamant

Committee in charge:

Professor Douglas Nitz, Co-Chair
Professor Hemal H. Patel, Co-Chair
Professor Laura Case
Professor Seana Coulson

2026

Copyright

Alex Jinich-Diamant, 2026

All rights reserved.

The Dissertation of Alex Jinich-Diamant is approved, and it is acceptable in quality and form for publication on microfilm and electronically.

University of California San Diego

2026

TABLE OF CONTENTS

DISSERTATION APPROVAL PAGE iii

TABLE OF CONTENTS iv

LIST OF FIGURES v

LIST OF TABLES vii

ACKNOWLEDGEMENTS ix

VITA x

ABSTRACT OF THE DISSERTATION xi

INTRODUCTION 1

CHAPTER 1: Higher Cortical Entropy Predicts Mindfulness Meditation-Based Pain Relief 9

CHAPTER 2: Neural and Molecular Changes During a Mind-Body Reconceptualization, Meditation, and Open Label Placebo Healing Intervention 49

CHAPTER 3: Experience as Medicine: Shared Neurobiological and Computational Mechanisms of Psychedelic, Contemplative, and Fasting-Induced Mystical Experience 139

CONCLUSION 347

LIST OF FIGURES

Figure 1.1: CONSORT flow diagram. 12
Figure 1.2: Experimental design. 14
Figure 1.3: fMRI cortical entropy analysis pipeline. 18
Figure 1.4: Post-pre change in psychophysical pain ratings (error bars = + 1 SEM). 22
Figure 1.5: Cortical Shannon entropy pre- and post-manipulation across the small-world range of densities 23
Figure 1.6: Pain ~ entropy regression model 1. 25
Figure 1.7: Pain ~ entropy regression model 2.. 26
Figure 1.8: Entropy modulated predictive coding of pain 28
Figure 2.1: Study Design, Participants, Data Collection, and Recruitment 52
Figure 2.2: Functional Magnetic Resonance Imaging (fMRI) 56
Figure 2.3: Neuronal Growth 61
Figure 2.4: Metabolic Effects 63
Figure 2.5: Plasma Proteome 65
Figure 2.6: Metabolomics 69
Figure 2.7: Exosome Transcriptomics. 72
Figure 2.8: Machine Learning and MEQ 74
Figure 2.9: Potential Cortical Implementation 78
Figure 3.1: Three converging routes to a shared computational neural state and mystical-like subjective phenomenology 143
Figure 3.2: Layer 5 pyramidal neurons, (A) apical amplification and (B) 5-HT2A agonism. 146
Figure 3.3: Predictive processing hierarchy under the normal waking state (A) and under the psychedelic state (B). 150
Figure 3.4: The brain's free energy landscape in the normal waking state (A) and in the psychedelic state (B). 155
Figure 3.5: Thalamic nuclei and thalamocortical connectivity patterns. 166
Figure 3.6: Corticothalamic circuits for attention and uncertainty. 168
Figure 3.7: Diffuse coupling theory of open monitoring meditation. 173
Figure 3.8: Olfacto-limbic interoceptive prior recalibration under focused attention meditation. 189
Figure 3.9: Three predictive regimes during FA meditation. 193
Figure 3.10: Metabolic relaxation of cortical priors (MRCP) mechanism 1. 227

Figure 3.11: MRCP 2 - Differential metabolic vulnerability of persistent activity across cortical levels 232
Figure 3.12: DMN-mediated synergy between caloric restriction and psychedelics. 241
Figure 3.13: Prior content versus structure – circular causation across levels. 260
Figure 3.14: Levels of biological organization, adapted from Noble et al. (2019)..... 262
Figure 3.15: Mystical state as a temporal window of expanded and exchanged degrees of freedom. 265
Figure 3.16: Hierarchically nested levels of the perceptual hierarchy..... 295
Figure 3.17: Field phenomena under subcritical (A) and near-critical (B) brain dynamics. 300

Supplemental Figure 1.1: Small-worldness (SW) per network density..... 31
Supplemental Figure 2.1: A. Resting State Functional Connectivity Networks..... 123
Supplemental Figure 2.2: Plasma Nanoparticle Size Distributions. 124
Supplemental Figure 2.3: Results of a proteomic enrichment analysis using g:Profiler 125
Supplemental Figure 2.4: Heatmap Representation of Enriched Biological Pathways..... 126
Supplemental Figure 2.5: Proteomic A Priori Protein Heat Maps..... 127
Supplemental Figure 2.6: Full Tryptophan Pathway 127

LIST OF TABLES

Table 1.1: Statistically Significant 2(group) X 2(pre/post) Repeated Measures ANOVA on Entropy. 24

Table 2.1: Statistically significant (pFWE < 0.05) rest-vs-meditation differences on resting state network regions (n=19 participants). 58

Table 2.2: Significant (pFDR < 0.05) pre-to-post differences on RSN component regions (n=19 participants). 60

Table 3.1: Empirical Predictions, Evidence, and Tests for the MRCP Theory. 236

Table 3.2: Empirical Predictions, Evidence, and Tests for DMN-Mediated Synergy Between Caloric Restriction and Psychedelics. 244

Table 3.3: Empirical Predictions, Evidence, and Tests for the Synergy Between Caloric Restriction and Meditation. 250

Supplemental Table 1.1: Repeated Measures ANOVAs on Entropy (Neutral). 32

Supplemental Table 1.2: Repeated Measures ANOVAs on Entropy (Heat) 34

Supplemental Table 1.3: Pre vs. post entropy paired t-tests (neutral, controls). 36

Supplemental Table 1.4: Pre vs. post entropy paired t-tests (neutral, meditators). 37

Supplemental Table 1.5: Pre vs. post entropy paired t-tests (heat, controls). 38

Supplemental Table 1.6: Pre vs. post entropy paired t-tests (heat, meditators). 39

Supplemental Table 1.7: Regression results, all densities, all subjects. 40

Supplemental Table 2.1: fMRI Framewise Displacement. 105

Supplemental Table 2.2: fMRI Two-Way (Scan X Time) Mean Framewise Displacement Repeated Measures ANOVA. 105

Supplemental Table 2.3: Montreal Neurologic Institute (MNI) Coordinates for 36 Regions of Interest Making up 7 Resting State Networks (source: Raichle 201191). 106

Supplemental Table 2.4: Montreal Neurologic Institute (MNI) Coordinates for 8 a priori Regions of Interest (DiFuMo atlas). 107

Supplemental Table 2.5: Statistically Significant (p < 0.05) Rest-vs-Meditation Paired t-tests Between A Priori Regions of Interest. 107

Supplemental Table 2.6: Whole-Brain Functional Connectivity Network Measures. 108

Supplemental Table 2.7: 2 (Time: Pre/Post) by 2 (Task: Rest/Meditation) Repeated Measures ANOVA on Whole-Brain Modularity, Characteristic Path Length, and Global Efficiency. 109

Supplemental Table 2.8: Pre- vs. Post-Intervention a Priori Regions Functional Connectivity. 110

Supplemental Table 2.9: Significant Anatomical Gray Matter Volume Clusters for Advanced > Novice Contrast. 111

Supplemental Table 2.10: fMRI Meditation Depth and Expectations Survey Results..... 112
Supplemental Table 2.11: ELISA Biomarker Levels and Wilcoxon Signed Rank Test (Pre- vs Post-Intervention). 112
Supplemental Table 2.12: Commercial ELISA Kits..... 112
Supplemental Table 2.13: UPLC Metabolomic Detection Conditions..... 113
Supplemental Table 2.14: Metabolomic Detection Mass Spectrum Conditions. 113
Supplemental Table 2.15: A-G: A Priori Protein Index Components. 114
Supplemental Table 2.16: SCFA Index. 115
Supplemental Table 2.17: Neuronal index..... 115
Supplemental Table 2.18: Glycolysis Pathway Index. 116
Supplemental Table 2.19: Endogenous Opioid Pathway Index..... 117
Supplemental Table 2.20: Pro-Inflammatory Pathways Index. 118
Supplemental Table 2.21: Anti-Inflammatory Pathways Index. 119
Supplemental Table 2.22: Oxidative Phorphorylation Index. 120
Supplemental Table 2.23: Metabolomic Pathway Analysis. 121

ACKNOWLEDGEMENTS

I would like to acknowledge the support of Professors Douglas Nitz and Hemal H. Patel as the co-chairs of my committee and Professors Seana Coulson and Laura Case as committee members.

Chapter 1, in full, is currently being prepared for submission for publication of the material. The dissertation author was the primary author of this material. The principal investigator of this material was Fadel Zeidan and additional authors include Grace Posey, Gabriel Riegner, and Youngkyoo Jung.

Chapter 2 is a reprint of the material as it appears in Alex Jinich-Diamant, Sierra Simpson, Juan P. Zuniga-Hertz, Ramamurthy Chitteti, Jan M. Schilling, Jacqueline A. Bonds, Laura Case,c, Andrei V. Chernov,c, Joe Dispenza, Jacqueline Maree, Natalia Esther Amkie Stahl, Michael Licamele, Narin Fazlalipour, Swetha Devulapalli, Leonardo Christov-Moore, Nicco Reggente, Michelle A. Poirier, Tobias Moeller-Bertram, Hemal H. Patel. Neural and molecular changes during a mind-body reconceptualization, meditation, and open label placebo healing intervention. Communications Biology, 8 (1525), 2025. The dissertation author was the primary author of this paper.

Chapter 3 contains unpublished material and is currently being prepared for submission for publication of the material. The dissertation author was the sole author of this material.

VITA

2012 Bachelor of Arts in Anthropology, Columbia University

2022 Master of Science in Cognitive Science, University of California San Diego

2026 Doctor of Philosophy in Cognitive Science, University of California San Diego

ABSTRACT OF THE DISSERTATION

From Pain Relief to Mystical Experience: Predictive Brain-Body Mechanisms of Transformative States

by

Alex Jinich-Diamant

Doctor of Philosophy in Cognitive Science

University of California San Diego, 2026

Professor Douglas Nitz, Co-Chair
Professor Hemal H. Patel, Co-Chair

The human brain is an organ of prediction. It does not passively receive sensory information but actively constructs perception, action, and the felt sense of the body by issuing precision-weighted predictions and updating them against ascending prediction error. Under this hierarchical predictive architecture, suffering and well-being are not only outcomes of peripheral physiology but configurations of the brain's generative model: how rigidly its priors are held,

where its attention is allocated, and how its high-level beliefs are coupled to interoceptive and exteroceptive signals. This dissertation investigates whether, and how, mind-body techniques transiently reorganize the predictive hierarchy, and what neural, molecular, and computational signatures accompany that reorganization.

Three complementary studies are presented. Chapter 1 reports a randomized controlled trial demonstrating that four days of mindfulness meditation training produces a 33% reduction in experimentally induced pain that is predicted, within meditators, by a meditation-induced rise in the Shannon entropy of cortical functional connectivity networks, consistent with a flattening of the prediction-driven attractor landscape that ordinarily sustains pain. Chapter 2 reports a multi-omics, fMRI, and behavioral characterization of a seven-day retreat combining meditation, cognitive reconceptualization, and open-label placebo healing rituals, showing that the intervention disengages the default mode and salience networks, increases circulating BDNF and endogenous opioid pathway proteins, enhances glycolytic metabolism, and modulates exosomal neurotransmission-related microRNAs. This coordinated brain-body reorganization is interpreted as the joint relaxation of high-level priors, the recalibration of embodied first priors, and the reopening of the predictive system to new beliefs. Finally, Chapter 3 develops a unifying theoretical framework arguing that serotonergic psychedelics, contemplative practice, and caloric restriction converge on a single computational endpoint, a transient near-critical regime of relaxed priors and expanded degrees of freedom in the generative model, and that the depth of the resulting mystical-like experience is the primary therapeutic agent. Together, these studies advance an empirically grounded, computationally explicit account of how transformative brain-body states are produced, how they heal, and how the science of such states may be pursued with greater precision.

INTRODUCTION

The human brain is a prediction machine. Across cortical, subcortical, and brainstem hierarchies, it continuously generates expectations about the causes of its sensory input, internal as well as external, and updates those expectations against the error signals that arrive when prediction and afferent data disagree. This view, formalized in predictive processing, active inference, and the free energy principle[1–3], has reframed how we understand perception, action, learning, and emotion, not as the assembly of representations from raw sensation, but as the moment-to-moment refinement of a hierarchical generative model. Based on this view, perception is controlled hallucination held in check by prediction error[2]; emotion is the affective consequence of expected and unexpected changes in interoceptive state[4,5]; and the body's homeostatic priors lie at the deepest, most slowly updated part of the predictive system[6].

This framework reorganizes how we think about suffering and wellbeing. Persistent pain, anxiety, depression, addiction, and trauma are increasingly understood not as the simple products of peripheral pathology or neurochemical deficit but as states of the generative model, i.e., as configurations in which high-level priors have grown rigid, attention is captured by their predictions, and the precision-weighting machinery that normally lets new evidence update belief becomes pathologically resistant to revision[7–9]. If suffering is, in part, a product of the predictive system, then relief from it must in some part follow from its reconfiguration.

Mind-body practices have, for millennia, claimed precisely this kind of reconfiguration as their effect. Across cultural and contemplative traditions, techniques as diverse as breath-based meditation, ritual healing, fasting, ecstatic dance, and ingestion of psychoactive plants and mushrooms have been reported to relieve suffering, provide access to insight, and occasion the structured phenomenological reorganization known as mystical experience[10,11]. Modern

cognitive neuroscience has begun to verify, in the language of brain imaging, neurochemistry, and behavioral measurement, that these techniques do reliably produce measurable changes in neural dynamics, plasma physiology, and self-reported experience[12–15]. What has lagged is a unifying account, a framework that explains, at the level of computation and biology, what these heterogeneous practices share and why their effects so often cluster around the same therapeutic endpoints.

The aim of this dissertation is to build such an account. It does so by approaching the same theoretical question–how does mind-body practice modulate the brain's predictive architecture, and what makes that modulation therapeutic, from three angles: a randomized controlled trial of brief mindfulness training for experimental pain (Chapter 1), an observational multi-omics study of a week-long retreat combining meditation, reconceptualization, and open-label placebo (Chapter 2), and a theoretical synthesis that places these findings alongside the literature on psychedelics and metabolic interventions to articulate a shared computational mechanism (Chapter 3). Each study probes a different scale: cortical network dynamics, brain-body molecular signaling, and computational architecture across techniques, with each contributing a different empirical or conceptual handle on the same underlying object.

Several theoretical commitments thread the studies together. The first is that the brain operates close to a critical regime, balanced between order and disorder, and that its distance from criticality determines its capacity for flexible inference and its level of consciousness[16–18]. When the system sits too deep in the ordered regime, priors are over-weighted and experience is rigid; as it moves toward the chaotic regime, priors are loosened and the generative model becomes more open to revision[12,19]. The entropy of large-scale neural network organization

indexes this distance from order and provides a tractable empirical handle on what the predictive hierarchy is doing[20,21].

The second commitment is that the predictive hierarchy is not confined to the cortex. Embodied physiology (metabolic state, autonomic tone, plasma-borne signaling molecules, etc.) is integral to the system, both because the body is the system's deepest prior and because high-level cortical predictions establish physiological setpoints through autonomic and metabolic regulation, closing a brain-body loop that mind-body techniques exploit[4,22,23]. The body, on this view, is not a passive substrate that the brain regulates from above but a participating member of inference whose own state shapes which predictions the brain can issue.

The third commitment is that mind-body techniques act on different levels of this hierarchy. Meditation acts on attention and on the precision weighting of present-moment sensation[24,25]. Cognitive reconceptualization acts on the content of high-level priors about the body and its capacities[26]. Placebo and ritual act on the expectation-driven priors that gate the physiological healing response[14,27,28]. Thus, these techniques are unlikely to be redundant alternatives, and understanding their unique mechanisms of action, which lie at the interface between computation and physiology, should help pave the way for a pharmacology that not only involves molecular mechanisms of action but also experience-mediated computational ones.

Chapter 1, the first study, asks whether mindfulness meditation reduces experimentally induced pain by modulating cortical entropy. Pain is an ideal model for this question because its intensity is known to be constructed in significant part by descending predictions about its threat and inevitability[24,28,29]. Forty pain-free, meditation-naïve volunteers were randomly assigned to four days of mindfulness training or to a book-listening control regimen and then scanned during noxious and innocuous heat, with and without their assigned meditation practice. Mindfulness

meditation produced large reductions in pain intensity and unpleasantness. Critically, a meditation-induced rise in the Shannon entropy of cortical functional connectivity networks predicted those reductions within the meditation group only. This is the first demonstration of a direct functional link between cortical network entropy and meditation-based pain relief, and it is consistent with the interpretation that meditation flattens the prediction-driven attractor landscape that ordinarily reinforces a painful percept.

Chapter 2 widens the lens. It asks what happens when a more intensive mind-body intervention, combining multiple techniques and lasting a full week, is studied simultaneously at the level of brain function, plasma proteomics, metabolomics, exosomal microRNA transcriptomics, and downstream plasma-transfer functional cellular assays. Twenty adults attending a structured retreat combining Kundalini-style meditation, didactic reconceptualization of the mind-body relationship, and open-label placebo healing rituals were assessed before and after the seven-day intervention. fMRI revealed lower modularity and reduced intra-network connectivity of the default mode and salience networks during meditation, consistent with the loosening of self-referential and allostatic priors. Post-intervention plasma, applied in vitro, drove enhanced neurite outgrowth and glycolytic metabolism, and contained elevated BDNF-pathway proteins, endogenous opioids, and modulated neurotransmission-associated exosomal microRNAs. This observational study is the first joint characterization of these three mind-body techniques across neural, molecular, metabolic, and cellular scales, and it is cautiously interpreted as potential evidence that distinct techniques acting on different levels of the predictive hierarchy can produce coordinated brain-body reorganization.

Chapter 3 develops the theoretical synthesis. It argues that serotonergic psychedelics, focused attention and open monitoring meditation, and caloric restriction converge, via three

physiologically distinct routes, on a single computational state–a transient near-critical neural regime characterized by relaxed precision on high-level priors, scale-free cortical dynamics, and an expansion of the degrees of freedom available to the brain's generative model. The chapter traces the known pharmacology of psychedelics via 5-HT_{2A} modulation of layer 5 pyramidal neurons for psychedelics and proposes set of novel, biologically grounded, and empirically falsifiable mechanistic models across molecular, circuit, network, and phenomenological levels for how meditation and fasting induce a convergent neural state, via diffuse thalamocortical coupling and olfacto-limbic interoceptive prior recalibration (for meditation) and metabolic destabilization of high-level cortical attractor states (for fasting). It also proposes a novel theoretical understanding of the mystical-like state produced under such states and a plausible accounting of the numinous, noetic content commonly encountered in its subjective phenomenology.

Together, the three studies move from a tightly controlled experimental demonstration that brief meditation training modulates cortical entropy dynamics in a manner that reduces pain (Chapter 1), to a multi-scale observational characterization of how a composite mind-body intervention produces a coordinated brain-body response interpretable as joint reorganization of the predictive hierarchy (Chapter 2), to a unifying theoretical proposal that situates these effects within a broader class of mystical-state-inducing interventions whose therapeutic action is, fundamentally, the experience itself (Chapter 3). The chapters can be read as a single line of argument, that the brain's predictive hierarchy is the proper level of analysis for understanding what mind-body practices do, that this hierarchy is modulable from many directions and in coordinated ways, and that the science of transformative states is now at the point where a

computationally explicit and biologically grounded account of their mechanism is both possible and necessary.

REFERENCES

1. Friston K. The free-energy principle: a unified brain theory? Nat Rev Neurosci. 2010;11:2. doi:10.1038/nrn2787

2. Clark A. Whatever next? Predictive brains, situated agents, and the future of cognitive science. Behav Brain Sci. 2013;36:181–204. doi:10.1017/S0140525X12000477 PubMed PMID: 23663408.

3. Hohwy J. The Predictive Mind. OUP Oxford; 2013. 294 p.

4. Seth AK. Interoceptive inference, emotion, and the embodied self. Trends Cogn Sci. 2013;17:565–73. doi:10.1016/j.tics.2013.09.007 PubMed PMID: 24126130.

5. Barrett LF. The theory of constructed emotion: an active inference account of interoception and categorization. Soc Cogn Affect Neurosci. 2017;12:1–23. doi:10.1093/scan/nsw154

6. Allen M, Tsakiris M. The body as first prior: Interoceptive predictive processing and the primacy of self-models. In: Tsakiris M, De Preester H, editors. The Interoceptive Mind: From Homeostasis to Awareness [Internet]. Oxford University Press; 2018 [cited 2026 Apr 3]. p. 0. Available from: https://doi.org/10.1093/oso/9780198811930.003.0002 doi:10.1093/oso/9780198811930.003.0002

7. Barrett LF, Quigley KS, Hamilton P. An active inference theory of allostasis and interoception in depression. Philos Trans R Soc Lond B Biol Sci. 2016;371:20160011. doi:10.1098/rstb.2016.0011 PubMed PMID: 28080969; PubMed Central PMCID: PMC5062100.

8. Friston KJ, Stephan KE, Montague R, Dolan RJ. Computational psychiatry: the brain as a phantastic organ. Lancet Psychiatry. 2014;1:148–58. doi:10.1016/S2215-0366(14)70275-5 PubMed PMID: 26360579.

9. Carhart-Harris RL, Friston KJ. REBUS and the Anarchic Brain: Toward a Unified Model of the Brain Action of Psychedelics. Barker EL, editor. Pharmacol Rev. 2019;71:316–44. doi:10.1124/pr.118.017160 PubMed PMID: 31221820.

10. James W. The Varieties of Religious Experience: A Study in Human Nature. Random House Publishing Group; 1999. 641 p.

11. Griffiths RR, Richards WA, McCann U, Jesse R. Psilocybin can occasion mystical-type experiences having substantial and sustained personal meaning and spiritual significance.

Psychopharmacology (Berl). 2006;187:268–83; discussion 284-292. doi:10.1007/s00213-006-0457-5 PubMed PMID: 16826400.

12. Carhart-Harris RL, Leech R, Hellyer PJ, Shanahan M, Feilding A, Tagliazucchi E, Chialvo DR, Nutt D. The entropic brain: a theory of conscious states informed by neuroimaging research with psychedelic drugs. Front Hum Neurosci. 2014;8:20. doi:10.3389/fnhum.2014.00020 PubMed PMID: 24550805; PubMed Central PMCID: PMC3909994.

13. Tang YY, Hölzel BK, Posner MI. The neuroscience of mindfulness meditation. Nat Rev Neurosci. 2015;16:213–25. doi:10.1038/nrn3916 PubMed PMID: 25783612.

14. Kaptchuk TJ. Open-Label Placebo: Reflections on a Research Agenda. Perspect Biol Med. 2018;61:311–34. doi:10.1353/pbm.2018.0045

15. Jinich-Diamant A, Garland E, Baumgartner J, Gonzalez N, Riegner G, Birenbaum J, Case L, Zeidan F. Neurophysiological Mechanisms Supporting Mindfulness Meditation–Based Pain Relief: an Updated Review. Curr Pain Headache Rep. 2020;24:56. doi:10.1007/s11916-020-00890-8

16. Cocchi L, Gollo LL, Zalesky A, Breakspear M. Criticality in the brain: A synthesis of neurobiology, models and cognition. Prog Neurobiol. 2017;158:132–52. doi:10.1016/j.pneurobio.2017.07.002 PubMed PMID: 28734836.

17. Müller EJ, Munn BR, Shine JM. Diffuse neural coupling mediates complex network dynamics through the formation of quasi-critical brain states. Nat Commun. 2020;11:6337. doi:10.1038/s41467-020-19716-7

18. Toker D, Pappas I, Lendner JD, Frohlich J, Mateos DM, Muthukumaraswamy S, Carhart-Harris R, Paff M, Vespa PM, Monti MM, Sommer FT, Knight RT, D'Esposito M. Consciousness is supported by near-critical slow cortical electrodynamics. Proc Natl Acad Sci. 2022;119:e2024455119. doi:10.1073/pnas.2024455119

19. Carhart-Harris RL. The entropic brain - revisited. Neuropharmacology. 2018;142:167–78. doi:10.1016/j.neuropharm.2018.03.010 PubMed PMID: 29548884.

20. Viol A, Palhano-Fontes F, Onias H, de Araujo DB, Viswanathan GM. Shannon entropy of brain functional complex networks under the influence of the psychedelic Ayahuasca. Sci Rep. 2017;7:7388. doi:10.1038/s41598-017-06854-0 PubMed PMID: 28785066; PubMed Central PMCID: PMC5547073.

21. Viol A, Palhano-Fontes F, Onias H, de Araujo DB, Hövel P, Viswanathan GM. Characterizing Complex Networks Using Entropy-Degree Diagrams: Unveiling Changes in Functional Brain Connectivity Induced by Ayahuasca. Entropy. 2019;21:128. doi:10.3390/e21020128 PubMed PMID: 33266844; PubMed Central PMCID: PMC7514607.

22. Tsakiris E by M, Preester HD, editors. The Interoceptive Mind: From Homeostasis to Awareness. Oxford, New York: Oxford University Press; 2018. 368 p.

23. Christov-Moore L, Jinich-Diamant A, Safron A, Lynch C, Reggente N. Cognitive Science Below the Neck: Toward an Integrative Account of Consciousness in the Body. Cogn Sci. 2023;47:e13264. doi:10.1111/cogs.13264

24. Zeidan F, Emerson NM, Farris SR, Ray JN, Jung Y, McHaffie JG, Coghill RC. Mindfulness Meditation-Based Pain Relief Employs Different Neural Mechanisms Than Placebo and Sham Mindfulness Meditation-Induced Analgesia. J Neurosci Off J Soc Neurosci. 2015;35:15307–25. doi:10.1523/JNEUROSCI.2542-15.2015 PubMed PMID: 26586819; PubMed Central PMCID: PMC4649004.

25. Lutz A, Slagter HA, Dunne JD, Davidson RJ. Attention regulation and monitoring in meditation. Trends Cogn Sci. 2008;12:163–9. doi:10.1016/j.tics.2008.01.005 PubMed PMID: 18329323; PubMed Central PMCID: PMC2693206.

26. Ashar YK, Gordon A, Schubiner H, Uipi C, Knight K, Anderson Z, Carlisle J, Polisky L, Geuter S, Flood TF, Kragel PA, Dimidjian S, Lumley MA, Wager TD. Effect of Pain Reprocessing Therapy vs Placebo and Usual Care for Patients With Chronic Back Pain: A Randomized Clinical Trial. JAMA Psychiatry. 2022;79:13–23. doi:10.1001/jamapsychiatry.2021.2669

27. Büchel C, Geuter S, Sprenger C, Eippert F. Placebo analgesia: a predictive coding perspective. Neuron. 2014;81:1223–39. doi:10.1016/j.neuron.2014.02.042 PubMed PMID: 24656247.

28. Wager TD, Rilling JK, Smith EE, Sokolik A, Casey KL, Davidson RJ, Kosslyn SM, Rose RM, Cohen JD. Placebo-induced changes in FMRI in the anticipation and experience of pain. Science. 2004;303:1162–7. doi:10.1126/science.1093065 PubMed PMID: 14976306.

29. Fardo F, Auksztulewicz R, Allen M, Dietz MJ, Roepstorff A, Friston KJ. Expectation violation and attention to pain jointly modulate neural gain in somatosensory cortex. NeuroImage. 2017;153:109–21. doi:10.1016/j.neuroimage.2017.03.041 PubMed PMID: 28341164; PubMed Central PMCID: PMC5460976.

CHAPTER 1: Higher Cortical Entropy Predicts Mindfulness Meditation-Based Pain Relief

Abstract

Pain is a multidimensional experience constructed by interactions between peripheral nociceptive afferents and a distributed predictive cortical architecture in which descending expectations shape how ascending sensory signals are perceived. Mindfulness meditation reliably reduces pain through multiple distinct neural mechanisms, yet the computational properties of the cortical reorganization that supports this effect remain underspecified. The Shannon entropy of large-scale functional connectivity networks indexes the stability of predictions encoded in the brain's generative model, with higher entropy corresponding to a less constrained, more flexible inferential regime. Here we tested whether mindfulness meditation-based analgesia is supported by an increase in cortical functional connectivity entropy. Forty healthy, pain-free, meditation-naïve adults were randomized to four days of mindfulness training (n = 20) or to a matched book-listening regimen (n = 20) and then underwent BOLD fMRI during alternating innocuous (35°C) and noxious (49°C) heat, both before and after engaging in their assigned practice. Functional connectivity networks were thresholded across the small-world range of densities (0.02 – 0.27), and Shannon entropy of the degree distribution was computed at each density. Meditation produced a 33% reduction in pain intensity and a 38% reduction in pain unpleasantness from rest to meditation ($p < .001$), while controls reported a 15–18% increase. During innocuous stimulation, meditators exhibited significantly higher cortical entropy from rest to meditation, and within meditators this entropy increase predicted the magnitude of pain relief across the majority of network densities (18 of 26; 0.07 < adjusted R^2 <

0.20). In controls, by contrast, higher entropy was associated with higher pain. These findings provide the first direct functional link between cortical network entropy and mindfulness-based analgesia and are consistent with the interpretation that meditation attenuates pain by flattening the prediction-driven attractor landscape that ordinarily sustains it.

Introduction

Pain is a multidimensional subjective experience constructed and modulated by interactions between peripheral nociceptive sensory afferents, cognitive-affective factors, and a distributed network of subcortical and cortical brain areas. Recent evidence[1–4] indicate that higher-order nociceptive processing may be driven by hierarchical probabilistic internal models that predict impending sensory events by integrating the expected probability of said events with ascending low-level afferent information[5–9]. Specifically, descending predictions and ascending sensory signals are integrated in proportion to their precision, and when the ascending sensory information does not match the expectation of said experience, the probabilistic internal model is updated to account for prediction error (violations of expected processing)[10,11].

Shannon entropy, a coarse-grained measure of a system's disorder or unpredictability, indexes the stability of predictions, with higher entropy corresponding to less stable predictions. As such, it is a potential mechanism supporting the modulation of the subjective experience of pain. Predictive coding considers the brain as a complex adaptive system performing active inference by dynamically minimizing its free energy (i.e., minimizing prediction error to avoid violating expectations)[8,12]. Stable attractors are characterized by accurate and consistently realized predictions of impending stimuli (i.e., non-violated expectations)[13]. In contrast, a higher

entropy system reflects inaccurate or weaker predictions of ongoing and imminent experience. The free energy principle[8] and the entropic brain hypothesis[14] are two theories that predict that under a higher entropic state, predictions are attenuated, prediction-based attractors become less stable (i.e., flatter), and maladaptive expectations may be replaced with novel adaptive predictions resulting in therapeutic outcomes, respectively[13]. Consequently, higher entropy reflects a less prediction-driven system in which predictions of pain are dampened, modulating the corresponding pain experience. However, it remains unknown if entropy is associated with pain.

Mindfulness meditation is a highly efficacious self-regulatory technique that directly attenuates nociception and pain through multiple unique mechanisms. Mindfulness meditation-based pain relief is associated with lower anticipatory electrophysiological[15] and neural mechanisms[16]. Mindfulness meditation also increases electrophysiological measures of entropy[17,18], suggesting that it generates a less prediction-driven state[19]. Thus, we postulate that the present-centered stance supporting mindfulness meditation reduces the influence of prior expectations and future anticipation to produce higher cortical Shannon entropy of functional connectivity networks[20,21] to reduce pain. The proposed randomized clinical trial combined blood oxygen level dependent functional magnetic resonance imaging (BOLD fMRI) with psychophysical pain testing [49°C] to determine if mindfulness-based pain relief is associated with higher cortical entropy.

Materials and Methods

The proposed study is part of a previously published study examining the neurofunctional connections supporting mindfulness-based pain relief [22].

Participants

Forty healthy, pain-free, and meditation-naïve human volunteers (M_{age}= 30 ± 10 years; 20 females, 20 males; 22 White, 13 Black, 3 Hispanic, 1 Asian, 1 Native American) were recruited from the local community and provided informed consent. Wake Forest School of Medicine's Institutional Review Board approved all study procedures.

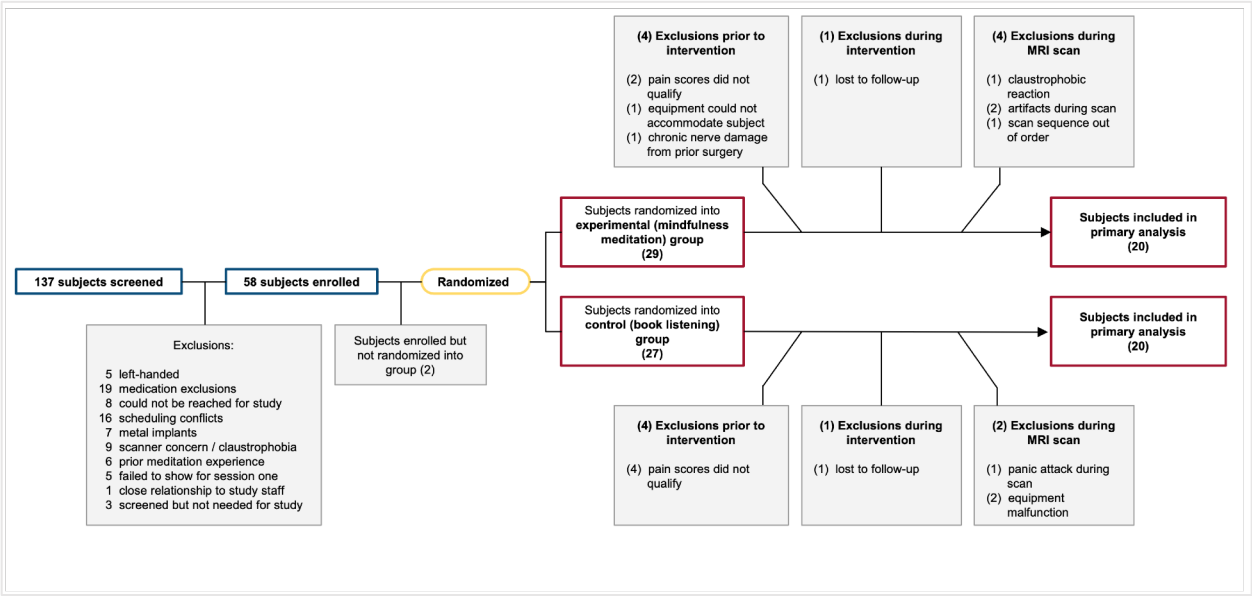


Figure 1.1: CONSORT flow diagram.

Stimuli

Noxious thermal stimuli were delivered to the posterior aspect of the right calf by a 16 × 16 mm^2 TSA II thermal stimulator (Medoc Inc). The thermal probe was moved to a new

stimulation site after each experimental series to reduce habituation, and subjects were free to escape the stimulator at any time by lifting their limb. All stimulus temperatures were ≤ 49°C.

Psychophysical Pain Assessment

Pain intensity and unpleasantness ratings were assessed with a 15 cm plastic sliding visual analog scale (VAS) [23] ranging from 0 ("no pain sensation" and "not at all unpleasant") to 10 ("most intense pain sensation imaginable" or "most unpleasant sensation imaginable"), respectively.

Anatomical MRI Acquisition

Participants were scanned on a 3T Siemens Skyra scanner with a 32-channel head coil. High-resolution T1-weighted structural images were obtained using a magnetization-prepared rapid acquisition gradient-echo (MP-RAGE) sequence (1 mm^3 voxels, TR = 2300ms, TE = 2.98ms, inversion time = 900ms, bandwidth = 240 Hz/Px, flip angle = 9°, % FOV = 93.75, matrix size = 256 x 256).

fMRI Acquisition

Whole-brain functional blood oxygen level dependent (BOLD) images were obtained with a gradient-recalled echo-planar imaging (EPI) sequence (4mm slice thickness, TE = 25ms,

TR = 2000ms, flip angle = 75°, % FOV = 100, matrix size = 64 x 64, bandwidth = 2230 Hz/Px), and stimuli were presented in a block design.

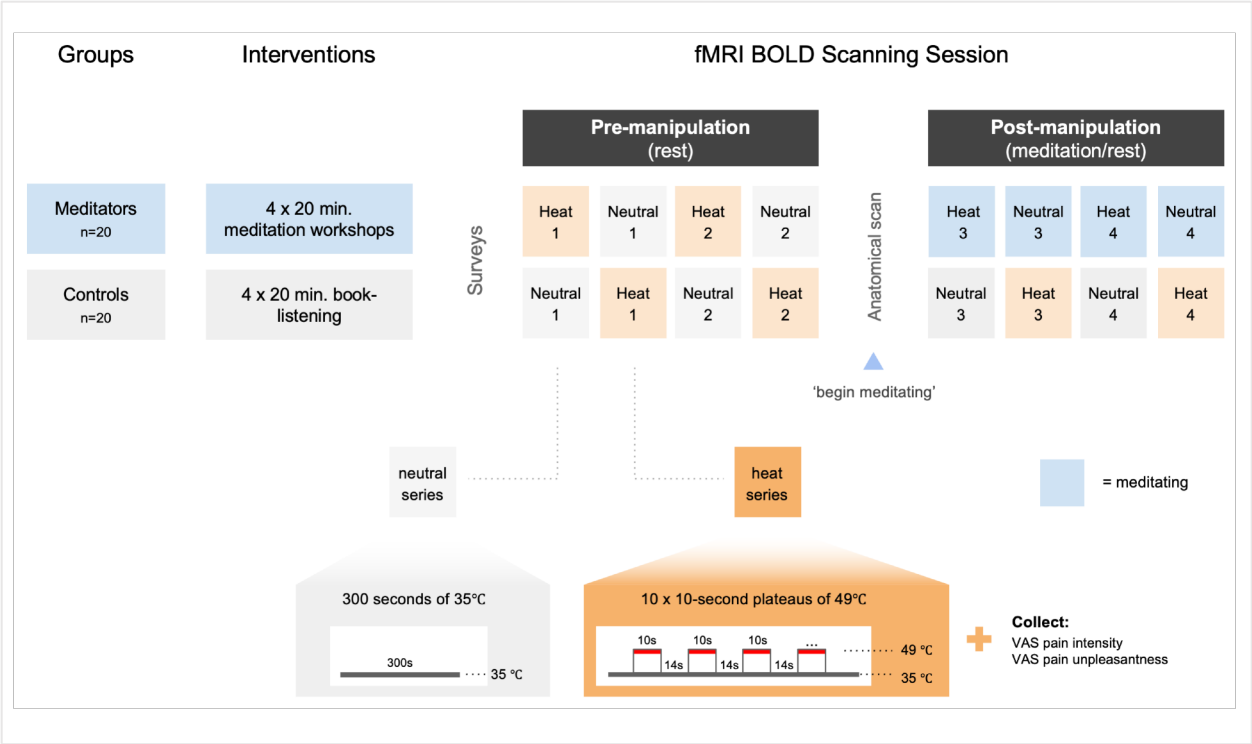


Figure 1.2: Experimental design.

Experimental Design

Experimental Session 1: Psychophysical Training and Baseline Pain Testing

Participants were familiarized with 32, 5-second stimuli (35-49º C) and use of the VAS for pain ratings (Figure 1.2). Baseline psychophysical responses to noxious heat were assessed by administering four "heat" series, each including 10 alternating 12-second plateaus of 49º C and 35º C stimulation to the back of the right calf. This *heat series* is identical to the *heat* paradigm used in subsequent MRI sessions. Participants were instructed to sit quietly and two *heat* series were delivered. Participants were then instructed to "continue to sit quietly" for 10

minutes to control for time elapsed in the post-manipulation MRI session. Two more *heat* series were then administered. VAS pain intensity and unpleasantness ratings were collected after each of the four series.

Randomization

After completing experimental session 1, participants were randomized into a four-session book listening control (n=20) or mindfulness meditation training regimen (n=20). Groups were matched on sex using a customized random number generator.

Experimental Sessions 2-5: Group Training

Mindfulness meditation training regimen:

As in previous studies[24,25], subjects in the meditation group participated in four separate days of mindfulness-based mental training for 20 minutes per day. Subjects were instructed to focus on the changing sensations of the breath while using a nonevaluative cognitive state, acknowledging arising sensations, thoughts, and/or feelings without judgment or emotional reaction and to simply return their attention back to the breath whenever such discursive events occurred. Subjects were also told that perceived sensory and affective events were "momentary and fleeting" and did not require interpretation or evaluation. In session 1, subjects were instructed to focus on breath sensations occurring at the tip of the nose. In session 2, subjects were told to expand their focus to the "full flow of the breath," including bodily sensations. On

sessions 3 and 4, subjects received minimal meditation instructions to allow them to meditate in silence while in the supine position with an audio recording of the MRI scanner to simulate the scanner environment. Subjects were not instructed to practice outside of the training sessions.

Book listening control regimen:

Subjects in the control group listened to an audio recording of *The Natural History of Selborne*[26], a book validated as a neutral comparison regimen for guided relaxation interventions[27,28], during 20 minutes per day across four separate days to control for facilitator attention and time elapsed in the meditation interventions. In session 3, MRI scanner sounds were introduced in the last 10 minutes of book listening. In session 4, subjects were instructed to lie in the supine position and listen to the audio book and scanner sounds.

Experimental Session 6: fMRI Scanning Session

Participants were positioned in the MRI scanner with a respiratory transducer placed around the chest and a pulse oximeter placed on the left index finger. Subjects positioned their right leg on the thermal probe. The following procedures were conducted:

1. During baseline "pre-manipulation" (rest), participants were instructed to "not move and keep eyes closed". Four *heat* and four *neutral* (*neutral series* = 300 seconds of continual 35º C) fMRI BOLD series were acquired (counterbalanced) across all participants. VAS pain ratings were collected after each series.

2. An MP-RAGE structural scan was conducted after the first four BOLD (2 *heat*, 2 *neutral*) series. Before MP-RAGE acquisition, meditation group participants were instructed to "begin meditating and continue to meditate until the end of the experiment." Participants in the control group were instructed to "not move and keep eyes closed."

3. Post-manipulation is characterized as "meditation" for the mindfulness group and as "control-rest" for the control group. During "post-manipulation" (meditation/rest), four *heat* and four *neutral* fMRI series were acquired. VAS pain ratings were collected after each series.

Behavioral Pain Analysis

I. Pain: A 2 manipulation (pre-manipulation vs. post-manipulation) X 2 group (mindfulness vs. control) X 2 session (session 1 vs. session 6) repeated measures ANOVA examined if mindfulness produced greater pain reductions than the controls. Simple effects tests were performed to identify significant main effects and interactions.

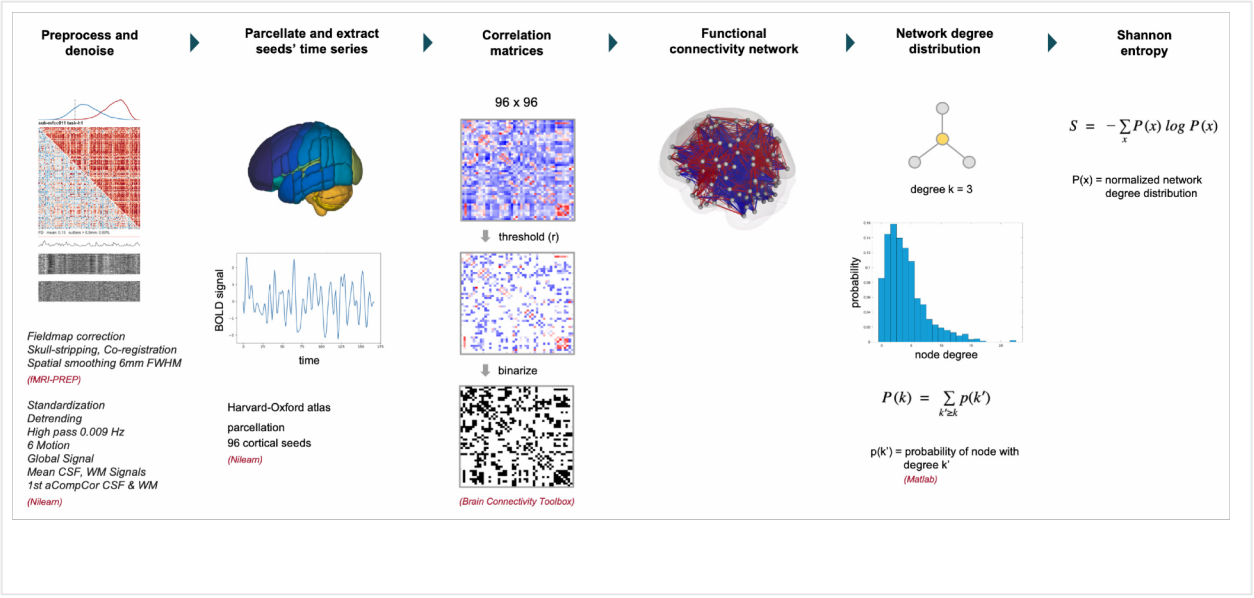


Figure 1.3: fMRI cortical entropy analysis pipeline.

Neuroimaging-Based Entropy Analysis

Following prior functional connectivity-based Shannon entropy studies[20,21], the entropy of functional connectivity networks was derived from functional BOLD acquisitions (Figure 1.3). Functional images were preprocessed, denoised, and segmented into 96 anatomically distinct cortical regions. Pearson correlations between every region's averaged BOLD time series were calculated to construct correlation matrices, which were thresholded and binarized to obtain connectivity networks. Finally, the Shannon entropy of networks' degree distributions was calculated and statistically compared across groups and conditions.

fMRI BOLD Preprocessing and Denoising

Eight BOLD series per participant (4 *heat* and 4 *neutral*) were preprocessed using a conventional analytical pipeline (fMRIPrep; v20.2.1)[29,30] using Nipype v1.5.1[31,32]. Distortion-corrected functional images were co-registered to their anatomical T1w references using FLIRT (FSL 5.0.9)[33], resampled onto native space to correct for head-motion and susceptibility distortions, and then resampled into standard MNI space. Images were spatially smoothed with an isotropic Gaussian kernel of 6mm FWHM (full-width half-maximum).

Functional images were denoised using Nilearn 0.6.2[34] by performing spike regression (removal of motion outliers defined as frames exceeding 0.9 mm framewise displacement or 1.5 standardized DVARS), detrending, standardizing, high-pass filtering (0.009 Hz), and performing confound regression of 6 motion parameters (3 rotation, 3 translation), mean global signal[35], and mean plus first five principal CSF and white matter components[36], respectively. Visual inspection of functional connectivity values centered around zero and homogeneous carpet plots confirmed the chosen parameters produced adequately denoised data while minimizing loss of degrees of freedom.

Functional Connectivity Matrices

Denoised functional images were converted to functional connectivity matrices[20,21] by segmenting them into 96 bilateral anatomically distinct, non-overlapping cortical regions according to the Harvard-Oxford 2mm cortical structural thresholded (25%) atlas[20,37]. Per region, a BOLD time series averaged across all voxels was computed (Nilearn 0.6.2). Pearson correlations between all region pairs' time series were calculated, yielding a 96 x 96 correlation

matrix per BOLD series (8 per participant: 2 pre-manipulation heat, 2 pre-manipulation neutral, 2 post-manipulation heat, and 2 post-manipulation neutral).

Correlation matrices were binarized to obtain adjacency matrices by applying a thresholding function (Brain Connectivity Toolbox)[38] such that if the absolute value of a Pearson correlation was larger than predetermined threshold *r*, a functional connectivity link was established and the pairwise element a_{ij} was binarized as "1". Elements that exhibited a correlation less than *r* were labeled as "0". To avoid non-generalizable threshold-specific effects[39], following previous work[20,21,40], a range of thresholds was used to produce networks with all possible network densities. Given it is known that the brain functions in the small-world range of densities[41], the small-worldness of all resulting adjacency matrices was calculated from the ratio of clustering coefficient and characteristic path length normalized to those of iso-dense random networks[42,43], and subsequent entropy calculations were performed only for the range of thresholds that produced non-fragmented graphs in the small world range (density range: 0.02 to 0.27, see Supplementary Figure 1.1). Comparisons performed between iso-dense networks pre- versus post-manipulation guarantee the density of links is equivalent such that any difference in entropy would result from network topology rather than density, which is more sensitive to movement artifacts.

Cortical Shannon Entropy

In line with Viol et al. (2017) and Viol et al. (2019)[20,21], the Shannon entropy of each adjacency matrix's degree distribution was computed. A node's degree (k) is defined as the number of nodes connected to it. Per BOLD series, cumulative degree distributions, $P(k) =$

$\sum_{k\prime \geq k} p(k')$ (Equation 1) where p(k') is the normalized probability of a region having degree k', were calculated and represented as normalized probability histograms[38,44]. The Shannon entropy (*S*) of nodal degree distributions was calculated according to $S = -\sum_x P(x) \log P(x)$ (Equation 2) (Python)[45] where P(x) is the normalized network degree distribution. Eight entropy values (8 per participant: [pre-manipulation] *heat* 1, *neutral* 1, *heat* 2, *neutral* 2, and [post-manipulation] *heat* 3, *neutral* 3, *heat* 4, *neutral* 4) were obtained and averaged by time-condition for statistical analysis (e.g., mean of *heat* 1 and *heat* 2 to obtain average entropy for *heat* pre-manipulation). Post- and pre-manipulation entropies were subtracted per group and heat/neutral condition to obtain (post-pre) changes in entropy.

Statistical Testing

Consistent with previous work[20,21], each network density threshold results in a different network configuration and is thus treated as a separate model, with statistical significance assessed independently.

II. Entropy:

To determine if mindfulness meditation produced a higher cortical entropy state when compared to rest and controls, a 2 (rest vs. manipulation) X 2 (group) repeated measures ANOVA was conducted on entropy values for noxious and innocuous heat separately across densities. Significant main effects and interactions were examined with planned simple effects tests.

III. Pain and Entropy:

To determine if mindfulness-based pain relief was associated with greater entropy, multivariate linear regression models were conducted. The change in pain was characterized as the dependent variables. Change post (rest) to post (manipulation) in framewise displacement and entropy were then entered. Group was entered to determine if the hypothesized relationship between entropy and pain varied by group. Follow-up within-group regressions examining the relationship of change in entropy by change of pain controlling from framewise displacement were performed as a post-hocs to test study hypotheses.

Results

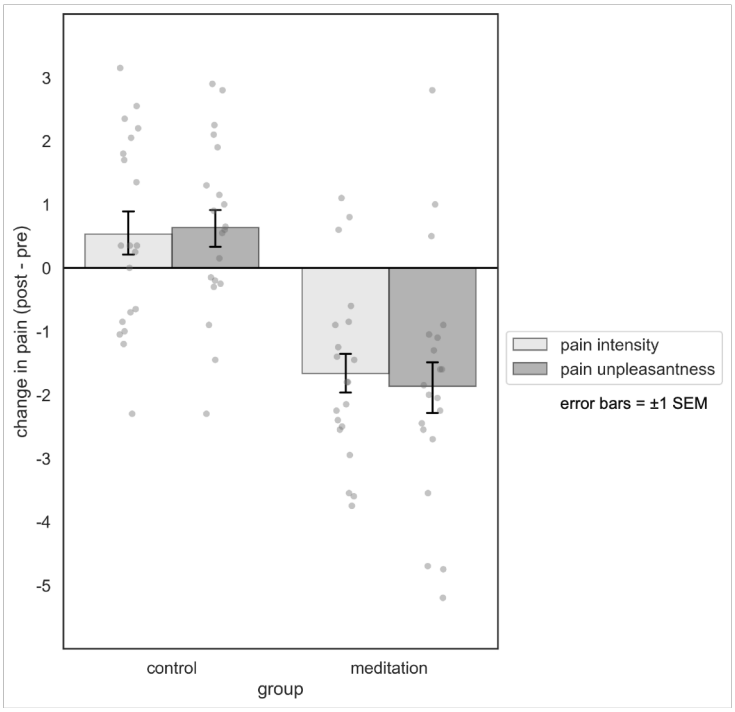


Figure 1.4: Post-pre change in psychophysical pain ratings (error bars = + 1 SEM).

I. Pain: Meditation significantly lowered pain intensity and unpleasantness ratings (Figure 1.4).

When controlling for baseline (session 1) pain ratings, the significant pre/post X group interaction, $F(1, 36) = 25.24$, $p < .001$, $\eta^2_p = .41$ was driven by the 33% percent reduction in pain intensity and 38% reduction in pain unpleasantness ratings from rest to meditation ($p<.001$). In contrast, the controls reported a significant 15% increase in pain intensity and 18% increase in pain unpleasantness ratings from pre to post manipulation. There was no significant pre vs. post $F(1, 36) = 2.36$, $p = .133$, $\eta^2_p = .06$ or group $F(1, 36) = .017$, $p = .90$, $\eta^2_p = 0.00$ main effect.

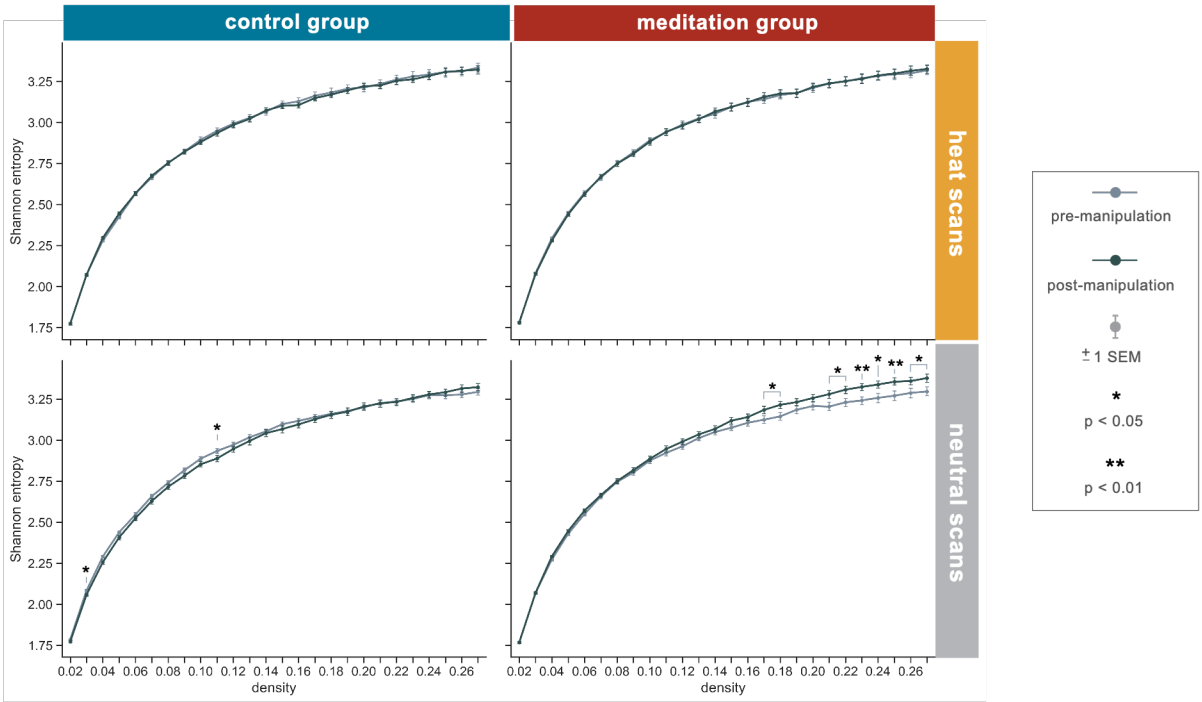


Figure 1.5: Cortical Shannon entropy pre- and post-manipulation across the small-world range of densities (error bars = ±1 SEM) for controls (left), meditators (right), heat BOLD series (top) and neutral BOLD series (bottom). Meditation resulted in significantly higher entropy during the innocuous condition (neutral scans) consistent at higher network densities, while weakly opposite (entropy decrease) changes were observed for controls. No significant entropy changes were observed during the noxious heat condition. Significant changes between iso-dense pre- and post-manipulation networks assessed with paired samples t-tests ($p < .05$ marked as *, $p < .01$ marked as **).

II. Entropy: Meditation significantly increases cortical Shannon entropy when compared to rest and controls.

A 2 (group) X 2 (pre/post) repeated measures ANOVA on entropy during neutral BOLD series performed across the small world density range (0.02 – 0.27) revealed a significant ($p < .05$) group by time interaction at 4 out of the 26 densities (see Table 1.1 for significant ANOVAs and Supplementary Tables 1.1-1.2 for complete ANOVAs) that were driven by the significant increase in entropy during meditation when compared to rest (p value range : $.011 < p < .048$ in paired samples t-tests at 9 out of 26 densities) and controls (no change in entropy for 25 out of 27 densities, $p > .05$, and significantly lower entropy at post session for 2 densities, $.024 < p < .038$) (Figure 1.5; See Supplementary Table 1.3-1.6). There were no significant main effects or interactions during noxious heat ($.06 < p < 1.0$; see Supplementary Table 1.2). Meditation thus significantly increased entropy during innocuous stimulation when compared to rest and controls.

Table 1.1: Statistically Significant 2(group) X 2(pre/post) Repeated Measures ANOVA on Entropy.

Density	Predictor	Sum of Squares	DF1	DF2	Mean Square	F	p	np2
0.04	group x time	0.014	1	38	0.014	5.235	0.028	0.121
0.11	group x time	0.024	1	38	0.024	4.196	0.047	0.099
0.15	group x time	0.026	1	38	0.026	4.282	0.045	0.101
0.18	group x time	0.029	1	38	0.029	4.458	0.041	0.105
0.23	time	0.039	1	38	0.039	5.298	0.027	0.122
0.24	time	0.037	1	38	0.037	4.259	0.046	0.101
0.25	time	0.054	1	38	0.054	6.985	0.012	0.155
0.26	time	0.059	1	38	0.059	6.780	0.013	0.151
0.27	time	0.061	1	38	0.061	5.829	0.021	0.133

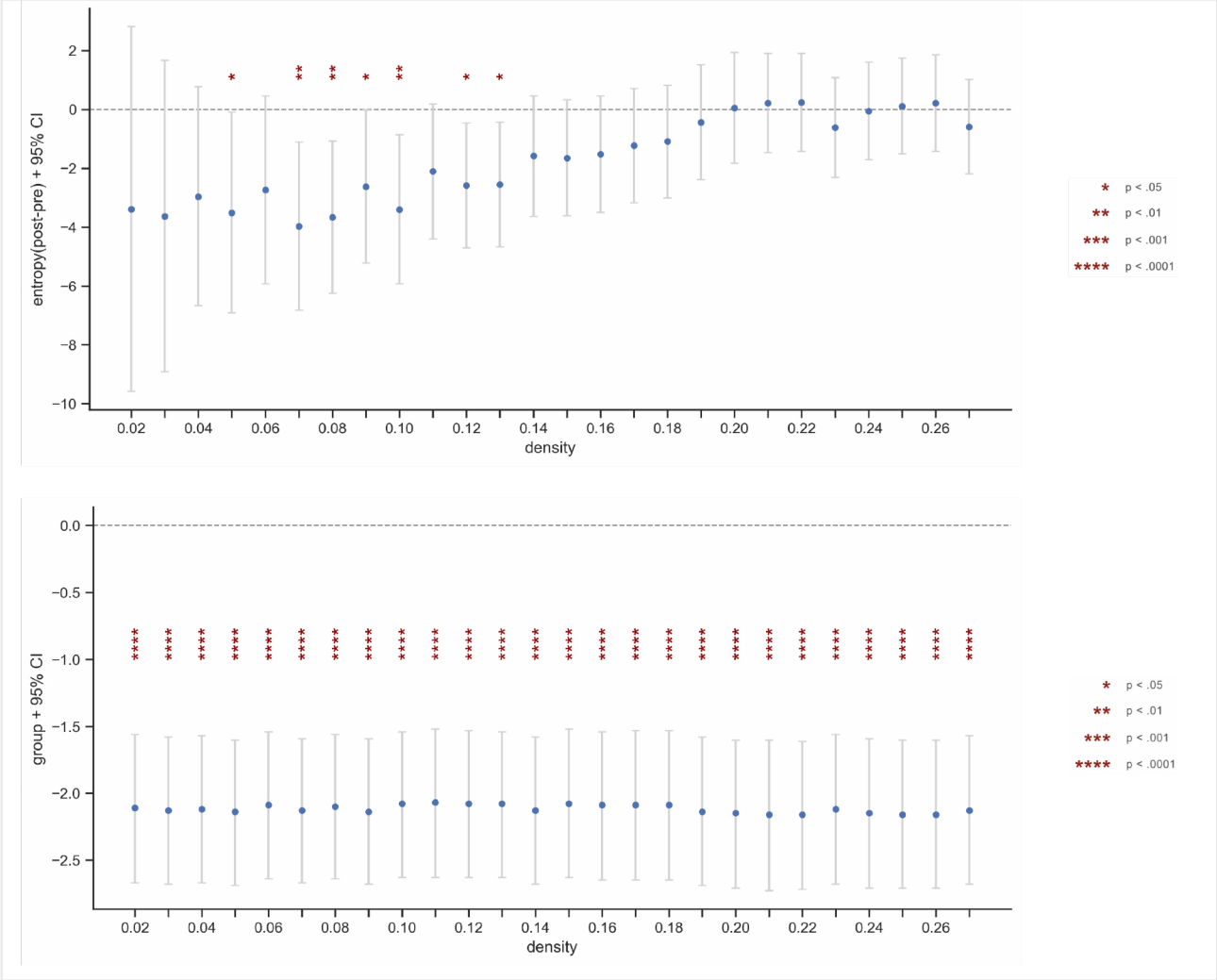


Figure 1.6: Pain ~ entropy regression model 1. Regression coefficients for regressors Group and Entropy(post-pre) from linear regression Model 1 performed for all subjects at each network density across the small-world range of densities.

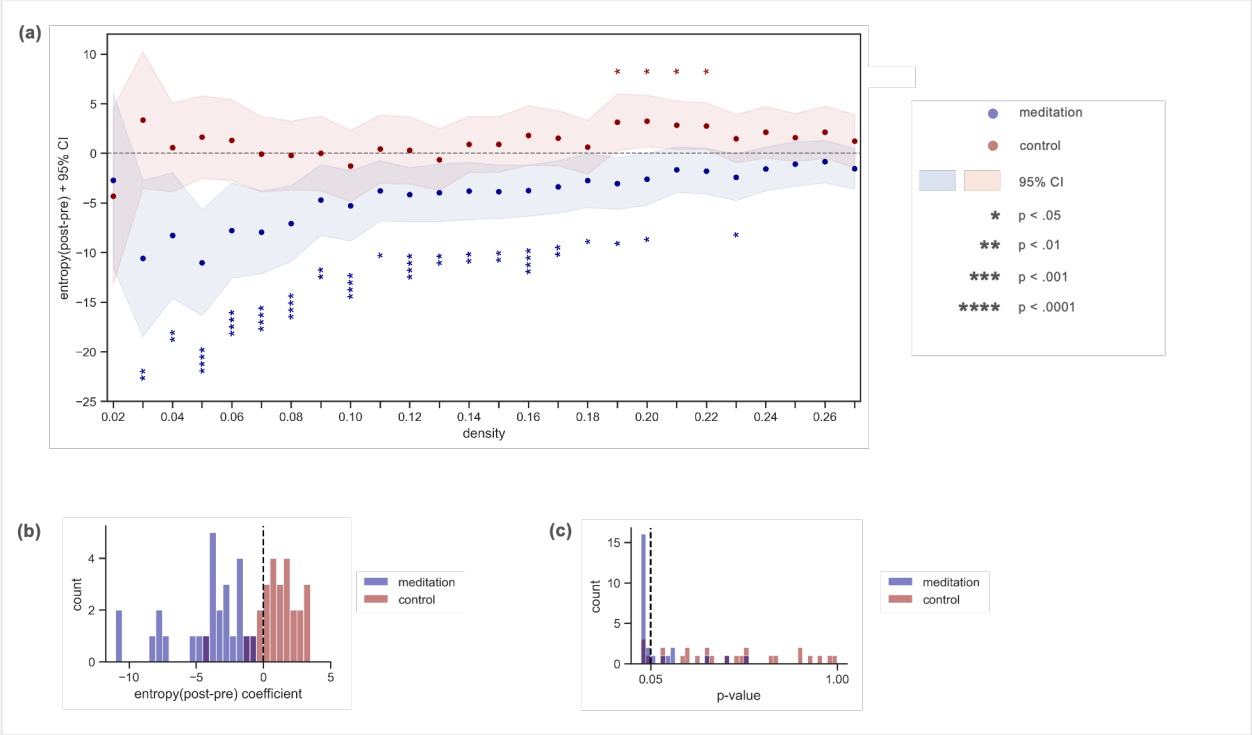


Figure 1.7: Pain ~ entropy regression model 2. (a) Regression coefficient for regressor *Entropy(post-pre)* from multivariate ordinary least squares (OLS) linear regression for Model 2: [Pain(post-pre) ~ 1 + Entropy(post-pre) + FramewiseDisplacement(post-pre)] performed separately for meditation (blue) and control (red) subjects at each density across the small-world range of network densities. (b) Histogram of *entropy(post-pre)* regressor coefficient values. (c) Histogram of Entropy(post-pre) regressor p-values.

III. Pain and Entropy: Higher meditation-associated cortical entropy predicts meditation-based pain relief

Meditators and controls differed in how changes in entropy predicted changes in pain (model 1). The relationship between entropy and pain varied by group across all densities ($p<0.0001$, adjusted $r^2 = 0.37$) (Figure 1.6). (See Supplementary Table 1.7 for detailed regression results).

Follow-up within group regressions revealed opposite association between pain and entropy for meditators and controls.

Mindfulness-induced higher entropy predicted lower pain.

For meditators, the significant increase in cortical entropy from rest to meditation during innocuous 35°C stimulation predicted the decrease in pain ratings from rest to meditation in 18 out of the 26 densities ($0.00 < ps < 0.04$; $0.07 <$ adjusted $r^2 < 0.20$) (Figure 1.7). In 13 out of 26 densities, higher framewise displacement during meditation was significantly associated with lower pain ($0.02 < ps < 0.04$; $0.05 <$ adjusted $r^2 < 0.14$).

Higher entropy was associated with higher pain in the controls.

For controls, an opposite, positive, relation between higher entropy and higher pain from rest to meditation during innocuous 35°C stimulation was found in 4 out of the 26 densities ($0.02 < ps < 0.03$; $0.04 <$ adjusted $r^2 < 0.06$). (See Supplementary Table 1.7 for detailed within-group regression results).

Discussion

The present findings are the first to demonstrate a functional relationship between cortical entropy and pain relief. After 80 minutes of meditation training, the degree distributions of meditators' functional connectivity networks under innocuous 35°C. stimulation exhibited significantly greater Shannon entropy during meditation than during rest and controls, showing that minimal training is sufficient to broaden the repertoire of functional connectivity states in

the cortex. These results complement previous neurophysiological findings[17,18] to show that meditation produces higher brain entropy markers and induces a less prediction-driven pattern of spontaneous neural dynamics consistent with a flatter attractor landscape[13,46,47]. Importantly, higher mindfulness meditation-induced entropy during innocuous 35°C stimulation predicted lower experimentally evoked pain, implicating cortical entropy modulation as a meditation-specific pain relief mechanism. Our results support the view that high-order nociceptive processing is a cortically mediated predictive process sensitive to entropy modulation[1–3,31] and that meditation attenuates the influence of self-fulfilling predictions of pain on the cortical circuits that construct the subjective experience of pain, resulting in pain relief (Figure 1.8).

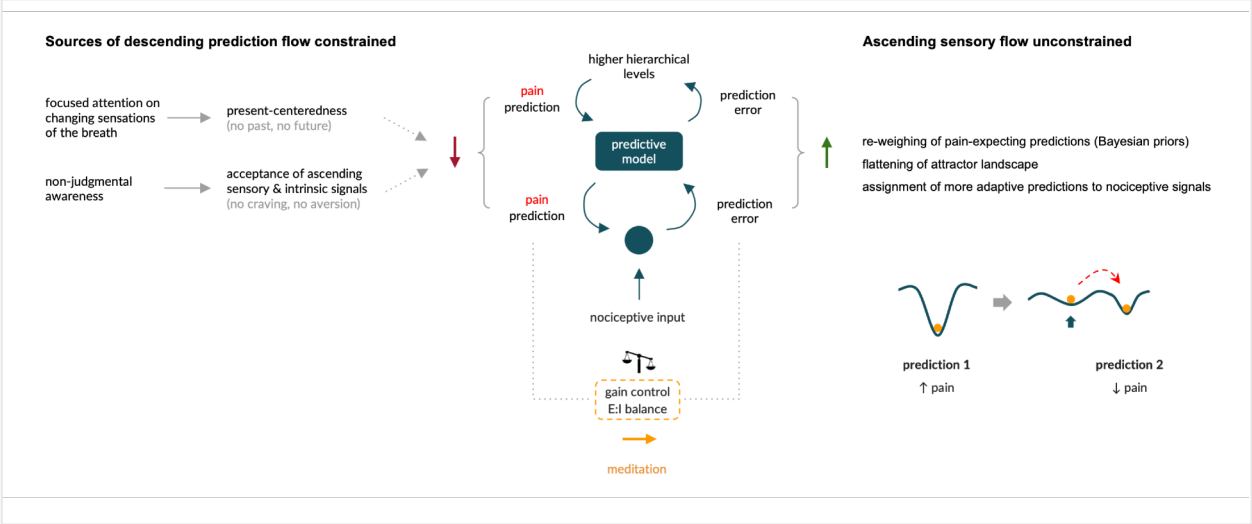


Figure 1.8: Entropy modulated predictive coding of pain. By limiting attention to the present moment via the breath and by removing judgments of exteroceptive and interoceptive sensations, mindfulness meditation constrains the very sources of self-fulfilling pain-expecting predictions, attenuating their influence and lowering the actual sensation of pain, while also allowing new, more adaptive predictions to be assigned to nociceptive signals.

Given that the brain minimizes the number of prediction-based attractors while still maintaining an adequate predictive model of the environment[8], higher meditation-induced

entropy is consistent with a flattened attractor landscape in which less confidence is assigned to predictions and more confidence is assigned to afferent sensory information. If higher-order nociceptive processing occurs via a confidence-weighted integration of ascending nociceptive and descending predictive signals[2,4], under a meditation-induced high entropy state the brain would assign less weight to pain-expecting predictions, reducing their influence on the overall level of pain. As the prediction-based component of pain is weakened, the experience of pain becomes more influenced by the ascending nociceptive afferent signal and less so by the prediction of pain, resulting in a lower overall level of painful suffering.

Of note, significant changes in entropy during noxious heat were not observed, and for meditators, entropy changes during innocuous heat predicted changes in pain during noxious heat. Focused attention has been shown to elicit lower entropy of spontaneous neural activity (subcritical dynamics)[48], and attention to the noxious stimulus during noxious heat may have counteracted the meditation-induced increases in entropy seen during innocuous heat. Alternatively, hemodynamic changes resulting from the block design of heat scan series may have reduced the functional connectivity networks' sensitivity to this entropy measure.

The present study is limited in that it calculates entropy from binarized networks, introducing possible threshold-specific effects, so results should be confirmed with different entropy measures. While denoising with aCompCor and mean CSF and WM confound regressors was necessary to produce functional connectivity distributions centered around zero, motion artifacts may have been reintroduced. Additionally, calculating entropy of functional connectivity networks during heat-based blocked design scans is methodologically novel and does not account for hemodynamic response. Finally, despite being consistent with theories of

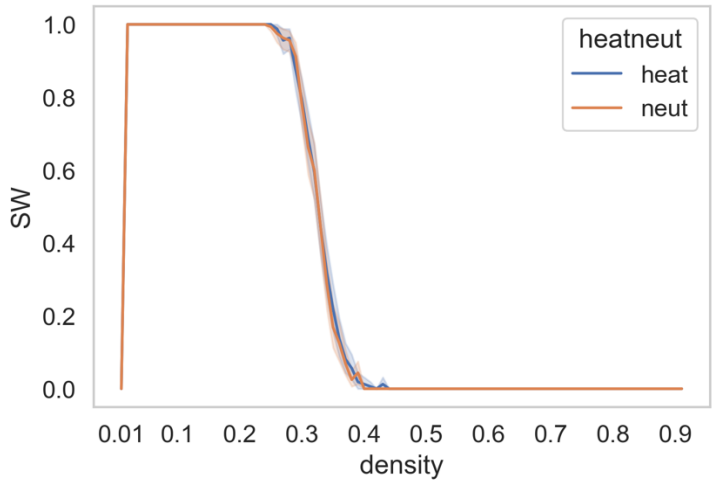
entropy-based gain modulation, the entropy-pain relation is inferred, and true causality remains to be demonstrated.

Conclusions

Consistent with our previous studies, mindfulness meditation after brief mental training significantly reduced experimentally induced pain. This is the first study to show that mindfulness meditation increases the Shannon entropy of cortical functional connectivity networks as compared to controls. Findings also revealed that greater meditation-based pain relief was predicted by higher cortical entropy, in line with nociceptive processing being neurally implemented by entropy-sensitive predictive coding mechanisms. Entropic modulation via meditative practice thus provides a mechanistic target for the treatment of psychosomatic pain conditions whose etiologies are distributed across the mind-body connection.

Acknowledgments

Chapter 1, in full, is currently being prepared for submission for publication of the material. The dissertation author was the primary author of this material. The principal investigator of this material was Fadel Zeidan and additional authors include Grace Posey, Gabriel Riegner, and Youngkyoo Jung.



Supplemental Figure 1.1: Small-worldness (SW) per network density.

Supplemental Table 1.1: Repeated Measures ANOVAs on Entropy (Neutral).
2(group) X 2(pre/post) Repeated Measures ANOVA on Entropy, Neutral Scans

Density	Predictor	Sum of Squares	DF1	DF2	Mean Square	*F*	*p*	np2
0.02	group	0.003	1	38	0.003	2.792	0.103	0.068
0.02	time	0.001	1	38	0.001	0.921	0.343	0.024
0.02	group x time	0.001	1	38	0.001	1.204	0.279	0.031
0.03	group	0.000	1	38	0.000	0.013	0.910	0.000
0.03	time	0.003	1	38	0.003	2.204	0.146	0.055
0.03	group x time	0.003	1	38	0.003	2.376	0.132	0.059
0.04	group	0.002	1	38	0.002	0.574	0.453	0.015
0.04	time	0.001	1	38	0.001	0.460	0.502	0.012
0.04	group x time	0.014	1	38	0.014	5.235	0.028	0.121
0.05	group	0.005	1	38	0.005	1.466	0.233	0.037
0.05	time	0.001	1	38	0.001	0.389	0.537	0.010
0.05	group x time	0.012	1	38	0.012	4.039	0.052	0.096
0.06	group	0.013	1	38	0.013	2.932	0.095	0.072
0.06	time	0.000	1	38	0.000	0.003	0.957	0.000
0.06	group x time	0.009	1	38	0.009	2.562	0.118	0.063
0.07	group	0.006	1	38	0.006	1.172	0.286	0.030
0.07	time	0.002	1	38	0.002	0.493	0.487	0.013
0.07	group x time	0.007	1	38	0.007	1.630	0.209	0.041
0.08	group	0.009	1	38	0.009	1.485	0.230	0.038
0.08	time	0.002	1	38	0.002	0.447	0.508	0.012
0.08	group x time	0.004	1	38	0.004	0.941	0.338	0.024
0.09	group	0.002	1	38	0.002	0.361	0.551	0.009
0.09	time	0.002	1	38	0.002	0.351	0.557	0.009
0.09	group x time	0.012	1	38	0.012	2.327	0.135	0.058
0.10	group	0.002	1	38	0.002	0.252	0.619	0.007
0.10	time	0.003	1	38	0.003	0.573	0.454	0.015
0.10	group x time	0.010	1	38	0.010	2.116	0.154	0.053
0.11	group	0.011	1	38	0.011	1.191	0.282	0.030
0.11	time	0.002	1	38	0.002	0.430	0.516	0.011
0.11	group x time	0.024	1	38	0.024	4.196	0.047	0.099
0.12	group	0.006	1	38	0.006	0.737	0.396	0.019
0.12	time	0.000	1	38	0.000	0.008	0.927	0.000
0.12	group x time	0.015	1	38	0.015	2.850	0.100	0.070
0.13	group	0.006	1	38	0.006	0.540	0.467	0.014
0.13	time	0.000	1	38	0.000	0.000	0.998	0.000
0.13	group x time	0.010	1	38	0.010	1.960	0.170	0.049
0.14	group	0.002	1	38	0.002	0.220	0.642	0.006
0.14	time	0.000	1	38	0.000	0.048	0.828	0.001
0.14	group x time	0.004	1	38	0.004	0.693	0.410	0.018
0.15	group	0.004	1	38	0.004	0.394	0.534	0.010
0.15	time	0.001	1	38	0.001	0.147	0.703	0.004

Supplemental Table 1.1: Repeated Measures ANOVAs on Entropy (Neutral). (Continued)
2(group) X 2(pre/post) Repeated Measures ANOVA on Entropy, Neutral Scans

Density	Predictor	Sum of Squares	DF1	DF2	Mean Square	*F*	*p*	np2
0.15	group x time	0.026	1	38	0.026	4.282	0.045	0.101
0.16	group	0.005	1	38	0.005	0.440	0.511	0.011
0.16	time	0.001	1	38	0.001	0.124	0.727	0.003
0.16	group x time	0.016	1	38	0.016	2.303	0.137	0.057
0.17	group	0.009	1	38	0.009	0.611	0.439	0.016
0.17	time	0.011	1	38	0.011	1.431	0.239	0.036
0.17	group x time	0.026	1	38	0.026	3.443	0.071	0.083
0.18	group	0.010	1	38	0.010	0.677	0.416	0.017
0.18	time	0.021	1	38	0.021	3.296	0.077	0.080
0.18	group x time	0.029	1	38	0.029	4.458	0.041	0.105
0.19	group	0.022	1	38	0.022	1.274	0.266	0.032
0.19	time	0.009	1	38	0.009	1.302	0.261	0.033
0.19	group x time	0.013	1	38	0.013	1.893	0.177	0.047
0.20	group	0.018	1	38	0.018	1.154	0.290	0.029
0.20	time	0.014	1	38	0.014	2.001	0.165	0.050
0.20	group x time	0.010	1	38	0.010	1.331	0.256	0.034
0.21	group	0.006	1	38	0.006	0.349	0.558	0.009
0.21	time	0.026	1	38	0.026	2.891	0.097	0.071
0.21	group x time	0.031	1	38	0.031	3.460	0.071	0.083
0.22	group	0.024	1	38	0.024	1.515	0.226	0.038
0.22	time	0.028	1	38	0.028	3.360	0.075	0.081
0.22	group x time	0.032	1	38	0.032	3.771	0.060	0.090
0.23	group	0.018	1	38	0.018	1.097	0.302	0.028
0.23	time	0.039	1	38	0.039	5.298	0.027	0.122
0.23	group x time	0.029	1	38	0.029	3.889	0.056	0.093
0.24	group	0.010	1	38	0.010	0.568	0.456	0.015
0.24	time	0.037	1	38	0.037	4.259	0.046	0.101
0.24	group x time	0.030	1	38	0.030	3.474	0.070	0.084
0.25	group	0.019	1	38	0.019	1.052	0.312	0.027
0.25	time	0.054	1	38	0.054	6.985	0.012	0.155
0.25	group x time	0.022	1	38	0.022	2.810	0.102	0.069
0.26	group	0.015	1	38	0.015	0.879	0.354	0.023
0.26	time	0.059	1	38	0.059	6.780	0.013	0.151
0.26	group x time	0.007	1	38	0.007	0.762	0.388	0.020
0.27	group	0.017	1	38	0.017	0.853	0.362	0.022
0.27	time	0.061	1	38	0.061	5.829	0.021	0.133
0.27	group x time	0.014	1	38	0.014	1.301	0.261	0.033

Supplemental Table 1.2: Repeated Measures ANOVAs on Entropy (Heat).
2(group) X 2(pre/post) Repeated Measures ANOVA on Entropy, Heat Scans

Density	Predictor	Sum of Squares	DF1	DF2	Mean Square	*F*	*p*	np2
0.02	group	0.001	1	38	0.001	0.605	0.442	0.016
0.02	time	0.000	1	38	0.000	0.111	0.740	0.003
0.02	group x time	0.000	1	38	0.000	0.115	0.737	0.003
0.03	group	0.001	1	38	0.001	1.063	0.309	0.027
0.03	time	0.000	1	38	0.000	0.350	0.558	0.009
0.03	group x time	0.000	1	38	0.000	0.131	0.719	0.003
0.04	group	0.000	1	38	0.000	0.016	0.898	0.000
0.04	time	0.000	1	38	0.000	0.036	0.850	0.001
0.04	group x time	0.005	1	38	0.005	3.682	0.063	0.088
0.05	group	0.002	1	38	0.002	0.357	0.554	0.009
0.05	time	0.001	1	38	0.001	0.385	0.539	0.010
0.05	group x time	0.004	1	38	0.004	2.157	0.150	0.054
0.06	group	0.000	1	38	0.000	0.000	0.996	0.000
0.06	time	0.000	1	38	0.000	0.148	0.702	0.004
0.06	group x time	0.000	1	38	0.000	0.105	0.748	0.003
0.07	group	0.000	1	38	0.000	0.031	0.861	0.001
0.07	time	0.001	1	38	0.001	0.449	0.507	0.012
0.07	group x time	0.000	1	38	0.000	0.018	0.893	0.000
0.08	group	0.000	1	38	0.000	0.025	0.876	0.001
0.08	time	0.000	1	38	0.000	0.000	0.983	0.000
0.08	group x time	0.000	1	38	0.000	0.005	0.944	0.000
0.09	group	0.002	1	38	0.002	0.157	0.694	0.004
0.09	time	0.001	1	38	0.001	0.166	0.686	0.004
0.09	group x time	0.000	1	38	0.000	0.066	0.798	0.002
0.10	group	0.000	1	38	0.000	0.002	0.968	0.000
0.10	time	0.002	1	38	0.002	0.557	0.460	0.014
0.10	group x time	0.000	1	38	0.000	0.035	0.852	0.001
0.11	group	0.000	1	38	0.000	0.000	0.988	0.000
0.11	time	0.001	1	38	0.001	0.099	0.755	0.003
0.11	group x time	0.001	1	38	0.001	0.253	0.618	0.007
0.12	group	0.000	1	38	0.000	0.028	0.867	0.001
0.12	time	0.001	1	38	0.001	0.128	0.722	0.003
0.12	group x time	0.000	1	38	0.000	0.002	0.969	0.000
0.13	group	0.000	1	38	0.000	0.009	0.923	0.000
0.13	time	0.001	1	38	0.001	0.071	0.792	0.002
0.13	group x time	0.000	1	38	0.000	0.004	0.951	0.000
0.14	group	0.002	1	38	0.002	0.102	0.751	0.003
0.14	time	0.002	1	38	0.002	0.252	0.619	0.007
0.14	group x time	0.000	1	38	0.000	0.028	0.868	0.001
0.15	group	0.003	1	38	0.003	0.174	0.679	0.005
0.15	time	0.001	1	38	0.001	0.067	0.797	0.002

Supplemental Table 1.2: Repeated Measures ANOVAs on Entropy (Heat). (Continued)
2(group) X 2(pre/post) Repeated Measures ANOVA on Entropy, Heat Scans

Density	Predictor	Sum of Squares	DF1	DF2	Mean Square	*F*	*p*	np2
0.16	group	0.001	1	38	0.001	0.047	0.829	0.001
0.16	time	0.003	1	38	0.003	0.387	0.538	0.010
0.16	group x time	0.002	1	38	0.002	0.246	0.623	0.006
0.17	group	0.001	1	38	0.001	0.037	0.848	0.001
0.17	time	0.000	1	38	0.000	0.001	0.975	0.000
0.17	group x time	0.004	1	38	0.004	0.491	0.488	0.013
0.18	group	0.001	1	38	0.001	0.023	0.881	0.001
0.18	time	0.000	1	38	0.000	0.008	0.927	0.000
0.18	group x time	0.002	1	38	0.002	0.252	0.619	0.007
0.19	group	0.009	1	38	0.009	0.387	0.538	0.010
0.19	time	0.001	1	38	0.001	0.076	0.784	0.002
0.19	group x time	0.000	1	38	0.000	0.040	0.842	0.001
0.20	group	0.000	1	38	0.000	0.013	0.908	0.000
0.20	time	0.001	1	38	0.001	0.096	0.758	0.003
0.20	group x time	0.000	1	38	0.000	0.003	0.960	0.000
0.21	group	0.001	1	38	0.001	0.053	0.820	0.001
0.21	time	0.000	1	38	0.000	0.025	0.874	0.001
0.21	group x time	0.001	1	38	0.001	0.043	0.837	0.001
0.22	group	0.001	1	38	0.001	0.026	0.874	0.001
0.22	time	0.000	1	38	0.000	0.013	0.910	0.000
0.22	group x time	0.000	1	38	0.000	0.031	0.861	0.001
0.23	group	0.000	1	38	0.000	0.010	0.920	0.000
0.23	time	0.002	1	38	0.002	0.183	0.671	0.005
0.23	group x time	0.001	1	38	0.001	0.061	0.806	0.002
0.24	group	0.000	1	38	0.000	0.005	0.945	0.000
0.24	time	0.000	1	38	0.000	0.010	0.919	0.000
0.24	group x time	0.001	1	38	0.001	0.063	0.803	0.002
0.25	group	0.003	1	38	0.003	0.094	0.761	0.002
0.25	time	0.000	1	38	0.000	0.008	0.930	0.000
0.25	group x time	0.000	1	38	0.000	0.009	0.925	0.000
0.26	group	0.001	1	38	0.001	0.027	0.870	0.001
0.26	time	0.002	1	38	0.002	0.152	0.699	0.004
0.26	group x time	0.001	1	38	0.001	0.043	0.837	0.001
0.27	group	0.001	1	38	0.001	0.025	0.875	0.001
0.27	time	0.000	1	38	0.000	0.011	0.917	0.000
0.27	group x time	0.002	1	38	0.002	0.193	0.663	0.005

Supplemental Table 1.3: Pre vs. post entropy paired t-tests (neutral, controls).

	Entropy							
	Pre		Post					
Density	Mean	SD	Mean	SD	*T*	DF	*p*	Cohen`s *d*
0.02	1.78	0.02	1.77	0.04	-2.01	19	0.06	-0.52
0.03	2.08	0.04	2.06	0.05	-2.21	19	0.04	-0.66
0.04	2.29	0.06	2.26	0.09	-1.88	19	0.08	-0.60
0.05	2.44	0.06	2.41	0.09	-1.83	19	0.08	-0.56
0.06	2.55	0.08	2.52	0.09	-1.16	19	0.26	-0.37
0.07	2.66	0.08	2.63	0.11	-1.38	19	0.18	-0.43
0.08	2.74	0.09	2.71	0.11	-1.12	19	0.28	-0.35
0.09	2.82	0.09	2.78	0.10	-1.85	19	0.08	-0.50
0.10	2.89	0.10	2.85	0.12	-1.80	19	0.09	-0.44
0.11	2.93	0.10	2.89	0.12	-2.47	19	0.02	-0.56
0.12	2.97	0.10	2.95	0.12	-1.78	19	0.09	-0.36
0.13	3.02	0.11	2.99	0.14	-1.14	19	0.27	-0.26
0.14	3.05	0.09	3.04	0.13	-0.52	19	0.61	-0.13
0.15	3.10	0.10	3.07	0.15	-1.43	19	0.17	-0.32
0.16	3.12	0.09	3.10	0.14	-1.08	19	0.29	-0.25
0.17	3.14	0.11	3.13	0.14	-0.63	19	0.54	-0.14
0.18	3.16	0.10	3.15	0.14	-0.35	19	0.73	-0.06
0.19	3.18	0.12	3.17	0.14	-0.29	19	0.78	-0.04
0.20	3.20	0.12	3.20	0.14	0.31	19	0.76	0.05
0.21	3.23	0.12	3.22	0.14	-0.20	19	0.84	-0.04
0.22	3.23	0.13	3.23	0.13	-0.13	19	0.90	-0.02
0.23	3.25	0.13	3.26	0.14	0.35	19	0.73	0.07
0.24	3.27	0.13	3.28	0.13	0.26	19	0.80	0.04
0.25	3.27	0.13	3.29	0.14	1.23	19	0.23	0.20
0.26	3.28	0.12	3.31	0.14	1.86	19	0.08	0.38
0.27	3.29	0.12	3.32	0.14	1.67	19	0.11	0.31

Supplemental Table 1.4: Pre vs. post entropy paired t-tests (neutral, meditators).

	Entropy							
	Pre		Post					
Density	Mean	SD	Mean	SD	*T*	DF	*p*	Cohen`s *d*
0.02	1.77	0.05	1.77	0.05	0.08	19	0.94	0.03
0.03	2.07	0.05	2.07	0.05	0.04	19	0.97	0.01
0.04	2.27	0.07	2.29	0.04	1.30	19	0.21	0.39
0.05	2.43	0.07	2.45	0.06	1.00	19	0.33	0.31
0.06	2.55	0.08	2.57	0.07	1.10	19	0.28	0.32
0.07	2.66	0.09	2.66	0.08	0.41	19	0.68	0.12
0.08	2.75	0.08	2.75	0.09	0.22	19	0.83	0.06
0.09	2.8	0.10	2.82	0.10	0.57	19	0.58	0.18
0.10	2.87	0.11	2.89	0.11	0.44	19	0.66	0.13
0.11	2.92	0.11	2.95	0.11	0.83	19	0.42	0.27
0.12	2.96	0.12	2.99	0.11	1.00	19	0.33	0.31
0.13	3.01	0.12	3.03	0.11	0.89	19	0.38	0.24
0.14	3.05	0.12	3.07	0.12	0.65	19	0.52	0.19
0.15	3.08	0.11	3.12	0.13	1.52	19	0.15	0.45
0.16	3.11	0.12	3.14	0.13	1.11	19	0.28	0.33
0.17	3.12	0.14	3.18	0.15	1.79	19	0.09	0.50
0.18	3.14	0.15	3.21	0.14	2.17	19	0.04	0.59
0.19	3.18	0.16	3.23	0.14	1.38	19	0.18	0.40
0.20	3.21	0.16	3.26	0.14	1.41	19	0.17	0.42
0.21	3.20	0.17	3.28	0.15	1.93	19	0.07	0.58
0.22	3.23	0.16	3.31	0.14	2.09	19	0.05	0.62
0.23	3.24	0.15	3.32	0.14	2.42	19	0.03	0.68
0.24	3.26	0.17	3.34	0.14	2.13	19	0.05	0.63
0.25	3.27	0.18	3.36	0.14	2.35	19	0.03	0.66
0.26	3.29	0.18	3.36	0.15	1.96	19	0.06	0.56
0.27	3.30	0.17	3.38	0.17	1.92	19	0.07	0.56

Supplemental Table 1.5: Pre vs. post entropy paired t-tests (heat, controls).

	Entropy							
	Pre		Post					
Density	Mean	SD	Mean	SD	*T*	DF	*p*	Cohen`s *d*
0.02	1.77	0.05	1.77	0.05	-0.00	19	1.00	-0.00
0.03	2.07	0.05	2.07	0.05	-0.15	19	0.88	-0.04
0.04	2.28	0.06	2.30	0.05	1.34	19	0.20	0.39
0.05	2.42	0.08	2.45	0.06	1.27	19	0.22	0.36
0.06	2.57	0.08	2.57	0.07	-0.04	19	0.97	-0.01
0.07	2.67	0.09	2.68	0.08	0.58	19	0.57	0.15
0.08	2.75	0.10	2.75	0.08	0.03	19	0.97	0.01
0.09	2.82	0.10	2.82	0.08	-0.10	19	0.92	-0.03
0.10	2.89	0.11	2.88	0.09	-0.64	19	0.53	-0.16
0.11	2.95	0.12	2.93	0.10	-0.59	19	0.56	-0.14
0.12	2.99	0.12	2.98	0.11	-0.29	19	0.77	-0.08
0.13	3.03	0.13	3.02	0.12	-0.24	19	0.81	-0.06
0.14	3.07	0.14	3.07	0.11	0.22	19	0.82	0.06
0.15	3.11	0.14	3.10	0.11	-0.36	19	0.72	-0.10
0.16	3.13	0.14	3.11	0.10	-0.82	19	0.42	-0.23
0.17	3.16	0.16	3.15	0.11	-0.44	19	0.66	-0.11
0.18	3.18	0.17	3.17	0.12	-0.37	19	0.71	-0.11
0.19	3.21	0.16	3.20	0.12	-0.31	19	0.76	-0.08
0.20	3.21	0.16	3.22	0.12	0.23	19	0.82	0.07
0.21	3.23	0.16	3.23	0.13	-0.24	19	0.81	-0.07
0.22	3.26	0.19	3.25	0.13	-0.19	19	0.85	-0.05
0.23	3.28	0.19	3.26	0.13	-0.45	19	0.66	-0.12
0.24	3.29	0.18	3.28	0.14	-0.25	19	0.80	-0.06
0.25	3.31	0.18	3.31	0.14	-0.00	19	1.00	-0.00
0.26	3.31	0.17	3.32	0.15	0.14	19	0.89	0.04
0.27	3.34	0.16	3.32	0.16	-0.40	19	0.69	-0.10

Supplemental Table 1.6: Pre vs. post entropy paired t-tests (heat, meditators).

	Entropy							
	Pre		Post					
Density	Mean	SD	Mean	SD	*T*	DF	*p*	Cohen`s *d*
0.02	1.78	0.04	1.78	0.03	0.51	19	0.61	0.16
0.03	2.08	0.04	2.08	0.04	-0.72	19	0.48	-0.22
0.04	2.29	0.06	2.28	0.05	-1.40	19	0.18	-0.34
0.05	2.45	0.07	2.44	0.07	-0.74	19	0.47	-0.14
0.06	2.57	0.08	2.56	0.09	-0.57	19	0.58	-0.11
0.07	2.66	0.10	2.67	0.09	0.37	19	0.71	0.08
0.08	2.75	0.12	2.75	0.10	-0.07	19	0.95	-0.01
0.09	2.82	0.11	2.81	0.11	-0.50	19	0.62	-0.10
0.10	2.89	0.12	2.88	0.12	-0.41	19	0.69	-0.08
0.11	2.94	0.13	2.94	0.12	0.13	19	0.90	0.03
0.12	2.99	0.14	2.98	0.14	-0.22	19	0.83	-0.05
0.13	3.02	0.15	3.02	0.14	-0.14	19	0.89	-0.03
0.14	3.05	0.15	3.07	0.15	0.50	19	0.62	0.10
0.15	3.09	0.15	3.09	0.15	-0.00	19	1.00	-0.00
0.16	3.13	0.16	3.12	0.15	-0.09	19	0.93	-0.02
0.17	3.14	0.16	3.16	0.16	0.56	19	0.58	0.11
0.18	3.17	0.16	3.18	0.16	0.34	19	0.74	0.06
0.19	3.18	0.16	3.18	0.16	-0.06	19	0.95	-0.01
0.20	3.21	0.16	3.22	0.15	0.21	19	0.83	0.04
0.21	3.24	0.17	3.24	0.17	0.04	19	0.97	0.01
0.22	3.25	0.18	3.25	0.18	0.05	19	0.96	0.01
0.23	3.27	0.19	3.27	0.18	-0.14	19	0.89	-0.03
0.24	3.28	0.18	3.29	0.17	0.10	19	0.92	0.02
0.25	3.29	0.18	3.30	0.17	0.14	19	0.89	0.03
0.26	3.3	0.18	3.31	0.17	0.39	19	0.70	0.10
0.27	3.32	0.18	3.33	0.17	0.23	19	0.82	0.05

Supplemental Table 1.7: Regression results, all densities, all subjects.

Density	Predictor	Beta (β)	SE	95% CI [LL, UL]	*t*	*p*	r^2	adjusted r^2
0.02	(intercept)	0.60	0.17	[0.26, 0.95]	3.45	0.00	0.38	0.37
0.02	Δ Framewise Displacement	-2.32	1.56	[-5.39, 0.76]	-1.49	0.14	0.38	0.37
0.02	Δ Entropy	-3.39	3.14	[-9.59, 2.81]	-1.08	0.28	0.38	0.37
0.02	Group dummy	-2.11	0.28	[-2.67, -1.56]	-7.52	0.00	0.38	0.37
0.03	(intercept)	0.57	0.18	[0.22, 0.92]	3.21	0.00	0.39	0.37
0.03	Δ Framewise Displacement	-2.03	1.56	[-5.10, 1.05]	-1.30	0.20	0.39	0.37
0.03	Δ Entropy	-3.63	2.68	[-8.92, 1.67]	-1.35	0.18	0.39	0.37
0.03	Group dummy	-2.13	0.28	[-2.68, -1.58]	-7.64	0.00	0.39	0.37
0.04	(intercept)	0.60	0.17	[0.26, 0.94]	3.45	0.00	0.39	0.38
0.04	Δ Framewise Displacement	-2.26	1.55	[-5.32, 0.80]	-1.46	0.15	0.39	0.38
0.04	Δ Entropy	-2.96	1.88	[-6.68, 0.77]	-1.57	0.12	0.39	0.38
0.04	Group dummy	-2.12	0.28	[-2.67, -1.57]	-7.60	0.00	0.39	0.38
0.05	(intercept)	0.60	0.17	[0.26, 0.94]	3.47	0.00	0.39	0.38
0.05	Δ Framewise Displacement	-1.92	1.55	[-4.98, 1.13]	-1.24	0.22	0.39	0.38
0.05	Δ Entropy	-3.51	1.73	[-6.92, -0.09]	-2.03	0.04	0.39	0.38
0.05	Group dummy	-2.14	0.28	[-2.69, -1.60]	-7.76	0.00	0.39	0.38
0.06	(intercept)	0.60	0.17	[0.25, 0.94]	3.43	0.00	0.39	0.38
0.06	Δ Framewise Displacement	-2.36	1.55	[-5.42, 0.70]	-1.52	0.13	0.39	0.38
0.06	Δ Entropy	-2.73	1.61	[-5.92, 0.46]	-1.69	0.09	0.39	0.38
0.06	Group dummy	-2.09	0.28	[-2.64, -1.54]	-7.47	0.00	0.39	0.38
0.07	(intercept)	0.58	0.17	[0.24, 0.92]	3.37	0.00	0.41	0.40
0.07	Δ Framewise Displacement	-1.72	1.53	[-4.75, 1.32]	-1.12	0.27	0.41	0.40
0.07	Δ Entropy	-3.97	1.45	[-6.83, -1.11]	-2.75	0.01	0.41	0.40
0.07	Group dummy	-2.13	0.27	[-2.67, -1.59]	-7.79	0.00	0.41	0.40

Supplemental Table 1.7: Regression results, all densities, all subjects. (Continued)

Density	Predictor	Beta (β)	SE	95% CI [LL, UL]	*t*	*p*	r^2	adjusted r^2
0.08	(intercept)	0.58	0.17	[0.24, 0.92]	3.40	0.00	0.41	0.40
0.08	Δ Framewise Displacement	-2.27	1.52	[-5.27, 0.74]	-1.49	0.14	0.41	0.40
0.08	Δ Entropy	-3.66	1.31	[-6.26, -1.07]	-2.79	0.01	0.41	0.40
0.08	Group dummy	-2.10	0.27	[-2.64, -1.56]	-7.67	0.00	0.41	0.40
0.09	(intercept)	0.57	0.17	[0.22, 0.91]	3.26	0.00	0.39	0.38
0.09	Δ Framewise Displacement	-1.76	1.56	[-4.84, 1.32]	-1.13	0.26	0.39	0.38
0.09	Δ Entropy	-2.63	1.31	[-5.22, -0.03]	-2.00	0.05	0.39	0.38
0.09	Group dummy	-2.14	0.28	[-2.68, -1.59]	-7.73	0.00	0.39	0.38
0.10	(intercept)	0.54	0.17	[0.20, 0.88]	3.10	0.00	0.40	0.39
0.10	Δ Framewise Displacement	-2.02	1.53	[-5.04, 1.00]	-1.32	0.19	0.40	0.39
0.10	Δ Entropy	-3.40	1.28	[-5.93, -0.86]	-2.65	0.01	0.40	0.39
0.10	Group dummy	-2.08	0.28	[-2.63, -1.54]	-7.58	0.00	0.40	0.39
0.11	(intercept)	0.56	0.18	[0.21, 0.91]	3.17	0.00	0.39	0.38
0.11	Δ Framewise Displacement	-2.10	1.55	[-5.15, 0.96]	-1.36	0.18	0.39	0.38
0.11	Δ Entropy	-2.10	1.16	[-4.39, 0.18]	-1.82	0.07	0.39	0.38
0.11	Group dummy	-2.07	0.28	[-2.63, -1.52]	-7.39	0.00	0.39	0.38
0.12	(intercept)	0.58	0.17	[0.24, 0.92]	3.38	0.00	0.40	0.39
0.12	Δ Framewise Displacement	-2.24	1.53	[-5.27, 0.78]	-1.46	0.15	0.40	0.39
0.12	Δ Entropy	-2.58	1.07	[-4.70, -0.46]	-2.41	0.02	0.40	0.39
0.12	Group dummy	-2.08	0.28	[-2.63, -1.53]	-7.52	0.00	0.40	0.39
0.13	(intercept)	0.59	0.17	[0.25, 0.93]	3.42	0.00	0.40	0.39
0.13	Δ Framewise Displacement	-2.31	1.53	[-5.34, 0.72]	-1.51	0.13	0.40	0.39
0.13	Δ Entropy	-2.55	1.07	[-4.67, -0.43]	-2.38	0.02	0.40	0.39
0.13	Group dummy	-2.08	0.28	[-2.63, -1.54]	-7.54	0.00	0.40	0.39

Supplemental Table 1.7: Regression results, all densities, all subjects. (Continued)

Density	Predictor	Beta (β)	SE	95% CI [LL, UL]	*t*	*p*	r^2	adjusted r^2
0.14	(intercept)	0.62	0.17	[0.28, 0.96]	3.58	0.00	0.39	0.38
0.14	Δ Framewise Displacement	-2.21	1.55	[-5.26, 0.85]	-1.42	0.16	0.39	0.38
0.14	Δ Entropy	-1.58	1.04	[-3.63, 0.46]	-1.53	0.13	0.39	0.38
0.14	Group dummy	-2.13	0.28	[-2.68, -1.58]	-7.63	0.00	0.39	0.38
0.15	(intercept)	0.59	0.17	[0.25, 0.94]	3.40	0.00	0.39	0.38
0.15	Δ Framewise Displacement	-2.29	1.55	[-5.35, 0.76]	-1.48	0.14	0.39	0.38
0.15	Δ Entropy	-1.65	1.00	[-3.61, 0.32]	-1.66	0.10	0.39	0.38
0.15	Group dummy	-2.08	0.28	[-2.63, -1.52]	-7.39	0.00	0.39	0.38
0.16	(intercept)	0.59	0.17	[0.25, 0.94]	3.38	0.00	0.39	0.38
0.16	Δ Framewise Displacement	-2.22	1.55	[-5.28, 0.84]	-1.43	0.15	0.39	0.38
0.16	Δ Entropy	-1.52	1.00	[-3.50, 0.46]	-1.52	0.13	0.39	0.38
0.16	Group dummy	-2.09	0.28	[-2.65, -1.54]	-7.47	0.00	0.39	0.38
0.17	(intercept)	0.61	0.17	[0.26, 0.95]	3.50	0.00	0.38	0.37
0.17	Δ Framewise Displacement	-2.26	1.55	[-5.33, 0.81]	-1.46	0.15	0.38	0.37
0.17	Δ Entropy	-1.23	0.98	[-3.17, 0.71]	-1.25	0.21	0.38	0.37
0.17	Group dummy	-2.09	0.28	[-2.65, -1.53]	-7.37	0.00	0.38	0.37
0.18	(intercept)	0.62	0.17	[0.27, 0.96]	3.54	0.00	0.38	0.37
0.18	Δ Framewise Displacement	-2.28	1.55	[-5.35, 0.79]	-1.47	0.14	0.38	0.37
0.18	Δ Entropy	-1.09	0.97	[-3.01, 0.82]	-1.13	0.26	0.38	0.37
0.18	Group dummy	-2.09	0.28	[-2.65, -1.53]	-7.39	0.00	0.38	0.37
0.19	(intercept)	0.62	0.17	[0.28, 0.97]	3.56	0.00	0.38	0.37
0.19	Δ Framewise Displacement	-2.26	1.56	[-5.35, 0.82]	-1.45	0.15	0.38	0.37
0.19	Δ Entropy	-0.44	0.99	[-2.39, 1.52]	-0.44	0.66	0.38	0.37
0.19	Group dummy	-2.14	0.28	[-2.69, -1.58]	-7.57	0.00	0.38	0.37

Supplemental Table 1.7: Regression results, all densities, all subjects. (Continued)

Density	Predictor	Beta (β)	SE	95% CI [LL, UL]	*t*	*p*	r^2	adjusted r^2
0.20	(intercept)	0.62	0.17	[0.28, 0.97]	3.57	0.00	0.38	0.37
0.20	Δ Framewise Displacement	-2.22	1.56	[-5.31, 0.86]	-1.43	0.16	0.38	0.37
0.20	Δ Entropy	0.05	0.95	[-1.83, 1.93]	0.05	0.96	0.38	0.37
0.20	Group dummy	-2.15	0.28	[-2.71, -1.60]	-7.67	0.00	0.38	0.37
0.21	(intercept)	0.63	0.17	[0.28, 0.97]	3.58	0.00	0.38	0.37
0.21	Δ Framewise Displacement	-2.20	1.56	[-5.29, 0.89]	-1.41	0.16	0.38	0.37
0.21	Δ Entropy	0.21	0.85	[-1.47, 1.90]	0.25	0.80	0.38	0.37
0.21	Group dummy	-2.16	0.28	[-2.73, -1.60]	-7.62	0.00	0.38	0.37
0.22	(intercept)	0.63	0.17	[0.28, 0.97]	3.58	0.00	0.38	0.37
0.22	Δ Framewise Displacement	-2.22	1.56	[-5.31, 0.86]	-1.43	0.16	0.38	0.37
0.22	Δ Entropy	0.24	0.84	[-1.42, 1.90]	0.28	0.78	0.38	0.37
0.22	Group dummy	-2.16	0.28	[-2.72, -1.61]	-7.66	0.00	0.38	0.37
0.23	(intercept)	0.62	0.17	[0.28, 0.97]	3.57	0.00	0.38	0.37
0.23	Δ Framewise Displacement	-2.28	1.56	[-5.36, 0.80]	-1.46	0.15	0.38	0.37
0.23	Δ Entropy	-0.61	0.86	[-2.31, 1.08]	-0.71	0.48	0.38	0.37
0.23	Group dummy	-2.12	0.28	[-2.68, -1.56]	-7.49	0.00	0.38	0.37
0.24	(intercept)	0.62	0.17	[0.28, 0.97]	3.58	0.00	0.38	0.37
0.24	Δ Framewise Displacement	-2.24	1.57	[-5.34, 0.86]	-1.43	0.16	0.38	0.37
0.24	Δ Entropy	-0.06	0.84	[-1.71, 1.60]	-0.07	0.95	0.38	0.37
0.24	Group dummy	-2.15	0.28	[-2.71, -1.59]	-7.54	0.00	0.38	0.37
0.25	(intercept)	0.62	0.17	[0.28, 0.97]	3.56	0.00	0.38	0.37
0.25	Δ Framewise Displacement	-2.22	1.56	[-5.30, 0.87]	-1.42	0.16	0.38	0.37
0.25	Δ Entropy	0.11	0.82	[-1.51, 1.74]	0.14	0.89	0.38	0.37
0.25	Group dummy	-2.16	0.28	[-2.71, -1.60]	-7.64	0.00	0.38	0.37
0.26	(intercept)	0.62	0.18	[0.27, 0.97]	3.53	0.00	0.38	0.37
0.26	Δ Framewise Displacement	-2.22	1.56	[-5.30, 0.86]	-1.42	0.16	0.38	0.37
0.26	Δ Entropy	0.21	0.83	[-1.42, 1.85]	0.26	0.80	0.38	0.37
0.26	Group dummy	-2.16	0.28	[-2.71, -1.60]	-7.69	0.00	0.38	0.37
0.27	(intercept)	0.63	0.17	[0.29, 0.97]	3.61	0.00	0.38	0.37
0.27	Δ Framewise Displacement	-2.27	1.56	[-5.35, 0.81]	-1.46	0.15	0.38	0.37
0.27	Δ Entropy	-0.59	0.81	[-2.19, 1.01]	-0.73	0.47	0.38	0.37
0.27	Group dummy	-2.13	0.28	[-2.68, -1.57]	-7.55	0.00	0.38	0.37

REFERENCES

1. Büchel C, Geuter S, Sprenger C, Eippert F. Placebo Analgesia: A Predictive Coding Perspective. Neuron. 2014;81:1223–39. doi:10.1016/j.neuron.2014.02.042

2. Fardo F, Auksztulewicz R, Allen M, Dietz MJ, Roepstorff A, Friston KJ. Expectation violation and attention to pain jointly modulate neural gain in somatosensory cortex. NeuroImage. 2017;153:109–21. doi:10.1016/j.neuroimage.2017.03.041

3. Grahl A, Onat S, Büchel C. The periaqueductal gray and Bayesian integration in placebo analgesia. Stephan KE, editor. eLife. 2018;7:e32930. doi:10.7554/eLife.32930

4. Mancini F, Zhang S, Seymour B. Learning the statistics of pain: computational and neural mechanisms [Internet]. bioRxiv; 2021 [cited 2022 Jun 10]. p. 2021.10.21.465270. Available from: https://www.biorxiv.org/content/10.1101/2021.10.21.465270v1 doi:10.1101/2021.10.21.465270

5. Clark A. Whatever next? Predictive brains, situated agents, and the future of cognitive science. Behavioral and Brain Sciences. 2013;36:181–204. doi:10.1017/S0140525X12000477

6. Friston K. A theory of cortical responses. Philosophical Transactions of the Royal Society B: Biological Sciences. 2005;360:815–36. doi:10.1098/rstb.2005.1622

7. Friston K. Hierarchical Models in the Brain. PLOS Computational Biology. 2008;4:e1000211. doi:10.1371/journal.pcbi.1000211

8. Friston K. The free-energy principle: a unified brain theory? Nat Rev Neurosci. 2010;11:127–38. doi:10.1038/nrn2787

9. Rao RPN, Ballard DH. Predictive coding in the visual cortex: a functional interpretation of some extra-classical receptive-field effects. Nat Neurosci. 1999;2:79–87. doi:10.1038/4580

10. Feldman H, Friston K. Attention, Uncertainty, and Free-Energy. Front Hum Neurosci. 2010;4. doi:10.3389/fnhum.2010.00215

11. Zeidan F, Lobanov OV, Kraft RA, Coghill RC. Brain mechanisms supporting violated expectations of pain. Pain. 2015;156:1772–85. doi:10.1097/j.pain.0000000000000231 PubMed PMID: 26083664; PubMed Central PMCID: PMC4545679.

12. Kirchhoff M, Parr T, Palacios E, Friston K, Kiverstein J. The Markov blankets of life: autonomy, active inference and the free energy principle. Journal of The Royal Society Interface. 2018;15:20170792. doi:10.1098/rsif.2017.0792

13. Carhart-Harris RL, Friston KJ. REBUS and the Anarchic Brain: Toward a Unified Model of the Brain Action of Psychedelics. Pharmacol Rev. 2019;71:316–44. doi:10.1124/pr.118.017160 PubMed PMID: 31221820.

14. Carhart-Harris RL, Leech R, Hellyer PJ, Shanahan M, Feilding A, Tagliazucchi E, Chialvo DR, Nutt D. The entropic brain: a theory of conscious states informed by neuroimaging research with psychedelic drugs. Front Hum Neurosci. 2014;8. doi:10.3389/fnhum.2014.00020

15. Brown CA, Jones AKP. Meditation experience predicts less negative appraisal of pain: electrophysiological evidence for the involvement of anticipatory neural responses. Pain. 2010;150:428–38. doi:10.1016/j.pain.2010.04.017 PubMed PMID: 20494517.

16. Lutz A, McFarlin DR, Perlman DM, Salomons TV, Davidson RJ. Altered anterior insula activation during anticipation and experience of painful stimuli in expert meditators. Neuroimage. 2013;64:538–46. doi:10.1016/j.neuroimage.2012.09.030 PubMed PMID: 23000783; PubMed Central PMCID: PMC3787201.

17. Kakumanu RJ, Nair AK, Venugopal R, Sasidharan A, Ghosh PK, John JP, Mehrotra S, Panth R, Kutty BM. Dissociating meditation proficiency and experience dependent EEG changes during traditional Vipassana meditation practice. Biological Psychology. 2018;135:65–75. doi:10.1016/j.biopsycho.2018.03.004

18. Martínez Vivot R, Pallavicini C, Zamberlan F, Vigo D, Tagliazucchi E. Meditation Increases the Entropy of Brain Oscillatory Activity. Neuroscience. 2020;431:40–51. doi:10.1016/j.neuroscience.2020.01.033

19. Laukkonen RE, Slagter HA. From many to (n)one: Meditation and the plasticity of the predictive mind. Neuroscience & Biobehavioral Reviews. 2021;128:199–217. doi:10.1016/j.neubiorev.2021.06.021

20. Viol A, Palhano-Fontes F, Onias H, de Araujo DB, Viswanathan GM. Shannon entropy of brain functional complex networks under the influence of the psychedelic Ayahuasca. Scientific Reports. 2017;7:1. doi:10.1038/s41598-017-06854-0

21. Viol A, Palhano-Fontes F, Onias H, de Araujo DB, Hövel P, Viswanathan GM. Characterizing Complex Networks Using Entropy-Degree Diagrams: Unveiling Changes in Functional Brain Connectivity Induced by Ayahuasca. Entropy. 2019;21:2. doi:10.3390/e21020128

22. Riegner G, Posey G, Oliva V, Jung Y, Mobley W, Zeidan F. Disentangling self from pain: mindfulness meditation-induced pain relief is driven by thalamic-default mode network decoupling. Pain. 2023;164:280–91. doi:10.1097/j.pain.0000000000002731 PubMed PMID: 36095039; PubMed Central PMCID: PMC9823141.

23. Price DD, Bush FM, Long S, Harkins SW. A comparison of pain measurement characteristics of mechanical visual analogue and simple numerical rating scales. Pain. 1994;56:217–26. doi:10.1016/0304-3959(94)90097-3 PubMed PMID: 8008411.

24. Zeidan F, Martucci KT, Kraft RA, Gordon NS, McHaffie JG, Coghill RC. Brain mechanisms supporting the modulation of pain by mindfulness meditation. J Neurosci.

2011;31:5540–8. doi:10.1523/JNEUROSCI.5791-10.2011 PubMed PMID: 21471390; PubMed Central PMCID: PMC3090218.

25. Zeidan F, Emerson NM, Farris SR, Ray JN, Jung Y, McHaffie JG, Coghill RC. Mindfulness Meditation-Based Pain Relief Employs Different Neural Mechanisms Than Placebo and Sham Mindfulness Meditation-Induced Analgesia. J Neurosci. 2015;35:15307–25. doi:10.1523/JNEUROSCI.2542-15.2015 PubMed PMID: 26586819; PubMed Central PMCID: PMC4649004.

26. White G. The Natural History of Selborne. Repressed Publishing. 2013.

27. Cropley M, Ussher M, Charitou E. Acute effects of a guided relaxation routine (body scan) on tobacco withdrawal symptoms and cravings in abstinent smokers. Addiction. 2007;102:989–93. doi:10.1111/j.1360-0443.2007.01832.x PubMed PMID: 17523994.

28. Ussher M, Cropley M, Playle S, Mohidin R, West R. Effect of isometric exercise and body scanning on cigarette cravings and withdrawal symptoms. Addiction. 2009;104:1251–7. doi:10.1111/j.1360-0443.2009.02605.x PubMed PMID: 19563567.

29. Esteban O, Markiewicz CJ, Blair RW, Moodie CA, Isik AI, Erramuzpe A, Kent JD, Goncalves M, DuPre E, Snyder M, Oya H, Ghosh SS, Wright J, Durnez J, Poldrack RA, Gorgolewski KJ. fMRIPrep: a robust preprocessing pipeline for functional MRI. Nature Methods. 2019;16:1. doi:10.1038/s41592-018-0235-4

30. Esteban O, Markiewicz CJ, Goncalves M, DuPre E, Kent JD, Salo T, Ciric R, Pinsard B, Blair RW, Poldrack RA, Gorgolewski KJ. fMRIPrep: a robust preprocessing pipeline for functional MRI [Internet]. Zenodo; 2020 [cited 2021 May 15]. Available from: https://zenodo.org/record/4252786 doi:10.5281/zenodo.4252786

31. Esteban O, Markiewicz CJ, Burns C, Goncalves M, Jarecka D, Ziegler E, Berleant S, Ellis DG, Pinsard B, Madison C, Waskom M, Notter MP, Clark D, Manhães-Savio A, Clark D, Jordan K, Dayan M, Halchenko YO, Loney F, Salo T, Dewey BE, Johnson H, Bougacha S, Keshavan A, Yvernault B, Hamalainen C, Christian H, Ćirić R, Dubois M, Joseph M, Cipollini B, Tilley II S, Visconti di Oleggio Castello M, Wong J, De La Vega A, Kaczmarzyk J, Huntenburg JM, Clark MG, Benderoff E, Erickson D, Kent JD, Hanke M, Giavasis S, Moloney B, Nichols BN, Tungaraza R, Frohlich C, Wassermann D, de Hollander G, Eshaghi A, Millman J, Mancini M, Nielson DM, Varoquaux G, Watanabe A, Mordom D, Guillon J, Koudoro S, Chetverikov A, Rokem A, Acland B, Forbes J, Markello R, Gillman A, Kong XZ, Geisler D, Salvatore J, Gramfort A, Doll A, Buchanan C, DuPre E, Liu S, Schaefer A, Kleesiek J, Sikka S, Schwartz Y, Lee JA, Mattfeld A, Richie-Halford A, Liem F, Perez-Guevara MF, Heinsfeld AS, Haselgrove C, Durnez J, Lampe L, Poldrack R, Glatard T, Tabas A, Cumba C, Pérez-García F, Blair R, Iqbal S, Welch D, Triplett W, Ghayoor A, Craddock RC, Correa C, Papadopoulos Orfanos D, Stadler J. nipy/nipype: 1.5.1 [Internet]. Zenodo; 2020 [cited 2021 May 15]. Available from: https://zenodo.org/record/4035081 doi:10.5281/zenodo.4035081

32. Gorgolewski K, Burns CD, Madison C, Clark D, Halchenko YO, Waskom ML, Ghosh SS. Nipype: A Flexible, Lightweight and Extensible Neuroimaging Data Processing Framework in Python. Front Neuroinform. 2011;5. doi:10.3389/fninf.2011.00013

33. Jenkinson M, Smith S. A global optimisation method for robust affine registration of brain images. Medical Image Analysis. 2001;5:143–56. doi:10.1016/S1361-8415(01)00036-6

34. Abraham A, Pedregosa F, Eickenberg M, Gervais P, Mueller A, Kossaifi J, Gramfort A, Thirion B, Varoquaux G. Machine learning for neuroimaging with scikit-learn. Front Neuroinform. 2014;8. doi:10.3389/fninf.2014.00014

35. Murphy K, Fox MD. Towards a consensus regarding global signal regression for resting state functional connectivity MRI. NeuroImage. 2017;Cleaning up the fMRI time series: Mitigating noise with advanced acquisition and correction strategies154:169–73. doi:10.1016/j.neuroimage.2016.11.052

36. Behzadi Y, Restom K, Liau J, Liu TT. A component based noise correction method (CompCor) for BOLD and perfusion based fMRI. NeuroImage. 2007;37:90–101. doi:10.1016/j.neuroimage.2007.04.042

37. Desikan RS, Ségonne F, Fischl B, Quinn BT, Dickerson BC, Blacker D, Buckner RL, Dale AM, Maguire RP, Hyman BT, Albert MS, Killiany RJ. An automated labeling system for subdividing the human cerebral cortex on MRI scans into gyral based regions of interest. NeuroImage. 2006;31:968–80. doi:10.1016/j.neuroimage.2006.01.021

38. Rubinov M, Sporns O. Complex network measures of brain connectivity: Uses and interpretations. NeuroImage. 2010;Computational Models of the Brain52:1059–69. doi:10.1016/j.neuroimage.2009.10.003

39. Ahmadi H, Fatemizadeh E, Nasrabadi AM. A Comparative Study of the Effect of Weighted or Binary Functional Brain Networks in fMRI Data Analysis. Frontiers in Biomedical Technologies. 2020;7:160–9. doi:10.18502/fbt.v7i3.4618

40. Hadley JA, Kraguljac NV, White DM, Ver Hoef L, Tabora J, Lahti AC. Change in brain network topology as a function of treatment response in schizophrenia: a longitudinal resting-state fMRI study using graph theory. npj Schizophr. 2016;2:1. doi:10.1038/npjschz.2016.14

41. Achard S, Bullmore E. Efficiency and cost of economical brain functional networks. PLoS Comput Biol. 2007;3:e17. doi:10.1371/journal.pcbi.0030017 PubMed PMID: 17274684; PubMed Central PMCID: PMC1794324.

42. Toppi J, De Vico Fallani F, Vecchiato G, Maglione AG, Cincotti F, Mattia D, Salinari S, Babiloni F, Astolfi L. How the Statistical Validation of Functional Connectivity Patterns Can Prevent Erroneous Definition of Small-World Properties of a Brain Connectivity Network. Computational and Mathematical Methods in Medicine. 2012;2012:e130985. doi:10.1155/2012/130985

43. Bassett DS, Bullmore ET. Small-World Brain Networks Revisited. Neuroscientist. 2017;23:499–516. doi:10.1177/1073858416667720

44. Onias H, Viol A, Palhano-Fontes F, Andrade KC, Sturzbecher M, Viswanathan G, de Araujo DB. Brain complex network analysis by means of resting state fMRI and graph analysis: Will it be helpful in clinical epilepsy? Epilepsy & Behavior. 2014;SI: NEWroscience 201338:71–80. doi:10.1016/j.yebeh.2013.11.019

45. Shannon CE. A mathematical theory of communication. The Bell System Technical Journal. 1948;27:379–423. doi:10.1002/j.1538-7305.1948.tb01338.x

46. Cocchi L, Gollo LL, Zalesky A, Breakspear M. Criticality in the brain: A synthesis of neurobiology, models and cognition. Progress in Neurobiology. 2017;158:132–52. doi:10.1016/j.pneurobio.2017.07.002

47. Poil SS, Hardstone R, Mansvelder HD, Linkenkaer-Hansen K. Critical-State Dynamics of Avalanches and Oscillations Jointly Emerge from Balanced Excitation/Inhibition in Neuronal Networks. J Neurosci. 2012;32:9817–23. doi:10.1523/JNEUROSCI.5990-11.2012 PubMed PMID: 22815496.

48. Fagerholm ED, Lorenz R, Scott G, Dinov M, Hellyer PJ, Mirzaei N, Leeson C, Carmichael DW, Sharp DJ, Shew WL, Leech R. Cascades and Cognitive State: Focused Attention Incurs Subcritical Dynamics. J Neurosci. 2015;35:4626–34. doi:10.1523/JNEUROSCI.3694-14.2015 PubMed PMID: 25788679.

CHAPTER 2: Neural and Molecular Changes During a Mind-Body Reconceptualization, Meditation, and Open Label Placebo Healing Intervention

Chapter 1 established a tight empirical claim. Four days of mindfulness training raised the Shannon entropy of cortical functional connectivity networks during innocuous stimulation, and within meditators this rise in entropy predicted the magnitude of subsequent pain relief. The result is consistent with the interpretation that meditation flattens the prediction-driven attractor landscape that ordinarily sustains a painful percept, allowing afferent input to be represented with less constraint from descending expectation. By tying a behavioral outcome, reduced pain, to a computational marker of prediction confidence, cortical entropy, Chapter 1 locates one of the most basic effects of mind-body practice within the predictive processing framework.

Two limitations of this first study motivate the next. The first is scope: a brief attentional intervention in healthy, pain-free volunteers cannot speak to the more sustained mind-body changes that practitioners describe and that more intensive interventions reportedly produce, nor to the joint operation of techniques that act on different levels of the predictive hierarchy. The second is the system in which the changes were measured. Chapter 1 reads the predictive hierarchy through cortical functional connectivity alone, but the brain's deepest priors are interoceptive; the precision-weighting machinery that gates new belief depends on neuromodulatory and metabolic state; and the body is both the regulated target and an active participant in the generative model. To test whether mind-body practice rearranges the predictive system in a way that is reflected at this broader brain-body level requires a more intensive intervention and a richer measurement palette. Chapter 2 takes up this task.

Abstract

Mind-body interventions offer promising avenues for improving physical and mental health, yet the comprehensive biological effects of increasingly popular mind-body retreat interventions remain poorly understood. The neural and molecular effects of a 7-day retreat intervention combining meditation, reconceptualization, and open-label placebo healing rituals are investigated in an observational study on 20 healthy human participants randomly selected from 561 retreat participants. BOLD fMRI functional connectivity during rest and meditation and whole plasma proteomics, metabolomics, exosome-specific miRNA transcriptomics, and neurite growth and real-time metabolism cellular assays are compared pre- and post-intervention. Meditation decreases functional integration in the default mode (p=0.00009) and salience networks (p=0.000003) and decreases whole-brain modularity (p=0.001). Compared to pre-intervention plasma, post plasma increases in vitro neurite outgrowth (p=0.01), enhances glycolytic metabolism (p=0.008), induces upregulation of BDNF (p=0.001), inflammatory (p=0.0001), anti-inflammatory (p=0.03), and endogenous opioid (p=0.03) pathways, and modulates tryptophan metabolism (pFDR=0.03) and neurotransmission-associated exosome miRNA transcripts. This intensive non-pharmacological mind-body intervention produces broad short-term neural and plasma-based molecular changes associated with enhanced neuroplasticity, metabolic reprogramming, and modulation of functional cell signaling pathways, highlighting the potential of mind-body techniques to modulate neural circuits and pathways important to health and well-being.

Introduction

Mind-body interventions–structured practices that harness the interaction between psychological processes and physiological systems–can significantly improve human physical and mental health, yet the neural and molecular effects of increasingly popular mind-body retreat interventions remain poorly understood. In a recent RCT, reconceptualizing pain as the product of plastic brain activity rather than of peripheral tissue injury reduced pain three times more than placebo and six times more than usual treatment[1]. Placebo effects, another mind-body intervention based on healing-centered rituals, symbols, and behaviors, affect every major organ system[2,3] and sometimes surpass routine surgical outcomes[4–6]. Interestingly, open-label placebos (administered without concealment such that the subject is aware of the placebo) conserve their effectiveness against many conditions[7–9], demonstrating that placebo responses do not require deception, expectations, or conditioning. Meditation, yet another intervention based on self-regulated attentional practices, can produce subjective mystical-type experiences[10], mental health improvements[11,12], and can alter neural[13–15], immune[16], autonomic[17,18] gene expression[19–21], proteomic[22–24], and metabolomic[25,26] activity.

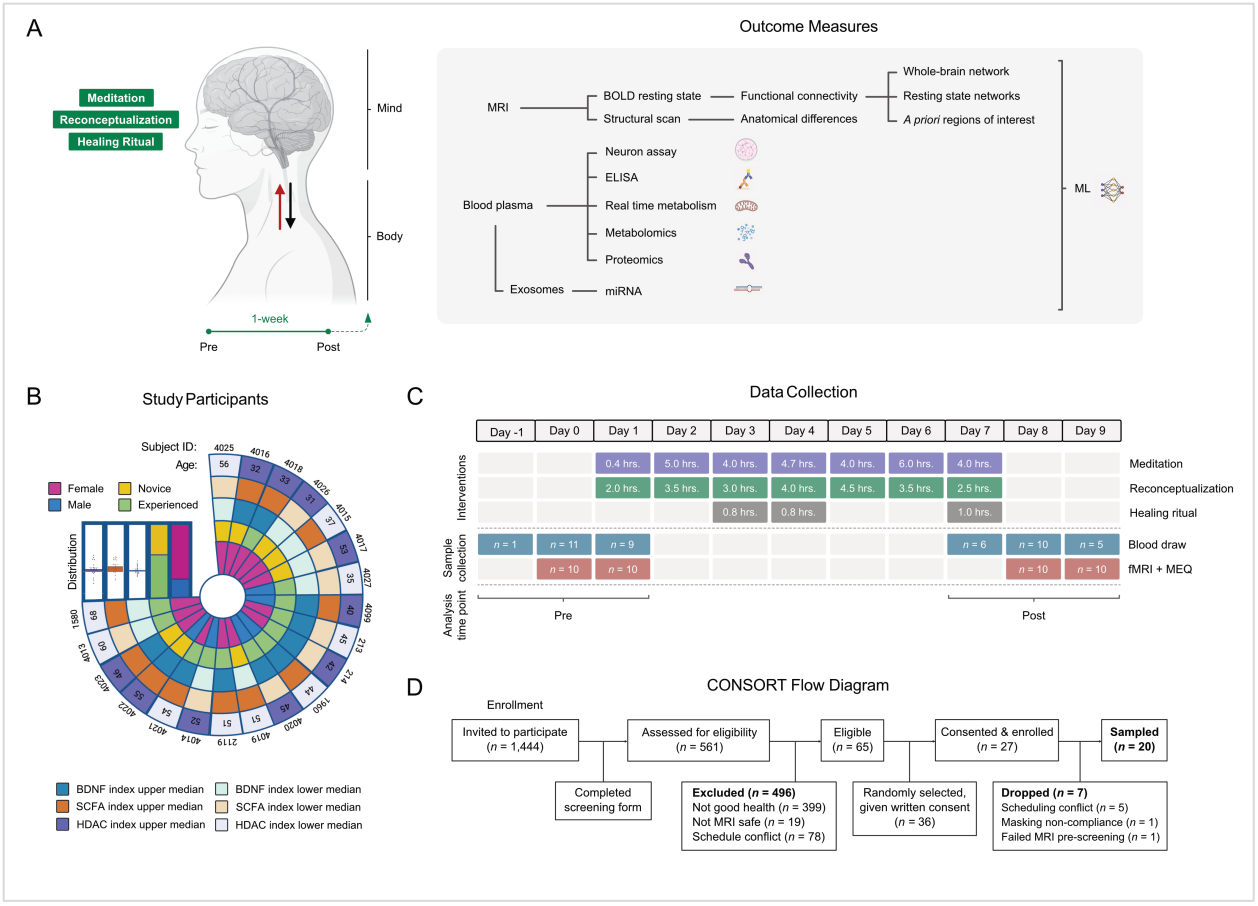


Figure 2.1: Study Design, Participants, Data Collection, and Recruitment. (A) Outcome measures to capture biological changes associated with brain and body. Created with BioRender. Simpson, S., Jinich, A. (2025). BioRender.com/ryzs1cd. (B) Participant characteristics, including age, subject, gender, meditation experience level, and top/bottom median scores for BDNF, short chain fatty acid (SCFA) metabolism, and HDAC proteomic pathways. (C) Intervention and data collection timeline. (fMRI = functional magnetic resonance imaging; MEQ = mystical experience questionnaire.) (D) CONSORT flow diagram.

Each of these interventions operates through partially distinct cognitive mechanisms, raising the possibility that they may complement one another to impact the brain and body synergistically. Reconceptualization operates through conscious, discursive, and volitional alteration of core beliefs, while meditation involves a willful yet non-discursive alteration of consciousness, and open-label placebo involves conscious awareness but operates unconsciously. While research on each technique exists, their combined neural and molecular effect has never

been studied. To do so, we conducted an exploratory observational study with functional magnetic resonance imaging (fMRI) and blood plasma-based high-throughput proteomics, metabolomics, exosome-specific miRNA transcriptomics; and neurite growth and real-time metabolism cellular assays (Figure 2.1A) on 20 healthy adult participants (14 females, age = 46.35 ± 10.06 (*SD*) years) (Figure 2.1B) sampled before and after a 7-day mind-body retreat (Figure 2.1C). While logistical limitations prevented us from including age and gender-matched controls to isolate and mechanistically describe the neural and physiological pathways engaged by each separate mind-body technique–an equally important but separate task–, our study provides evidence for the breadth and depth of physiological effects following a holistic, multifaceted experience commonly described by participants as personally transformational.

The 7-day retreat combined lectures, meditation, and healing rituals. Daily lectures (25 total hours) emphasized the body's self-healing abilities, the mind's capacity to shape lived reality, and the healing power of present-centeredness and mystical-type experiences. All meditations (33 total hours) were guided, delivered with atmospheric music, and taught Kundalini techniques, which combine conscious meta-awareness and conscious breathing exercises with slow, ascending, focused interoceptive attention on purported energetic centers along the midline (e.g., brow, throat, heart) which, according to practitioners, can reprocess embodied trauma and catalyze adaptive mental and physical changes[27,28]. Guidance also emphasized sustaining a heart-centered state devoid of thinking or judgment and focusing awareness on a void beyond one's normal sense of space and time – a common theme in some contemplative practices[29]. Guided healing rituals (5 total hours) brought 6-8 "healers" around one "healee" in which the former were instructed to practice loving-kindness compassion meditation while focusing attention on their heart, hands, and on the latter's body. A healing

mechanism was not presented, but the possibility that healing could occur on either party because of the ritual was mentioned, similarly to how open-label placebos are presented in trials[30]. All study subjects participated as healers. Of the 20 participants, 11 were "advanced" meditators who had practiced the techniques taught for at least six months, while 9 were "novices" who had not. No pharmacological substances, including any psychedelics, were involved in the retreat.

We characterized the resting and meditation states experienced by participants pre- and post-intervention. Consistent with previous meditation studies[31,32], we observed higher meditation-associated whole-brain functional integration and reduced intra-network connectivity in the default mode and salience networks. Comparing pre- to post-intervention whole plasma, we report evidence of enhanced neuroplasticity and glycolytic metabolism, as well as activation of endogenous opioid and neuromodulatory pathways.

Results

Functional Brain Activity

To characterize the neural signature of the meditative state, participants underwent structural and blood-oxygenation-level-dependent (BOLD) functional MRI scans during rest (5 minutes) and meditation (15 minutes). Mystical experience questionnaire (MEQ) scores reflective of the scanner meditation increased significantly following the intervention (n=20; pre = 2.37 ± 1.26 (*SD*); post = 3.02 ± 1.44) (Wilcoxon signed rank test $W = 35.0$, $p = 0.03$), indicating a deepening of the meditative state between sessions. One participant's data was

excluded from further analysis due to corrupt T1w data. Participants moved more during meditation than rest, a potential confound revealed by the significant effect of task (meditation, rest) on mean framewise displacement on a two-way (task X time) repeated measures ANOVA (n=19, $F_{(1,18)} = 25.1$, $p = 0.00009$, $\eta^2 p = 0.58$) (Supplementary Tables 2.1-2.2).

Meditation Versus Rest

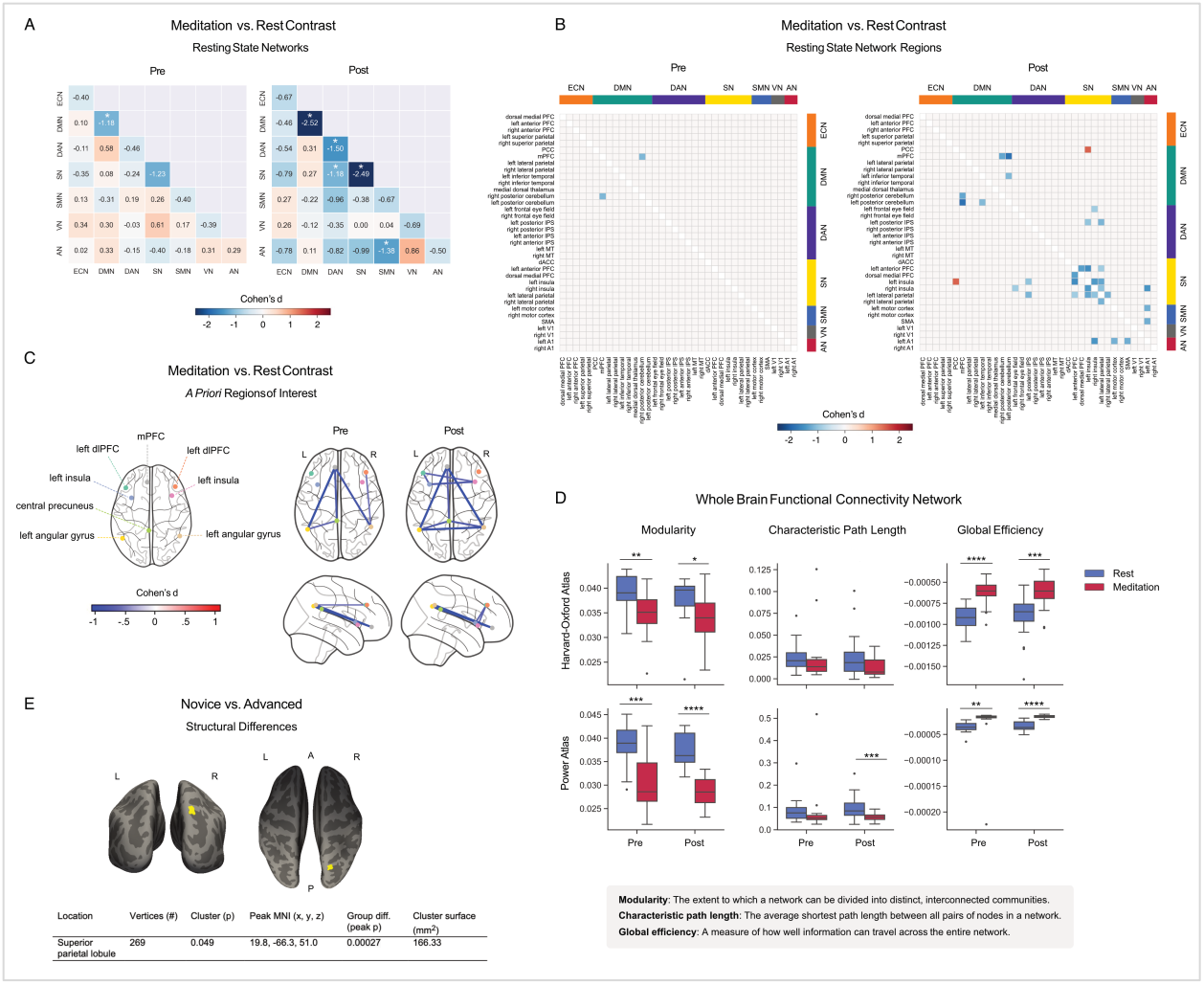


Figure 2.2: Functional Magnetic Resonance Imaging (fMRI) (n=19 participants). (A) Meditation vs. rest RSN functional connectivity pre- and post-intervention. Cell values and color scale represent Cohen's *d* effect size values from paired t-tests. Asterisks denote $p_{FWE} < 0.05$ significance (28 multiple comparisons). ECN (executive control network), DMN (default mode network), DAN (dorsal attention network), SN (salience network), SMN (somatomotor network), VN (visual network), and AN (auditory network). (B) Meditation vs. rest RSN-region functional connectivity pre- and post-intervention. Cell values and color scale represent Cohen's *d* effect size values from paired t-tests. Asterisks denote $p_{FWE} < 0.05$ (630 multiple comparisons). (C) Significant ($p < 0.05$) meditation-induced functional connectivity changes between *a priori* ROIs pre- and postintervention. Color scale represents Cohen's *d* effect sizes from paired t-tests. (D) Whole-cortex/brain network measures for 48-region Harvard-Oxford cortical atlas and Power (2011) 264-region brain atlas (*n*=19). Asterisks denote * ($p < 0.05$), ** ($p < 0.01$), *** ($p < 0.001$), **** ($p < 0.0001$). (E) Anatomical Structure. Coronal and axial views with superior parietal lobule cluster (yellow) where advanced practitioners had greater gray matter volume than novices at baseline.

We examined functional connectivity in seven resting state networks (RSNs) (Figure 2.2A-B), eight regions of interest (ROIs) (Figure 2.2C) (coordinates in Supplementary Tables 2.3-4), and two whole brain networks (Figure 2.2D), comparing meditation with rest (n=19, p_{FWE} = 0.0018 for 28 network pairs). All resting state networks had higher intra- than inter-network connectivity (Supplementary Figure 2.1A). Compared to rest, meditation reduced intra-network connectivity in the salience network pre- and post-intervention (pre: t = -4.32, p = 0.0004, Cohen's d = -0.87; post: t = -6.71, p = 0.000003, Cohen's d = -1.76), default mode network post-intervention (DMN) (t = -5.04, p = 0.00009, Cohen's d = -1.78), and dorsal attention network (DAN) post-intervention (t = -3.71, p = 0.002, Cohen's d = -1.06) (Figure 2.2A). Meditation also showed reduced inter-network connectivity post-intervention between the salience and dorsal attention networks (t = -4.09, p = 0.0007, Cohen's d = -1.18) and between the somatomotor and auditory networks (t = -5.30, p = 0.00005, Cohen's d = -1.38).

Table 2.1: Statistically significant (pFWE < 0.05) rest-vs-meditation differences on resting state network regions (n=19 participants).

Session	RSN Component Region Pair		RSN(s)	*t*	*p*	Cohen's *d*
pre	R post. Cerebellum	medial PFC	DMN	-4.44	0.0003	-1.15
post	R post. Cerebellum	medial PFC	DMN	-5.81	0.00002	-1.30
post	L post. Cerebellum	medial PFC	DMN	-6.30	0.000006	-1.87
post	L post. Cerebellum	L inferior temporal	DMN	-4.56	0.0002	-1.13
post	R anterior PFC	L anterior PFC	SN	-7.41	0.0000007	-1.38
post	L insula	L posterior IPS	SN	-4.32	0.0004	-1.01
post	L insula	L anterior PFC	SN	-5.30	0.00005	-1.57
post	R insula	L insula	SN	-5.58	0.00003	-1.44
post	L lateral parietal	L anterior PFC	SN	-4.62	0.0004	-0.88
post	L lateral parietal	L insula	SN	-7.30	0.0000009	-1.30
post	L lateral parietal	R insula	SN	-6.01	0.00001	-1.02
post	R lateral parietal	L lateral parietal	SN	-4.41	0.0003	-1.18
post	L insula	PCC	SN-DMN	4.50	0.0003	1.47
post	R insula	L frontal eye field	SN-DAN	-4.24	0.0005	-0.89
post	L lateral parietal	L posterior IPS	SN-DAN	-4.66	0.0002	-1.15
post	L A1	R insula	AN-SN	-4.68	0.0002	-1.47
post	L A1	L motor cortex	AN-SMN	-4.67	0.0002	-1.19
post	L A1	SMA	AN-SMN	-4.55	0.0002	-1.22

For individual network-component regions (Figure 2.2B; Table 2.1), both pre- and post-intervention, meditation reduced connectivity between the right posterior cerebellum and medial prefrontal cortex (pre: $t = -4.44$, $p = 0.0003$, Cohen's $d = -1.15$; post: $t = -5.81$, $p = 0.00002$, Cohen's $d = -1.30$) and bilateral connectivity between insular cortices, lateral parietal cortices, and anterior prefrontal cortices (all $p \leq 0.0003$; Table 2.1), network hubs associated with sensory, affective, and cognitive functions that shape the prediction-driven conscious state[33]. Interestingly, the only meditation-driven connectivity increase was post-intervention between the left insula and posterior cingulate cortex ($t = 4.50$, $p = 0.0003$, Cohen's $d = 1.47$), a finding previously reported during absorptive trance states[34]. ROIs also revealed lower functional

connectivity between key network hubs, including medial prefrontal cortex (mPFC), precuneus, bilateral insular cortices, and bilateral angular gyri (Supplementary Table 2.5), serving as an internal replication and returning results agreeable with the RSN data-driven approach.

To observe meditation-induced changes at the whole-brain/cortex level, we parcellated the brain into 48 cortical regions using the Harvard-Oxford atlas[35–37] and into 264 brain regions using the Power atlas[38] and calculated whole-brain/cortex network measures (Supplementary Table 2.6). For the cortical parcellation, a 2 (pre/post) by 2 (rest/meditation) repeated measures ANOVA (Supplementary Table 2.7) (n=19) revealed a significant effect of meditation on network modularity ($F_{(1,18)} = 15$, $p = 0.001$, $\eta^2 p = 0.45$) and global efficiency ($F_{(1,18)} = 48$, $p = 0.000002$, $\eta^2 p = 0.73$), and no significant effect on characteristic path length, with similarly significant whole-brain results. Post-hoc Wilcoxon signed rank tests confirmed that meditation decreased modularity (pre: $W = 18.0$, $p = 0.001$, Cohen's $d = -1.07$; post: $W = 45.0$, $p = 0.04$, Cohen's $d = -0.77$) and increased global efficiency (pre: $W = 3.0$, $p = 0.00002$, Cohen's $d = 2.04$; post: $W = 10.0$, $p = 0.0002$, Cohen's $d = 1.26$) as compared to rest (Figure 2.2D). These results were robust to excluding BOLD runs with mean framewise displacement > 0.3 mm, indicating they were not due to higher meditation-associated head motion.

Meditation thus reduced functional connectivity in the default mode and salience networks and induced a whole-brain functional state less segregated into distinct modules that allows for more efficient information flow.

Pre Versus Post

Pre- to post-intervention, functional connectivity during meditation decreased between executive control and salience networks (t = -2.61, p = 0.02, Cohen's d = -0.62) but did not survive correction for multiple comparisons (p_{FWE} = 0.0018) (Supplementary Figure 2.1B). For network component regions, connectivity during meditation decreased significantly pre-to-post between the left posterior intra-parietal sulcus and auditory cortex and between the left posterior intra-parietal sulcus and left lateral parietal cortex (Table 2.2). No significant changes were found between *a priori* ROIs (Supplementary Table 2.8).

Table 2.2: Significant (pFDR < 0.05) pre-to-post differences on RSN component regions (n=19 participants).

Task	RSN Component Region Pair		RSN(s)	t	p	Cohen's d
meditation	L posterior IPS	L A1	DAN-AN	-4.72	0.0002	-1.01
meditation	L posterior IPS	L lateral parietal	DAN-SN	-4.44	0.0003	-0.80

Neuroanatomical Differences

No significant anatomical changes were observed pre-to-post intervention, but advanced practitioners showed greater gray matter volume in the right superior parietal lobule at baseline (n=19, p = 0.049) (Figure 2.2E), a region linked to spatial awareness and body representation, which has been reported to have greater cortical thickness in experienced Zen meditators[39]. This difference warrants further investigation with larger samples and comparisons with age-matched non-meditator controls.

Whole Plasma

Having characterized the neural state induced by meditation, we turned our attention to the broader metabolic and molecular changes in whole plasma.

Enhanced Neuroplasticity

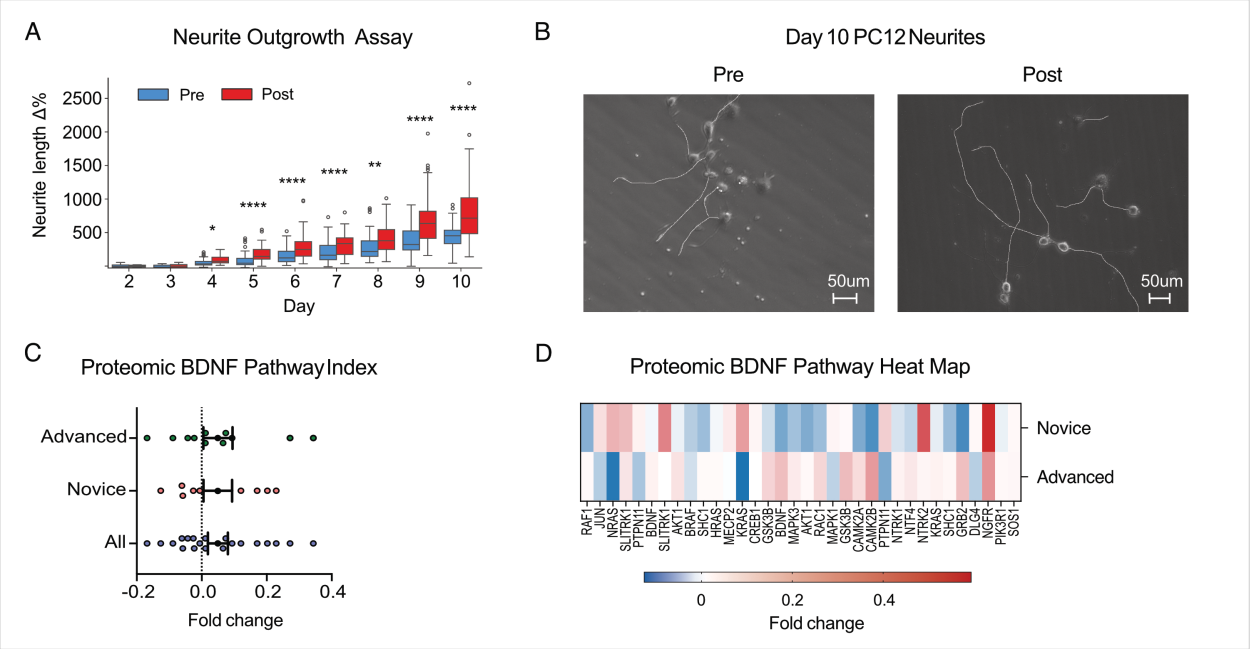


Figure 2.3: Neuronal Growth (n=20 participants). (A) PC12 neurite growth: Percent change in mean neurite length from baseline (day 2 post-NGF treatment). Asterisks denote * ($p < 0.05$), ** ($p < 0.01$), *** ($p < 0.001$), **** ($p < 0.0001$). (B) Phase contrast 20X microscopy images of PC12 cells on day 10 post-NGF treated with pre- and post-intervention plasma with longest neurite per cell body traced. (C) BDNF pathway index pre-to-post fold change. Error bars denote SEM. Fold change levels significantly above zero signal upregulated pathway or protein cluster. (D) BDNF Pathway Heat Map. Fold change per protein for advanced and novice participants.

Participants' anecdotal reports consistently emphasize radical psychological breakthroughs, and previous meditation studies have reported increased BDNF (brain-derived

neurotrophic factor) levels[22] consistent with enhanced neuroplasticity. To investigate whether the intervention affected circulating plasma factors conducive to neuroplasticity, we treated cultured dopaminergic PC12 neuroendocrine cells with NGF (nerve growth factor) and 1% pre- and post-intervention plasma and quantified neurite outgrowth length. Starting on day 4 post-NGF treatment, post-plasma-treated cells exhibited significantly longer neurites than pre-plasma-treated cells (t = -2.52, p = 0.01, Cohen's d = 0.59) and continued to do so until the end of the experiment (Figure 2.3A-B).

To investigate proteomic factors driving this effect, we quantitatively measured 7,596 protein targets using the high-throughput SomaScan assay and constructed a BDNF pathway 26-protein pre-to-post foldchange index (Figure 2.3C-D), which was significantly upregulated (1-sample t-test: t = 3.21, p = 0.001, Cohen's d = 0.12). While BDNF itself was not significantly affected, SLITRK1 (SLIT and NTRK-like family member 1), a protein that promotes excitatory synapse development and neurite outgrowth[40,41], increased significantly pre-to-post (W = 39.0, p = 0.01, CLES = 0.35). NGFR (nerve growth factor receptor), a TNF receptor that binds to NGF and BDNF and plays an essential role in neural cell differentiation and survival, also increased (W = 58.0, p = 0.08, CLES = 0.35).

Metabolic Reprogramming

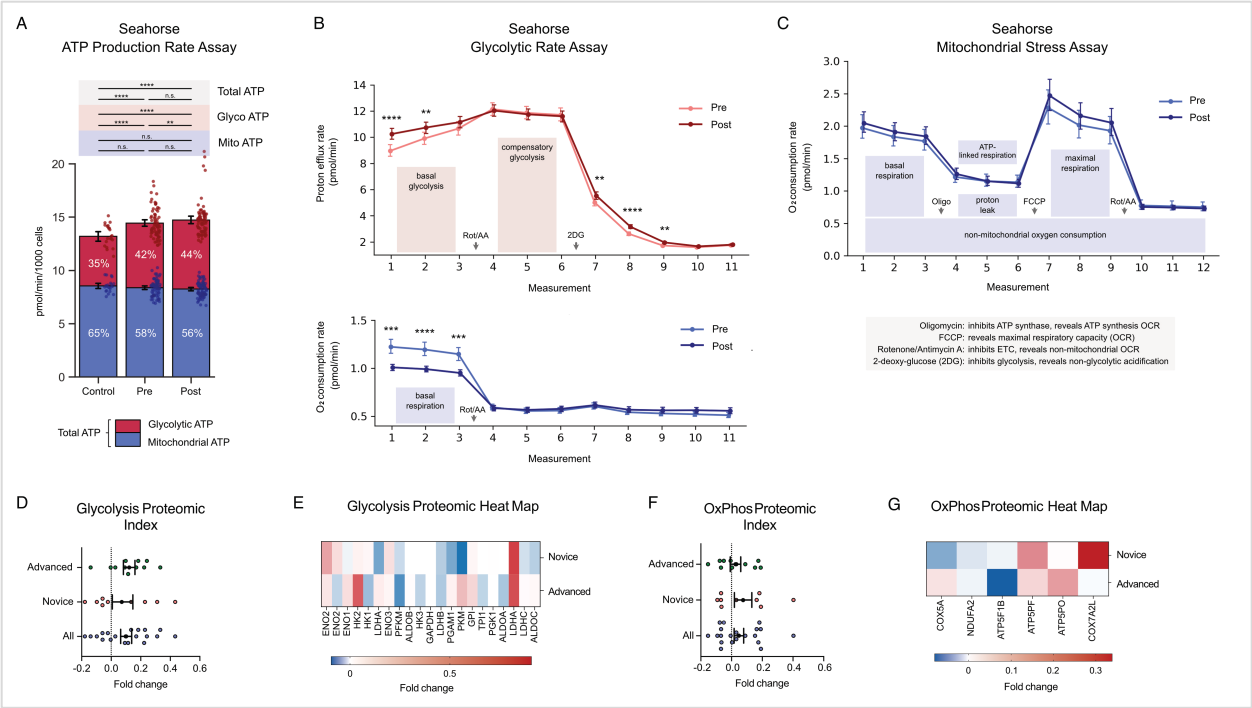


Figure 2.4: Metabolic Effects (n=20 participants). (A-C) Seahorse XF analyzer real time cellular metabolic assays with BE(2)M17 human neuroblastoma cells treated with 1% pre- and post-retreat plasma for 60-min or assay buffer (control). Mean ± 95% CI error bars. (A) ATP production rate assay with total ATP production rate (mean ± 95% CI) broken into glycolytic and mitochondrial ATP production rates. (B) Glycolytic rate assay, including basal and compensatory glycolytic rates (top) and basal mitochondrial respiration rate (bottom). Mean ± 95% CI error bars. (C) Mitochondrial respiration stress assay. Mean ± 95% CI error bars. Asterisks denote * ($p < 0.05$), ** ($p < 0.01$), *** ($p < 0.001$), **** ($p < 0.0001$). (D) Glycolysis pathway index pre-to-post fold change. Error bars denote SEM. Index fold change levels significantly above zero signal an upregulated pathway or protein cluster. (E) Glycolysis pathway heat map. Fold change level per component protein for advanced and novice participants. (F) Oxidative phosphorylation pathway index with pre-to-post fold change. (G) Heat map for advanced and novice participants. Error bars denote SEM.

Previous studies have characterized meditation as a hypometabolic state[42] and reported enhanced glycolysis in Tibetan Buddhist monks[24]. To test the intervention's effect on real-time metabolism, we treated BE(2)M17 human neuroblastoma cells with 1% plasma from all participants for 60 minutes and performed Seahorse XF assays. An ATP Rate assay (Figure 2.4A) revealed that changes in plasma produced during the intervention induced a compensatory shift from mitochondrial to glycolytic ATP production, with post-plasma-treated cells showing

significantly higher basal glycolytic rate than pre-plasma-treated cells (t = 2.95, p = 0.008, Cohen's d = 0.36) despite no significant differences in mitochondrial (t = -1.04, p = 0.31, Cohen's d = -0.28) or total ATP production rate (t = 1.46, p = 0.16, Cohen's d = 0.25). A glycolytic rate assay (Figure 2.4B) confirmed that, compared to pre-plasma, post-plasma increased basal glycolytic rate (t = 3.39, p = 0.003, Cohen's d = 0.63) and lowered basal respiration rate (t = -4.80, p = 0.0001, Cohen's d = -1.26). Mitochondrial stress parameters (Figure 2.4C) did not significantly differ between cells exposed to pre- and post-plasma, while, compared to cells exposed to growth medium only, plasma-exposed cells displayed significantly higher ATP production and glycolytic rates.

As before, to see if the plasma proteome reflected these changes, we pre-selected 19 proteins involved in glycolysis and oxidative phosphorylation and calculated pre-to-post foldchanges and an index average (Figure 2.4D-G). The glycolysis index increased significantly pre-to-post (t = 3.37, p = 0.0008, Cohen's d = 0.23), with 12 upregulated targets led by ENO2 (enolase 2, a neuron-specific converter of 2-phosphoglycerate into phosphoenolpyruvate) (W = 48.0, p = 0.03, CLES = 0.33) and LDHA (lactate dehydrogenase A, converter of pyruvate into lactate in anaerobic glycolysis (W = 38.0, p = 0.01, CLES = 0.22). Oxidative phosphorylation associated proteins trended upwards (t = 1.38, p = 0.17, Cohen's d = 0.13) but did not reach statistical significance.

Functional Cellular Signaling

Having investigated specific pathways of interest, we performed an exploratory, hypothesis-free analysis of proteomic and metabolomic results.

Proteomics

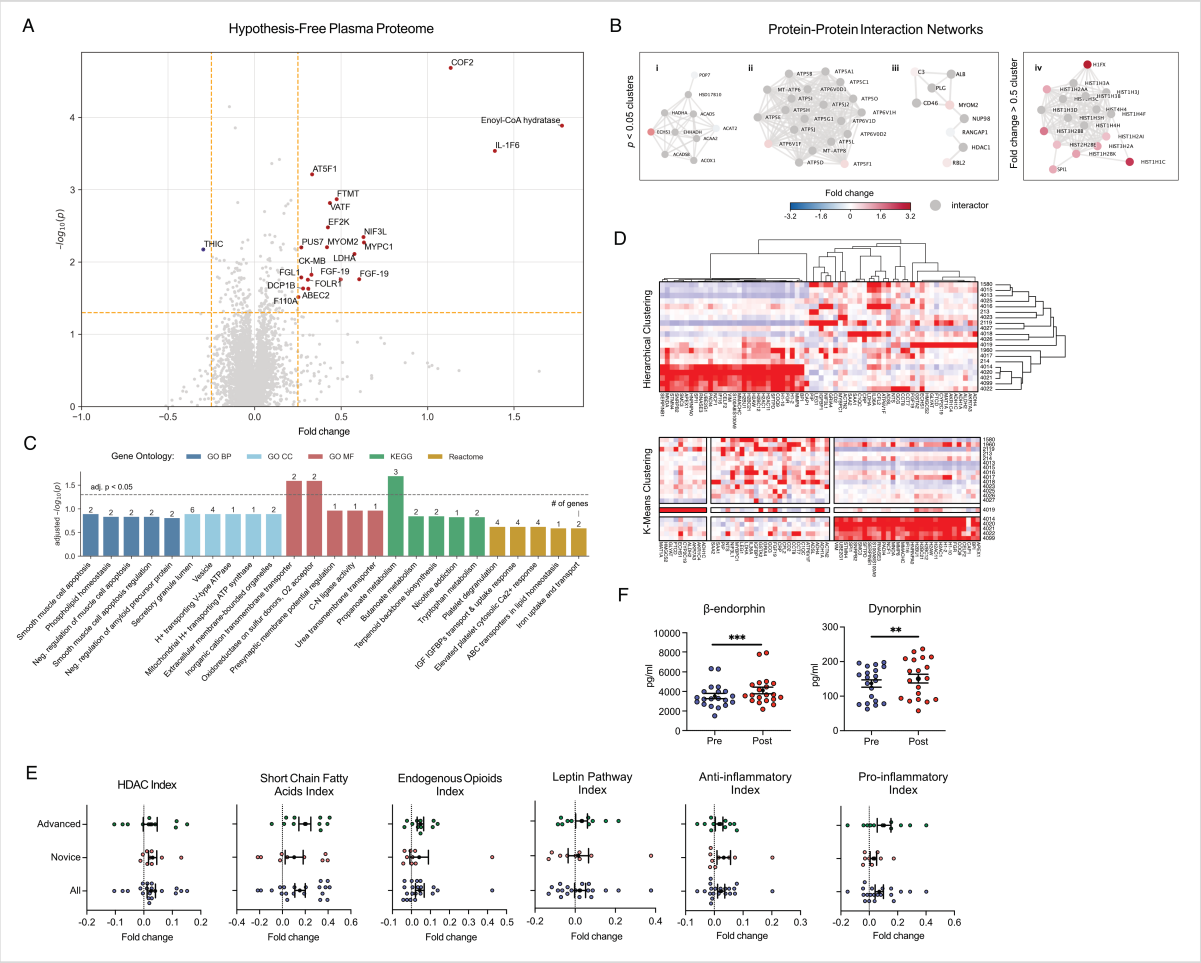


Figure 2.5: Plasma Proteome (n=20 participants). (A) Plasma Proteome. Volcano plot of pre/post fold changes (x-axis) and paired t-test –log(*p*-values) (y-axis) for 7,596 proteins. Vertical yellow dashed lines mark a linear fold change of 0.25 in either direction; horizontal yellow dashed line marks $p = 0.05$ cutoff. Proteins in top right/left quadrants are significantly up/down-regulated. (B) Protein-Protein Interactions. Heat-diffused network clusters with ≤ 20 interactors for proteins with pre/post (i-iii) $p < 0.05$ and (iv) |foldchange| > 0.5. Top gene enrichment terms for each cluster are: (i) fatty acid metabolism, (ii) proton-transporting two-sector ATPase complex, (iii) complement system, and (iv) nucleosome organization. (C) Gene Enrichment. Enrichment analysis (Enrichr) with pre/post significantly altered proteins ($p < 0.01$) and assay targets as background. (D) Proteome Cluster Analysis. Hierarchical and K-means clustering of |fold changes| > 0.5 proteins. Dendrogram branch lengths indicate degree of similarity between expression profiles. Nodes represent protein targets; colors indicate fold change. (E) Proteomic A Priori Gene Indices. Mean pre/post fold change for protein clusters or pathways. Index proteins in Supplementary Table 2.15. Mean ± SEM error bars. (F) ELISA Assay Biomarkers. Mean ± 95% CI error bars. Asterisks denote * ($p < 0.05$), ** ($p < 0.01$), *** ($p < 0.001$).

Volcano plot analysis (Figure 2.5A) revealed 21 significantly altered proteins. Cofilin-2 (COF2) and Enoyl-CoA hydratase were significantly upregulated, which suggests enhanced cellular processes related to cytoskeletal regulation and fatty acid metabolism. IL1-F6 (interleukin-36 alpha), MYPC1 (myosin binding protein C1), LDHA, and FGF-19 (fibroblast growth factor 19) exhibited moderate upregulation.

Protein-protein interaction networks (Figure 2.5B) revealed three significantly altered protein clusters related to mitochondrial energy production (ATP5F1, ATP6V1F); fatty acid metabolism (ECHS1, POP7 and ACAT2); nucleosome organization (HDAC1, RANGAP1, RBL2, C3, and MYOM2).

Pathway enrichment analysis (Figure 2.5C) showed upregulated proteins associated with muscle cell apoptosis, amyloid precursor protein catabolism, and mitochondrial proton transport pathways ($p_{\text{adjusted}} < 0.05$), suggesting alterations in metabolic pathways and muscle-related cellular processes. Interestingly, pathways related to butanoate, propanoate metabolism, and tryptophan biosynthesis were enriched, suggesting shifts in key metabolic routes. (See Supplementary Figures 2.3-2.4 for g:Profiler enrichment and pathway heatmaps.)

We also created proteomic indices to examine inflammation, epigenetic regulation, and short-chain fatty acid (SCFA) metabolism pathways, comparing across timepoint (pre/post) and experience level (novice/advanced) (Figure 2.5E) (Supplementary Figure 2.5). The epigenetic (HDAC) index demonstrated elevated sirtuins and HDAC expression in the advanced group, reflecting increased epigenetic regulation and possible stress resilience. In contrast, the novice group showed differences in mitochondrial function and chromatin remodeling. SCFA index showed increased expression of acyl-CoA dehydrogenase short chain (ACADS) and fatty acid

synthase (FASN) in the advanced group, suggesting a shift toward enhanced fatty acid oxidation and improved metabolic efficiency.

Inflammation, Anti-Inflammation, and Cellular Turnover

To assess whether the intervention elicited inflammatory or anti-inflammatory cascades, we examined a panel of 23 inflammatory and 21 anti-inflammatory proteins (Figure 2.5E). We found significant upregulation of inflammatory markers ($t = 3.81$, $p = 0.0001$, Cohen's $d = 0.15$), driven by increases in S100A8 (calgranulin A) ($W = 30.0$, $p = 0.004$, CLES = 0.33) and CCL2 (C-C motif chemokine 2) ($W = 47.0$, $p = 0.03$, CLES = 0.33) and trending increases in IL-6, S100A9 (S100 calcium-binding protein A9; calgranulin B), and PTGS2 (prostaglandin G/COX-2). These findings align with the role of S100A8 and S100A9 as alarmins – endogenous molecules released in response to cellular damage or stress known to induce secretion of inflammatory mediators IL-6, IL-8, and CCL2[43,44].

Interestingly, we also observed a significantly upregulated anti-inflammatory markers index ($t = 2.25$, $p = 0.03$, Cohen's $d = 0.09$), with positively trending levels of TGF-b1 (transforming growth factor beta-1), NFKBIA (NF-kappa-B inhibitor), STAT6 (signal transducer and activator of transcription 6), CEBPB (CCAAT/enhancer-binding protein beta**)**, IL1, SOCS3 (suppressor of cytokine signaling 3), and TNFAIP3 (TNF alpha-induced protein 3). Concurrent activation of both pathways suggests a dynamic process of immune modulation, possibly reflecting enhanced cellular turnover or repair mechanisms. We also measured plasma nanoparticles and found no significant change in total nanoparticle concentration ($t = -0.17$, $p = 0.87$, Cohen's $d = -0.03$), but did find a significant decrease in the percentage of particles in the

exosome range (20-120nm diameter) (t = -2.09, p = 0.04, Cohen's d = -0.65) (Supplementary Figures 2.2A-B) consistent with both higher cellular turnover and metabolic suppression.

Endogenous Opioids

Placebo effects are known to engage endogenous opioid and endocrine systems. We assessed levels of 15 proteomic targets within the endogenous opioid pathway and found the pathway index to be significantly upregulated (t = 2.14, p = 0.03, Cohen's d = 0.12), driven by positively trending increases in opioid peptide precursor PENK (proenkephalin-A), opioid peptide PDYN (dynorphin A), GABR2:CD (GABBA B receptor subunit 2: cytoplasmic domain), and CAMK2B (calcium/calmodulin-dependent protein kinase type II), which is known to increase after opioid administration (Figure 2.5E). ELISA assays to confirm these findings (Supplementary Table 2.11) revealed significant increases of beta-endorphin (W = 14.0, p = 0.0002, Cohen's d = 0.42) and dynorphin (W = 37.0, p = 0.009, Cohen's d = 0.27).

Metabolomics

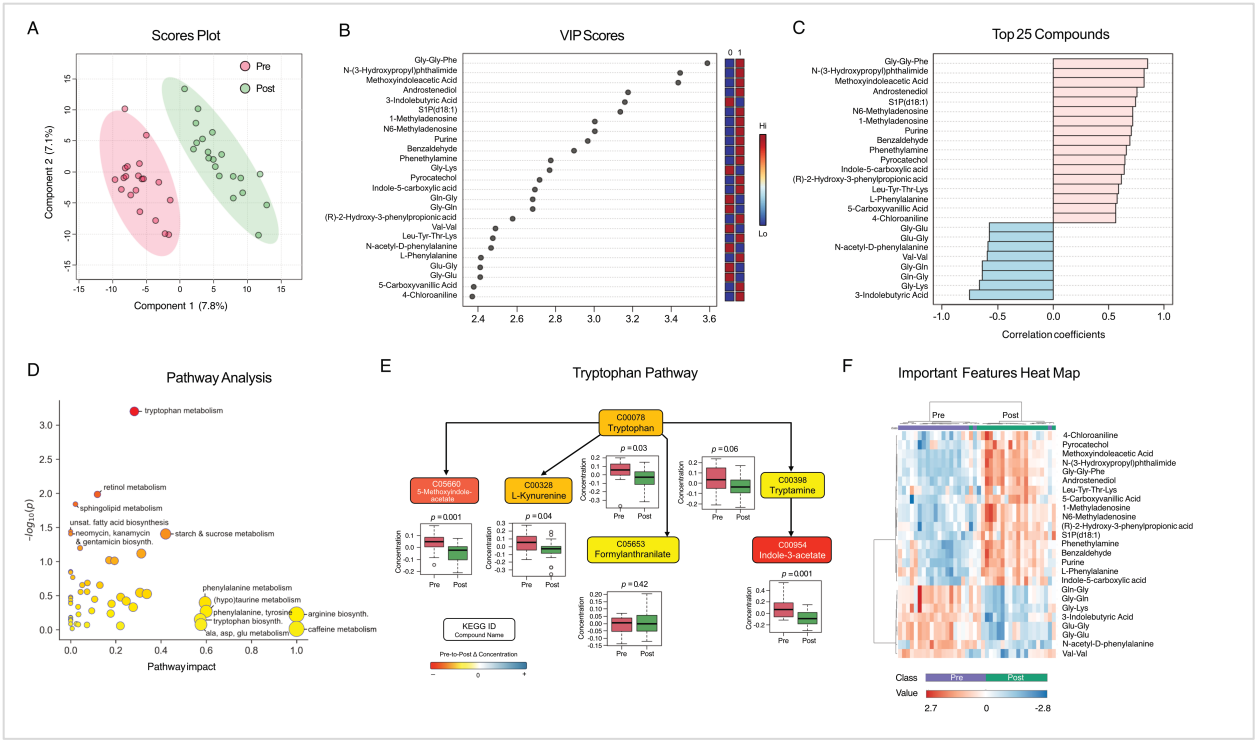


Figure 2.6: Metabolomics (n=20 participants). (A) PLS-DA Scores Plot. Scatter plot shows 2 principal components with greatest variation. Ovals show 95% confidence intervals. Similar observations cluster together. Component 1 (x-axis) contains 7.8% of total variation; component 2 contains 7.1%. Oval cluster spatial separation indicates systematic differences between timepoints. (B) PLS-DA Variable Importance in Projection (VIP) Scores. VIP scores indicate metabolite's contribution to timepoint separation, ranked in descending order. Top metabolites are involved in neurotransmitter regulation, lipid signaling, and RNA modification, suggesting the intervention induced broad metabolic and molecular adaptations. (C) Top PLS-DA Compounds. Correlation coefficients between metabolites and PLS-DA discriminant function. Each metabolite's correlation coefficient indicates strength and direction of association with timepoint separation (positive = direct, negative = inverse, closer to ± 1 = more influential in driving group separation). Top metabolites highlight changes in neurotransmitter precursors, lipid signaling, and amino acid metabolism. (D) Pathway Analysis. Metabolite pathways' impact scores (x-axis) and *p*-values (y-axis, -log$_{10}$ transformed). Larger impact values indicate greater contribution to the pathway. Bubble size reflects the pathway's enrichment score, and bubble color corresponds to significance level (darker indicating lower *p*-value). (E) Tryptophan Pathway. Colored boxes represent detected metabolites. Color scale represents magnitude of pre-to-post change. Box plots show pre and post concentration distributions and paired t-test values with raw p-values. (F) Important Features Heat Map showing top differentially expressed metabolites, including several phenylalanine-related metabolites involved in neurotransmitter synthesis and metabolic regulation. Color scale indicates relative abundance (red = higher; blue = lower). Clustering highlights metabolic pathway shifts, including phenylalanine metabolism and lipid signaling.

We performed liquid chromatography-mass spectrometry-based metabolomic analysis on plasma. Partial least squares discriminant analysis (PLS-DA) (Figure 2.6A) revealed distinct metabolic profiles between time points, with key metabolites involved in synaptic plasticity, metabolism, RNA modulation, neurotransmitter availability, and inflammation and over 25 metabolites with VIP (variable importance in projection) scores > 2 (Figure 2.6B-C).

MetaboAnalyst pathway enrichment detected 53 impacted pathways (Figure 2.6D; Supplementary Table 2.16). Six showed significant pre-to-post changes ($p < 0.05$), led by tryptophan metabolism ($p_{FDR} = 0.03$) (Figure 2.6E; Supplementary Figure 2.6), with decreases in upstream and downstream metabolites, including L-tryptophan ($p = 0.03$), tryptamine ($p = 0.04$), L-kynurenine ($p = 0.04$), indole-3-acetate ($p = 0.001$), and 5-methoxyindoleacetate ($p = 0.001$). The steroid hormone biosynthesis pathway showed lower androstenediol ($p = 0.04$), testosterone ($p = 0.19$), cortisol ($p = 0.06$), cortisone ($p = 0.07$), 21-deoxycortisol ($p = 0.77$), corticosterone ($p = 0.07$), and 11-dehydrocorticosterone ($p = 0.02$). Lower cortisol levels reported in previous meditation studies, were interpreted as signs of improved stress response regulation[45].

Among top-ranking metabolites, three were related to phenylalanine metabolism, including CAN-2-Hydroxy-3-phenylpropionic acid, N-acetyl-D-phenylalanine, and phenethylamine, which can act as neurotransmitter storage, contribute to stress adaptation, and enhance dopamine, norepinephrine, and serotonin release. Two RNA-related metabolites, 1-methyladenosine and N6-methyladenosine, were linked to inflammatory responses, with roles in RNA metabolism, methylation, and cellular signaling. 3-indolebutyric acid, associated with tryptophan metabolism, may influence neurotransmitter synthesis and synaptic plasticity. Several dipeptides were identified as enhancers of gut microbial activity, promoting SCFA production, which is crucial for regulating inflammation and immune function. S1P (d18:1), a signaling lipid,

may reflect gut barrier integrity and inflammatory pathway alterations. Figure 2.6F shows a distinct clustering of metabolites by relative abundance, highlighting these key contributors.

Exosome-Specific Transcriptomics

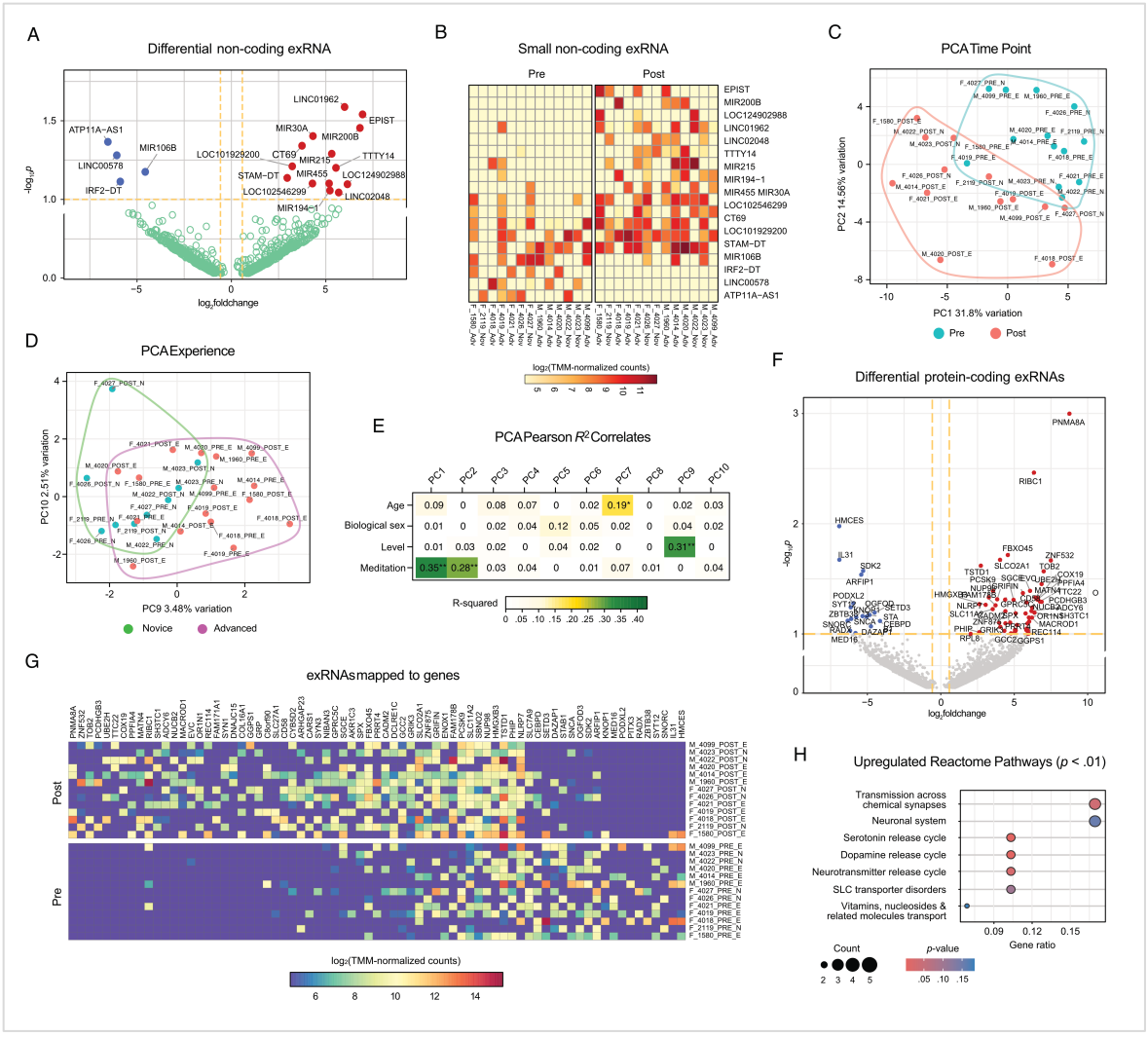


Figure 2.7: Exosome Transcriptomics (n=16 participants). (A) Differential non-coding exRNAs (miRNAs, ncRNAs) on volcano plot of -$\log_{10}p$ versus $\log_2$FC (pre/post difference). Blue/red dots denote exRNAs prevalent in pre/post-intervention exosomes, respectively; green dots denote exRNAs without significant difference. Dashed orange lines indicate $p < 0.1$ and $\log_2\text{FC} > \pm 0.58$ thresholds. Full list of exRNAs on Supplementary Table 2.17. (B) Differential expression ($\log_2$-transformed TMM-normalized counts) of 18 non-coding exRNAs. Colors indicate counts. Sample name: (M, male; F, female)_participantID_(pre; post)_(E, advanced; N, novice). (C-D) Principal component analysis of top normalized exRNA counts. Encircled are clusters corresponding to (C) pre/post, and (D) novice/advanced. (E) Eigenvector plot showing the correlation of PCs to variables' metadata and test significances (** $p < 0.01$; * $p < 0.05$). Values correspond to Pearson R^2 values. (F) Differential protein-coding exRNAs (excluding ncRNAs) on volcano scatter plot of -$\log_{10}p$ versus $\log_2$FC (post–pre). Blue/red dots denote exRNAs prevalent in pre/post exosomes, respectively; green dots denote exRNAs without significant difference. Dashed orange lines indicate $p < 0.1$, $\log_2\text{FC} > \pm 0.58$ thresholds. (G) TMM-normalized counts of $\log_2$-transformed protein-coding exRNAs with highest variance across samples. Color scale indicates counts. (H) Reactome pathway analysis of enriched protein-coding exRNAs. Color indicates p-value; circle size indicates exRNA count per pathway.

We analyzed differentially expressed exosome-specific extracellular microRNAs, non-coding RNAs, and RNAs mapping to protein-coding mRNAs. Data from 6 participants was excluded at preprocessing (n=16). At least 18 non-coding exRNAs ($p < 0.1$, $\log_2FC > \pm 0.58$) exhibited distinct expression profiles on pre and post timepoints (Figure 2.7A-B). Principal components (PC) explain 46.3% of the total timepoint variation (Figure 2.7C), indicating significant shifts in non-coding exRNA expression during the intervention. At least 5.99% of the variance was attributed to experience levels, with partial separation between novice and advanced meditators (Figure 2.7D). Correlations between principal components and key variables such as timepoint and experience reveal that PC1 and PC2 strongly correlate with timepoint (R^2 = 0.35 and 0.28, respectively), while PC9 moderately correlates with experience (R^2 = 0.31), indicating that both influence exRNA expression (Figure 2.7E).

We also identified exRNAs mapped to at least 66 annotated protein-coding mRNAs upregulated or downregulated post-intervention (Figure 2.7F-G). Some of the upregulated exRNAs could be mapped to ras/rab interactor 1 (*RIBC1*), synapsin 3 (*SYN3*), and glutamate ionotropic receptor kainite type subunit 3 (*GRIK3*), genes linked to synaptic function and neurotransmission. The enrichment of exRNAs specific to solute carrier family 27 member 1 (*SLC27A1*) and proprotein convertase subtilisin/kexin type 9 (*PCSK9*) could enhance neural signaling and metabolic regulation. Downstream functional analysis of exRNAs in pre-vs-post exosome fractions against the Reactome database[46] (Figure 2.7H) predicted pathways related to neurotransmission (Serotonin/Dopamine Neurotransmitter Release Cycle), further highlighting the enhancement of synaptic activity post-intervention. Metabolic pathways, including Transport of Vitamins and Nucleosides, could reflect broader metabolic changes.

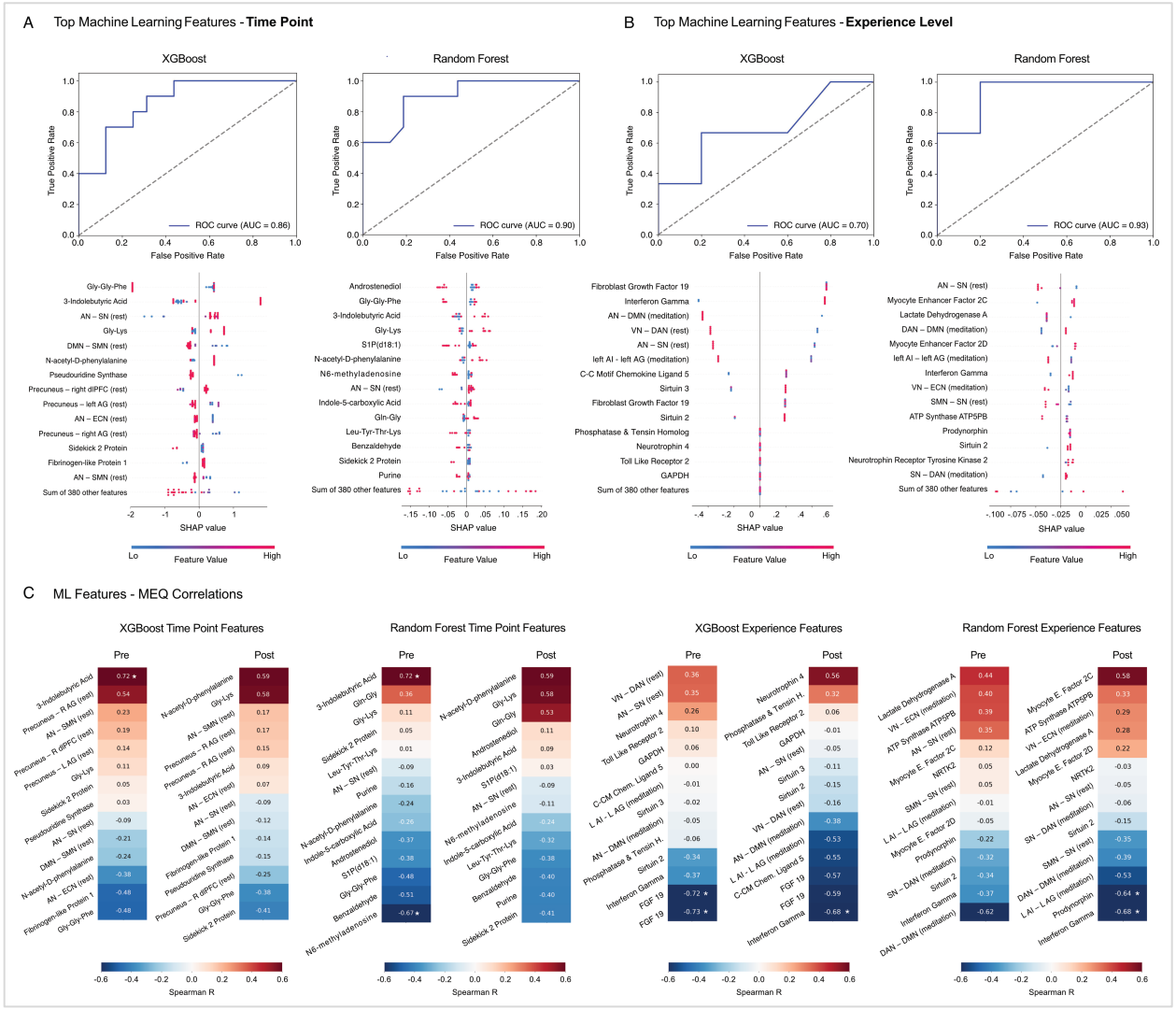


Figure 2.8: Machine Learning and MEQ – Features Correlations (n=20 participants). (A) ROC curves and SHAP plots for XGBoost and Random Forest models predicting pre/post classification: AUC = 0.86 (XGBoost) and 0.90 (Random Forest) indicate good classification performance. SHAP plots display the top contributing features ranked by impact on model output. (B) ROC curves and SHAP plots for XGBoost and Random Forest models predicting novice/advanced classification: AUC = 0.70 (XGBoost) and 0.93 (Random Forest). Abbreviations: R (right), L (left), AN (auditory network), SN (salience network), DMN (default mode network), SMN (somatomotor network), ECN (executive control network), VN (visual network), DAN (dorsal attention network), dlPFC (dorsolateral prefrontal cortex), AI (anterior insula), AG (angular gyrus), GAPDH (glyceraldehyde-3-phosphate dehydrogenase), ATP5PB (ATP synthase peripheral stalk membrane subunit B), FGF (fibroblast growth factor), NTRK2 (neurotrophin receptor tyrosine kinase 2). (C) Heatmaps of Spearman R correlations between Mystical Experience Questionnaire (MEQ) scores and the top machine learning features per model and time point, with * denoting FDR-adjusted statistical significance ($p_{FDR} < 0.05$).

To identify features differentiating timepoints and experience levels across metabolomic, proteomic, fMRI, and RNA outcomes, we evaluated the data using Random Forest and XGBoost models. After normalization and dimensionality reduction, performance was assessed with 10-fold cross-validation using F1 score, precision, recall, and area under the receiver operating characteristic (AUROC). Both models demonstrated robust classification across conditions, with AUC values ranging from 0.70–0.93. SHAP analyses revealed key contributors spanning metabolites, fMRI connectivity features, proteins, and non-coding RNAs (Figure 2.8A–B).

Focusing first on timepoint classification, both models achieved strong discrimination between pre- and post-meditation states (XGBoost AUC = 0.86; Random Forest AUC = 0.90). Top XGBoost predictors included Gly-Gly-Phe, 3-indolebutyric acid, Gly-Lys, and connectivity between the anterior and salience networks, default mode–salience, and precuneus regions. Random Forest highlighted overlapping features alongside additional metabolites such as Androstenediol, S1P(d18:1), N6-methyladenosine, and purine derivatives. Many of these metabolites are linked to amino acid metabolism, neurotransmitter balance, and cellular stress signaling, while sphingolipids such as Androstenediol and S1P(d18:1) implicate lipid signaling and neuroendocrine function. Connectivity differences involving salience, executive and default mode networks (SN, ECN, DMN,PC) align with prior literature that mediation can reorganize large-scale brain networks that govern salience[47], attention[48], interoception[49], and self-referential processing[47]. Taken in concert, timepoint differences identify shifts that integrate across neurofunctional and metabolic layers, reinforcing the concept that mediation acts as a systemic regulator of mind-body physiology.

To evaluate the influence of meditation experience, post–pre deltas were compared between novice and advanced practitioners. XGBoost achieved modest classification

performance (AUC = 0.70), while Random Forest reached higher discrimination (AUC = 0.93). SHAP analysis indicated that immune- and stress-related proteins, including fibroblast growth factor 19, interferon-γ, C-C motif chemokine ligand 5, and Toll-like receptor 2, were major contributors in XGBoost, whereas Random Forest emphasized metabolic and mitochondrial features such as myocyte enhancer factors, lactate dehydrogenase A, ATP synthase ATP5PB, and Sirtuin 2. Across both models, large-scale connectivity differences involving salience, executive, and default mode networks (e.g., AN–SN, VN–DMN, SN–DAN) emerged as consistent drivers of classification. These findings indicate that long-term meditation experience is associated with distinct molecular and network-level adaptations that support resilience and energy regulation.

Finally, to explore links between biological features and subjective outcomes, we correlated model-identified predictors with Mystical Experience Questionnaire (MEQ) scores. Several metabolites and connectivity measures showed nominal associations ($p < 0.05$), with a subset surviving FDR correction (asterisks, Figure 2.8C). In the timepoint analysis, baseline 3-indolebutyric acid correlated positively with MEQ ($r = 0.72$, $q < 0.05$), whereas N6-methyladenosine correlated negatively ($r = –0.67$, $q < 0.05$). At the experience level, immune markers including FGF19 and interferon-γ were negatively associated with MEQ deltas ($r = –0.59$ to $–0.73$, $q < 0.05$), and reductions in network connectivity (DAN–DMN, LAI–LAG) were inversely correlated with MEQ outcomes in experienced meditators ($r = –0.64$ to $–0.68$, $q < 0.05$). Together, these exploratory findings suggest that both peripheral metabolic and immune markers and central network dynamics are tied to reported mystical experience levels during meditation.

Discussion

Our study shows how an intensive non-pharmacological mind-body intervention produced broad short-term neural and plasma-based molecular changes associated with enhanced neuroplasticity, metabolic reprogramming, and modulation of functional cell signaling pathways.

fMRI data showed that this meditation style functionally disrupts the default mode and salience networks (responsible for self-referential thought and allostatic regulation[32,50] and cerebellum-prefrontal predictive processing circuits involved in integrating internal models with external sensory data[51]. This complements studies showing meditation-induced changes in DMN connectivity[32,52]. Mindfulness meditation has been linked to DMN deactivation[32,53] and stronger connectivity between DMN-Salience and DMN-Executive Control networks[47], likely reflecting an increased capacity to switch in/out of default mode dominance. Here, the main effect we observed was a meditation-driven decrease in intra-network DMN connectivity and a broad desynchronization of whole-brain connectivity. Meditation also reduced prefrontal-cerebellar connectivity both pre- and post-intervention, suggesting a state-dependent suppression of self-referential and evaluative processing consistent with focused interoceptive awareness, non-judgmental awareness, and a state that transcends the self – all features of the guided meditations. DMN-cerebellar connectivity alterations have been reported for depressive disorder and during previous meditation studies, albeit with opposite (higher connectivity) effects[54,55]. Our machine learning analyses further reinforced these findings by demonstrating that meditation-related shifts in fMRI connectivity were embedded within broader molecular changes across metabolomic, proteomic, and transcriptomic layers. The convergence of neural and peripheral predictors, including amino acid metabolites, lipid signaling molecules, immune

regulators, and network-level connectivity, underscores that meditation engages a systemic mind-body axis rather than isolated pathways.

We can interpret these findings with a Bayesian brain framework, which posits that the brain probabilistically predicts incoming sensory information based on prior beliefs to allostatically regulate the body's energy needs, with experience and behavior largely shaped by the system's priors and predictive architecture[56]. Predictive brain regions project efferent copies to the subcortical nuclei that regulate metabolic, endocrine, immune, and other physiological setpoints[33,57] based on current and predicted energy needs. Thus, physiological and psychological health can be targeted by shifting the priors and functioning of the predictive system.

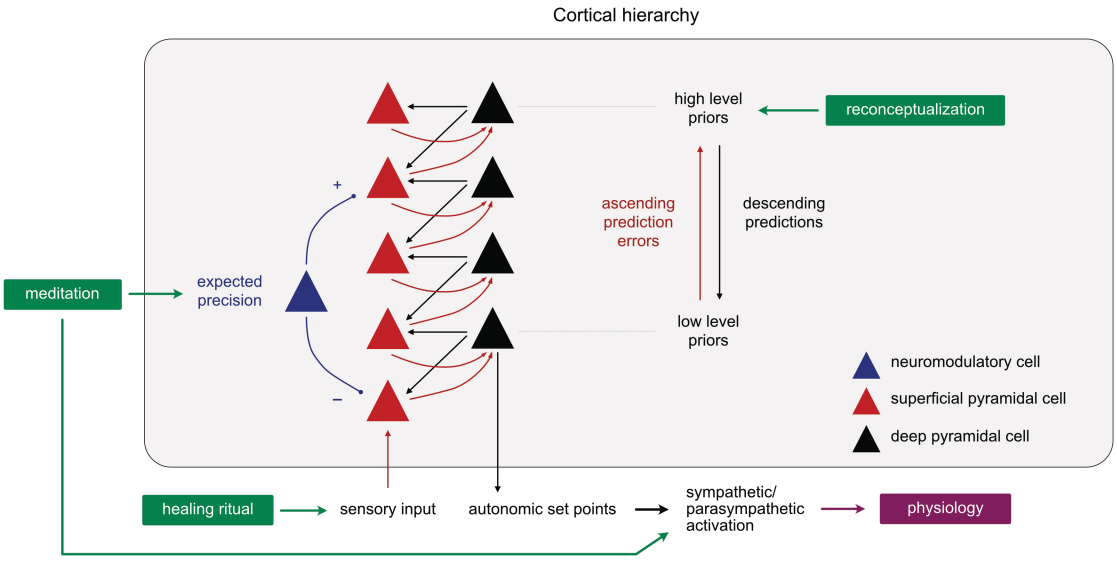


Figure 2.9: Potential Cortical Implementation. Hierarchical predictive coding scheme showing how the three mind-body techniques may synergistically facilitate a more flexible and adaptive predictive system: Reconceptualization remodels priors and hyper-priors; the healing ritual, acting as an open label placebo, opens the system to new predictive avenues; and meditation weakens descending predictions to facilitate their replacement with new beliefs and present-centered sense data and activates sympathetic and parasympathetic autonomic responses. New predictions alter allostatic setpoints and autonomic regulation.

Each mind-body technique in the study may be thought of as acting on a different part of the predictive architecture (Figure 2.9): Reconceptualization changes how participants believe their minds construct reality and affect their bodies, which is equivalent to reconfiguring the priors (beliefs about the causes of symptoms or sense data) and hyperpriors (beliefs about beliefs about the causes of sense data) that structure how interoceptive and exteroceptive sensory signals are interpreted and experienced. The open label placebo-like healing ritual enacts a known health-promoting behavior (healing) that does not conform to rational norms, creating a mismatch between motor/affective behavior and the experience-driven self-fulfilling prediction of sense data, which opens the system to new predictive (sensory and allostatic) paths[30]. Finally, meditation, by focusing attention on the present, weakens the predictive processes themselves to produce a state of pure awareness that is free from the predicted self[50] in which priors are more easily replaced with present-centered sense data. The three techniques may therefore work synergistically to facilitate a more flexible and adaptive prediction system, accounting for the personal transformations anecdotally reported by participants and the downstream neuroplastic and molecular changes. The observed changes in blood biomarkers may have resulted from the endocrine, immune, and other regulatory changes evoked by the intervention's effects on these predictive allostatic mechanisms, as well as from meditation-induced effects on both sympathetic and parasympathetic branches of the autonomic nervous system[58], a finding common to other meditation studies[59], which may also account for the concomitant upregulation of inflammatory and anti-inflammatory proteins during the intervention.

MEQ-30 scores revealed that participants experienced mystical-type experiences during meditation, reflected in neural activity by strengthened connectivity between the left insula and the PCC – a hallmark sign of trance states – and diminished DMN connectivity and whole-brain

modularity – consistent with previous meditation studies[32,60]. Elevated post-intervention plasma levels of SLITRK1 and NGFR and the inducement of greater glutamatergic dendritic growth by post-intervention plasma are both similar to effects by serotoninergic entheogens, which some have compared to meditative states,[61,62] and consistent with neuroplastic changes mediated by the BDNF pathway. While follow-up mechanistic studies are needed to establish causality, we provide converging evidence at multiple scales to suggest that the mind-body intervention produced neuroplastic changes mediated by these BDNF-associated proteins.

Beyond neural changes, we found that post-intervention plasma enhanced glycolysis in treated cells and contained higher levels of glycolysis-associated proteins ENO2 and LDHA. While the in vitro results may be interpreted as a Warburg effect on neuroblastoma cells, our proteomic data suggests that glycolysis became enhanced in participants. Notably, a similar phenomenon was observed in experienced Tibetan monks[24], for whom the enhanced glycolytic phenotype was associated with a cardioprotective plasma proteome, improved oxygen release, and decreased atherosclerosis. This underscores the complex interplay between neural and non-neural mechanisms in mind-body interventions and warrants further investigation. Since the brain's predictive architecture is evolutionarily geared towards regulating metabolic outlays, we speculate that the present-centered, sensory-driven brain state induced by meditation requires a more dynamic energetic profile made possible by glycolysis' fast response times.

The significant pre-to-post intervention increases in beta-endorphin and dynorphin point to the engagement of the endogenous opioid system without deception. We suggest that reconceptualization altered high-level priors about the mind's ability to influence the body, leading to new predictions that modulated endorphin levels. Since reconceptualization creates a steady belief state, this effect is likely sustained for longer than deception-based placebos. In a

world in which up to 50% of American physicians regularly and knowingly prescribe placebo medications[63], interventions that activate a self-mediated, conscious, and non-deceptive pain relief mechanism carry great potential, especially for pain conditions without a well described physical etiology. Future research should investigate which specific beliefs associated with health, disease, mind, and body sustainably optimize endogenous opioid modulation, as well as if and how meditation aids in initiating and sustaining these changes.

Our transcriptomic analyses reveal significant changes in circulating exRNAs implicated in neural activity, metabolic processes, and cellular signaling. Specifically, key upregulated transcripts such as *RIBC1* (*RIB43A* domain with coiled-coils 1) and *MIR455* (microRNA 455) mapped to pathways involved in neurotransmission and glycolysis. Pathway enrichment analysis highlighted upregulated Reactome pathways related to synaptic transmission and neurotransmitter cycling, consistent with the observed neural connectivity and neuroplasticity changes. Together, these results provide multi-level evidence that the mind-body retreat induced metabolic reprogramming, neuroplastic changes, and endogenous opioid modulation, potentially mediated by dynamic exRNA activity and glycolytic adaptation.

Interestingly, simultaneous activation of inflammatory and anti-inflammatory protein pathways is reminiscent of prior findings showing mind-body techniques can enhance resilience to environmental stressors via gene expression[64]. Cytokines like IL-6 are known to have both pro-and anti-inflammatory roles depending on the context acting as both acute-phase reactants during stress but also stimulating IL-1 receptor antagonist and IL-10 in exercise and repair settings[65]. While inflammation is often viewed as a harmful response, increased cellular turnover and tissue remodeling could occur as part of an adaptive response to these interventions – another area worthy of further investigation.

While our study provides valuable insights into the broad effects of mind-body interventions, we acknowledge several important limitations. First, the uncontrolled observational design limits our ability to infer causality or disentangle the relative contributions of meditation, placebo, reconceptualization, and other factors such as expectations, diet, and relaxation or distance from routine stressors. Future studies should implement more rigorous, controlled designs to test how these elements interact and whether the non-predictive meditation state facilitates the replacement of maladaptive priors during reconceptualization. Additionally, the small sample size and partial reliance on experienced meditators may limit the generalizability of our findings, and future research should include larger, more diverse cohorts. Additional mechanistic studies should investigate the molecular targets implicated by this study to causally link the neuroplastic and phenomenological changes to the molecular pathways implicated by our work.

Specific methodological limitations include the following. Although data on meditation experience and practice frequency were collected for retreat-based meditations within the study cohort, equivalent information regarding other forms of meditation practice—apart from the binary indication of their presence or absence—was not obtained. Potential circadian and metabolic confounds were introduced by variable blood collection times (up to 8-hour range on Day 8), pre-collection fasting durations, and time elapsed after the meditation intervention ended (up to 48 hours for blood collections and 24 hours for fMRI acquisition) between participants. Dietary factors and fasting may also have introduced confounds in proteomic and metabolomic measures since no standardized diet was implemented and fasting times beyond 30-minutes pre-blood collection were not controlled during the intervention. The short duration of the resting state scan can limit our ability to attribute connectivity-derived features solely to the

experimental variables[65–67]. The open eyes paradigm during fMRI BOLD acquisition, chosen to reduce the risk of drowsiness, likely introduced potential visual confounds. Finally, denoising with ICA-AROMA + WM/CSF regression is limited in removing physiological noise in regions with strong cardiac or respiratory activity, which may have resulted in additional confounds.

Conclusions

This observational study is the first to investigate the joint effects of three mind-body interventions–meditation, reconceptualization, and open-label placebo healing rituals–on neural activity and plasma physiology. Our findings show these techniques may act synergistically to produce mystical-type experiences, enhance neuroplasticity, reprogram metabolic pathways, and modulate endogenous opioids, highlighting the potential of mind-body interventions to effect profound changes in neural activity and physiology.

Methods

Participant Recruitment

The study was advertised to all 1,444 registered retreat attendees via email invitation, of which 561 expressed interest by answering an online questionnaire to determine eligibility (Figure 2.1D). Inclusion criteria included being an English speaker; being at least 21 years of age; being in good general health; being able to provide blood samples before, during, and after the retreat; and agreeing to undergo fMRI neuroimaging before and after the retreat. Exclusion

criteria included inability to consent, inability to follow or comply with study procedures, current use of psychoactive medications, contraindications for phlebotomy, and contraindications for MRI (pregnancy, history of seizures, electronic or ferromagnetic medical implants or devices, claustrophobia). Of 65 eligible participants, 36 were randomly selected to participate and provided written informed consent. Of 27 who consented, five were dropped due to scheduling conflicts; one participant was dropped for not complying with MRI facility masking requirements; and one participant failed MRI screening due to a heart stent. The study size was determined by the scanning time available at the fMRI facility (1 MRI scanner for 2 days pre- and post-intervention). Our study included male (n=6) and female (n=14) participants (gender identity), and similar findings are reported for both genders. Of the 6 male participants, 2 had been practicing the meditations carried out in the workshop daily for more than 1 year, 3 had been practicing the meditations daily for less than 1 year (one of whom practiced a different form of meditation), and 1 participant had not previously practiced the meditations before attending the retreat, though he had a different meditation practice. Of the 14 female participants, 8 had been practicing the retreat meditations for over 1 year (most being a daily practice), and 1 of the 8 also practiced a different form of meditation. Six of the 8 females had been practicing the meditations for less than 1 year, with only 3 reporting an almost daily practice, and 4 of the 8 reported having a different meditation practice. One of the 8 females had not previously practiced the meditations before attending the retreat, though she had a different meditation practice. The retreat began at 5 pm on Day 1 and ended at 1:30 pm on Day 7 and was conducted in April 2022 at the Manchester Grand Hyatt (San Diego, CA, USA). The diet was provided by the hotel. There were no adverse events.

The study was conducted in accordance with the Declaration of Helsinki principles and all relevant ethical regulations. Experimental protocols were approved by the Western Institutional Review Board (WIRB; now WCG-IRB; Protocol MED02#20211477) and registered on clinicaltrials.gov (NCT 06615531). Whole blood and buccal cells were collected but not analyzed due to budgetary constraints. Quantitative electroencephalography (qEEG) and heart rate variability (HRV) data were also collected and not analyzed due to poor data quality. Written informed consent was obtained from all participants prior to study inclusion, and clinical records are housed at VitaMed Research (Palm Desert, CA) as mandated by federal laws. All ethical regulations relevant to human research participants were followed.

Functional Magnetic Resonance Imaging (fMRI)

Acquisition

fMRI was performed off-site at the UCSD Center for Functional MRI pre-intervention (Day 0: 8am-8pm and Day 1: 8am-4pm) and post-intervention (Days 8 and 9: 8am-6pm). Participants were positioned in the MRI scanner (Siemens Prisma 3T with standard 32-channel head coil) with a respiratory transducer placed around the chest, a pulse oximeter placed on the left index finger, and MRI-safe headphones. A structural scan, two functional blood oxygen level dependent (BOLD) scans (resting state and meditation), and a diffusion tensor imaging (DTI) scan (not described here) were acquired.

Structural Scan

Participants were instructed to “not move and keep eyes closed.” High resolution structural images were acquired with a T1-weighted magnetization-prepared rapid gradient-echo (MPRAGE) sequence with TR = 2400ms, TE = 2.22ms, TI = 1000ms, flip angle = 8°, FOV = 224mm, voxel size = 0.7mm isotropic, 320 slices, slice thickness 0.80mm, saggital orientation, bandwidth = 210 Hz/Px, and acquisition time = 7min. 40s.

Functional Scans

During the 5-minute BOLD resting state scan, participants were instructed to “not move, keep eyes open, stay awake, and think about whatever you want, but do not meditate.” During the subsequent 15-minute BOLD meditation scan, an auditory recording of a guided meditation from the retreat was played and participants were instructed to “not move, listen to the guided meditation soundtrack, and meditate as suggested by the audio while keeping your eyes open.” An eyes open paradigm was chosen to reduce the risk of drowsiness or sleep during the meditation run, which was deemed a potentially greater risk than the presence of visual confounds to accurately comparing active meditation with passive rest[68,69]. One rest and one meditation run were collected per scan. The audio consisted of continuous expansive atmospheric music with an intermittent ethereal voice repeatedly instructing listeners to “tune into nothingness”, “no time”, “nowhere”, and “love”, combining loving-kindness meditation with focused awareness of the experiencing self and its potential dissolution into pure awareness. BOLD images were obtained with a gradient-recalled echo-planar imaging (EPI) sequence with TR = 800ms, TE = 37ms, flip angle = 52°, FOV = 208mm, voxel size = 2mm isotropic, 2mm

slice thickness, 72 slices, number of volumes = 1200, matrix size = 104 x 90, bandwidth = 2290 Hz/Px, and acquisition time = 5 min. (rest) and 15 min. (meditation).

Post-Scan Questionnaire

Immediately after each scanning session, participants were asked to assess their experience meditating by completing the Mystical Experience Questionnaire (MEQ-30)[70].

fMRI Preprocessing and Denoising

Anatomical and functional data were preprocessed using fMRIPrep v21.0.2[71]. B0-fieldmaps were estimated with Topup[72]. Anatomical T1-weighted (T1w) images were corrected for intensity non-uniformity using ANTS 2.3.3[73], skull-stripped, segmented using Fast (FSL 6.0.5)[74], and normalized to standard space (MNI152Nlin2009cAsym) with nonlinear registration (ANTs 2.3.3). Brain surfaces were reconstructed using recon-all (FreeSurfer 6.0.1)[75]. Due to a corrupted T1w image for participant 4023, co-registration failed, and 4023 was excluded from fMRI analysis.

BOLD head-motion parameters were estimated using MCFLIRT (FSL 6.0.5)[76]. Functional runs were co-registered to anatomical T1w references using boundary-based registration (FreeSurfer) and resampled to standard space. Confounding time-series were calculated for CSF/WM region-wise global signals, and motion artifacts were identified using independent component analysis (ICA-AROMA)[77]. Non-steady state volumes were removed and spatial smoothing with an isotropic Gaussian kernel of 6mm FWHM (full-width half-maximum)

was applied. Denoising using Nilearn 0.9.2[78] was performed by detrending, standardizing, and bandpass filtering (0.01 – 0.1 Hz) time series data, and by regressing ICA-AROMA motion artifacts and mean CSF+WM signals[79]. Physiological noise was addressed via ICA-AROMA + CSF/WM regressions rather than with physiological recordings. Additional denoising for whole-brain network analyses involved regressing global signal and excluding BOLD runs with mean FD > 0.3 mm to obtain functional connectivity distributions mean-centered around zero, which were confirmed by visual inspection.

Functional Connectivity Analysis

Functional connectivity analyses were performed on seven canonical resting state networks (RSNs), eight a priori defined regions of interest (ROIs), and whole-brain networks (Nilearn 0.9.2) (Brain Connectivity Toolbox[80]). To understand how this meditation style influences large-scale neural dynamics, we examined functional connectivity and whole-brain network measures, capturing the integration, segregation, and reorganization of brain networks.

Resting State Networks and Regions of Interest

RSNs examined included the default mode network (DMN), dorsal attention network (DAN), executive control network (ECN), salience network (SN), sensorimotor network (SMN), visual network (VN) and auditory network (AN). While preregistration discussed DMN, all seven canonical RSNs were included for analysis. The Montreal Neurological Institute (MNI) coordinates for the 36 regions that comprise them were extracted from the Raichle (2011) atlas[81]

(Supplementary Table 2.3). Mean denoised BOLD time series were extracted from 10mm-radius (523-voxel) spheres centered on the MNI coordinates. Between-region Pearson correlations were calculated and z-transformed to obtain a measure of connectivity strength. Within-network connectivity was calculated as the mean connectivity between each unique pair of ROIs within a given network, and between-network connectivity was calculated as mean connectivity between all ROIs from two networks, with each ROI pair containing one region per network. Eight a priori ROIs, not preregistered as an outcome, were additionally selected for a hypothesis-driven analysis based on task-induced and connectivity changes in other meditation studies[82–85]: medial prefrontal cortex (mPFC), right and left dorsolateral prefrontal cortices (r/l dlPFC), right and left insular cortices (r/l IC), right and left angular gyri (r/l AG), and central precuneus, with MNI coordinates extracted from the DiFuMo atlas[86] (Supplementary Table 2.4). Mean denoised BOLD time series per region were extracted from 10mm-radius (523-voxel) spheres centered on the MNI coordinates, and between-region Pearson correlations were calculated.

Whole-Cortex/Brain Networks

Networks were constructed from the 25%-thresholded 48-region Harvard Oxford 2mm cortical atlas[37] and from the 264-region whole-brain Power (2011) atlas[38] by extracting mean denoised BOLD time series per region per parcellation and calculating between-region Fisher z-transformed correlations for all possible pairs. We constructed weighted undirected graphs and computed modularity, global efficiency, and characteristic path length per network to assess integrated whole-brain functional connectivity changes, as per preregistration. Functional connectivity value distributions were visually inspected, and one outlier run not mean-centered

around zero was excluded from Power atlas analysis. Network measures were recalculated while excluding runs with mean framewise displacement > 0.3 mm to check if any significant effects were due to motion artifacts.

Statistics

We investigated scanner head motion per session and condition with a 2 (pre/post) X 2 (meditation/rest) repeated measures ANOVA on mean and maximum framewise displacement per BOLD run with post-hoc effects confirmed with Wilcoxon signed rank tests. MEQ score differences were compared between sessions with Wilcoxon signed rank tests (*n=18,* two subjects missing data).

After confirming normality and heteroskedasticity, paired *t*-tests compared RSNs, their component regions, a priori ROIs, and whole cortex/brain networks pre- and post- intervention (separately for rest and meditation scans) plus rest and meditation (separately for pre- and post-scans) to investigate effects of time and of meditation, respectively. On rest vs. meditation comparisons, the last 5 minutes of the 15-minute meditation scan were used to compare equal-length scans. *P*-values were corrected for multiple comparisons using Bonferroni-Holm family wise error correction and Benjamini-Hochberg false discovery rate when no results reached $p_{FWE} < 0.05$.

Anatomical Data

Preprocessed skull-stripped segmented T1w data was resampled to the MNI fsaverage template using mris_preproc (FreeSurfer 7.3.2) and cortical surface was inflated to an average spherical surface. Hemispheres were automatically parcellated into regions of interest, and vertex-wise volumetric and cortical thickness calculations were performed. Images were spatially smoothed with a 5mm FWHM Gaussian kernel. Pre-vs-post differences were assessed by repeated measures ANOVA, and group differences between novice and advanced participants at each timepoint were assessed by fitting a general linear model using mri_glmfit-sim. Total intracranial volume and age were included as covariates, and results were cluster corrected with a cluster-wise *p*-threshold = 0.01.

Human Plasma Collection

Human plasma was collected and processed, as described in[87], via venous puncture by registered nurses, physicians, and phlebotomists, at pre-intervention either off-site ("Day -1", 2 days pre-retreat, 2-4 pm) or on-site ("Day 0", 1 day pre-retreat, 11 am-4 pm) and post-intervention ("Day 8", on-site, 9-5 pm). Participants were offered the same food options for all breakfast, lunch, and snacks throughout the week, although food choices were not monitored. All participants were required to fast for at least 30 minutes prior to blood collection. Blood was collected in EDTA-coated tubes (BD, Franklin Lakes, NJ) and kept at 4°C (wet ice) for less than 30 minutes. Plasma was isolated by centrifugation at 3000 RPM for 15 min in an E8 Touch tabletop centrifuge (LW Scientific, Lawrenceville, GA), aliquoted into 1.5 mL Eppendorf tubes, and immediately frozen on dry ice. At the end of the retreat, samples were shipped to UCSD and stored at -80 ºC.

Plasma Nanoparticle Tracking Analysis

Plasma Nanoparticle Tracking Analysis (NTA) measured circulating plasma nanoparticle size and concentration with a NanoSight NS300 instrument (Malvern Instruments Ltd., UK). Samples were thawed on ice and diluted in PBS (100X) to prevent aggregation. Measurements were performed at room temperature under continuous video recording (16 X 30-sec. acquisitions/sample) and 532 nm laser illumination. Mean hydrodynamic diameter, size distribution, and particle concentration were obtained per sample with NTA 3.3 software.

ELISA

To investigate plasma concentrations of oxytocin, beta-endorphin, dynorphin, anandamide, cocaine and amphetamine-regulated transcript (CART), c-reactive protein (CRP), and neuropeptide Y (NPY), pre- and post-intervention plasma samples were tested with commercially available ELISA kits listed in Supplementary Table 2.12 following manufacturers' instructions. Absorbance was measured with a Tecan Spark 10M microplate reader, and concentrations were calculated by interpolating absorbance values against the standard curve, previously fit with a 3-parameter logistic curve. Pre- and post-intervention concentrations were compared with Wilcoxon signed-rank tests.

Plasma Proteomics

To investigate the intervention's effects on the plasma proteome, 7,596 proteins were quantified with the SomaScan Assay v4.1 (SomaLogic, Boulder, CO, USA).

SomaScan Assay

Samples were thawed on ice, diluted in SomaLogic plasma diluent, and loaded onto SomaScan 96-well plates containing capture SOMAmer reagents for 7,596 unique human protein targets. Plates were incubated for protein capture, unbound material was washed away, and biotinylated capture antibodies were added to hybridize with SOMAmer-bound proteins. Streptavidin-conjugated Cy3 dye was added to label the antibodies, plates were washed to remove unbound dye, and protein-bound SOMAmer reagents were eluted and hybridized to custom DNA microarrays containing complementary sequences to each SOMAmer. Cy3 fluorescence intensity in relative fluorescence units (RFU) measured protein abundance. Hybridization control normalization removed sample variance between microarrays and scanners; median signal normalization removed within-plate inter-sample differences; and calibration normalization removed variance across assay runs. Performance and quality were monitored with blank wells, technical replicates, and spiked protein controls, and precision was assessed by calculating coefficients of variation for all measurements. Background subtraction RFU calculations were performed with SomaLogic Discovery Server software.

Data Processing

RFU values were normalized, log10-transformed, and auto-scaled (mean-centered and divided by each variable's standard deviation), and outliers above two SDs were flagged. Foldchange and paired *t*-tests tested pre/post-intervention differences, and hierarchical clustering and k-means clustering revealed correlated variation expression patterns. Functional enrichment analysis (Enrichr-KG) on differentially expressed proteins (pre/post $p < 0.01$), with all SOMAmer targets as background, assessed enriched biological processes, molecular pathways, and cellular components. Enriched pathways were considered significant at $p_{FDR} < 0.05$. Protein-protein interaction subnetworks of significant proteins ($p < 0.05$ or $|\text{fold change}| \geq 0.5$) were created in Cytoscape with ≤30 interactor nodes and heat diffusion using the STRING database[88].

Plasma Metabolomics

640 metabolites in whole plasma were detected via liquid chromatography-mass spectrometry analysis using the widely-targeted Metware platform (Metware Biotechnology, Woburn, MA, USA).

Metabolite Detection

Plasma samples were extracted with a 1:4 ACN:methanol solution and centrifuged at 12,000 RPM (10 min, 4°C) and again at 12,000 RPM (3 min, 4°C) after 30 min. at -20°C. Supernatants were analyzed by ultra-HPLC (UPLC) (ExionLC 2.0, Sciex, Framingham, MA, USA) on a UPLC column with a gradient elution system for metabolite separation (UPLC conditions listed in Supplementary Table 2.13). Eluted metabolites were detected based on mass

and fragmentation patterns by Tandem Mass Spectrometry (MS/MS) using a quadrupole-time of flight mass spectrometer (QTRAP®6500+, Sciex) with an electrospray ionization (ESI) Turbo Ion-Spray interface, operating in positive and negative ion mode. Untargeted qualitative metabolite identification was performed by matching ion features to references from Metware, HMDB[89], METLIN[90], and KEGG[91] databases. Identified metabolites were then quantified using triple quadrupole mass spectrometry with multiple reaction monitoring (mass spectrum conditions in Supplementary Table 2.14). Mass spectrometry chromatographic peaks were corrected with MultiQuant software (Sciex). Reproducibility, cross-contamination, and inter-sample quality were controlled with control samples, internal standard peaks from blank samples, and internal standards, respectively.

Metabolite Analysis

Quantified metabolite features were variance-filtered via inter-quartile range (max 25% filtered out), normalized, and log10-transformed. Outliers above 2 standard deviations were flagged. Dietary factors and fasting may have introduced confounds in proteomic and metabolomic measures, as no standardized diet was implemented and fasting times beyond 30 minutes pre-blood collection were not controlled. Exogenous compounds annotated as dietary or drug-related by HMDB were monitored using the MetaboAnalyst pipeline and were flagged or removed if observed among the top 25 features. PCA, hierarchical cluster analysis (HCA), partial least squares discriminant analysis (PLS-DA), and FDR-corrected pre/post paired *t*-tests (Scikit-learn[92]) identified differentially expressed metabolites. Correlation heatmaps were generated using Pearson r distance measures. Metabolic pathway analysis comparing pre- to post- samples

was performed with MetaboAnalyst v5.0 based on the KEGG database. Pathway enrichment was first assessed using MetaboAnalyst, and false discovery rate (FDR) correction was applied to control for multiple comparisons. Significant pathways ($p_{FDR} < 0.05$) were then selected for follow-up analysis. For these pathways, we examined the distribution of normalized feature values and report the corresponding p-values for group comparisons after normalization.

Real Time Cellular Metabolic Analysis

To investigate the effects of human plasma on cellular metabolism, we performed Seahorse XF mitochondrial stress, glycolytic rate, and ATP production assays on BE(2)M17 cells (ATCC), a human neuroblastoma cell line, exposed to plasma following Song et al. (2023) and Kopp et al. (2023)[93,94] methods.

Cell Culture and Plasma Treatment

BE(2)M17 cells were cultured in complete DMEM/F12 medium supplemented with 10% FBS and 1% penicillin/streptomycin under standard conditions (37°C, 5% CO_2). Cells were harvested, washed, and seeded onto microplates pre-coated with poly-L-lysine at a 40,000 cells/well density and incubated overnight. Cells were resuspended in XF assay medium and treated with 1% plasma for 1 hour at 37°C, with 4 technical replicate wells per plasma sample, and stained with DAPI for post-assay cell counting.

Seahorse XF Assays

Seahorse XF96 Analyzer (Agilent, Santa Clara, CA, USA) was calibrated according to manufacturer's instructions, and the following injection protocols were implemented: Mitochondrial Stress Test (kit #103015-100): Oligomycin (1.5 μM), FCCP (2.0 μM), and Rotenone/Antimycin A (0.5 μM) were sequentially injected to measure basal respiration, proton leak, maximal respiration, and spare respiratory capacity, with oxygen consumption rate (OCR) monitoring. Glycolytic Rate Test (kit #103344-100): Rotenone/antimycin A (0.5 μM) and 2-deoxyglucose (50 mM) were injected to assess basal glycolytic rate, glycolytic reserve, and non-glycolytic acidification, monitored by extracellular acidification rate (ECAR). ATP Production Rate Test (kit #103592-100): Injections of oligomycin (1.5 μM) and rotenone/antimycin A (0.5 μM) enabled real-time calculation of ATP production rates from OCR and ECAR.

Data Analysis and Statistics

We used Seahorse XF software (v.2.6) to analyze raw OCR and ECAR data, normalizing results by cell counts, and compared metabolic parameters between control, pre-, and post-intervention groups with paired *t*-tests ($p < 0.05$ considered significant). We assessed cell viability pre- and post-treatment and included four non-cellular blank well controls per plate to ensure assay quality.

Neurite Differentiation

To investigate the effects of human plasma on neurite growth, PC12 neuroendocrine cells were differentiated to their neuronal phenotype, treated with plasma, and live-imaged following published methods[95].

Cell Culture and Differentiation

PC12 cells (ATCC, Manassas, VA, USA) were cultured in RPMI 1640 medium supplemented with 10% horse serum, 5% FBS, and 1% penicillin/streptomycin under standard conditions (37°C, 5% CO_2). On Day 0, differentiation was induced by plating cells onto poly-D-lysine-coated plates at a 1.0 x 10^4 cells/cm^2 density and culturing them with Opti-MEM medium supplemented with 0.5% FBS, 1% penicillin/streptomycin, 50 ng/mL nerve growth factor (NGF), and either 1% human plasma pooled from pre- and post-intervention or no plasma (control cells) with 2 technical replicate wells per condition. Medium was replaced every 48 hours. Media was supplemented with 1% Culture One from Day 2 onwards to support neuronal differentiation.

Live-Cell Imaging and Neurite Analysis

Differentiated cells were live-imaged every 24 hours for 10 days at 20X in a live cell imaging microscope (Keyence BZ-X700) equipped with a phase contrast objective and an incubation chamber at 37 °C, 5% CO_2, and controlled humidity. Images were acquired under consistent illumination across groups and time points, and background subtraction and image thresholding were applied to enhance neurite visualization. The single longest neurite per cell,

for cells for which it was longer than the cell body diameter, was manually traced in FIJI software (v1.0). Neurite lengths were compared with two-tailed independent samples t-tests between plasma-treated and control groups at each time point. Treatment wells remained blinded until completion to avoid bias.

Exosome-Specific Small RNA Transcriptomics

Exosome Isolation

Exosomes were isolated from plasma samples (300-500 µl) by centrifugation at 300 x g for 10 min at 4°C to remove cell debris. Supernatants were transferred to microcentrifuge tubes, filled with 1x PBS, balanced for mass, placed in a pre-cooled Beckman Coulter Type 70.1 rotor, and centrifuged at 10,000 × g for 30 min at 4°C with maximum acceleration and gradual deceleration. Supernatants were transferred to new tubes, exosome pellets were resuspended in 100 µl 1x PBS, and another round of ultracentrifugation at 100,000 × g for 2 hrs. at 4°C was performed. Final exosome pellets were resuspended in 150 µl 1x PBS, analyzed by nanoparticle tracking using the same protocol as whole plasma, and stored at -80°C.

Exosome RNA sequencing

Total RNAs were purified from exosome pellets using Direct Zol RNA mini kit (Zymo Research). RNAs were eluted in 20 µl of RNAse-free water and concentrated to 5 µl using SpeedVac Vacuum Concentrator (Thermo Fisher Scientific). 44 to 523 ng of exosome-specific

extracellular small RNAs (exRNAs) were obtained from 28 human plasma samples. exRNA quantity and integrity were determined using the NanoDrop ND-1000 spectrophotometer (Thermo Fisher Scientific) and the Bioanalyzer 2100 (Agilent, Santa Clara, CA, USA), respectively. Small exRNA libraries were generated using NEXTFlex Small RNA-seq Kit v4 with UDIs (Revvity Inc, Waltham, MA, USA) according to modified manufacturer's protocol to account for low exRNA concentrations in exosome samples. The strategy for small RNA libraries aimed at a range of 16-120 nucleotide (nt)-long transcripts for accurate identification and quantification of exosome-specific extracellular microRNAs, ncRNAs, and protein-coding RNAs. NEXTFLEX® 3' Adenylated Adapter v4 was ligated at 25°C for 1h. Following 3' Adenylated Adapter inactivation, NEXTFLEX 5' Adapter v4 was ligated at 20°C for 1h. Reverse Transcription-First Strand Synthesis from 5' and 3' NEXTFLEX® Adapter Ligated RNA templates was conducted at 50°C for 1h, followed by inactivation at 90°C for 5 min. First Strand Synthesis products were purified using NEXTFLEX Cleanup Beads by two washes in 80% ethanol. RNA templates were combined with NEXTFLEX UDI Barcoded Primer Mixes v4 diluted 1:4 and amplified by PCR for 24 cycles. PCR products size selection and cleanup were done using NEXTFLEX Cleanup Beads. Small exRNA libraries were eluted from beads in 15 µl and concentrations were determined using Qubit dsDNA HS Assay (Life Technologies). DNA fragment profile in small exRNA libraries was analyzed on the Bioanalyzer 2100. RNA-seq was conducted on the NovaSeq X Plus Short-Read Sequencer (Illumina, San Diego, CA) at the Genomics Research and Technology Hub, University of California Irvine.

RNA-seq Data Processing

Sequencing read data were converted to FASTQ format for bioinformatic processing using Lonestar6 supercomputer at the Texas Advanced Computing Center and bioinformatically processed according to guidelines developed for NEXTFLEX Small RNA-Seq (Revvity Inc., Waltham, MA, USA). In brief, flanking forward (TGG AAT TCT CGG GTG CCA AGG) and reverse (AGA TCG GAA GAG CGT CGT GTA GGG AAA GA) adapter sequences were trimmed prior to alignment with Cutadapt[96]. Paired reads above 16 nucleotides with quality scores above 20 were mapped to the human genome primary assembly (Release 47, GRCh38.p14). Reads-to-genome alignment was conducted using STAR aligner[97]. Mapping quality was assessed using MultiQC tool[98].

Detection of Differential Exosomal RNAs

The differential analysis of sequence read count data was done using a generalization of a paired *t*-test using EdgeR software[99–101] in which exosome RNA pools in pre- and post-intervention samples per participant were compared separately and the baseline differences between participants were subtracted. Transcripts with fewer than 10 counts were removed from analysis. Trimmed Mean of M-values (TMM) normalization[102,103] was applied to account for compositional difference between samples. exRNA were annotated using org.Hs.eg.db[104] and miRbase[105] databases. Sequences corresponding to non-coding RNAs (ncRNAs) and exhibiting the highest variance across all samples were analyzed by PCA of TMM-normalized counts using PCAtools Bioconductor package. Functional analysis of differential exRNA was done using ClusterProfiler[106] and the Reactome Pathways Knowledgebase[46]. A paired design in the negative binomial (NB) generalized linear model (GLM) detected the effect of the intervention on the

composition of exRNAs from paired post- intervention (n=14) vs pre-intervention (n=14) samples, while adjusting for differences between participants. Participants' experience level (9 advanced, 5 novices), gender (8 females, 6 males), and age were included as additional covariates.

Machine Learning and MEQ-Features Correlation Analyses

We applied machine learning to identify the most biologically relevant features across time point (pre/post) and experience level (novice/advanced) datasets. Each dataset was preprocessed (log-transformed and auto-centered) and missing data was imputed to ensure feature scaling, normalization consistency, and data integrity and comparability across modalities[107]. Post-preprocessing, ELISA, metabolomics, transcriptomics, and proteomics datasets were concatenated into a single feature matrix used as input for an eXtreme Gradient Boosting (XGBoost)[108] classifier chosen for its ability to handle high-dimensional data. To obtain a unified impact metric per feature, the dataset was passed through a Shapley Additive exPlanations (SHAP)[109] explainer model. Spearman correlations were then calculated between MEQ scores and the top 14 features per model and corrected for multiple comparisons to explore whether the top molecular changes were linked to subjective outcomes.

Statistics and Reproducibility

Given the n=20 sample size (n=19 for fMRI), nonparametric Wilcoxon signed-rank statistics were performed throughout when comparing paired samples, except when $n \geq 30$ (e.g.

protein targets) or when normality and homoskedasticity were ascertained, in which case two-tailed paired *t*-tests were employed. Given that proteomic and metabolomic analyses were hypothesis free and data driven, False Discovery Rate (FDR) correction was applied using the Benjamini-Hochberg procedure, and reported p-values are labelled as FDR-adjusted, with nominal p-values included for transparency. Seahorse XF plates were prepared with 4 technical replicates (wells) per participant and time point. PC12 assay plates were prepared with pooled plasma (*n=20*) with 2 technical replicates (wells) per treatment (pre plasma/post plasma/no treatment).

Ethics and Inclusion Statement

Data collection and analysis was performed locally in San Diego, CA, USA and included local researchers. Roles and responsibilities were agreed amongst collaborators ahead of the research, and clinical practice and biospecimen handling trainings were provided to all researchers. The study was approved by a local research ethics committee and did not result in personal risk to study participants. Researchers who handled biospecimens during collection and analysis wore adequate personal protective equipment. fMRI researchers and participants were thoroughly screened for MRI safety before being allowed inside the fMRI magnet room.

Data Availability

Values for all data points in plots and reported means are available (Supplementary Data 1). RNAseq data is available from GEO repository (accession #GSE291700). Proteomics data is

available from PRIDE repository (dataset PAD000010). Any other data is available from the corresponding author on reasonable request.

Code Availability

Analytic code can be obtained from the corresponding author on reasonable request.

Funding

Support for this research was provided by the Inner Science Research Fund (HHP) and a Research Career Scientist Award from the Veterans Administration (BX005229 to HHP).

Acknowledgments

Chapter 2 is a reprint of the material as it appears in Alex Jinich-Diamant, Sierra Simpson, Juan P. Zuniga-Hertz, Ramamurthy Chitteti, Jan M. Schilling, Jacqueline A. Bonds, Laura Case,c, Andrei V. Chernov,c, Joe Dispenza, Jacqueline Maree, Natalia Esther Amkie Stahl, Michael Licamele, Narin Fazlalipour, Swetha Devulapalli, Leonardo Christov-Moore, Nicco Reggente, Michelle A. Poirier, Tobias Moeller-Bertram, Hemal H. Patel. Neural and molecular changes during a mind-body reconceptualization, meditation, and open label placebo healing intervention. Communications Biology, 8 (1525), 2025. The dissertation author was the primary author of this paper.

Supplemental Table 2.1: fMRI Framewise Displacement.

	Pre		Post	
Task	*M*	*SD*	*M*	*SD*
meditation	0.157	0.113	0.140	0.121
rest	0.086	0.095	0.088	0.096

Supplemental Table 2.2: fMRI Two-Way (Scan X Time) Mean Framewise Displacement Repeated Measures ANOVA.

Source	*SS*	*DF1*	*DF2*	*MS*	*F*	*p*	η^2p
scan	0.072	1	18	0.072	25.1	0.0001	0.58
time	0.001	1	18	0.001	0.6	0.44	0.03
scan * time	0.002	1	18	0.002	1.3	0.26	0.07

Supplemental Table 2.3: Montreal Neurologic Institute (MNI) Coordinates for 36 Regions of Interest Making up 7 Resting State Networks (source: Raichle 201191).

		MNI Coordinate		
Region of Interest	Network	*x*	*y*	*z*
dorsal medial PFC	ECN	0	24	46
left anterior PFC	ECN	-44	45	0
right anterior PFC	ECN	44	45	0
left superior parietal	ECN	-50	-51	45
right superior parietal	ECN	50	51	45
PCC	DMN	0	-52	27
mPFC	DMN	-1	54	27
left lateral parietal	DMN	-46	-66	30
right lateral parietal	DMN	49	-63	33
left inferior temporal	DMN	-61	-24	-9
right inferior temporal	DMN	58	-24	-9
medial dorsal thalamus	DMN	0	-12	9
right posterior cerebellum	DMN	-25	-81	-33
left posterior cerebellum	DMN	25	-81	-33
left frontal eye field	DAN	-29	-9	54
right frontal eye field	DAN	29	-9	54
left posterior IPS	DAN	-26	-66	48
right posterior IPS	DAN	26	-66	48
left anterior IPS	DAN	-44	-39	45
right anterior IPS	DAN	41	-39	45
left MT	DAN	-50	-66	-6
right MT	DAN	53	-63	-6
dorsal ACC	SN	0	21	36
left anterior PFC	SN	-35	45	30
right anterior PFC	SN	32	45	30
left insula	SN	-41	3	6
right insula	SN	41	3	6
left lateral parietal	SN	-62	-45	30
right lateral parietal	SN	62	-45	30
left motor cortex	SMN	-39	-26	51
right motor cortex	SMN	38	-26	48
SMA	SMN	0	-21	48
left V1	VN	-7	83	2
right V1	VN	7	83	2
left A1	AN	-62	-30	12
right A1	AN	59	-27	15

PFC: prefrontal cortex; PCC: posterior cingulate cortex; IPS: intraparietal sulcus; MT: middle temporal region; ACC: anterior cingulate cortex; SMA: supplementary motor area; V1: primary visual cortex; A1: primary auditory cortex; ECN: executive control network; DMN: default mode network; DAN: dorsal attention network; SN: salience network; SMN: somatomotor network; VN: visual network; AN: auditory network.

Supplemental Table 2.4: Montreal Neurologic Institute (MNI) Coordinates for 8 a priori Regions of Interest (DiFuMo atlas).

	MNI Coordinate		
Region of Interest	*x*	*y*	*z*
left dlPFC	-6	44	-6
right dlPFC	52	-52	32
left anterior insula	-50	-56	30
right anterior insula	-3	-42	25
central precuneus	38	20	-2
left angular gyrus	-34	16	2
right angular gyrus	44	36	32
mPFC	-44	34	32

dlPFC: dorsolateral prefrontal cortex; mPFC: medial prefrontal cortex.

Supplemental Table 2.5: Statistically Significant ($p < 0.05$) Rest-vs-Meditation Paired t-tests Between A Priori Regions of Interest.

Session	A Priori Region Pair		*t*	*p*	Cohen's *d*
pre	L angular gyrus	precuneus	-2.77	0.01	-0.81
pre	R angular gyrus	R dlPFC	-2.93	0.009	-0.67
pre	mPFC	precuneus	-2.66	0.02	-0.83
pre	mPFC	L angular gyrus	-3.67	0.002	-1.05
pre	mPFC	R angular gyrus	-2.33	0.03	-0.86
post	L anterior insula	L dlPFC	-2.18	0.04	-0.69
post	R anterior insula	L dlPFC	-2.14	0.05	-0.61
post	R anterior insula	L anterior insula	-2.17	0.04	-0.78
post	L angular gyrus	precuneus	-2.52	0.02	-0.70
post	R angular gyrus	precuneus	-2.40	0.03	-0.70
post	R angular gyrus	L angular gyrus	-2.88	0.01	-0.91
post	mPFC	precuneus	-2.12	0.05	-0.69
post	mPFC	L angular gyrus	-3.18	0.005	-0.97
post	mPFC	R angular gyrus	-3.51	0.002	-1.07

dlPFC: dorsolateral prefrontal cortex; mPFC: medial prefrontal cortex.

Supplemental Table 2.6: Whole-Brain Functional Connectivity Network Measures.

		Rest				Meditation			
		Pre		Post		Pre		Post	
Atlas	Measure	*M*	*SD*	*M*	*SD*	*M*	*SD*	*M*	*SD*
Harvard-Oxford	Characteristic Path Length	0.0173	0.0151	0.0184	0.0237	0.0171	0.0280	0.0071	0.0101
	Global Efficiency	-0.0009	0.0002	-0.0009	0.0003	-0.0006	0.0002	-0.0006	0.0002
	Modularity	0.0389	0.0045	0.0374	0.0042	0.0347	0.0042	0.0327	0.0060
Power	Characteristic Path Length	0.0788	0.0549	0.0895	0.0493	0.0748	0.0953	0.0540	0.0177
	Global Efficiency	-0.00004	0.00001	-0.00003	0.00001	-0.00003	0.00005	-0.00002	0.000003
	Modularity	0.0388	0.0045	0.0373	0.0045	0.0307	0.0062	0.0286	0.0029

Supplemental Table 2.7: 2 (Time: Pre/Post) by 2 (Task: Rest/Meditation) Repeated Measures ANOVA on Whole-Brain Modularity, Characteristic Path Length, and Global Efficiency.

Atlas	Measure	Source	*SS*	*DF1*	*DF2*	*MS*	*F*	*p*	η^2p
Harvard-Oxford	Modularity	task	0.00038	1	18	0.0004	20	0.0003	0.53
		session	6e-5	1	18	6e-5	3.3	0.09	0.15
		task * sess.	1e-6	1	18	1e-6	0.04	0.9	0.002
	Char. Path Length	task	0.00062	1	18	0.0006	1.5	0.2	0.08
		session	0.00038	1	18	0.0004	1.1	0.3	0.06
		task * sess.	0.00058	1	18	0.0006	1.4	0.25	0.07
	Global Efficiency	task	1.7e-6	1	18	2e-6	48	0.000002	0.73
		session	2e-9	1	18	3e-9	0.07	0.8	0.004
		task * sess.	3e-9	1	18	3e-9	0.11	0.8	0.006
Power	Modularity	task	0.0013	1	17	0.0013	54	1.1e-06	0.76
		session	6e-05	1	17	6e-05	2.3	0.14	0.12
		task * sess.	2.1e-06	1	17	2.1e-06	0.092	0.77	0.0054
	Char. Path Length	task	0.007	1	17	0.007	2	0.17	0.11
		session	0.00046	1	17	0.00046	0.12	0.74	0.0068
		task * sess.	0.0045	1	17	0.0045	1.5	0.23	0.083
	Global Efficiency	task	3.2e-09	1	17	3.2e-09	5	0.039	0.23
		session	8.7e-10	1	17	8.7e-10	1.5	0.23	0.083
		task * sess.	6e-10	1	17	6e-10	0.89	0.36	0.05

Supplemental Table 2.8: Pre- vs. Post-Intervention a Priori Regions Functional Connectivity.

Task	A Priori Region Pair		*t*	*p*	Cohen's d
rest	right dlPFC	left dlPFC	-0.06	0.95	-0.01
rest	left anterior insula	left dlPFC	1.02	0.32	0.29
rest	left anterior insula	right dlPFC	0.22	0.82	0.05
rest	right anterior insula	left dlPFC	0.11	0.91	0.03
rest	right anterior insula	right dlPFC	-1.15	0.26	-0.32
rest	right anterior insula	left anterior insula	-0.12	0.90	-0.04
rest	central precuneus	left dlPFC	0.79	0.44	0.23
rest	central precuneus	right dlPFC	-1.46	0.16	-0.31
rest	central precuneus	left anterior insula	-1.23	0.23	-0.34
rest	central precuneus	right anterior insula	-0.64	0.53	-0.18
rest	left angular gyrus	left dlPFC	-0.14	0.89	-0.04
rest	left angular gyrus	right dlPFC	-0.96	0.35	-0.24
rest	left angular gyrus	left anterior insula	-0.48	0.64	-0.15
rest	left angular gyrus	right anterior insula	0.07	0.94	0.02
rest	left angular gyrus	central precuneus	0.22	0.83	0.08
rest	right angular gyrus	left dlPFC	0.43	0.68	0.10
rest	right angular gyrus	right dlPFC	-1.41	0.18	-0.43
rest	right angular gyrus	left anterior insula	-0.23	0.82	-0.06
rest	right angular gyrus	right anterior insula	-1.06	0.30	-0.28
rest	right angular gyrus	central precuneus	1.01	0.33	0.32
rest	right angular gyrus	left angular gyrus	1.47	0.16	0.52
rest	mPFC	left dlPFC	-0.48	0.64	-0.12
rest	mPFC	right dlPFC	-0.20	0.84	-0.06
rest	mPFC	left anterior insula	0.68	0.50	0.15
rest	mPFC	right anterior insula	0.97	0.35	0.23
rest	mPFC	central precuneus	-0.83	0.42	-0.21
rest	mPFC	left angular gyrus	0.27	0.79	0.08
rest	mPFC	right angular gyrus	0.35	0.73	0.09
meditation	right dlPFC_	left dlPFC	-0.00	1.00	-0.00
meditation	left anterior insula	left dlPFC	0.17	0.87	0.04
meditation	left anterior insula	right dlPFC	-1.30	0.21	-0.35
meditation	right anterior insula	left dlPFC	-0.03	0.98	-0.01
meditation	right anterior insula	right dlPFC	-0.77	0.45	-0.19
meditation	right anterior insula	left anterior insula	-0.24	0.81	-0.07
meditation	central precuneus	left dlPFC	0.12	0.91	0.03
meditation	central precuneus	right dlPFC	-0.08	0.94	-0.02
meditation	central precuneus	left anterior insula	-0.24	0.81	-0.08

Supplemental Table 2.8: Pre- vs. Post-Intervention a Priori Regions Functional Connectivity. (Continued)

Task	A Priori Region Pair		*t*	*p*	Cohen's d
meditation	central precuneus	right anterior insula	-0.69	0.50	-0.21
meditation	left angular gyrus	left dlPFC	1.01	0.32	0.28
meditation	left angular gyrus	right dlPFC	0.32	0.75	0.10
meditation	left angular gyrus	left anterior insula	0.35	0.73	0.10
meditation	left angular gyrus	right anterior insula	-0.73	0.47	-0.21
meditation	left angular gyrus	central precuneus	0.65	0.53	0.17
meditation	right angular gyrus	left dlPFC	-1.16	0.26	-0.33
meditation	right angular gyrus	right dlPFC	-0.89	0.39	-0.25
meditation	right angular gyrus	left anterior insula	-1.08	0.30	-0.28
meditation	right angular gyrus	right anterior insula	-1.17	0.26	-0.26
meditation	right angular gyrus	central precuneus	-0.80	0.43	-0.23
meditation	right angular gyrus	left angular gyrus	-0.98	0.34	-0.30
meditation	mPFC	left dlPFC	-1.22	0.24	-0.29
meditation	mPFC	right dlPFC	-0.60	0.55	-0.21
meditation	mPFC	left anterior insula	-0.03	0.98	-0.01
meditation	mPFC	right anterior insula	-0.97	0.34	-0.29
meditation	mPFC	central precuneus	-0.70	0.49	-0.25
meditation	mPFC	left angular gyrus	0.14	0.89	0.04
meditation	mPFC	right angular gyrus	-0.37	0.72	-0.13

Supplemental Table 2.9: Significant Anatomical Gray Matter Volume Clusters for Advanced > Novice Contrast.

Location	Vertices (#)	Cluster (*p*)	Peak MNI (x, y, z)	Group diff. (peak *p*)	Cluster surface (mm^2)
Superior parietal lobule	269	0.049	19.8, -66.3, 51.0	0.00027	166.33

Supplemental Table 2.10: fMRI Meditation Depth and Expectations Survey Results.

	Pre		Post	
	M	*SD*	*M*	*SD*
How well/deeply did you meditate (1 to 10)?	6.05	1.75	6.89	1.91
Meditation depth compared to recent meditation experience (-5 to 5).	-0.11	2.85	-0.32	2.71
Retreat expectation (pre) and perceived effect (post) on meditation ability.	8.95	1.47	8.74	1.79

Supplemental Table 2.11: ELISA Biomarker Levels and Wilcoxon Signed Rank Test (Pre- vs Post-Intervention).

	Pre		Post		Pre vs. Post	
ELISA	*M*	*SD*	*M*	*SD*	*p*	Cohen's d
CART (pg/ml)	413.34	497.1	395.32	363.22	0.37	0.10
CRP (μg/ml)	1.4	1.39	1.45	1.35	0.35	0.01
NPY (ng/ml)	21.58	8.05	19.39	9.33	0.21	-0.42
anandamide (ng/ml)	4.79	4.04	4.56	3.53	0.20	-0.06
beta-endorphin (pg/ml)	3530.6	1198.07	4105.5	1508.76	0.0002	0.42
dynorphin (ng/ml)	136.52	47.56	150.75	56.18	0.009	0.27
leptin (pg/ml)	1794.87	1759.65	1619.6	1760.35	0.097	-0.10
oxytocin (pg/ml)	1038.87	1025.59	1102.5	1306.43	0.97	0.00

Supplemental Table 2.12: Commercial ELISA Kits.

Target	Kit Model	Manufacturer
Oxytocin	ADI-900-153A	ENZO Life Sciences, Farmingdale NY, USA
Beta-endorphin	NBP2-78774	Novus Biologicals, Centennial CO, USA
Dynorphin	EIA-DYN	RayBiotech, Norcross GA, USA
Anandamide	MBS167217	MyBioSource, San Diego CA, USA
Cocaine and amphetamine regulated transcript (CART)	IHUCARTPTKT	Innovative Research, Novi MI, USA
C-reactive protein (CRP)	DCRP00B	USA R&D Systems, Minneapolis MN, USA
Neuropeptide Y (NPY)	EIA-NPY	RayBiotech, Norcross GA, USA

Supplemental Table 2.13: UPLC Metabolomic Detection Conditions.

Component	Condition
Column	Acquity HSS T3 (2.1 mm x 100 mm, 1.8 μm)
Solvent A	Ultrapure water with 0.1% formic acid
Solvent B	Acetonitrile with 0.1% formic acid
Linear gradient elution	5% B to 90% B over 11 minutes
Flow rate	0.4 mL/min
Injection volume	2 μL

Supplemental Table 2.14: Metabolomic Detection Mass Spectrum Conditions.

Parameter	ESI+	ESI-
Curtain Gas (psi)	25	25
IonSpray Voltage (V)	5500	4500
Temperature (°C)	500	500
Ion Source Gas 1 (psi)	50	50
Ion Source Gas 2 (psi)	50	50
Declustering Potential	80	-80
Collision Energy	30	-30
Collision Energy Spread	15	15
Collision Gas (CAD) (widely targeted phase)	High	High

Instrument tuning and mass calibration were performed with 10 and 100 μmol/L polypropylene glycol solutions in QQQ and LIT modes, respectively. A specific set of MRM transitions were monitored for each period according to the metabolites eluted within that period.

Supplemental Table 2.15: A-G: A Priori Protein Index Components.

Gene Symbol	Target Name	UniProt	Gene ID	Dilution
RAF1	RAF protooncogene serine/threonine-protein kinase	P04049	5894	20
JUN	Transcription factor AP-1	P05412	3725	20
NRAS	GTPase NRas	P01111	4893	20
PTPN11	Tyrosine-protein phosphatase non-receptor type 11	Q06124	5781	20
BDNF	Brain-derived neurotrophic factor	P23560	627	0.5
SLITRK1	SLIT and NTRK-like protein 1	Q96PX8	114798	20
BRAF	Serine/threonine-protein kinase B-raf	P15056	673	20
SHC1	SHC-transforming protein 1:Phosphotyrosine Interaction Domain	P29353	6464	20
HRAS	GTPase HRas	P01112	3265	0.5
MECP2	Methyl-CpG-binding protein 2	P51608	4204	20
KRAS	GTPase KRas	P01116	3845	20
CREB1	cAMP response element-binding protein	P16220	1385	20
BDNF	Brain-derived neurotrophic factor	P23560	627	20
MAPK3	Mitogen-activated protein kinase 3	P27361	5595	20
AKT1	RAC-alpha serine/threonine-protein kinase	P31749	207	20
RAC1	Ras-related C3 botulinum toxin substrate 1	P63000	5879	0.5
MAPK1	Mitogen-activated protein kinase 1	P28482	5594	20
GSK3B	Glycogen synthase kinase-3 beta	P49841	2932	20
CAMK2A	Calcium/calmodulin-dependent protein kinase type II subunit alpha	Q9UQM7	815	20
CAMK2B	Calcium/calmodulin-dependent protein kinase type II subunit beta	Q13554	816	20
NTRK1	High affinity nerve growth factor receptor	P04629	4914	20
NTF4	Neurotrophin-4	P34130	4909	20
NTRK2	BDNF/NT-3 growth factors receptor	Q16620	4915	20
KRAS	GTPase KRas	P01116	3845	20
SHC1	SHC-transforming protein 1:Src Homology domain	P29353	6464	20
GRB2	Growth factor receptor-bound protein 2	P62993	2885	20
DLG4	Disks large homolog 4	P78352	1742	20
NGFR	Tumor necrosis factor receptor superfamily member 16	P08138	4804	20
PIK3R1	Phosphatidylinositol 3-kinase regulatory subunit alpha	P27986	5295	20
SOS1	Son of sevenless homolog 1	Q07889	6654	20

Supplemental Table 2.16: SCFA Index.

Entrez Gene Symbol	Target Full Name	UniProt	Entrez Gene ID	Dilution
SLC5A8	Sodium-coupled monocarboxylate transporter 1	Q8N695	160728	0.5
LDHA	L-lactate dehydrogenase A chain	P00338	3939	0.5
ACADS	Short-chain specific acyl-CoA dehydrogenase; mitochondrial	P16219	35	20
ACOX1	Peroxisomal acyl-coenzyme A oxidase 1	Q15067	51	20
ACSS2	Acetyl-coenzyme A synthetase; cytoplasmic	Q9NR19	55902	20
LDHB	L-lactate dehydrogenase B chain	P07195	3945	0.005
FASN	Fatty acid synthase	P49327	2194	20
LDHA	L-lactate dehydrogenase A chain	P00338	3939	0.5

Supplemental Table 2.17: Neuronal index.

Entrez Gene Symbol	Target Name	UniProt	Entrez Gene ID	Dilution
SIRT5	NAD-dependent protein deacylase sirtuin-5; mitochondrial	Q9NXA8	23408	20
CREBBP	CREB-binding protein	Q92793	1387	0.5
RBBP4	Histone-binding protein RBBP4	Q09028	5928	20
SIRT3	NAD-dependent protein deacetylase sirtuin-3; mitochondrial	Q9NTG7	23410	20
HDAC2	Histone deacetylase 2	Q92769	3066	20
SIRT1	NAD-dependent protein deacetylase sirtuin-1	Q96EB6	23411	20
SIRT6	silent mating type information regulation 2 homolog	Q8N6T7	51548	20
SIRT2	NAD-dependent protein deacetylase sirtuin-2	Q8IXJ6	22933	20
MEF2D	Myocyte-specific enhancer factor 2D	Q14814	4209	20
HDAC6	Histone deacetylase 6	Q9UBN7	10013	20
HDAC4	Histone deacetylase 4	P56524	9759	20
HDAC8	Histone deacetylase 8	Q9BY41	55869	20
SIRT2	NAD-dependent protein deacetylase sirtuin-2	Q8IXJ6	22933	0.5
MEF2C	Myocyte-specific enhancer factor 2C	Q06413	4208	20

Supplemental Table 2.18: Glycolysis Pathway Index.

Entrez Gene Symbol	Target Name	UniProt	Entrez Gene ID	Dilution
ENO2	Gamma-enolase	P09104	2026	20
ENO2	Gamma-enolase	P09104	2026	20
ENO1	Alpha-enolase	P06733	2023	0.5
HK2	Hexokinase-2	P52789	3099	20
HK1	Hexokinase-1	P19367	3098	20
LDHA	L-lactate dehydrogenase A chain	P00338	3939	0.5
ENO3	Beta-enolase	P13929	2027	20
PFKM	ATP-dependent 6-phosphofructokinase; muscle type	P08237	5213	0.5
ALDOB	Fructose-bisphosphate aldolase B	P05062	229	0.5
HK3	Hexokinase-3	P52790	3101	20
GAPDH	Glyceraldehyde-3-phosphate dehydrogenase	P04406	2597	0.005
LDHB	L-lactate dehydrogenase B chain	P07195	3945	0.005
PGAM1	Phosphoglycerate mutase 1	P18669	5223	20
PKM	Pyruvate kinase PKM	P14618	5315	0.5
GPI	Glucose-6-phosphate isomerase	P06744	2821	20
TPI1	Triosephosphate isomerase	P60174	7167	0.5
PGK1	Phosphoglycerate kinase 1	P00558	5230	20
ALDOA	Fructose-bisphosphate aldolase A	P04075	226	0.005
LDHA	L-lactate dehydrogenase A chain	P00338	3939	0.5
LDHC	L-lactate dehydrogenase C chain	P07864	3948	20
ALDOC	Fructose-bisphosphate aldolase C	P09972	230	0.5

Supplemental Table 2.19: Endogenous Opioid Pathway Index.

Entrez Gene Symbol	Target Name	UniProt	Entrez Gene ID	Dilution
GABBR1	Gamma-aminobutyric acid type B receptor subunit 1	Q9UBS5	2550	20
GNAI3	Guanine nucleotide-binding protein G(k) subunit alpha	P08754	2773	20
GABBR2	Gamma-aminobutyric acid type B receptor subunit 2:Extracellular domain	O75899	9568	20
PNOC	Prepronociceptin	Q13519	5368	20
GNAI1	Guanine nucleotide-binding protein G(i) subunit alpha-1	P63096	2770	20
PDYN	Dynorphin A (1-17)	P01213	5173	20
CREB1	cAMP response element-binding protein	P16220	1385	20
POMC	Beta-endorphin	P01189	5443	20
CAMK2A	Calcium/calmodulin-dependent protein kinase type II subunit alpha	Q9UQM7	815	20
CAMK2B	Calcium/calmodulin-dependent protein kinase type II subunit beta	Q13554	816	20
PRKACA	cAMP-dependent protein kinase catalytic subunit alpha	P17612	5566	20
POMC	Corticotropin	P01189	5443	20
PENK	Proenkephalin-A	P01210	5179	20
POMC	Pro-opiomelanocortin	P01189	5443	20
GABBR2	Gamma-aminobutyric acid type B receptor subunit 2:Cytoplasmic domain	O75899	9568	20

Supplemental Table 2.20: Pro-Inflammatory Pathways Index.

Entrez Gene Symbol	Target Name	UniProt	Entrez Gene ID	Dilution
STAT3	Signal transducer & activator of transcription 3	P40763	6774	20
STAT1	Signal transducer & activator of transcription 1-alpha/beta	P42224	6772	20
STAT6	Signal transducer & activator of transcription 6	P42226	6778	20
TLR4	Toll-like receptor 4	O00206	7099	20
IL10	Interleukin-10	P22301	3586	20
IL12B	Interleukin-12 subunit beta	P29460	3593	20
IFNG	Interferon gamma	P01579	3458	20
IRAK4	Interleukin-1 receptor-associated kinase 4	Q9NWZ3	51135	20
S100A8	Calgranulin A	P05109	6279	20
CCL5	C-C motif chemokine 5	P13501	6352	20
IL6	Interleukin-6	P05231	3569	20
CCL2	C-C motif chemokine 2	P13500	6347	20
MAPK3	Mitogen-activated protein kinase 3	P27361	5595	20
IFNG	Interferon gamma	P01579	3458	20
IL1B	Interleukin-1 beta	P01584	3553	20
MAPK1	Mitogen-activated protein kinase 1	P28482	5594	20
CXCL8	Interleukin-8	P10145	3576	20
IL17A	Interleukin-17A	Q16552	3605	20
PTGS2	Prostaglandin G/H synthase 2	P35354	5743	20
TLR2	Toll-like receptor 2	O60603	7097	20
IL6	Interleukin-6	P05231	3569	20
S100A9	Protein S100-A9	P06702	6280	20
CCL5	C-C motif chemokine 5	P13501	6352	0.5
IL18	Interleukin-18	Q14116	3606	20
TNF	Tumor necrosis factor	P01375	7124	20
NFKB1	Nuclear factor NF-kappa-B p105 subunit	P19838	4790	20

Supplemental Table 2.21: Anti-Inflammatory Pathways Index.

Entrez Gene Symbol	Target Name	UniProt	Entrez Gene ID	Dilution
STAT6	Signal transducer and activator of transcription 6	P42226	6778	20
MSR1	Macrophage scavenger receptor types I and II:Extracellular domain	P21757	4481	20
SOCS3	Suppressor of cytokine signaling 3	O14543	9021	0.5
IL4	Interleukin-4	P05112	3565	20
IL10	Interleukin-10	P22301	3586	20
TNFAIP3	Tumor necrosis factor alpha-induced protein 3	P21580	7128	20
IL13	Interleukin-13	P35225	3596	20
TGFB1	Transforming growth factor beta-1	P01137	7040	20
MSR1	Macrophage scavenger receptor types I and II:Extracellular domain	P21757	4481	20
CEBPB	CCAAT/enhancer-binding protein beta	P17676	1051	20
STAT5B	Signal transducer and activator of transcription 5B	P51692	6777	20
HMOX1	Heme oxygenase 1	P09601	3162	0.5
KLF4	Krueppel-like factor 4	O43474	9314	20
NFKBIA	NF-kappa-B inhibitor alpha	P25963	4792	20
STAT5A	Signal transducer and activator of transcription 5A	P42229	6776	20
TGFB1	Transforming growth factor beta-1	P01137	7040	20
FOXP3	Forkhead box protein P3	Q9BZS1	50943	20
CEBPB	CCAAT/enhancer-binding protein beta	P17676	1051	20
TGFB1	Transforming growth factor beta-1	P01137	7040	20
PPARG	Peroxisome proliferator activated receptor gamma	P37231	5468	20
MRC1	Macrophage mannose receptor 1	P22897	4360	0.5
MSR1	Macrophage scavenger receptor types I and II:Extracellular domain	P21757	4481	20
CD274	Programmed cell death 1 ligand 1	Q9NZQ7	29126	20
IL1RN	Interleukin-1 receptor antagonist protein	P18510	3557	20
ARG1	Arginase-1	P05089	383	20

Supplemental Table 2.22: Oxidative Phorphorylation Index.

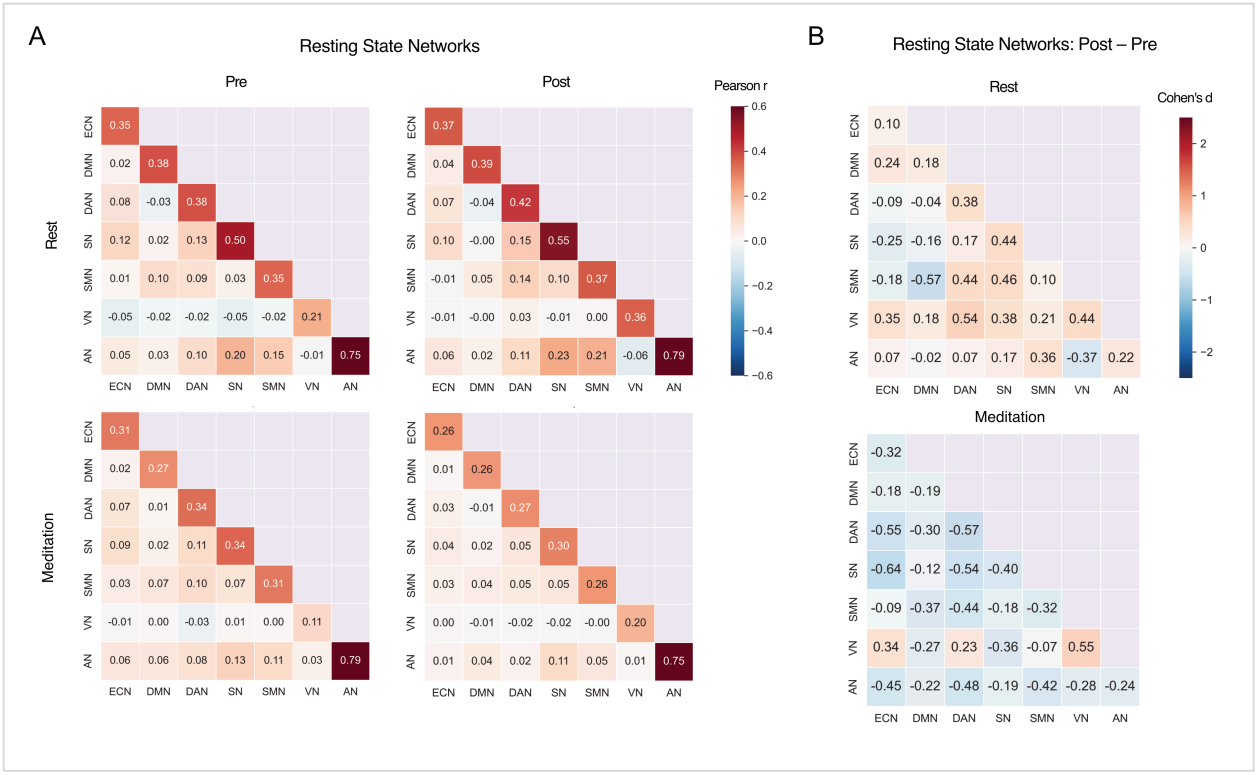
Entrez Gene Symbol	Target Name	UniProt	Entrez Gene ID	Dilution
COX5A	Cytochrome c oxidase subunit 5A (mitochondrial)	P20674	9377	20
NDUFA2	NADH dehydrogenase 1 alpha subcomplex subunit 2	O43678	4695	20
ATP5F1B	ATP synthase subunit beta (mitochondrial)	P06576	506	20
ATP5PF	ATP synthase-coupling factor 6 (mitochondrial)	P18859	522	20
ATP5PO	ATP synthase subunit O (mitochondrial)	P48047	539	20
COX7A2L	Cytochrome c oxidase subunit 7A-related protein	O14548	9167	20

Supplemental Table 2.23: Metabolomic Pathway Analysis.

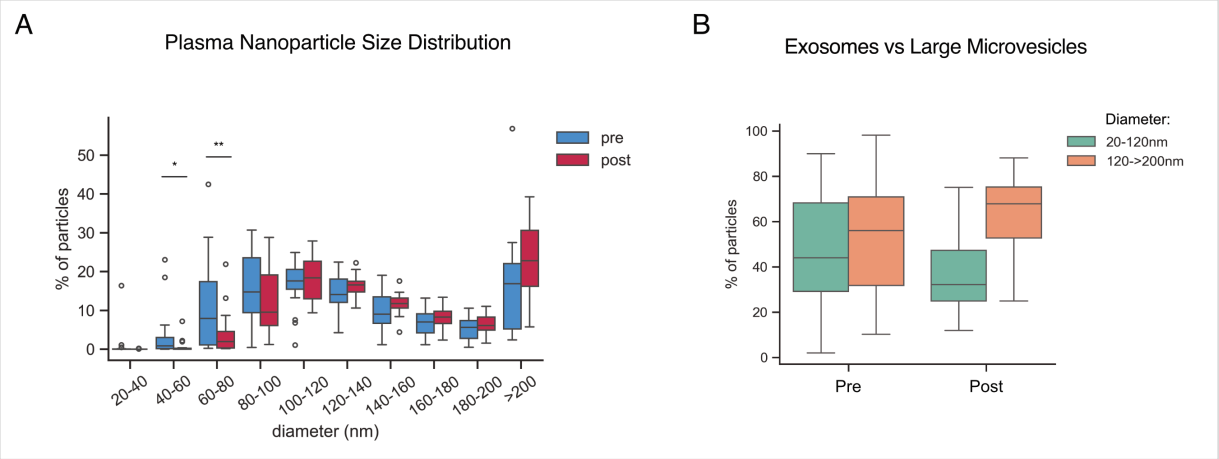
	Total cmpds	Hits	Raw *p*	-log10(*p*)	Holm adjust	FDR	Impact
Tryptophan metabolism	41	6	0.00	3.20	0.03	0.03	0.28
Retinol metabolism	17	1	0.01	1.98	0.54	0.25	0.12
Sphingolipid metabolism	32	3	0.01	1.84	0.74	0.25	0.02
Biosynthesis of unsaturated fatty acids	36	1	0.04	1.44	1	0.35	0.00
Starch and sucrose metabolism	18	1	0.04	1.40	1	0.35	0.42
Neomycin, kanamycin and gentamicin biosynthesis	2	1	0.04	1.40	1	0.35	0.00
Glycerophospholipid metabolism	36	2	0.06	1.20	1	0.48	0.04
Arginine and proline metabolism	36	6	0.08	1.12	1	0.51	0.31
Steroid hormone biosynthesis	87	8	0.10	1.02	1	0.52	0.17
Nicotinate and nicotinamide metabolism	15	4	0.10	1.01	1	0.52	0.19
Drug metabolism - other enzymes	39	1	0.14	0.85	1	0.59	0.00
One carbon pool by folate	9	2	0.14	0.84	1	0.59	0.00
Folate biosynthesis	27	1	0.14	0.84	1	0.59	0.00
Amino sugar and nucleotide sugar metabolism	42	3	0.17	0.77	1	0.65	0.01
Porphyrin metabolism	31	2	0.21	0.69	1	0.69	0.07
Glutathione metabolism	28	4	0.22	0.66	1	0.69	0.05
Inositol phosphate metabolism	30	1	0.22	0.65	1	0.69	0.13
Purine metabolism	70	4	0.28	0.56	1	0.69	0.07
Ether lipid metabolism	20	1	0.28	0.55	1	0.69	0.04
Cysteine and methionine metabolism	33	7	0.29	0.54	1	0.69	0.31
Glycine, serine and threonine metabolism	33	5	0.30	0.53	1	0.69	0.34
Lipoic acid metabolism	28	1	0.33	0.48	1	0.69	0.00
Histidine metabolism	16	5	0.33	0.48	1	0.69	0.22
Butanoate metabolism	15	4	0.34	0.47	1	0.69	0.00
Fatty acid biosynthesis	47	1	0.34	0.46	1	0.69	0.00
Lysine degradation	30	1	0.36	0.45	1	0.69	0.11
Propanoate metabolism	22	3	0.37	0.43	1	0.69	0.00
Tyrosine metabolism	42	4	0.38	0.42	1	0.69	0.25
Phenylalanine metabolism	8	4	0.40	0.40	1	0.69	0.60
Nitrogen metabolism	6	2	0.41	0.39	1	0.69	0.00
Ascorbate and aldarate metabolism	9	2	0.41	0.39	1	0.69	0.00

Supplemental Table 2.23: Metabolomic Pathway Analysis. (Continued)

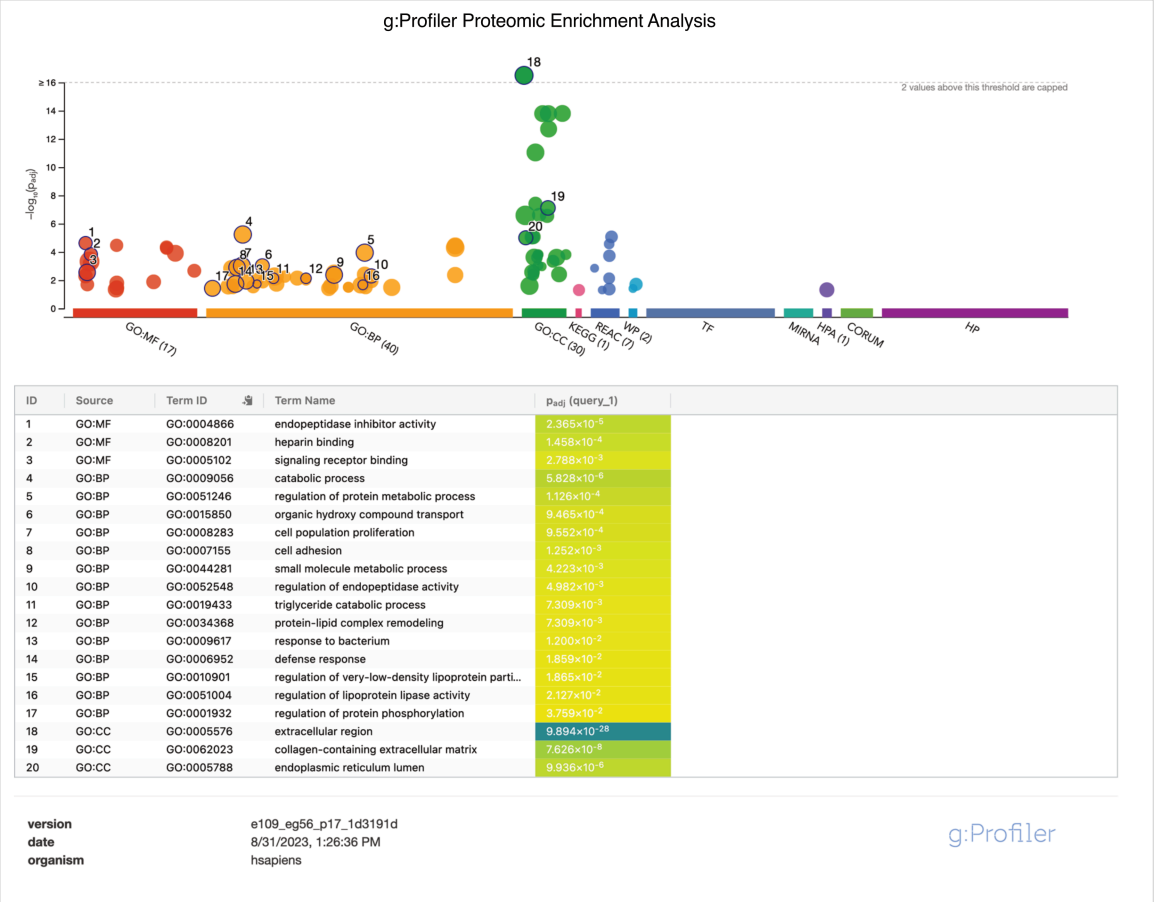
	Total cmpds	Hits	Raw *p*	-log10(*p*)	Holm adjust	FDR	Impact
Pentose phosphate pathway	23	4	0.42	0.38	1	0.69	0.18
Fructose and mannose metabolism	20	3	0.46	0.34	1	0.73	0.03
Citrate cycle (TCA cycle)	20	5	0.47	0.33	1	0.73	0.28
Glycerolipid metabolism	16	1	0.53	0.28	1	0.79	0.09
Taurine and hypotaurine metabolism	8	2	0.54	0.27	1	0.79	0.60
Glyoxylate and dicarboxylate metabolism	32	6	0.58	0.24	1	0.81	0.18
Galactose metabolism	27	5	0.59	0.23	1	0.81	0.03
Phenylalanine, tyrosine and tryptophan biosynthesis	4	2	0.60	0.22	1	0.81	1.00
Ubiquinone and other terpenoid-quinone biosynthesis	18	1	0.66	0.18	1	0.86	0.00
Vitamin B6 metabolism	9	1	0.67	0.17	1	0.86	0.00
Arginine biosynthesis	14	8	0.71	0.15	1	0.86	0.57
Linoleic acid metabolism	5	1	0.71	0.15	1	0.86	0.00
beta-Alanine metabolism	21	4	0.71	0.15	1	0.86	0.00
Valine, leucine and isoleucine biosynthesis	8	2	0.74	0.13	1	0.87	0.00
Primary bile acid biosynthesis	46	5	0.82	0.09	1	0.90	0.03
D-Amino acid metabolism	15	1	0.82	0.08	1	0.90	0.00
Valine, leucine and isoleucine degradation	40	3	0.84	0.08	1	0.90	0.03
Alanine, aspartate and glutamate metabolism	28	9	0.84	0.08	1	0.90	0.58
Pentose and glucuronate interconversions	19	1	0.85	0.07	1	0.90	0.07
Pyrimidine metabolism	39	7	0.88	0.06	1	0.91	0.22
Pantothenate and CoA biosynthesis	20	4	0.96	0.02	1	0.97	0.01
Caffeine metabolism	10	9	0.97	0.01	1	0.97	1.00



Supplemental Figure 2.1: A. Resting State Functional Connectivity Networks. Within- and between-network resting-state connectivity during rest and meditation, pre- and post-intervention. Cell values and color scale represent mean Pearson correlation values across participants. As expected, intra-network connectivity is stronger than inter-network connectivity, validating data quality. B. Pre Versus Post-Intervention Changes in Functional Connectivity. Pre- versus post-retreat resting state network connectivity during (Left) rest and (Right) meditation. Cell values and color scale represent Cohen's d effect size values from paired samples t-tests. No statistically significant results adjusted for 28 multiple comparisons, $p_{FWE} < 0.05$; however, pre-to-post intervention there is generally weaker intra and inter-network connectivity during meditation (with exceptions clustered around the visual network), and generally stronger connectivity during rest, except for SMN-DMN, SMN-ECN, SN-ECN, SN-DMN, and AN-VN.



Supplemental Figure 2.2: A. Plasma Nanoparticle Size Distributions. Asterisks denote statistical significance for pre vs post two-tailed paired t-tests: * ($p < 0.05$), ** ($p < 0.01$). B. Exosomes Versus Larger Microvesicles. Percentage of plasma exosomes (20-120nm) versus larger microvesicles (120-200nm) pre- and post-intervention. Asterisks denote statistical significance on two-tailed t-tests, * ($p < 0.05$), ** ($p < 0.01$), *** ($p < 0.001$).

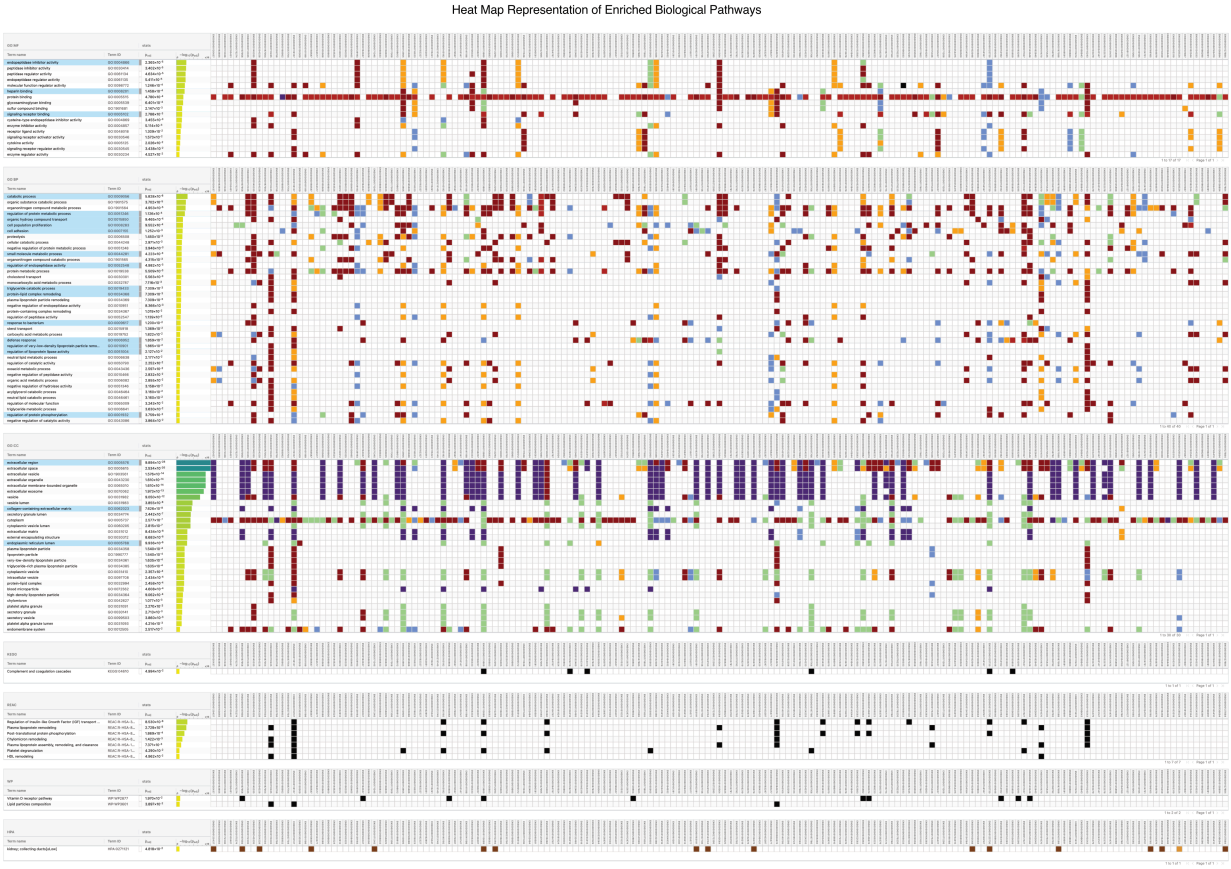


ID	Source	Term ID	Term Name	p_{adj} (query_1)
1	GO:MF	GO:0004866	endopeptidase inhibitor activity	2.365×10^{-5}
2	GO:MF	GO:0008201	heparin binding	1.458×10^{-4}
3	GO:MF	GO:0005102	signaling receptor binding	2.788×10^{-3}
4	GO:BP	GO:0009056	catabolic process	5.828×10^{-6}
5	GO:BP	GO:0051246	regulation of protein metabolic process	1.126×10^{-4}
6	GO:BP	GO:0015850	organic hydroxy compound transport	9.465×10^{-4}
7	GO:BP	GO:0008283	cell population proliferation	9.552×10^{-4}
8	GO:BP	GO:0007155	cell adhesion	1.252×10^{-3}
9	GO:BP	GO:0044281	small molecule metabolic process	4.223×10^{-3}
10	GO:BP	GO:0052548	regulation of endopeptidase activity	4.982×10^{-3}
11	GO:BP	GO:0019433	triglyceride catabolic process	7.309×10^{-3}
12	GO:BP	GO:0034368	protein-lipid complex remodeling	7.309×10^{-3}
13	GO:BP	GO:0009617	response to bacterium	1.200×10^{-2}
14	GO:BP	GO:0006952	defense response	1.859×10^{-2}
15	GO:BP	GO:0010901	regulation of very-low-density lipoprotein parti...	1.865×10^{-2}
16	GO:BP	GO:0051004	regulation of lipoprotein lipase activity	2.127×10^{-2}
17	GO:BP	GO:0001932	regulation of protein phosphorylation	3.759×10^{-2}
18	GO:CC	GO:0005576	extracellular region	9.894×10^{-28}
19	GO:CC	GO:0062023	collagen-containing extracellular matrix	7.626×10^{-8}
20	GO:CC	GO:0005788	endoplasmic reticulum lumen	9.936×10^{-6}

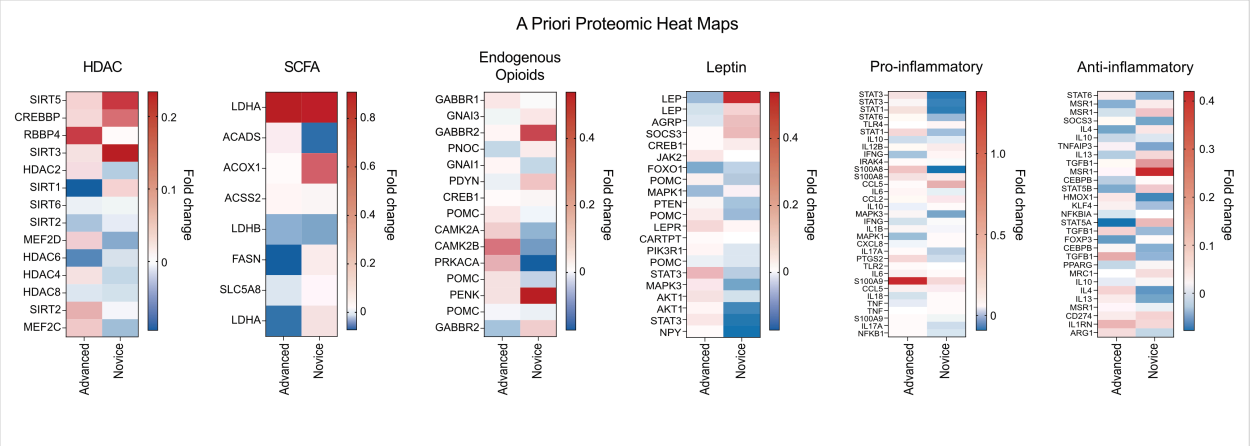
version	e109_eg56_p17_1d3191d
date	8/31/2023, 1:26:36 PM
organism	hsapiens

g:Profiler

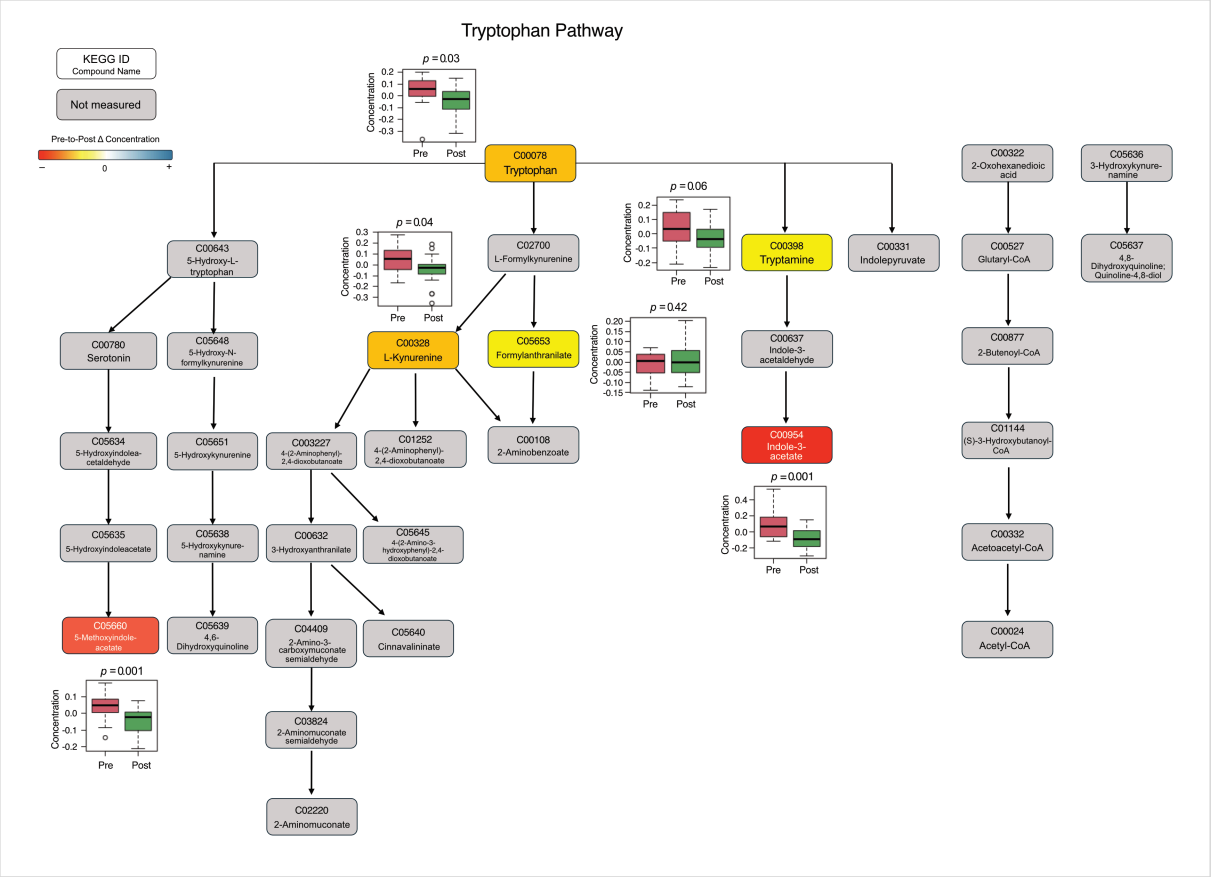
Supplemental Figure 2.3: Results of a proteomic enrichment analysis using g:Profiler. The top panel shows a multi-category Manhattan plot where significant gene ontology (GO) terms, pathways, and protein complexes are visualized. Each dot represents an enriched term, with the x-axis indicating the category (e.g., GO: Molecular Function [MF], GO: Biological Process [BP], KEGG pathways, Reactome, CORUM) and the y-axis showing the -log10 adjusted p-value (p_{adj}) of enrichment. Terms with $p_{adj} < 0.05$ are considered significant. Two values exceed the threshold and are capped at the top of the plot. The bottom table lists the top 20 enriched terms, including their source, term ID, term name, and adjusted p-value. The most enriched terms include "extracellular region" ($p_{adj} = 9.894 \times 10^{-28}$), "collagen-containing extracellular matrix" ($p_{adj} = 7.626 \times 10^{-8}$), and "endoplasmic reticulum lumen" ($p_{adj} = 9.936 \times 10^{-6}$). The analysis highlights key molecular functions, biological processes, and cellular components relevant to the proteomic dataset under investigation.



Supplemental Figure 2.4: Heatmap Representation of Enriched Biological Pathways.
The heatmap depicts the enrichment of various biological pathways and functional terms across multiple samples using g:Profiler analysis. The y-axis lists the enriched terms grouped by categories, including Gene Ontology: Molecular Function (GO:MF), Biological Process (GO:BP), Cellular Component (GO:CC), KEGG pathways, Reactome pathways, CORUM complexes, and transcription factors (TF). The x-axis represents individual samples. Each colored cell indicates the presence and significance of a specific term in a corresponding sample, with color intensity reflecting the level of enrichment (adjusted p-value). Darker colors indicate stronger enrichment (lower p-values). Terms that are significantly enriched ($p_{adj} < 0.05$) are highlighted, emphasizing distinct biological processes and cellular functions enriched in subsets of the dataset. The top-ranked terms in each category, such as "endocytic vesicle membrane," "lipid catabolic process," and "extracellular matrix," are shown alongside a bar plot indicating their relative significance across the dataset. This visualization highlights key differences in functional enrichment across samples, providing insights into the underlying biological variations.



Supplemental Figure 2.5: Proteomic A Priori Protein Heat Maps. Heat maps for a priori protein indices showing fold change levels per protein for advanced and novice participants.



Supplemental Figure 2.6: Full Tryptophan Pathway. Colored boxes represent detected metabolites. Color scale represents the magnitude of pre-to-post change in concentration. Box plots show pre and post concentration distributions and two-tailed paired t-test p-values.

REFERENCES

1. Ashar YK, Gordon A, Schubiner H, Uipi C, Knight K, Anderson Z, Carlisle J, Polisky L, Geuter S, Flood TF, Kragel PA, Dimidjian S, Lumley MA, Wager TD. Effect of Pain Reprocessing Therapy vs Placebo and Usual Care for Patients With Chronic Back Pain: A Randomized Clinical Trial. JAMA Psychiatry. 2022;79:13–23. doi:10.1001/jamapsychiatry.2021.2669

2. Benedetti F, Carlino E, Pollo A. How Placebos Change the Patient's Brain. Neuropsychopharmacology. 2011;36:339–54. doi:10.1038/npp.2010.81 PubMed PMID: 20592717; PubMed Central PMCID: PMC3055515.

3. Benedetti F, Piedimonte A, Frisaldi E. How do placebos work? Eur J Psychotraumatology. 2018;9:1533370. doi:10.1080/20008198.2018.1533370 PubMed PMID: 30397427; PubMed Central PMCID: PMC6211282.

4. Jonas WB, Crawford C, Colloca L, Kaptchuk TJ, Moseley B, Miller FG, Kriston L, Linde K, Meissner K. To what extent are surgery and invasive procedures effective beyond a placebo response? A systematic review with meta-analysis of randomised, sham controlled trials. BMJ Open. 2015;5:e009655. doi:10.1136/bmjopen-2015-009655 PubMed PMID: 26656986.

5. Probst P, Grummich K, Harnoss JC, Hüttner FJ, Jensen K, Braun S, Kieser M, Ulrich A, Büchler MW, Diener MK. Placebo-Controlled Trials in Surgery: A Systematic Review and Meta-Analysis. Medicine (Baltimore). 2016;95:e3516. doi:10.1097/MD.0000000000003516

6. Beecher HK. Surgery as Placebo: A Quantitative Study of Bias. JAMA. 1961;176:1102–7. doi:10.1001/jama.1961.63040260007008

7. Hoenemeyer TW, Kaptchuk TJ, Mehta TS, Fontaine KR. Open-Label Placebo Treatment for Cancer-Related Fatigue: A Randomized-Controlled Clinical Trial. Sci Rep. 2018;8:1. doi:10.1038/s41598-018-20993-y

8. Carvalho C, Caetano JM, Cunha L, Rebouta P, Kaptchuk TJ, Kirsch I. Open-label placebo treatment in chronic low back pain: a randomized controlled trial. Pain. 2016;157:2766–72. doi:10.1097/j.pain.0000000000000700 PubMed PMID: 27755279; PubMed Central PMCID: PMC5113234.

9. Schaefer M, Harke R, Denke C. Open-Label Placebos Improve Symptoms in Allergic Rhinitis: A Randomized Controlled Trial. Psychother Psychosom. 2016;85:373–4. doi:10.1159/000447242

10. Zanesco AP, King BG, Conklin QA, Saron CD. The Occurrence of Psychologically Profound, Meaningful, and Mystical Experiences During a Month-Long Meditation Retreat. Mindfulness. 2023;14:606–21. doi:10.1007/s12671-023-02076-w

11. Kuyken W, Warren FC, Taylor RS, Whalley B, Crane C, Bondolfi G, Hayes R, Huijbers M, Ma H, Schweizer S, Segal Z, Speckens A, Teasdale JD, Van Heeringen K, Williams M, Byford S, Byng R, Dalgleish T. Efficacy of Mindfulness-Based Cognitive Therapy in Prevention of Depressive Relapse: An Individual Patient Data Meta-analysis From Randomized Trials. JAMA Psychiatry. 2016;73:565–74. doi:10.1001/jamapsychiatry.2016.0076

12. Goyal M, Singh S, Sibinga EMS, Gould NF, Rowland-Seymour A, Sharma R, Berger Z, Sleicher D, Maron DD, Shihab HM, Ranasinghe PD, Linn S, Saha S, Bass EB, Haythornthwaite JA. Meditation Programs for Psychological Stress and Well-being: A Systematic Review and Meta-analysis. JAMA Intern Med. 2014;174:357–68. doi:10.1001/jamainternmed.2013.13018

13. Fox KCR, Dixon ML, Nijeboer S, Girn M, Floman JL, Lifshitz M, Ellamil M, Sedlmeier P, Christoff K. Functional neuroanatomy of meditation: A review and meta-analysis of 78 functional neuroimaging investigations. Neurosci Biobehav Rev. 2016;65:208–28. doi:10.1016/j.neubiorev.2016.03.021

14. Afonso RF, Kraft I, Aratanha MA, Kozasa EH. Neural correlates of meditation: a review of structural and functional MRI studies. Front Biosci-Sch. 2020;12:1. doi:10.2741/S542

15. Lomas T, Ivtzan I, Fu CHY. A systematic review of the neurophysiology of mindfulness on EEG oscillations. Neurosci Biobehav Rev. 2015;57:401–10. doi:10.1016/j.neubiorev.2015.09.018

16. Oyler DL, Hulett JM, Pratscher SD, Price-Blackshear MA, Murphy EA, Bettencourt BA. The Influence of Meditative Interventions on Immune Functioning: A Meta-Analysis. Mindfulness. 2023;14:1815–51. doi:10.1007/s12671-023-02157-w

17. Davidson JM. The Physiology of Meditation and Mystical States of Consciousness. Perspect Biol Med. 1976;19:345–80.

18. Tang YY, Ma Y, Fan Y, Feng H, Wang J, Feng S, Lu Q, Hu B, Lin Y, Li J, Zhang Y, Wang Y, Zhou L, Fan M. Central and autonomic nervous system interaction is altered by short-term meditation. Proc Natl Acad Sci. 2009;106:8865–70. doi:10.1073/pnas.0904031106

19. Álvarez-López MJ, Conklin QA, Cosín-Tomás M, Shields GS, King BG, Zanesco AP, Kaliman P, Saron CD. Changes in the expression of inflammatory and epigenetic-modulatory genes after an intensive meditation retreat. Compr Psychoneuroendocrinology. 2022;11:100152. doi:10.1016/j.cpnec.2022.100152

20. Buric I, Farias M, Jong J, Mee C, Brazil IA. What Is the Molecular Signature of Mind–Body Interventions? A Systematic Review of Gene Expression Changes Induced by Meditation and Related Practices. Front Immunol [Internet]. 2017 [cited 2023 Dec 24];8. Available from: https://www.frontiersin.org/articles/10.3389/fimmu.2017.00670

21. Venditti S, Verdone L, Reale A, Vetriani V, Caserta M, Zampieri M. Molecules of Silence: Effects of Meditation on Gene Expression and Epigenetics. Front Psychol [Internet]. 2020 [cited 2023 Dec 24];11. Available from: https://www.frontiersin.org/articles/10.3389/fpsyg.2020.01767

22. Cahn BR, Goodman MS, Peterson CT, Maturi R, Mills PJ. Yoga, Meditation and Mind-Body Health: Increased BDNF, Cortisol Awakening Response, and Altered Inflammatory Marker Expression after a 3-Month Yoga and Meditation Retreat. Front Hum Neurosci [Internet]. 2017 [cited 2023 Dec 24];11. Available from: https://www.frontiersin.org/articles/10.3389/fnhum.2017.00315

23. Morin-Alain V, Larouche E, Chouinard AM, Audet MC, Goulet S, Rousseau LS, Hudon C. Effects of a Mindfulness-Based Intervention on Circulating Cytokine Levels in Individuals with Amnestic Mild Cognitive Impairment: A Pilot Study. OBM Integr Complement Med. 2020;5:2. doi:10.21926/obm.icm.2002022

24. Xue T, Chiao B, Xu T, Li H, Shi K, Cheng Y, Shi Y, Guo X, Tong S, Guo M, Chew SH, Ebstein RP, Cui D. The heart-brain axis: A proteomics study of meditation on the cardiovascular system of Tibetan Monks. eBioMedicine. 2022;80. doi:10.1016/j.ebiom.2022.104026 PubMed PMID: 35525203.

25. Chen W, Zeng J, Wang W, Yang B, Zhong L, Zhou J. Comprehensive Metabolomic and Lipidomic Analysis Reveals Metabolic Changes After Mindfulness Training. Mindfulness. 2020;11:1390–400. doi:10.1007/s12671-020-01359-w

26. Raman M, Vishnubhotla R, Ramay HR, Gonçalves MCB, Shin AS, Pawale D, Subramaniam B, Sadhasivam S. Isha yoga practices, vegan diet, and participation in Samyama meditation retreat: impact on the gut microbiome & metabolome – a non-randomized trial. BMC Complement Med Ther. 2023;23:107. doi:10.1186/s12906-023-03935-8

27. Greenwell B. Energies of Transformation: A Guide to the Kundalini Process. Motilal Banarsidass Publishe; 2002. 354 p.

28. Krishna G. Kundalini: The Evolutionary Energy in Man. Shambhala Publications; 2018. 308 p.

29. Hopkins J. Meditation on Emptiness. Simon and Schuster; 2014. 717 p.

30. Kaptchuk TJ. Open-Label Placebo: Reflections on a Research Agenda. Perspect Biol Med. 2018;61:311–34.

31. Prakash RS, Shankar A, Tripathi V, Yang WFZ, Fisher M, Bauer CCC, Betzel R, Sacchet MD. Mindfulness Meditation and Network Neuroscience: Review, Synthesis, and Future Directions. Biol Psychiatry Cogn Neurosci Neuroimaging. 2024. doi:10.1016/j.bpsc.2024.11.005

32. Brewer JA, Worhunsky PD, Gray JR, Tang YY, Weber J, Kober H. Meditation experience is associated with differences in default mode network activity and connectivity. Proc Natl Acad Sci. 2011;108:20254–9. doi:10.1073/pnas.1112029108

33. Barrett LF, Simmons WK. Interoceptive predictions in the brain. Nat Rev Neurosci. 2015;16:7. doi:10.1038/nrn3950

34. Hove MJ, Stelzer J, Nierhaus T, Thiel SD, Gundlach C, Margulies DS, Van Dijk KRA, Turner R, Keller PE, Merker B. Brain Network Reconfiguration and Perceptual Decoupling During an Absorptive State of Consciousness. Cereb Cortex. 2016;26:3116–24. doi:10.1093/cercor/bhv137

35. Makris N, Goldstein JM, Kennedy D, Hodge SM, Caviness VS, Faraone SV, Tsuang MT, Seidman LJ. Decreased volume of left and total anterior insular lobule in schizophrenia. Schizophr Res. 2006;83:155–71. doi:10.1016/j.schres.2005.11.020 PubMed PMID: 16448806.

36. Frazier JA, Chiu S, Breeze JL, Makris N, Lange N, Kennedy DN, Herbert MR, Bent EK, Koneru VK, Dieterich ME, Hodge SM, Rauch SL, Grant PE, Cohen BM, Seidman LJ, Caviness VS, Biederman J. Structural brain magnetic resonance imaging of limbic and thalamic volumes in pediatric bipolar disorder. Am J Psychiatry. 2005;162:1256–65. doi:10.1176/appi.ajp.162.7.1256 PubMed PMID: 15994707.

37. Desikan RS, Ségonne F, Fischl B, Quinn BT, Dickerson BC, Blacker D, Buckner RL, Dale AM, Maguire RP, Hyman BT, Albert MS, Killiany RJ. An automated labeling system for subdividing the human cerebral cortex on MRI scans into gyral based regions of interest. NeuroImage. 2006;31:968–80. doi:10.1016/j.neuroimage.2006.01.021 PubMed PMID: 16530430.

38. Power JD, Cohen AL, Nelson SM, Wig GS, Barnes KA, Church JA, Vogel AC, Laumann TO, Miezin FM, Schlaggar BL, Petersen SE. Functional Network Organization of the Human Brain. Neuron. 2011;72:665–78. doi:10.1016/j.neuron.2011.09.006

39. Grant JA, Duerden EG, Courtemanche J, Cherkasova M, Duncan GH, Rainville P. Cortical thickness, mental absorption and meditative practice: Possible implications for disorders of attention. Biol Psychol. 2013;92:275–81. doi:10.1016/j.biopsycho.2012.09.007

40. Aruga J, Mikoshiba K. Identification and characterization of Slitrk, a novel neuronal transmembrane protein family controlling neurite outgrowth. Mol Cell Neurosci. 2003;24:117–29. doi:10.1016/S1044-7431(03)00129-5

41. Beaubien F, Raja R, Kennedy TE, Fournier AE, Cloutier JF. Slitrk1 is localized to excitatory synapses and promotes their development. Sci Rep. 2016;6:27343. doi:10.1038/srep27343 PubMed PMID: 27273464; PubMed Central PMCID: PMC4895136.

42. Jevning R, Wallace RK, Beidebach M. The physiology of meditation: A review. A wakeful hypometabolic integrated response. Neurosci Biobehav Rev. 1992;16:415–24. doi:10.1016/S0149-7634(05)80210-6

43. Cremers NAJ, van den Bosch MHJ, van Dalen S, Di Ceglie I, Ascone G, van de Loo F, Koenders M, van der Kraan P, Sloetjes A, Vogl T, Roth J, Geven EJW, Blom AB, van Lent PLEM. S100A8/A9 increases the mobilization of pro-inflammatory Ly6Chigh monocytes to the synovium during experimental osteoarthritis. Arthritis Res Ther. 2017;19:217. doi:10.1186/s13075-017-1426-6

44. Crowe LAN, McLean M, Kitson SM, Melchor EG, Patommel K, Cao HM, Reilly JH, Leach WJ, Rooney BP, Spencer SJ, Mullen M, Chambers M, Murrell GAC, McInnes IB, Akbar M, Millar NL. S100A8 & S100A9: Alarmin mediated inflammation in tendinopathy. Sci Rep. 2019;9:1463. doi:10.1038/s41598-018-37684-3 PubMed PMID: 30728384; PubMed Central PMCID: PMC6365574.

45. Pascoe MC, Thompson DR, Jenkins ZM, Ski CF. Mindfulness mediates the physiological markers of stress: Systematic review and meta-analysis. J Psychiatr Res. 2017;95:156–78. doi:10.1016/j.jpsychires.2017.08.004 PubMed PMID: 28863392.

46. Milacic M, Beavers D, Conley P, Gong C, Gillespie M, Griss J, Haw R, Jassal B, Matthews L, May B, Petryszak R, Ragueneau E, Rothfels K, Sevilla C, Shamovsky V, Stephan R, Tiwari K, Varusai T, Weiser J, Wright A, Wu G, Stein L, Hermjakob H, D'Eustachio P. The Reactome Pathway Knowledgebase 2024. Nucleic Acids Res. 2024;52:D672–8. doi:10.1093/nar/gkad1025 PubMed PMID: 37941124; PubMed Central PMCID: PMC10767911.

47. Bremer B, Wu Q, Mora Álvarez MG, Hölzel BK, Wilhelm M, Hell E, Tavacioglu EE, Torske A, Koch K. Mindfulness meditation increases default mode, salience, and central executive network connectivity. Sci Rep. 2022;12:13219. doi:10.1038/s41598-022-17325-6

48. Vishnubhotla RV, Radhakrishnan R, Kveraga K, Deardorff R, Ram C, Pawale D, Wu YC, Renschler J, Subramaniam B, Sadhasivam S. Advanced Meditation Alters Resting-State Brain Network Connectivity Correlating With Improved Mindfulness. Front Psychol. 2021;12. doi:10.3389/fpsyg.2021.745344

49. Datko M, Lutz J, Gawande R, Comeau A, To MN, Desel T, Gan J, Desbordes G, Napadow V, Schuman-Olivier Z. Increased insula response to interoceptive attention following mindfulness training is associated with increased body trusting among patients with depression. Psychiatry Res Neuroimaging. 2022;327:111559. doi:10.1016/j.pscychresns.2022.111559 PubMed PMID: 36308976.

50. Laukkonen RE, Slagter HA. From many to (n)one: Meditation and the plasticity of the predictive mind. Neurosci Biobehav Rev. 2021;128:199–217. doi:10.1016/j.neubiorev.2021.06.021

51. Van Overwalle F, Mariën P. Functional connectivity between the cerebrum and cerebellum in social cognition: A multi-study analysis. NeuroImage. 2016;124:248–55. doi:10.1016/j.neuroimage.2015.09.001

52. Guidotti R, D'Andrea A, Basti A, Raffone A, Pizzella V, Marzetti L. Long-Term and Meditation-Specific Modulations of Brain Connectivity Revealed Through Multivariate Pattern Analysis. Brain Topogr. 2023;36:409–18. doi:10.1007/s10548-023-00950-3

53. Garrison KA, Zeffiro TA, Scheinost D, Constable RT, Brewer JA. Meditation leads to reduced default mode network activity beyond an active task. Cogn Affect Behav Neurosci. 2015;15:712–20. doi:10.3758/s13415-015-0358-3 PubMed PMID: 25904238; PubMed Central PMCID: PMC4529365.

54. Guo W, Liu F, Xue Z, Gao K, Liu Z, Xiao C, Chen H, Zhao J. Abnormal resting-state cerebellar-cerebral functional connectivity in treatment-resistant depression and treatment sensitive depression. Prog Neuropsychopharmacol Biol Psychiatry. 2013;44:51–7. doi:10.1016/j.pnpbp.2013.01.010 PubMed PMID: 23352887.

55. Shen YQ, Zhou HX, Chen X, Castellanos FX, Yan CG. Meditation effect in changing functional integrations across large-scale brain networks: Preliminary evidence from a meta-analysis of seed-based functional connectivity. J Pac Rim Psychol. 2020;14:e10. doi:10.1017/prp.2020.1

56. Friston K. The free-energy principle: a unified brain theory? Nat Rev Neurosci. 2010;11:2. doi:10.1038/nrn2787

57. Seth AK. Interoceptive inference, emotion, and the embodied self. Trends Cogn Sci. 2013;17:565–73. doi:10.1016/j.tics.2013.09.007 PubMed PMID: 24126130.

58. Cahn BR, Goodman MS, Peterson CT, Maturi R, Mills PJ. Yoga, Meditation and Mind-Body Health: Increased BDNF, Cortisol Awakening Response, and Altered Inflammatory Marker Expression after a 3-Month Yoga and Meditation Retreat. Front Hum Neurosci. 2017;11. doi:10.3389/fnhum.2017.00315

59. Sezer I, Sacchet MD. Advanced and long-term meditation and the autonomic nervous system: A review and synthesis. Neurosci Biobehav Rev. 2025;173:106141. doi:10.1016/j.neubiorev.2025.106141

60. van Lutterveld R, van Dellen E, Pal P, Yang H, Stam CJ, Brewer J. Meditation is associated with increased brain network integration. NeuroImage. 2017;158:18–25. doi:10.1016/j.neuroimage.2017.06.071

61. Calder AE, Hasler G. Towards an understanding of psychedelic-induced neuroplasticity. Neuropsychopharmacology. 2023;48:104–12. doi:10.1038/s41386-022-01389-z

62. Smigielski L, Scheidegger M, Kometer M, Vollenweider FX. Psilocybin-assisted mindfulness training modulates self-consciousness and brain default mode network connectivity with lasting effects. NeuroImage. 2019;196:207–15. doi:10.1016/j.neuroimage.2019.04.009 PubMed PMID: 30965131.

63. Tilburt JC, Emanuel EJ, Kaptchuk TJ, Curlin FA, Miller FG. Prescribing "placebo treatments": results of national survey of US internists and rheumatologists. BMJ. 2008;337:a1938. doi:10.1136/bmj.a1938 PubMed PMID: 18948346.

64. Saatcioglu F. Regulation of gene expression by yoga, meditation and related practices: A review of recent studies. Asian J Psychiatry. 2013;This issue includes a special section on Spirituality and Psychiatry6:74–7. doi:10.1016/j.ajp.2012.10.002

65. Laumann TO, Snyder AZ, Gratton C. Challenges in the measurement and interpretation of dynamic functional connectivity. Imaging Neurosci. 2024;2:1–19. doi:10.1162/imag_a_00366

66. Vadaq N, van de Wijer L, van Eekeren LE, Koenen H, de Mast Q, Joosten LAB, Netea MG, Matzaraki V, van der Ven AJAM. Targeted plasma proteomics reveals upregulation of distinct inflammatory pathways in people living with HIV. iScience. 2022;25:105089. doi:10.1016/j.isci.2022.105089 PubMed PMID: 36157576; PubMed Central PMCID: PMC9494231.

67. Vadaq N, van de Wijer L, van Eekeren LE, Koenen H, de Mast Q, Joosten LAB, Netea MG, Matzaraki V, van der Ven AJAM. Targeted plasma proteomics reveals upregulation of distinct inflammatory pathways in people living with HIV. iScience. 2022;25:105089. doi:10.1016/j.isci.2022.105089 PubMed PMID: 36157576; PubMed Central PMCID: PMC9494231.

68. Garrison K, Santoyo J, Davis J, Thornhill T, Kerr C, Brewer J. Effortless awareness: using real time neurofeedback to investigate correlates of posterior cingulate cortex activity in meditators' self-report. Front Hum Neurosci. 2013;7. doi:10.3389/fnhum.2013.00440

69. Tagliazucchi E, Laufs H. Decoding wakefulness levels from typical fMRI resting-state data reveals reliable drifts between wakefulness and sleep. Neuron. 2014;82:695–708. doi:10.1016/j.neuron.2014.03.020 PubMed PMID: 24811386.

70. Maclean KA, Leoutsakos JMS, Johnson MW, Griffiths RR. Factor Analysis of the Mystical Experience Questionnaire: A Study of Experiences Occasioned by the Hallucinogen Psilocybin. J Sci Study Relig. 2012;51:721–37. doi:10.1111/j.1468-5906.2012.01685.x PubMed PMID: 23316089; PubMed Central PMCID: PMC3539773.

71. Esteban O, Markiewicz CJ, Blair RW, Moodie CA, Isik AI, Erramuzpe A, Kent JD, Goncalves M, DuPre E, Snyder M, Oya H, Ghosh SS, Wright J, Durnez J, Poldrack RA, Gorgolewski KJ. fMRIPrep: a robust preprocessing pipeline for functional MRI. Nat Methods. 2019;16:1. doi:10.1038/s41592-018-0235-4

72. Andersson JLR, Skare S, Ashburner J. How to correct susceptibility distortions in spin-echo echo-planar images: application to diffusion tensor imaging. NeuroImage. 2003;20:870–88. doi:10.1016/S1053-8119(03)00336-7

73. Avants BB, Epstein CL, Grossman M, Gee JC. Symmetric diffeomorphic image registration with cross-correlation: Evaluating automated labeling of elderly and neurodegenerative brain. Med Image Anal. 2008;Special Issue on The Third International Workshop on Biomedical Image Registration – WBIR 200612:26–41. doi:10.1016/j.media.2007.06.004

74. Zhang Y, Brady M, Smith S. Segmentation of brain MR images through a hidden Markov random field model and the expectation-maximization algorithm. IEEE Trans Med Imaging. 2001;20:45–57. doi:10.1109/42.906424

75. Dale AM, Fischl B, Sereno MI. Cortical Surface-Based Analysis: I. Segmentation and Surface Reconstruction. NeuroImage. 1999;9:179–94. doi:10.1006/nimg.1998.0395

76. Jenkinson M, Smith S. A global optimisation method for robust affine registration of brain images. Med Image Anal. 2001;5:143–56. doi:10.1016/S1361-8415(01)00036-6

77. Pruim RHR, Mennes M, van Rooij D, Llera A, Buitelaar JK, Beckmann CF. ICA-AROMA: A robust ICA-based strategy for removing motion artifacts from fMRI data. NeuroImage. 2015;112:267–77. doi:10.1016/j.neuroimage.2015.02.064

78. Abraham A, Pedregosa F, Eickenberg M, Gervais P, Mueller A, Kossaifi J, Gramfort A, Thirion B, Varoquaux G. Machine learning for neuroimaging with scikit-learn. Front Neuroinformatics. 2014;8. doi:10.3389/fninf.2014.00014

79. Pruim RHR, Mennes M, van Rooij D, Llera A, Buitelaar JK, Beckmann CF. ICA-AROMA: A robust ICA-based strategy for removing motion artifacts from fMRI data. NeuroImage. 2015;112:267–77. doi:10.1016/j.neuroimage.2015.02.064

80. Rubinov M, Kötter R, Hagmann P, Sporns O. Brain connectivity toolbox: a collection of complex network measurements and brain connectivity datasets. NeuroImage. 2009;Organization for Human Brain Mapping 2009 Annual Meeting47:S169. doi:10.1016/S1053-8119(09)71822-1

81. Raichle ME. The restless brain. Brain Connect. 2011;1:3–12. doi:10.1089/brain.2011.0019 PubMed PMID: 22432951; PubMed Central PMCID: PMC3621343.

82. De Filippi E, Escrichs A, Càmara E, Garrido C, Marins T, Sánchez-Fibla M, Gilson M, Deco G. Meditation-induced effects on whole-brain structural and effective connectivity. Brain Struct Funct. 2022;227:2087–102. doi:10.1007/s00429-022-02496-9

83. Zhang Z, Luh WM, Duan W, Zhou GD, Weinschenk G, Anderson AK, Dai W. Longitudinal effects of meditation on brain resting-state functional connectivity. Sci Rep. 2021;11:1. doi:10.1038/s41598-021-90729-y

84. Cristofori I, Bulbulia J, Shaver JH, Wilson M, Krueger F, Grafman J. Neural correlates of mystical experience. Neuropsychologia. 2016;80:212–20. doi:10.1016/j.neuropsychologia.2015.11.021

85. Josipovic Z. Neural correlates of nondual awareness in meditation. Ann N Y Acad Sci. 2014;1307:9–18. doi:10.1111/nyas.12261

86. Dadi K, Varoquaux G, Machlouzarides-Shalit A, Gorgolewski KJ, Wassermann D, Thirion B, Mensch A. Fine-grain atlases of functional modes for fMRI analysis. NeuroImage. 2020;221:117126. doi:10.1016/j.neuroimage.2020.117126

87. Zuniga-Hertz JP, Simpson S, Chitetti R, Hsu CF, Huang HP, Jinich-Diamant A, Chernov AV, Onton JA, Cuomo R, Dispenza J, Davis D, Christov-Moore L, Reggente N, Gu W, Kong M, Bonds JA, Maree J, Simonson TS, Ahn AC, Poirier MA, Moeller-Bertram T, Patel HH. Multidimensional Analysis of Twin Sets During an Intensive Week-Long Meditation Retreat: A Pilot Study. Mindfulness. 2025;16:1634–55. doi:10.1007/s12671-025-02584-x PubMed PMID: 40535580; PubMed Central PMCID: PMC12170707.

88. Szklarczyk D, Gable AL, Lyon D, Junge A, Wyder S, Huerta-Cepas J, Simonovic M, Doncheva NT, Morris JH, Bork P, Jensen LJ, Mering C von. STRING v11: protein–protein association networks with increased coverage, supporting functional discovery in genome-wide experimental datasets. Nucleic Acids Res. 2019;47:D607–13. doi:10.1093/nar/gky1131 PubMed PMID: 30476243; PubMed Central PMCID: PMC6323986.

89. Wishart DS, Tzur D, Knox C, Eisner R, Guo AC, Young N, Cheng D, Jewell K, Arndt D, Sawhney S, Fung C, Nikolai L, Lewis M, Coutouly MA, Forsythe I, Tang P, Shrivastava S, Jeroncic K, Stothard P, Amegbey G, Block D, Hau DavidD, Wagner J, Miniaci J, Clements M, Gebremedhin M, Guo N, Zhang Y, Duggan GE, MacInnis GD, Weljie AM, Dowlatabadi R, Bamforth F, Clive D, Greiner R, Li L, Marrie T, Sykes BD, Vogel HJ, Querengesser L. HMDB: the Human Metabolome Database. Nucleic Acids Res. 2007;35:D521–6. doi:10.1093/nar/gkl923

90. Smith CA, Maille GO, Want EJ, Qin C, Trauger SA, Brandon TR, Custodio DE, Abagyan R, Siuzdak G. METLIN: A Metabolite Mass Spectral Database. Ther Drug Monit. 2005;27:747. doi:10.1097/01.ftd.0000179845.53213.39

91. Kanehisa M, Furumichi M, Sato Y, Kawashima M, Ishiguro-Watanabe M. KEGG for taxonomy-based analysis of pathways and genomes. Nucleic Acids Res. 2023;51:D587–92. doi:10.1093/nar/gkac963 PubMed PMID: 36300620; PubMed Central PMCID: PMC9825424.

92. Pedregosa F, Varoquaux G, Gramfort A, Michel V, Thirion B, Grisel O, Blondel M, Prettenhofer P, Weiss R, Dubourg V, Vanderplas J, Passos A, Cournapeau D, Brucher M, Perrot M, Duchesnay É. Scikit-learn: Machine Learning in Python. J Mach Learn Res. 2011;12:2825–30.

93. Song Y, Leem J, Dhanani M, McKirnan MD, Ichikawa Y, Braza J, Harrington EO, Hammond HK, Roth DM, Patel HH. Impact of blood factors on endothelial cell metabolism and function in two diverse heart failure models. PLOS ONE. 2023;18:e0281550. doi:10.1371/journal.pone.0281550 PubMed PMID: 36780477; PubMed Central PMCID: PMC9924994.

94. Kopp EL, Deussen DN, Cuomo R, Lorenz R, Roth DM, Mahata SK, Patel HH. Modeling and Phenotyping Acute and Chronic Type 2 Diabetes Mellitus In Vitro in Rodent Heart and Skeletal Muscle Cells. Cells. 2023;12:2786. doi:10.3390/cells12242786 PubMed PMID: 38132105; PubMed Central PMCID: PMC10741513.

95. Karliner J, Merry DE. Differentiating PC12 cells to evaluate neurite densities through live-cell imaging. STAR Protoc. 2023;4:101993. doi:10.1016/j.xpro.2022.101993

96. Martin M. Cutadapt removes adapter sequences from high-throughput sequencing reads. EMBnet.journal. 2011;17:1. doi:10.14806/ej.17.1.200

97. STAR: ultrafast universal RNA-seq aligner | Bioinformatics | Oxford Academic [Internet]. [cited 2025 Jul 31]. Available from: https://academic.oup.com/bioinformatics/article/29/1/15/272537

98. Ewels P, Magnusson M, Lundin S, Käller M. MultiQC: summarize analysis results for multiple tools and samples in a single report. Bioinformatics. 2016;32:3047–8. doi:10.1093/bioinformatics/btw354

99. Tuch BB, Laborde RR, Xu X, Gu J, Chung CB, Monighetti CK, Stanley SJ, Olsen KD, Kasperbauer JL, Moore EJ, Broomer AJ, Tan R, Brzoska PM, Muller MW, Siddiqui AS, Asmann YW, Sun Y, Kuersten S, Barker MA, De La Vega FM, Smith DI. Tumor transcriptome sequencing reveals allelic expression imbalances associated with copy number alterations. PloS One. 2010;5:e9317. doi:10.1371/journal.pone.0009317 PubMed PMID: 20174472; PubMed Central PMCID: PMC2824832.

100. Robinson MD, McCarthy DJ, Smyth GK. edgeR: a Bioconductor package for differential expression analysis of digital gene expression data. Bioinformatics. 2010;26:139–40. doi:10.1093/bioinformatics/btp616

101. McCarthy DJ, Chen Y, Smyth GK. Differential expression analysis of multifactor RNA-Seq experiments with respect to biological variation. Nucleic Acids Res. 2012;40:4288–97. doi:10.1093/nar/gks042 PubMed PMID: 22287627; PubMed Central PMCID: PMC3378882.

102. Robinson MD, Oshlack A. A scaling normalization method for differential expression analysis of RNA-seq data. Genome Biol. 2010;11:R25. doi:10.1186/gb-2010-11-3-r25

103. Risso D, Ngai J, Speed TP, Dudoit S. Normalization of RNA-seq data using factor analysis of control genes or samples. Nat Biotechnol. 2014;32:896–902. doi:10.1038/nbt.2931

104. Carlson M, Falcon S, Pages H, Li N. org. Hs. eg. db: Genome wide annotation for Human. R Package Version. 2019;3:3.

105. Kozomara A, Birgaoanu M, Griffiths-Jones S. miRBase: from microRNA sequences to function. Nucleic Acids Res. 2019;47:D155–62. doi:10.1093/nar/gky1141

106. Wu T, Hu E, Xu S, Chen M, Guo P, Dai Z, Feng T, Zhou L, Tang W, Zhan L, Fu X, Liu S, Bo X, Yu G. clusterProfiler 4.0: A universal enrichment tool for interpreting omics data. Innov Camb Mass. 2021;2:100141. doi:10.1016/j.xinn.2021.100141 PubMed PMID: 34557778; PubMed Central PMCID: PMC8454663.

107. Song M, Greenbaum J, Luttrell J, Zhou W, Wu C, Shen H, Gong P, Zhang C, Deng HW. A Review of Integrative Imputation for Multi-Omics Datasets. Front Genet. 2020;11. doi:10.3389/fgene.2020.570255

108. Chen T, Guestrin C. XGBoost: A Scalable Tree Boosting System. In: Proceedings of the 22nd ACM SIGKDD International Conference on Knowledge Discovery and Data Mining [Internet]. 2016 [cited 2024 Dec 5]. p. 785–94. Available from: http://arxiv.org/abs/1603.02754 doi:10.1145/2939672.2939785

109. Lundberg S, Lee SI. A Unified Approach to Interpreting Model Predictions [Internet]. arXiv; 2017 [cited 2024 Dec 5]. Available from: http://arxiv.org/abs/1705.07874 doi:10.48550/arXiv.1705.07874

CHAPTER 3: Experience as Medicine: Shared Neurobiological and Computational Mechanisms of Psychedelic, Contemplative, and Fasting-Induced Mystical Experience

Chapter 2 demonstrated that a one-week mind-body intervention combining meditation, reconceptualization, and open-label placebo healing produces coordinated reorganization across the brain and body. fMRI showed reduced whole-brain modularity and lower intra-network connectivity of the default mode and salience networks during meditation; plasma proteomics, metabolomics, and exosomal transcriptomics revealed elevated BDNF-pathway proteins, upregulated endogenous opioid signaling, enhanced glycolysis, and changes in exRNAs implicated in neurotransmission; and downstream cellular assays confirmed that post-intervention plasma enhanced neurite outgrowth and shifted cellular metabolism. The combination of techniques is most readily interpreted as acting on different levels of the predictive hierarchy: meditation lowers descending predictive constraint on present-moment sensation; reconceptualization edits the content of high-level priors about the body's healing capacity; open-label placebo recruits the expectation-driven priors that gate physiological response. Their composite effect is a brain-body state more characteristic of the kind of transient reorganization that more intensive transformative interventions are known to produce—including ones with no apparent pharmacological or behavioral relationship to these techniques.

That observation invites the question Chapter 3 takes up. Mystical-type experiences are reported across pharmacological (classic psychedelics), contemplative (deep meditation), and metabolic (fasting) routes that share nothing at the level of mechanism narrowly construed, and yet the experiences they produce exhibit a remarkably consistent phenomenology and predict

comparable therapeutic outcomes across indications. If the empirical findings of Chapters 2 and 3 reflect a general property of the predictive hierarchy under modulation, that property should be visible across these otherwise unrelated routes. Chapter 4 argues that it is and develops a unifying account.

Abstract

Psychedelics, contemplative practice, and fasting are physiologically unrelated interventions that nevertheless converge, across cultures and centuries, on a common experiential endpoint: the mystical state. Here I propose that this convergence reflects shared disruption of a single computational architecture, the precision-weighted predictive hierarchy, through three mechanistically distinct but functionally equivalent routes. Serotonergic psychedelics sensitize layer 5 pyramidal neurons and disinhibit higher-order thalamic nuclei, relaxing the gain on top-down priors; open-monitoring meditation shifts thalamocortical coupling geometry toward diffuse, matrix-type connectivity, elevating cortical entropy; and caloric restriction attenuates the metabolic machinery sustaining high-level attractor states, destabilizing the default mode network from below. All three routes terminate in a transient near-critical regime characterized by relaxed priors, scale-free cortical dynamics, and expanded degrees of freedom in the brain's generative model, conditions I identify as the neurobiological substrate of mystical experience. Critically, the depth of this state, not its pharmacological or procedural occasion, is the primary predictor of lasting therapeutic benefit, implicating conscious experience itself as the mechanistic agent of change. I further argue that near-critical dynamics may constitute the conditions under which field-theoretic and quantum-coherent contributions to consciousness become empirically

detectable. This framework generates testable predictions across molecular, circuit, and phenomenological levels, and positions the neuroscience of mystical states as a tractable frontier for understanding how the brain constructs, maintains, and fundamentally reorganizes its model of reality.

Introduction

Meditation techniques and serotonergic psychedelics like psilocybin and N,N-dimethyltryptamine (N,N-DMT) have garnered significant scientific and clinical attention thanks to their ability to produce altered states of consciousness and to alleviate otherwise difficult-to-treat conditions like depression, post-traumatic stress disorder (PTSD), addiction, and chronic pain, whose etiology lies in the mind-body connection. Fasting practices too have been recognized across cultures and millennia as producing states of consciousness with similar phenomenological and spiritual character to meditation and psychedelics. Despite their profound differences in mechanism, timescale, and cultural origin (psychedelics are fast-acting ingestible tryptamine or phenethylamine molecules; meditation consists of a variety of self-mediated attentional practices; fasting operates through metabolic restriction) all three reliably and reproducibly converge on the same extraordinary territory, the mystical-type experience, characterized by a profound sense of unity, sacredness, noetic quality, ineffability, deeply felt positive mood, and transcendence of time and space. The three techniques also converge clinically in their ability to alleviate psychosomatic and psychiatric conditions for which traditional pharmacological agents have had limited success. Neurophysiologically, all three attenuate the default mode network (DMN), the resting state brain network associated with self-

referential processing, mental time travel, and counterfactual thinking; increase brain-wide measures of neural entropy, complexity, and criticality; and show evidence of prior relaxation and reduction in prediction-driven processing. Historically, all three were originally embedded within contemplative and indigenous spiritual traditions and are now increasingly being studied, prescribed, and practiced in secular and biomedical contexts.

This convergence is not merely of phenomenological interest. It is also a remarkable scientific opportunity. When three physiologically and mechanistically distinct interventions reliably produce the same richly structured output, the neuroscientist encounters a system that can be probed from three orthogonal angles simultaneously. Psychedelics, meditation, and fasting are, in this sense, perturbation experiments on the mechanisms of conscious experience. Each perturbs the system through a different entry point–molecular pharmacology, attentional self-regulation, and metabolic restriction–, at a different timescale, and through a distinct biological pathway. Their convergence on overlapping phenomenological and neurophysiological output constrains theory in a way that no single intervention could. Comparative analysis of the three routes thus offers a rare lens through which to examine the mechanics of mystical experience: the question of how the biological substrate of the brain and body produces these states, what computational principles govern them, and what the constraints imposed by their convergence reveal about how the brain generates and modulates conscious experience more broadly.

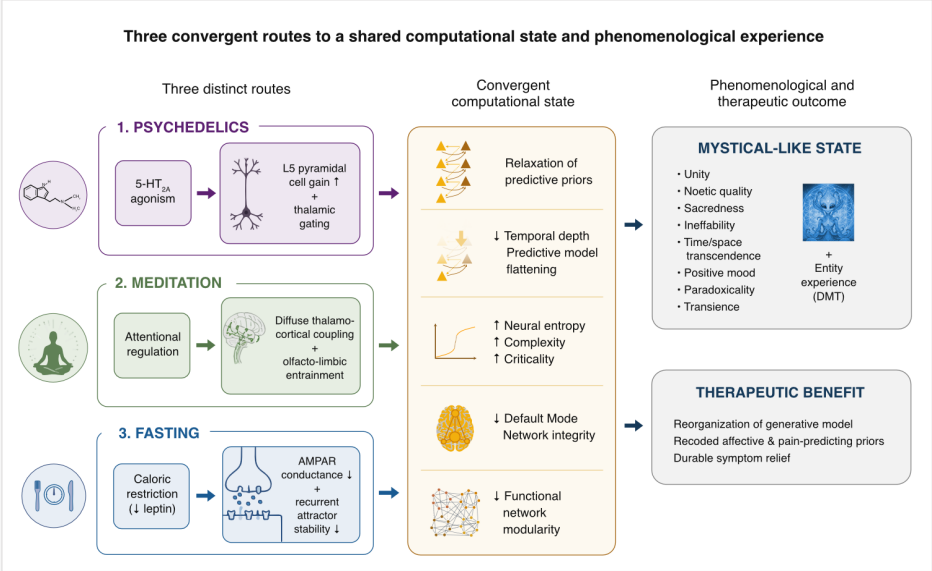


Figure 3.1: Three converging routes to a shared computational neural state and mystical-like subjective phenomenology.

The scientific value of this lens extends beyond the study of altered states. The conditions for which psychedelic-assisted therapy, mindfulness-based interventions, and their allied metabolic approaches show the most robust clinical efficacy–depression, PTSD, addiction, and anxiety disorders–share a computational signature: pathological rigidity of high-level predictive priors, in which self-reinforcing loops of negatively valenced predictions suppress the ascending prediction errors that would normally update the generative model and relieve suffering. The mystical state directly targets this computational signature through the relaxation of high-level priors, the flattening of the predictive hierarchy, and the recoupling of the perceptual system to ascending sensory evidence. Understanding the mechanics of this state therefore advances two scientific goals at once. The first is a fundamental account of how the brain generates and modulates conscious experience, and the second is a biologically grounded mechanistic explanation for why these approaches work, for whom, and under what conditions. Importantly, this includes, taking seriously the most challenging features of the mystical state's

phenomenology, the consistently numinous and noetic character of entity encounter experiences, which resist existing mechanistic accounts, are among the most therapeutically active features of these experiences, and bear directly on the question of what the brain is doing in these states.

This paper builds a theoretical framework for the mechanics of mystical experience by tracing three distinct biological routes to a shared computational destination. Section 1 reviews existing empirical and theoretical work on how classic psychedelics modulate consciousness via 5-HT_{2A} action on layer 5 cortical pyramidal neurons and the predictive processing circuits they comprise. Section 2 proposes novel mechanistic frameworks for how open monitoring and focused attention meditation techniques produce effects parallel to those of psychedelics through, respectively, attentional modulation of diffuse thalamocortical coupling and olfacto-limbic entrainment of interoceptive prior recalibration. Section 3 connects these dynamics to the body via metabolism, proposing how caloric restriction produces convergent neurophysiological changes through metabolic relaxation of cortical priors. Section 4 develops a biologically grounded computational account of the mystical state itself, treating it as the perturbation of a multi-scale predictive architecture and examining it through the complementary lenses of criticality, computational irreducibility, and stochastic noise. Section 5 examines the implications of this account through the lens of field theories of consciousness, asking what the numinous, noetic, and entity-encountering phenomenology of the mystical state may reveal about the nature of consciousness and its physical substrate. Sections 1, 2, and 3 present three roads to Rome; Sections 4 and 5 ask what Rome is and what it might mean to face what one encounters there.

Section 1: **Classic psychedelics act on consciousness via 5-HT_{2A} modulation of layer 5 cortical pyramidal neurons**

5-HT_{2A} Receptor Pharmacology and the Cellular Basis of Psychedelic Action

Despite variations in chemical structure and receptor affinity, classic psychedelics like LSD, psylocibin, mescaline, and N,N-DMT produce similar experiences in humans and create cross-tolerance, pointing to a unitary mechanism of action mediated by the 5-HT_2 receptor family[1]. Subjective psychedelic effects correlate with 5-HT_{2A} receptor occupancy[2] and are abolished when 5-HT_{2A} antagonist ketanserin and mixed D_2/5-HT_{2A} antagonist risperidone are administered[1]; yet, not all 5-HT_{2A} agonists are psychedelic, demonstrating that 5-HT_{2A} agonism is necessary but not sufficient. Psychedelic effects are thought to originate from specific 5-HT_{2A} receptor circuits and from biased agonism, whereby different agonists acting on the same G protein coupled target receptor elicit different cellular signaling cascades by stabilizing different receptor conformational states[3]. Complex interactions with 5-$HT_{1A,1B,1C}$, sigma-1 receptors, and serotonin transporter (SERT) inhibition (with the molecule acting as a transporter substrate) also likely play a role[4].

5-HT_{2A} binding sites are widely distributed throughout the human brain, with the highest densities found in the claustrum and neocortex, where they are primarily expressed in layer V pyramidal (L5p) neurons[5]. Moderate-to-low expression levels are also found in the hippocampus, amygdala, nucleus accumbens, striatum, and hypothalamus, and in parvalbumin-expressing GABAergic interneurons[5]. 5-HT_{2A} receptors modulate nitric oxide production, cAMP production, and arachidonic acid release, and interact with arrestins, caveolin-1, and microtubule associated proteins (MAPs)[5]; however, psychedelic effects are believed to be primarily mediated by 5-HT_{2A}-evoked excitatory post-synaptic potentials (EPSPs) in neocortical L5p cells[6].

In mice, psychedelic 5-HT$_{2A}$ stimulation increases cortical excitability by means of higher excitatory post-synaptic current (EPSC) activity in a subpopulation of prefrontal cortex (PFC) glutamatergic L5p neurons that are highly sensitive to 5-HT$_{2A}$ agonists and also express μ-opioid receptors[4,7]. In rats, the psychedelic DOI (2,5-Dimethoxy-4-iodoamphetamine) increases the frequency of spontaneous EPSPs and increases the amplitude of evoked EPSPs in L5p neurons[6,8], and 5-MeO-DMT increases cortical pyramidal neuron firing rate and burst activity[9]. While there is much to be learned about the cortical circuits that sustain consciousness, psychedelics' effects appear to be driven by these 5-HT$_{2A}$-evoked irregular postsynaptic increases in L5p excitability (or gain) on the corticocortical and thalamocortical circuits that underlie conscious perception.

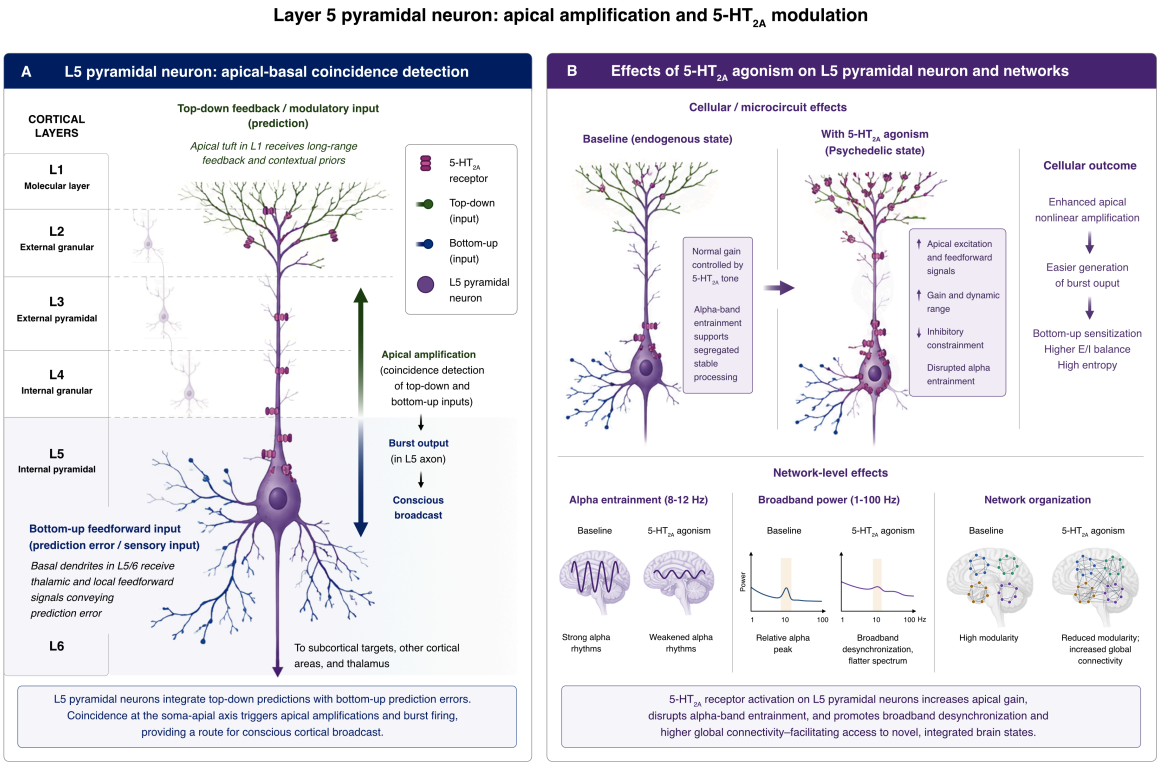


Figure 3.2: Layer 5 pyramidal neurons, (A) apical amplification and (B) 5-HT2A agonism.

Layer 5 Pyramidal Neurons: Gatekeepers of Conscious Content

L5p neurons integrate bottom-up (feedforward) sensory signals via their basal dendrites with top-down (feedback) prediction and modulatory signals via their apical dendrites, making them gatekeepers, broadcasters, and amplifiers of consciously relevant content (Figure 3.2A)[10]. When L5p apical and basal inputs coincide, a burst output is generated, which enhances transmission and correlates with stimulus awareness thresholds, while isolated basal (bottom-up) input produces weaker single spikes[10,11]. L5p bursts are associated with attention in awake cortex, while during deep sleep and anesthesia their apical tuft becomes isolated[12], suggesting that L5p apical-basal coincidence (known as apical amplification) is essential for broadcasting conscious content[12,13].

L5p neurons also integrate inputs from many cortical sources, serving as cortical hubs linking corticocortical and cortico-thalamo-cortical circuits and participating in intracolumnar, lateral, feedforward, and feedback pathways[14]. In sensory cortices, L5p neurons innervate higher-order thalamic nuclei (e.g. medial dorsal (MD) and pulvinar), whose matrix cells project diffusely back to cortex, where they target L5p neurons at their apical (L1) and basal (L5) dendrites[15]. L5p dendritic excitability gates sensory information into conscious perception via these cortico-thalamo-cortical loops[11,16]. Indeed, when these deep (L5/L6) cells are stimulated they produce complex responses in conscious states that are not produced with superficial layer stimulation[17].

The ability of bursts to propagate through cortico-thalamo-cortical loops, in turn, depends on the population-level oscillatory synchrony and neural resonance (responsiveness to inputs at specific frequencies) that support consciousness. Signals that arrive during a depolarized up-state

translate into spiking activity, which travels across cortex and thalamus during waking and REM sleep. In contrast, signals that arrive during down-states lead to the signal loss observed during NREM sleep, anesthesia, and coma[18]. GABAergic anesthetics like barbiturates and propofol block apical amplification, stopping dendrosomatic spike propagation to induce unconsciousness by either suppressing L5p apical dendrites with inhibition or by targeting the higher-order thalamic nuclei that control cortical pyramidal neurons' sensitivity to the feedback signals which arrive at distal apical dendrites[19]. In contrast, psychedelics amplify apical processing via 5-HT_{2A}-induced excitation (or gain), resulting in cortical excitability and broadband desynchronization of cortical oscillatory rhythms (Figure 3.2B)[20]. Psychedelics therefore do not attenuate consciousness but rather modulate it to produce unique states tuned by this altered cortical synchrony. Understanding the electrodynamic and computational characteristics of this altered state is therefore important to explain how $5HT_{2A}$ action accounts for the subjective phenomenology and clinical effects of the psychedelic state.

In humans, psychedelics dramatically decrease low frequency α and β oscillatory activity in a manner that correlates to the intensity of subjective effects[20,21]. Similarly, DOI decreases the amplitude of low-frequency (0.3–4 Hz) cortical oscillations in rats and disrupts the temporal association between pyramidal firing and the active phase of the local field potential (LFP)[22]. Alpha power is associated with default mode network (DMN) activity and with a state in which top-down expectations about sensory stimuli dominate, while the beta rhythm is associated to top-down (expectations-driven) motor activity[23–25]. Normally, L5p bursts are entrained to alpha rhythm troughs, corresponding to when inhibition is lifted and input integration peaks[26]. By increasing L5p cells' dendritic gain via 5-HT_{2A}, psychedelics disrupt burst-inducing apical amplification (integration of apical prediction-driven input and basal sensory-driven input),

increasing cortical excitability and dysregulating the population-level low frequency oscillations associated with an expectations-driven state. The result is a conscious state supported by more excitable, less prediction-driven neural circuits. Since perception is prediction-driven, these changes produce profound perceptual alterations, tuning consciousness away from the prediction-driven perceptual state that characterizes normal wakefulness. Active inference accounts of perception that describe the computational dynamics of prediction further elucidate how these effects likely arise.

Predictive Processing and the Computational Architecture of Perception

Active inference accounts describe how the circuits supporting conscious awareness are predictive in nature, with perception being equivalent to statistical inference about the hidden causes of sensory input[27,28] ("hidden" because they must be inferred from their sensory consequences). Predictions are issued by a generative model that represents the sensorium, is constructed from past experience, and is calibrated by prediction errors. Such a system likely evolved as a metabolically efficient way to maximize survival by filtering conscious experience to be adaptively relevant. Given that the world is highly correlated in both time and space (e.g., the color of any point in our visual field is correlated to that of the point next to it and to itself on the next time point), it is metabolically more efficient to develop a model of the world that generates predictions, which are dynamically weighed against sensory evidence and are updated via prediction errors, than to open the gates of perception, perceiving everything high-dimensionally and reducing dimensionality moment-by-moment.

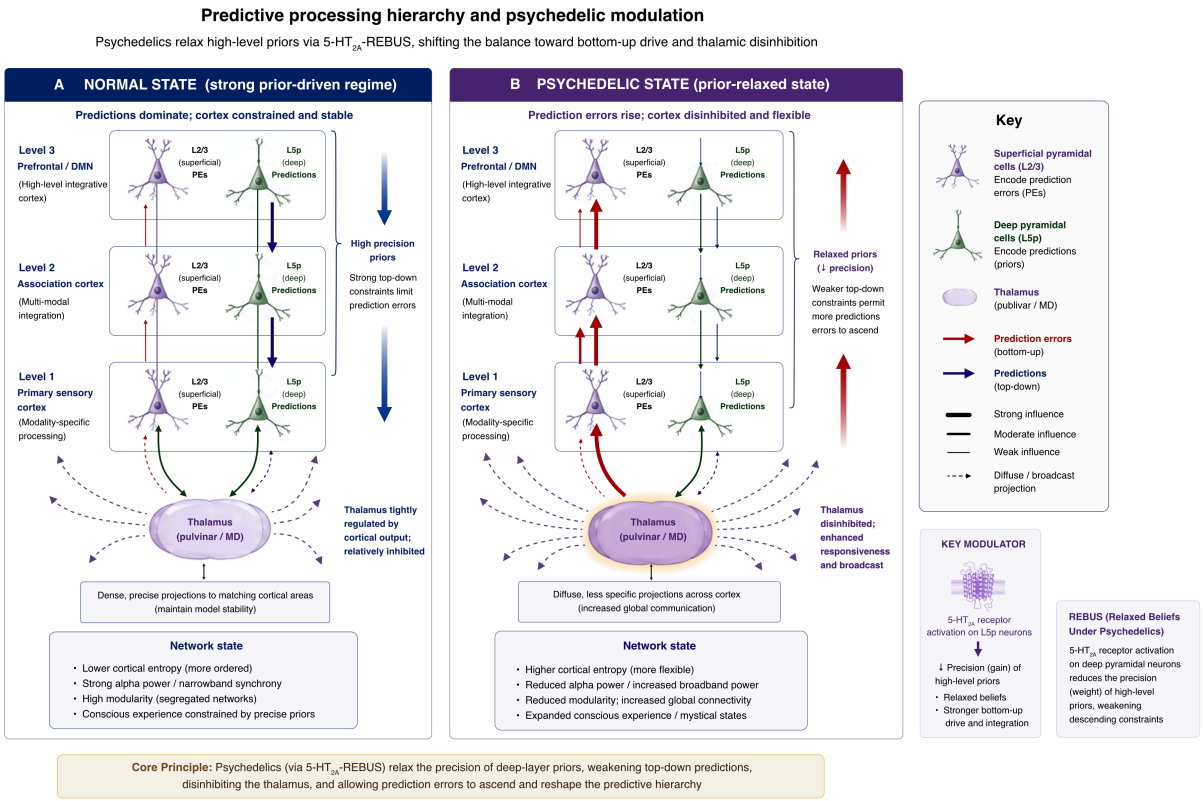


Figure 3.3: Predictive processing hierarchy under the normal waking state (A) and under the psychedelic state (B).

Under such a predictive architecture, neuronal activity encodes beliefs (or probability distributions) over states of the world that cause sensations, and inference is performed by hierarchically comparing the descending predictions to ascending afferent input, with mismatches (prediction errors) traveling up the hierarchy to update higher-level predictions so as to reduce future mismatches. Said inference is mathematically equivalent to a Bayesian precision-based weighing of descending priors and ascending sensory evidence, where priors are recursively updated to minimize prediction error; the posterior corresponds to the perceived gestalt; precision weights influence the relative contribution of top-down priors and bottom-up afferent data to the posterior; and precision is equivalent to inverse variance, such that a narrower distribution will carry more weight than a wider (more uncertain) one. Perception, therefore,

results from the moment-to-moment precision-weighted matching of prior expectations about the hidden causes of sensory input, with new rounds of expectations being updated by previous mismatches. What we perceive, under such an architecture, is what the brain predicts. It follows that modifying the predictive processing system will alter what is consciously perceived.

In canonical cortical microcircuits, superficial pyramidal neurons (which provide feedforward connections) are thought to encode prediction errors on hidden causes, passing them forward to update expectations at higher levels of the hierarchy, while deep pyramidal neurons (including L5p, which provide feedback connections) are thought to encode the higher-level conditional expectations (or priors) that predict lower level representations (Figure 3.3A)[29]. Beyond the cortex, L5p neurons are thought to carry prediction signals about the sensorium from cortex to higher order thalamic nuclei, where they update the contextual belief states that underlie perception and project them back to the cortex[30,31]. Within this cortico-thalamo-cortical circuit, the thalamus is thought to act as a higher-order Bayesian observer that performs contextual modulation of cortical processing by integrating prediction signal inputs from many different cortical areas (via convergent L5p traffic into the pulvinar and medial dorsal nuclei), computing a context-informed belief (posterior distribution) about the state of the environment by selectively enhancing the impact of some inputs over others in a task-dependent manner, and propagating the resulting posterior distribution diffusely back to the cortex to update sensory expectations by modulating the gain of superficial pyramidal cells[30,32]. These cortico-thalamo-cortical circuits provide a precision control mechanism associated with attention[31], which increases the precision of attended sensory data vis-à-vis competing inputs[33].

Crucially, the brain must adjust and encode the precision of prediction errors that compete to update higher-level expectations so as to only assimilate precise information in deep

hierarchical layers and to dynamically adjust the sensitivity of perception to predictions versus afferent input based on their relative uncertainty. This encoding of precision is thought to be performed by the synapse-level gain (excitability) control of the neuronal populations that encode priors and prediction errors through neuromodulatory receptors, including 5-HT[34] and D_1 (dopamine), synaptic gain control mechanisms like N-methyl-D-aspartate (NMDA) receptors, and cortical excitation-inhibition balance[35]. Attention circuits, comprised of cortico-thalamo-cortical loops, also modulate the encoding of precision such that the precision of a percept that one attends to increases relative to that of rest of the sensorium.

Neuromodulation of these circuits' excitability, including via 5-HT modulation of neural gain, allows the brain to regulate sleep-wake transitions (via apical amplification and the ascending arousal system), to modulate the selective processing of cognitively relevant perceptual features (attentional segregation), and to dynamically adapt conscious perception to varying levels of uncertainty. As uncertainty varies exogenously (or endogenously via attention), the relative precision of predictions and prediction errors adjusts dynamically. Indeed, when contextual uncertainty increases, the cortex shifts from a rhythmic to an excited asynchronous regime characterized by higher signal entropy, reduced alpha engagement, and upregulated thalamic activity[36], all consistent with a less prediction-driven state that is encoding higher-precision prediction errors and lower-precision predictions. Via 5-HT_{2A}-driven excitability of L5p neurons, psychedelics are thought to modulate these same precision-control pathways and profoundly alter the inference system.

Psychedelic Modulation of the Predictive Hierarchy

Active inference-based models like REBUS (relaxed beliefs under psychedelics) account for the perceptual, emotional, and cognitive effects of psychedelics by proposing that the psychedelic-driven 5-HT_{2A} sensitization of the deep pyramidal neurons that encode expectations and issue predictions reduces their precision, making them more sensitive to ascending prediction errors (Figure 3.3B)[37]. Sensitizing these neurons is thus computationally equivalent to weakening the precision of higher-level priors and the influence of the expectations that they encode over the posterior. This, in turn, disrupts the normal process by which high-level generative predictions explain away lower level perceptual, cognitive, and emotional data; increases bottom up signaling; and allows prediction errors to ascend the cortical hierarchy and remodel the higher-level layers that issue predictions. In short, psychedelics lower the threshold for prediction errors to be deemed too large for descending predictions to explain them away, altering the dynamic balance between descending predictions and ascending sensory data within the cortex in favor of the latter.

Psychedelics also likely disrupt predictive dynamics in the broader thalamo-cortico-thalamic system by disrupting the selective thalamic relay gating that selectively excites superficial pyramidal cells. Serotonin hyperpolarizes the higher-order thalamic relay nuclei (mediodorsal and pulvinar)[38], which, as described above, receive cortical prediction signals about the sensorium via convergent L5p traffic and project diffusely back to cortex. Under the normal waking state, these diffuse matrix projections update sensory expectations in the cortex by modulating the gain of superficial pyramidal cells in a context and task dependent manner. The mediodorsal and pulvinar also express the highest concentration of 5-HT_{2A} receptors within the thalamus[39], and psychedelics modulate their activity in a manner that correlates to subjective effects[40,41]. Like serotonin, psychedelics are thought to bias the system toward feedforward

processing[38,42] by disinhibiting relay nuclei[41], leading to broad increases in the gain of cortical superficial pyramidal cells that encode prediction errors (bottom-up signals).

Criticality, Entropy, and the Annealing of the Generative Model

As predictive feedback traffic weakens and feedforward prediction error traffic strengthens following psychedelic-induced modulation of both cortical and thalamo-cortico-thalamic predictive dynamics, perceptual processes become less constrained by predictions, loosening or dissolving the prediction-driven perceptual, emotional, and cognitive categories that structure and constrain normal waking awareness. This is consistent with a more entropic perceptual experience that departs from the normal waking one and is rich in numinous content, emotional breakthroughs, epiphanic insights, and perceptual anomalies–the hallmark psychedelic state. And yet, while this may explain some perceptual anomalies via an overall noisier signaling, it does not explain where the epiphanic or numinous content comes from, which is an intriguing question.

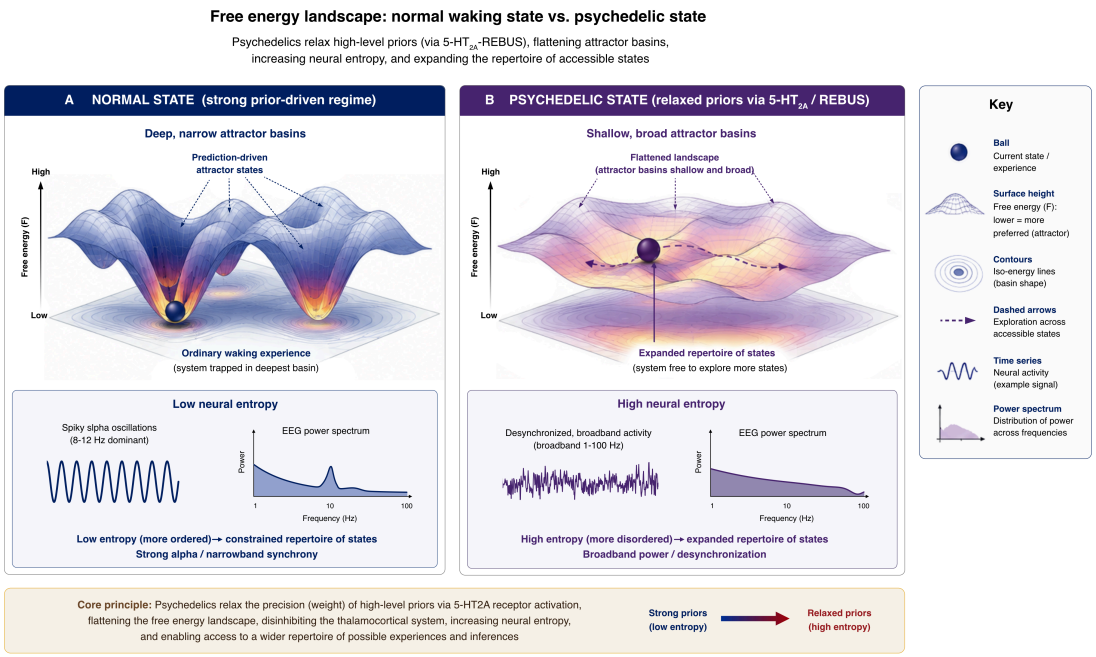


Figure 3.4: The brain's free energy landscape in the normal waking state (A) and in the psychedelic state (B).

Computationally, this less prediction-driven state corresponds to a topological flattening of the brain's free energy landscape, which is a way to describe the brain's dynamics in terms of valleys (low free energy attractor regions that correspond to stable and predictable patterns) and hills (high free energy unstable or unlikely regions). Under the normal waking state, the imperative of the system to minimize prediction errors means that the brain constrains itself to a limited number of prediction-driven, low-surprise attractor states that adequately minimize variational free energy, which is equivalent to the long-term average of surprise (Figure 3.4A). Subjective experience under the sober state is therefore constrained by the system frequenting this limited number of states. Under psychedelics, the loosening of priors and the increased bottom-up influence on the cortical hierarchy flatten the free-energy landscape, producing shallower valleys, which allow neuronal dynamics to more easily escape them and explore a

wider range of states (Figure 3.4B). This is reflected in neural electrodynamics, which, under psychedelics, exhibit greater complexity, entropy, and diversity, and in functional connectivity network geometry, which shows reduced modularity, increased efficiency, and higher entropy – all consistent with the system frequenting a more diverse and less prediction-driven range of states[43–45].

During the normal waking state, the brain operates close to the edge-of-chaos critical point–the phase transition that gives rise to neuronal avalanches. While the precise nature of the dynamical phases lying on either side of the critical point and whether the brain is normally poised on the chaotic or stable phase remain a matter of debate, it is well known that conscious awareness arises within a critical zone near the phase transition from stable to chaotic dynamics (the edge-of-chaos criticality) and disappears as the system moves far enough into either the stable or chaotic regimes[43], for example, in disorders of consciousness, anesthesia, and NREM sleep. Many systems maximize their information processing capacity at the edge-of-chaos critical point, and it is in this quasicritical region which supports consciousness that the brain can maximize its sensitivity to small but potentially important sensory fluctuations without falling into dangerous self-perpetuating excitatory cascades (super-critical regime), remaining maximally sensitive to the external and internal milieus while simultaneously being able to carry out predictive computations based on them[46]. The system's distance from the critical point has been variously measured or inferred via the largest Lyapunov exponent (a formal measure of chaoticity), Lempel-Ziv complexity (a measure of nonredundant or noncompressible information), closeness to power-law statistics (a scale-free distribution characteristic of critical systems), and diverse entropy and complexity measures. An organism's level of consciousness can therefore be indexed by the entropy of low-frequency cortical electrodynamics, entropy

being a dimensionless measure of randomness, uncertainty, or variability. It is also worth noting that entropy peaks at criticality, the state at which the system has access to the largest repertoire of metastable microstates without collapsing into randomness or rigidity[47,48].

The brain can dynamically adjust its computational architecture and its network topology in a task and uncertainty-sensitive manner by tuning its distance from the edge of criticality. Neuromodulation of cortical gain across the thalamocortical system, including by serotonin, acetylcholine, and noradrenaline, tune how far the system operates from the critical edge in order to dynamical alter its functional network topology towards either a more segregated network topology (associated with subcritical states) that facilitates greater information storage, or a more integrated network topology (associated with supercritical states) that facilitates greater information transfer[42,49]. A more prediction-driven state is associated with the system operating farther from the critical edge, a deeper free energy landscape, and lower electrodynamic complexity/entropy, while a more bottom-up-driven state is associated with a flatter energy landscape, with higher electrodynamic entropy, and with operating closer to the edge of criticality.

In addition to whole brain entropy changes, activation and functional connectivity fMRI findings also support the notion of lower psychedelic-mediated predictive brain activity, with one hallmark study showing that an acute dose of psilocybin disrupts default-mode network (DMN) connectivity and causes only decreases in BOLD signal and cerebral blood flow (CBF), which are largest in hub regions, including thalamus, anterior cingulate cortex (ACC), posterior cingulate cortex (PCC), and medial prefrontal cortex (mPFC)[50]–the latter two being DMN hubs. Lower activity in these hubs likely allows for more unconstrained cognition by reducing their constraint on the rest of the brain. Indeed, the DMN has been proposed to be a central generator

of predictions[51,52], and its activity is associated with alpha power, which is linked to top-down expectations about sensory stimuli[23].

In the psychedelic state, cortical electrodynamics move closer to the edge-of-chaos critical point[43,44], where the entropy and information richness of cortical activity increase as the system sheds the constraints of prediction-driven dynamics and operates beyond the attractors frequented during the normal waking state. The result is a richer-than-normal range of sensations, perceptions, emotions, and thoughts associated with the loosening of rigid cognitive patterns[53,54]. While it is well established that the entropy of cortical electrodynamics increases during the psychedelic state and that this is associated with a richer content of experience, the source of the increased richness is not known. Nonetheless, a less prediction-driven and more sensory-driven state would suggest that it is at least partly the product of sensory signals from the periphery, both interoceptive and exteroceptive, along with the dissolution of the high-level priors and hyper-priors that structure epistemic, self-related, and other fundamental predictive categories. Importantly, the transient state in which the inference system is annealed (a term borrowed from metallurgy that describes the higher flexibility facilitated by the transient higher-entropy state) and priors are relaxed or dissolved allows for older priors to be replaced with new, potentially more adaptive ones, which, after the psychedelic effects wear off, can stabilize as high-level encodings that explain away lower-level sensory, affective, and cognitive signals. This can explain why a single dose regimen can produce longstanding clinical improvements across many psychiatric conditions and why set, setting, and intentionality are crucial determinants of both the psychedelic experience and the subsequent degree of clinical improvement.

Neuroplasticity, Glutamatergic Interactions, and Longevity

Finally, it is worth briefly mentioning additional glutamateric interactions with 5-HT_{2A} receptor-mediated psychedelic activity, which include that NMDA antagonists potentiate psychedelic effects in mice and that group II mGluR agonists counteract psychedelic effects[4]. Psychedelics have also been shown to have effects on neuroplasticity and longevity, with structural remodeling, including neuritogenesis, spinogenesis, and synaptogenesis, occurring quickly (within 24 hours) after exposure and remaining long after a single dose[55,56]. These plastogenic effects are mediated by changes in gene expression triggered by 5-HT_{2A}-induced glutamate release and by direct binding to BDNF receptor TrkB in the mTOR pathway[57–59]. Psilocybin has also been shown to significantly increase cellular lifespan and delay senescence, likely via SIRT1-dependent reduction of oxidative stress and neuroprotection[60].

Interim Summary

In summary, classic psychedelics produce their characteristic subjective effects through a mechanism mediated by 5-HT_{2A} receptor activation, particularly in layer V pyramidal (L5p) neurons of the neocortex where these receptors are most densely expressed. Psychedelic 5-HT_{2A} stimulation increases cortical excitability by enhancing excitatory post-synaptic potentials in L5p neurons, which serve as critical integrators of bottom-up sensory signals (via basal dendrites) and top-down predictive signals (via apical dendrites) within cortico-thalamo-cortical circuits that underlie conscious perception. This 5-HT_{2A}-mediated excitation disrupts the normal entrainment of L5p bursts to alpha rhythm oscillations, resulting in broadband desynchronization and

decreased low-frequency α and β oscillatory activity that correlates with subjective psychedelic intensity.

Within the framework of active inference and predictive processing, psychedelics are proposed to modulate precision-control mechanisms by reducing the precision of higher-level priors encoded by deep pyramidal neurons while simultaneously increasing the gain of superficial pyramidal cells that encode prediction errors through disruption of thalamic relay gating. This computational rebalancing weakens the influence of top-down predictive feedback and strengthens bottom-up prediction error signals, disrupting the normal hierarchical process whereby high-level generative predictions explain away lower-level perceptual, cognitive, and affective data. The resulting perturbation of predictive dynamics produces a topological flattening of the brain's free energy landscape, allowing neuronal dynamics to escape prediction-driven attractor states and explore a more diverse range of states characterized by increased entropy and a tuning of neural dynamics closer to the critical edge of chaos. This manifests subjectively as the loosening of prediction-driven perceptual, cognitive, and emotional categories.

Section 2: **Meditation techniques mimic the psychedelic state via attentional modulation of diffuse thalamocortical coupling and olfacto-limbic entrainment of interoceptive prior recalibration**

Meditation is a loose construct that refers to self-regulated mental training practices that allow practitioners to attain transient non-ordinary states of consciousness, improve attentional and emotional wellbeing, and cultivate insight into the nature of reality[61]. While there is a wide

range of meditation techniques, each originating in a distinct tradition and for a specific purpose, they have been classified into three families based on the cognitive mechanisms involved (Box 1)[62].

Box 3.1 – Popular Varieties of Meditation
(Categories and cognitive mechanisms adapted from Dahl, Lutz, and Davidson, 2015[1])

- **Attentional** (mechanism: attentional regulation and meta-awareness):
    - **Focused attention (FA) meditation**: Sustaining narrowly focused attention on the moment-to-moment quality of a sensory, emotional, or cognitive phenomenon like the breath and re-orienting attention to the chosen object when distractions arise.
    - **Open monitoring (OM) meditation**: Wide monitoring of the moment-to-moment content of sensory, affective, and cognitive experience without evaluation or reaction.

- **Constructive** (mechanism: perspective taking and reappraisal by cultivating adaptive beliefs, emotions, intentions, and gestures):
    - **Loving-kindness and compassion (LKC) meditation**: Focusing attention on the intention to feel and spread loving-kindness and compassion to other beings.
    - **Prayer**: Intentional thought, speech, or action toward a transcendent agent.

- **Deconstructive** (mechanism: inquiry into the nature of self and experience):
    - **Mindfulness, insight, or Vipassana meditation**: Cultivating focused attention and open monitoring to non-judgmentally witness the content of consciousness and elicit insight into the nature of experience.
    - **Non-dual (ND) meditation**: Cultivating an experiential state not structured by self/other, subject/object, mind/body structural divisions.

Meditation techniques are heterogeneous, and the borders between them are porous. For example, focused attention (FA), which involves attending to the dynamic moment-to-moment quality of a sensory, emotional, or cognitive phenomenon like the breath, and non-judgmentally re-orienting attention to it when distraction arises, tends to naturally transition into an open monitoring (OM) state in which moment-to-moment sensory, affective, and cognitive experience are widely monitored without evaluation. Open monitoring may, in turn, reduce self-referential processing to produce a state of pure non-dual (ND) awareness that is free from the predicted self. A categorization based on cognitive mechanisms is useful but misses the importance of embodied processes, leaving out practices like Kundalini meditation in which sustained interoceptive awareness combined with intentionality, meta-awareness, and breathing exercises may awaken a subtle embodied process that, according to practitioners, can catalyze adaptive mental and physical changes and reprocess embodied trauma[63,64]. Of these, mindfulness meditation, which includes FA and OM, is the most studied.

Different meditation techniques produce different subjective experiences; within these, practitioners report similarities to psychedelic experiences, including the dissolution of time, space, and self, and mystical-type experiences characterized by a profound sense of unity, compassion, ineffability, positive mood, and transcendence[65]. While there are important differences between states of consciousness elicited by meditation and psychedelics, as well as within different styles of meditation and among the various psychedelics, the resulting expanded states of consciousness could be argued to be more alike to each other than different. Indeed, anthropologists have characterized meditation as the "hard" path towards ecstatic states in contrast to the "easy" path offered by psychedelic substances[66]. Separately, historians have speculated that meditation emerged as a substitute for the psychedelic referred to as "soma" in

the Indian Vedas, which likely disappeared due to climate changes in the Indian subcontinent[67]. In parallel fashion, as psychedelics became legally banned in the 1970s, psychedelic-assisted therapists developed and used meditation techniques able to induce psychedelic-like states to continue to access the therapeutic benefits of these states in contexts where psychedelics became psychologically, medically, or legally contraindicated[68].

Neurobiologically, meditation and psychedelics may engage overlapping or complementary neural mechanisms[69–71]. Both increase the complexity of neural dynamics[72], with studies showing that multiple meditation techniques increase neural entropy and enhance the neural signature of edge-of-chaos criticality[45,73–77]. Additionally, like psychedelics, meditation has been shown to increase neuroplasticity (including BDNF levels[78]), deactivate the default mode network (DMN, implicated in mental time travel and imagination of counterfactuals)[79–81], reduce anticorrelations between the DMN and resting state networks associated with exteroceptive processing[82,83], and reduce alpha power[84] (associated with predictive activity[23]).

Given these convergences and the relevance of DMN, alpha power, and neural complexity measures to predictive dynamics, meditation has been proposed to relax predictive neural activity in a similar manner to psychedelics. Notably, Laukkonen and Slagter[1] argue that, by bringing the meditator into the present moment, focused attention, open monitoring, and non-dual meditation progressively reduce hierarchically deep predictive processing, halting or diminishing any mental process that involves temporally deep processing; i.e., most cognitive, perceptual, and affective processes, which rely on anticipation of sensory inputs based on past experience. Specifically, they argue that focused attention stabilizes attention in the present moment, increasing the precision weighing of one source of present sensory experience while reducing that of all processes that rely on deep temporal models and of predictions from higher

in the hierarchy. Open monitoring also stabilizes attention in the present moment but treats all signals equally and assigns them low precision, making deeper levels of the hierarchy perceptible. Finally, as models with any temporal thickness fall away, the sense of time, space, body, self, and agency dissolve and become replaced with an experience of pure awareness–a non-dual state devoid of a narrative self and of subject-object divisions.

Put differently, they propose that as the meditator becomes anchored in the here and now, the brain's predictive hierarchy flattens, halting counterfactual processing–the issuing of predictions or hypotheses about the hidden causes of perceptual input conditional on sensory evidence. Counterfactuals predict the future states that minimize free energy under different scenarios[85]; i.e., they allow the system to maintain stability in the face of present and predicted stressors (i.e., to perform allostasis) by charting multiple potential paths so that one that minimizes long term surprise can be chosen. As meditative depth increases, these counterfactuals become "pruned" by a system anchored in the present, producing not only a non-prediction-driven state of awareness, but also unlocking novel, more flexible and parsimonious counterfactuals derived from this new experience and from high-level priors through insight-generating fact free learning (or Bayesian model reduction)[86].

Importantly, this process is largely equivalent to how psychedelics are thought to act on the predictive architecture, by attenuating temporally deep processing and reducing the relative weight of predictions and increasing that of prediction errors. The idea that, as meditative depth increases, counterfactual depth decreases, is therefore a meditation equivalent to the 5-HT_{2A}-mediated relaxation of priors via gain modulation of L5p cortical neurons and higher-order thalamic relay nuclei. It provides a plausible and parsimonious algorithmic description of how meditation relaxes predictive activity by modulating attention to modify precision weighing and

relax predictive activity, and it is consistent with the studies showing that meditation, like psychedelics, increases the entropy of neural dynamics[73–77]. However, it does not provide a plausible biological mechanism through which these meditation-evoked effects on predictive dynamics occur, making empirical verification difficult. Here, I present a plausible and falsifiable biological mechanism through which meditation techniques like mindfulness and FA-OM-ND may operate in the brain, which can account for how self-mediated attentional practices can produce a state with similar neural, phenomenological, and therapeutic effects to those induced by psychedelic $5HT_{2A}$ agonists.

Open Monitoring Meditation

Although mindfulness meditators tend to begin with focused attention (FA) practice and transition to open monitoring (OM) and non-dual (ND) states, I begin with a proposed mechanism for OM meditation.

As described above, psychedelics are thought to modulate the circuits that support conscious awareness by (a) sensitizing the deep pyramidal cells that encode expectations in cortical circuits and (b) disinhibiting the second-order thalamic relay nuclei that receive convergent L5p cortical prediction signals about the sensorium and project back to cortex. Both pathways increase cortical excitability, the entropy or complexity of neural dynamics, and tilt the system towards assigning higher precision to ascending sensory signals and less precision to descending predictive signals to produce a high entropy state that pushes the brain to operate closer to the edge of criticality. I propose that OM meditation endogenously achieves very similar effects by attentionally modulating the degree of matrix-to-core thalamocortical coupling

by second-order thalamic nuclei. To understand how this may be the case, we must briefly examine the anatomy and physiology of thalamic nuclei and of the cortico-thalamic-cortical (CTC) circuits involved in conscious awareness.

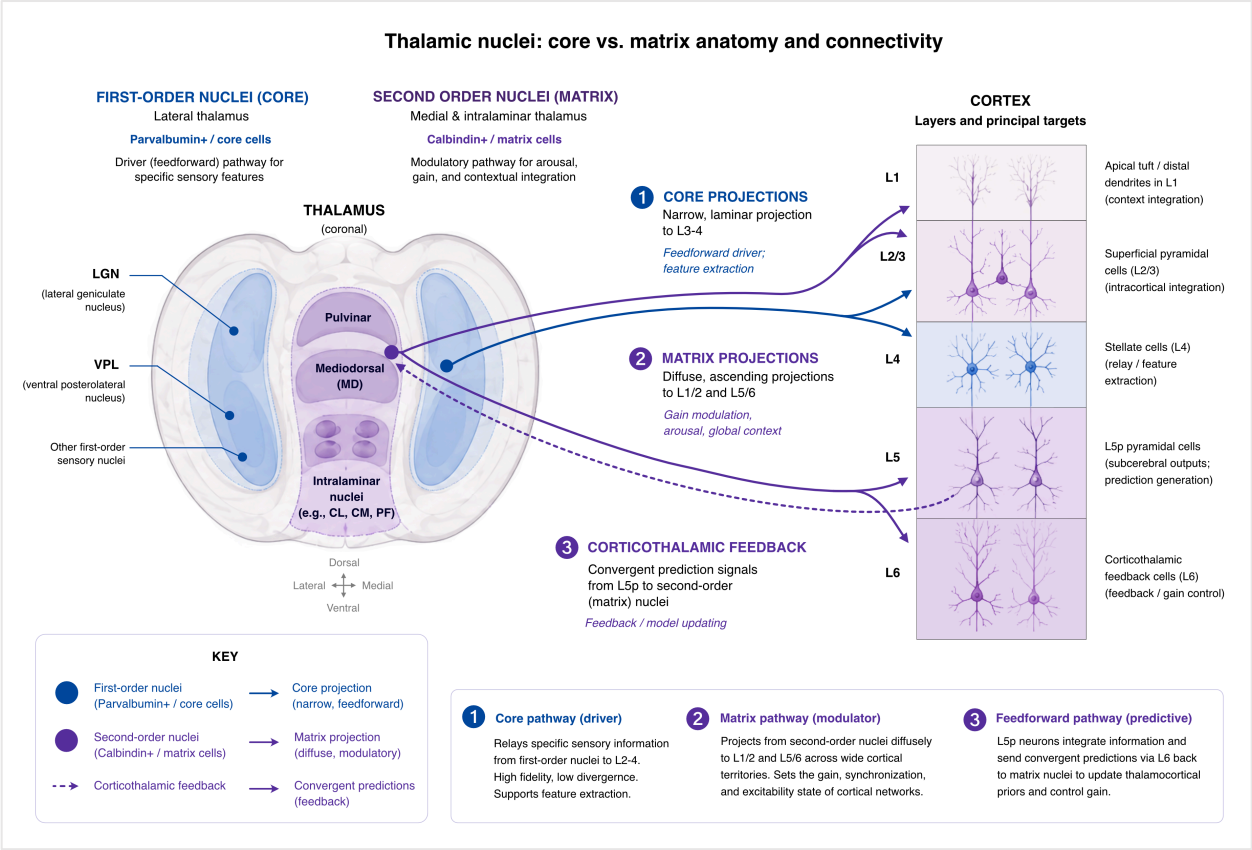


Figure 3.5: Thalamic nuclei and thalamocortical connectivity patterns.

Thalamic Nuclei

The thalamus contains two types of nuclei (Figure 3.5): First order nuclei, like the lateral geniculate nucleus (LGN), mainly act as thalamocortical *relays* between ascending sensory input and low-level cortical areas. For example, ascending retinal input projects from the optic nerve to

LGN, which then narrowly projects to primary visual cortex (V1) for low-level visual feature extraction. In contrast, second order thalamic nuclei, like the pulvinar, medial dorsal (MD), intralaminar, and midline nuclei, have a different circuit topology that receives and *integrates* convergent L5p input from cortex, *amplifies* task-relevant stimuli, and *suppresses* competing tasks' stimuli patterns via balanced amplification, gain adjustment, and divisive normalization[30,87,88]. These second order nuclei are at the center of the CTC circuits for attentional selection–the ability to select sensory inputs and suppress distractors in a task-relevant manner–, and they project broadly back to cortex, forming a re-entrant loop[30,88]. Tellingly, while first order nuclei activity is modulated by the physical presence of a stimulus, it is the awareness of a stimulus and not its presence that modulates the activity of second order nuclei[18].

In predictive coding terms, first order thalamic nuclei are central to feedforward computations that extract features, while second order nuclei are central to feedback computations that synthesize and update expectations based on attention, uncertainty, and the internal predictive model. Specifically, second order nuclei receive prediction signals from multiple cortical sources via convergent L5p traffic, compute a posterior distribution via selective gating (a likelihood function conditional on cortical context), and send the updated posterior back to cortex, where it can directly drive cortical spiking or modulate the impact of other inputs[30].

These types of processing are reflected in different anatomical connectivity patterns. Thalamocortical (TC) projections have traditionally been split into core and matrix types. Parvalbumin-containing "core" neurons, found primarily in first order thalamic nuclei, project *narrowly* to the middle cortical layers (layers 3-4) of a single cortical field, where they produce

large EPSPs and drive feedforward computations. In contrast, calbindin-containing "matrix" neurons are mostly found in second order thalamic nuclei and project *diffusely* to superficial or deep cortical layers of dispersed cortical fields, where they modulate activity and drive feedback computations[18,89]. Matrix neurons, together with thick-tufted layer 5 pyramidal (ttL5p) neurons, coordinate the widespread low-frequency oscillatory synchrony between cortical and thalamic neuronal populations, allowing thalamocortical signals to arrive in the "up" state of cortical oscillations and not be lost–a necessary condition for sustaining the conscious state[18].

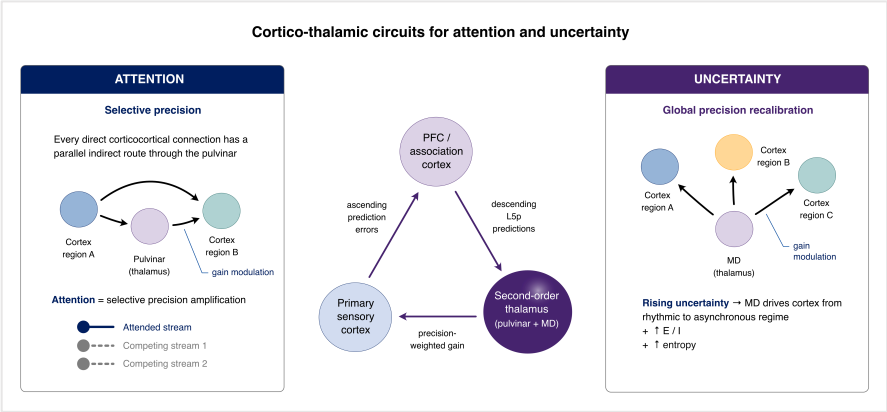


Figure 3.6: Corticothalamic circuits for attention and uncertainty.

Cortico-Thalamo-Cortical Circuits for Attention and Uncertainty

Besides tuning the rhythms that sustain consciousness, matrix neurons and second order nuclei are thought to encode and modulate the expected precision of prediction errors to control attention and adjust the brain's response to uncertainty (Figure 3.6). Attention and uncertainty are intimately linked: Attention reduces uncertainty by increasing the precision of sensory

signals from the attended object, and rising uncertainty redirects attention to keep overall surprise levels low.

The MD and pulvinar nuclei play an essential role in attentional dynamics. When attending to a particular stimulus, MD circuits amplify the recurrent connectivity patterns arriving from the prefrontal cortex that match that stimulus and suppress others that do not match it to maintain attention on the stimulus[30,88]. The pulvinar encodes attended objects with high precision and does not encode ignored objects[90], and pulvinar neurons are thought to encode the expected precision of information used in perceptual decisions[91]. Anatomically, every direct connection between two cortical regions has a matching indirect parallel connection through the pulvinar[92]. This unique circuit architecture facilitates selective neuronal synchronization (communication by coherence) between cortical regions, with pulvinar matrix neurons encoding the top-down expected precision of corticocortical signals and modulating the postsynaptic gain of corticocortical connections[31,93,94]. Therefore, not only do second order nuclei tune the rhythms that sustain the conscious state; they also orchestrate which signals between cortical regions get amplified or suppressed to shape the contents of consciousness. Note that this cortico-thalamic-cortical mechanism is central for the brain's ability to direct attention and is itself modulated by attention.

The same second-order nuclei involved in attention also drive dynamic CTC adjustments in response to uncertainty. MD neural populations, for example, separately encode sensory uncertainty and rule uncertainty (uncertainty in the underlying principles or rules governing the environment) to drive prefrontal reconfiguration as the organism switches between contexts[95]. Human EEG and fMRI studies show that heightened uncertainty increases cortical excitability, shifting the cortex from a rhythmic to an asynchronous regime, increasing sample entropy, and

flattening 1/f power spectral density slopes in a manner that correlates with BOLD signal increases in medial thalamic nuclei, especially MD[36]. This MD-mediated response to uncertainty also increases cortical excitation-to-inhibition (E/I) balance–the dynamic competitive balance between excitatory and inhibitory neuronal populations[96]. In other words, second order thalamic nuclei respond to higher uncertainty by increasing cortical E/I balance and the entropy of cortical rhythms, which corresponds to a re-weighting of neural precision. Since second order thalamus performs this through matrix-based TC projections that increase the gain of corticocortical signals, higher uncertainty drives diffuse thalamocortical coupling under the normal waking state.

This makes computational sense: Higher uncertainty means low precision about sensory evidence, hidden states, or the predictive model itself. Under increased sensory uncertainty, the surprise-minimizing system can only benefit from (a) increasing sensory precision (i.e., trusting prediction errors more), (b) increasing prior precision if sensory evidence is noisy or unreliable, or (c) increasing precision by identifying and attending to the source of uncertainty (i.e., attentional selection). Under uncertainty about hidden states or about the model itself, the system benefits by increasing sensory precision (i.e., trusting prediction errors more). In all these cases but one (noisy sensory evidence), and barring active inference (reducing uncertainty by acting on the world), the optimal response involves increasing sensory precision to shift away from a prediction-driven oscillatory low-entropy regime and toward a high-complexity quasi-critical regime that assigns more weight to ascending predictions errors and is capable of sending and responding to weaker and more unpredictable environmental perturbations[97].

Under heightened uncertainty, increasing sensitivity to inputs increases the probability of finding sensory signals to update or select higher-level predictions that match the environment

and explain hidden causes of sensory input to reduce uncertainty. It is thus adaptive for the system to respond to higher uncertainty by increasing cortical excitability, entropy, and criticality. Recall that increasing sensory precision can be done by increasing the gain of the deep pyramidal neurons that encode predictions and are the targets of matrix cells to make them more sensitive to ascending prediction errors. At a population-level, the resulting state is one in which firing rates can sustain a high sensitivity to inputs while preventing the system from saturating, i.e., one in which individual nodes become more susceptible to perturbations–more excitable–while stability is preserved at the network level. Recall as well that serotonin encodes expected uncertainty, with 5-HT_{1A} receptors reducing cortical gain by hyperpolarizing pyramidal cells and 5-HT_{2A} receptors increasing cortical excitability by enhancing pyramidal cells' sensitivity to bottom-up sensory signals and prediction errors.

Crucially, in silico biophysical corticothalamic models confirm that increasing the ratio of diffuse matrix-type versus targeted core-type connectivity stretches the brain's critical regime, allowing it to get closer to the edge of criticality without transitioning into a globally synchronized pathological state[98]. Tuning the thalamocortical system towards matrix-type connectivity therefore produces a higher entropy quasi-critical state consistent with both increased uncertainty and the diffuse and open attention practiced during OM meditation. Since superficial pyramidal neurons' gain, which is computationally equivalent to the precision assigned to ascending prediction errors, depends on the local excitation-to-inhibition (E/I) balance, increasing diffuse TC coupling increases cortical E/I balance, which is equivalent to increasing the excitability (or postsynaptic gain) of the superficial pyramidal cells that encode prediction errors on hidden causes of sensory input[99].

Diffuse Coupling Theory of OM Meditation

We now return to OM meditation, during which attention is non-reactively directed towards the overall content of experience as the practitioner remains anchored to the present and simultaneously aware of any arising sensory, affective, or cognitive events in a non-evaluative manner. As it is usually practiced with eyes closed and in a serene environment, the salience of exteroceptive sense data is diminished relative to that of interoceptive, affective, and cognitive content, increasing the relative importance of re-entrant, second order nuclei-based CTC streams vis-à-vis relay traffic from first order nuclei. Moreover, stillness precludes active inference (acting on the world) as an avenue for surprise-minimization, leaving modulation of sensory precision as the main free energy minimization mechanism available. Crucially, during OM, the practitioner resists the natural tendency to focus attention on a specific percept (i.e., to selectively amplify and assign high precision to signals associated to one percept) in favor of non-reactively monitoring the whole contents of experience. As a result, the system is assigning high precision to many streams of sensory, affective, and cognitive content simultaneously and maintaining this high precision during the practice. High precision is, in turn, implemented via thalamic matrix cells, which increase the gain of multiple streams of corticocortical processing. By the mechanisms just described, this increases the ratio of matrix-to-core thalamocortical connectivity, raises cortical E/I balance, and induces a higher-entropy cortical regime.

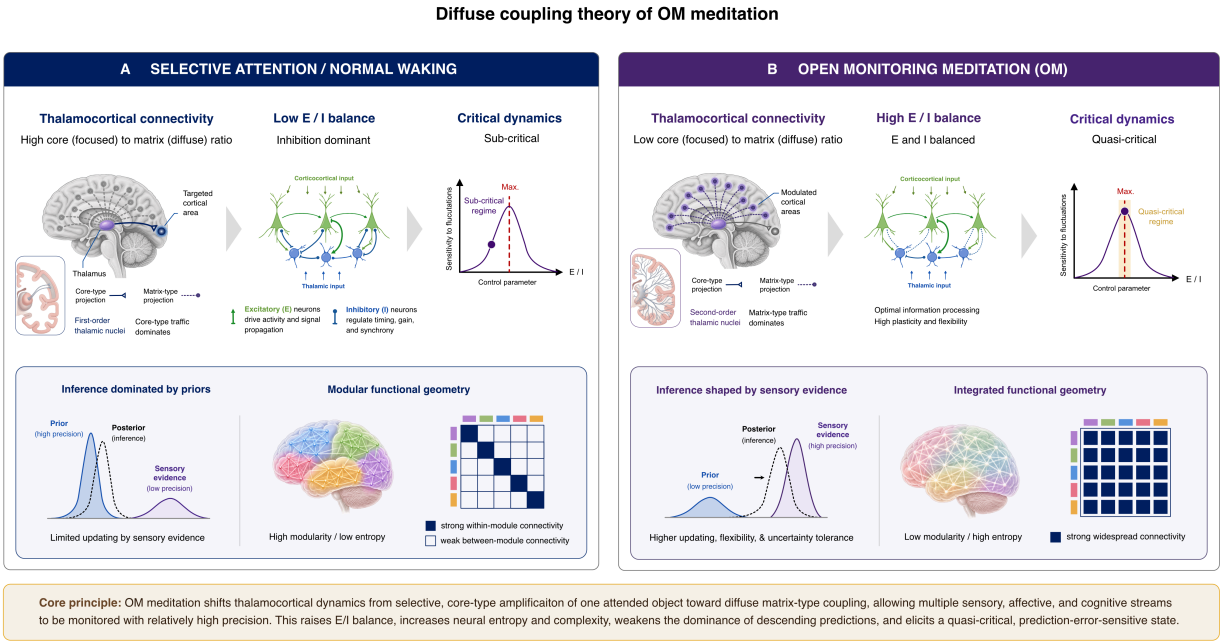


Figure 3.7: Diffuse coupling theory of open monitoring meditation.

We therefore propose that by limiting attention to the present moment and cultivating a nonevaluative state devoid of judgments of exteroceptive and interoceptive stimuli that is simultaneously broadly aware of such stimuli, OM meditation modulates attention to simultaneously assign high precision to more cortical streams than under the normal wakeful state (Figure 3.7). This, in turn, shifts thalamocortical functional geometry towards diffuse matrix-based coupling, which increases population-level cortical excitation-to-inhibition balance and cortical excitability (gain) to produce a higher entropy cortical regime in which the cortex operates closer to criticality, becoming more perturbable by smaller fluctuations and showing greater signatures of complexity. Since the intrinsic excitability (gain) of the superficial pyramidal cells that encode prediction errors on hidden causes normally results from the competition between excitatory and inhibitory neuronal populations[99], a higher E/I balance corresponds to a relative dampening of predictions on predictive coding circuits and to a more

feedforward-driven state with predictions assigned a lower relative weight vis-à-vis prediction errors–a state that can also be characterized as producing a flattened predictive hierarchy and less counterfactual processing.

This biologically plausible mechanism explains how regulating attention during meditation can produce the observed signatures of higher cortical complexity and criticality, which mimic those induced by psychedelics. It also explains how OM meditation alters consciousness in a similar manner to psychedelics to produce an experience in which the prior-based models of self, body, world, and reality loosen their grip on perception to allow for the emergence of what practitioners call an expanded state of consciousness. The proposed mechanism implicates many of the same circuits thought to be responsible for psychedelics' effects on consciousness. Recall, for example, that the mediodorsal and pulvinar nuclei express the highest concentration of 5-HT_{2A} receptors within the thalamus[39] and that psychedelics modulate their activity in a manner that correlates to subjective effects[40,41]. By disinhibiting these relay nuclei[41] and by increasing the gain of cortical superficial pyramidal cells that encode prediction errors, psychedelics are thought to bias the system toward bottom-up feedforward processing[38,42]. Moreover, psychedelic 5-HT_{2A} agonists modulate the same L5p neurons that project from cortex to the second-order thalamic nuclei that can tune core-to-matrix TC coupling via attention and uncertainty. It is likely that the proposed mechanism is one of multiple mechanisms operating during mediation, and it cannot explain the significant differences between and heterogeneity within the states of consciousness and mystical experiences induced by psychedelics and OM meditation. Nevertheless, it provides a parsimonious and empirically falsifiable mechanism that accounts for the neurophysiological, computational, phenomenological, and clinical similarities between psychedelics and OM meditation.

Empirical Predictions

The diffuse coupling theory of meditation can be tested empirically with a combination of activation, functional connectivity, and complexity/criticality-based neuroimaging techniques. It predicts that thalamocortical functional connectivity under OM meditation will have a more diffuse geometry, with second-order thalamus having a higher degree distribution than under the normal waking state. It also predicts a less modular cortical functional connectivity network under OM meditation, with increases in diffuse thalamocortical functional geometry and decreases in cortical modularity proportional to increases in cortical entropy and complexity measures and to subjective effects like time, space, and ego dissolution on scales of mindfulness and mystical experience.

Additionally, more diffuse coupling would correspond not only to a higher E/I balance and greater entropy, complexity, and a stretched quasi-critical regime, but also to attenuated predictive processing with lighter relative weights on descending priors vis-à-vis ascending prediction errors. Therefore, perceptual processes subject to predictive processing, including pain perception, visual/auditive/somatosensory perception, saccadic eye movements, speech/language perception, face/emotion perception, and time/agency/self-related perception, should be altered under OM meditation, with perception becoming less prediction-driven in a manner proportional to increases in cortical entropy and excitability.

Implications

Before continuing to address the second major component of mindfulness meditation–focused attention (FA) meditation–two noteworthy observations derive from the diffuse coupling theory and its constituent components.

First, the ability of second order thalamic nuclei to encode sensory and rule uncertainty separately and to modulate cortex-wide excitability, oscillatory dynamics, and corticocortical synchronization via cortical gain control implicates these nuclei as orchestrators of thalamocortical functional geometry and supports the possible role of the thalamus as Bayesian observer[30]. By modulating the strength of each cortico-cortical signal along L5p neurons, which have been shown to be highly relevant to conscious content, these thalamic circuits seem to influence the contents of consciousness by adjusting the target of attention and tuning the degree to which the system is prior- versus prediction error-driven to minimize prediction errors in a task relevant manner.

Second, by modulating cortical E/I balance, OM meditation not only alters the contents of consciousness but also the level of consciousness. The entropy of neural dynamics is a reliable correlate of level of consciousness, with the entropy and complexity of signals being greatest in fully alert states and falling in states with loss of awareness or consciousness like NREM sleep and anesthesia[100,101]. Interestingly, second order thalamic nuclei and core-matrix functional geometry are implicated as modulators of perceptual thresholds and level of consciousness. Mice studies show that lesions to higher-order thalamic nuclei that project to cortical ttL5p neurons via matrix cells increase the animals' perceptual thresholds, implying that conscious perception thresholds are mediated by a re-entrant loop between matrix thalamus and ttL5B cells that transition the latter from rhythmic spiking (unconscious) to a bursting (conscious) regime[11,18,102]. Importantly, the converse is also true: Loss of consciousness due to anesthesia is accompanied

not only by a decrease in entropy and complexity but also by a shift from balanced core-matrix functional geometry to a matrix-deficient one[103]. Thus, the state produced by meditation, characterized by a matrix-dominant functional geometry and higher levels of complexity and entropy than under the normal waking state, is consistent with a level of consciousness that lies *above* that of normal wakefulness–an intriguing status. While the potential meaning of this is beyond the scope of the neurophysiological mechanism, both meditation practitioners and psychedelics users colloquially refer to the states attained as elevated and expanded states of consciousness.

Focused Attention Meditation

Focused attention (FA) meditation consists of maintaining attention on a target stimulus, most commonly the breath, while disengaging from unrelated distractors and reorienting attention back to the chosen stimulus in a neutral, nonjudgmental manner when it strays[104,105]. With training, attention remains focused for longer, and the practitioner tends to experience increasingly deeper and longer absorptive states, which can be experienced as mental bliss. FA meditation is often taught as a precursor technique to other types of meditation, which require the ability to sustain inwardly focused attention. Buddhist FA meditation practices like Ānāpānasati (mindfulness of breathing) are meant to calm and concentrate the mind to overcome distraction, develop insight and mental stability, and overcome suffering.

Mechanistic predictive processing accounts of FA meditation, like that by Lutz et al.[106], focus on the bidirectional shift between the focused attention and the mind-wandering states and characterize FA as a precision-modulation regime in which interoceptive sensory channels

associated with respiration are selectively up-weighted. Specifically, they posit that by focusing on the breath, the practitioner adopts breathing as a stable low-variance prior, with top-down predictions about breathing-related interoceptive input becoming increasingly precise, while competing high-level priors—e.g., autobiographical thought, exteroceptive distractions—becoming down-regulated via reduced precision weighting. The low variance and novelty from sensory channels causes the salience of the breath to fade and low-level sensory prediction errors to be explained away. This causes precision to drift upward in the predictive hierarchy toward higher-level cognitive predictions, endogenous mental material, and autobiographical priors, which come to the fore as mind-wandering[106]. Mind-wandering continues until interoceptive and proprioceptive prediction errors signaling deviation from the focused attention policy trigger a perceptual update, at which point distraction is noticed and attention is reallocated back to the breath. Lutz et al. conclude that, with practice, progressively earlier error detection shortens mind wandering episodes, and that, as the mind becomes better able to represent mental contents with reduced precision, epistemic insight reveals the impermanent and constructed nature of mental contents while weakening the grip of high-precision habitual priors.

Lutz and colleagues build a compelling algorithmic case for how FA meditation modulates competing sensory and cognitive priors to regulate attention, including monitoring and disengaging from distractions and redirecting focus. However, their view, along with that of most FA contemplative science, reduces FA practices like Ānāpānasati to switching between selective attention and mind-wandering, while Buddhist accounts treat mindfulness of breathing as not just a precursor attentional regulation technique but rather as a complex insight practice in its own right[107,108]. Here, I build on their and others' work by proposing a broader algorithmic theory that accounts for the affective, cognitive, epistemic, and absorptive phenomenology of

this style of meditation, along with a plausible biological implementation that accounts for the hallmark neurophysiological and information theoretical markers of the FA meditative state. Since FA meditation is usually focused on the breath, we first trace the effect of oscillatory and breathing rhythms on intrinsic brain oscillatory activity.

Attentional Entrainment to Rhythmic Stimuli

Selective attention can be understood as a rhythmic, oscillation-based process that synchronizes internal neural dynamics to the temporal structure of relevant stimuli[109], aligning periods of higher neural excitability with the moments new stimuli are expected to arrive. Low frequency delta and theta oscillations align their phase with the rhythm of an attended stimulus in primary sensory cortex and motor cortex, with oscillations becoming selectively entrained with attended streams over ignored ones and with entrainment strength scaling with the predictability of the stream[110,111]. Entrainment enhances and stabilizes the neural representations of attended stimuli, and its periodicity aligns with an individual's intrinsic alpha frequency, indicating that attention exploits endogenous oscillatory dynamics[112].

Since low-frequency oscillation phase hierarchically modulates higher frequency amplitude, rhythmic attentional entrainment has hierarchical consequences. Aligning low-frequency phase to an attended stimulus sharpens its temporal processing, boosts gamma-band power (associated with bottom-up sensory encoding) and suppresses alpha/beta power (linked to prediction, top-down inhibition, and reduced uncertainty)[109,113], with the latter known as event-related desynchronization. Furthermore, as compared to a less predictable rhythmic stimulus, a more predictable one causes pre-stimulus alpha power (associated with prediction) to strengthen

and post-stimulus gamma power (associated with sensory processing) to weaken[113]. This, in turn, matches a predictive processing logic: Facing a more predictable stimulus, the system can rely more on its predictions without generating large prediction errors, whereas facing a less predictable stimulus requires that higher precision be assigned to ascending sensory/prediction error signals.

In summary, attention rhythmically tunes intrinsic neural oscillations based on the rhythm and predictability of the attended stimulus to optimize the timing and gain of sensory processing and to balance the precision weighing of sensory- versus prediction-driven signals.

Nasal Breathing Entrains Limbic Oscillations

We can think of the breath as both an endogenously generated oscillation and a sensory stimulus that is perceivable, for example, by orienting attention to sensations in the nasal passages. While respiratory drive originates in bursting pacemaker brainstem neurons, the frequency and amplitude of the breath are influenced by affective and cognitive states. For example, inspiratory time and tidal volume are reduced when human participants are amused; inspiratory pauses are prolonged during disgust[114]; and sympathetic activation, which can be triggered by anticipation and remembrance of a stimulus, alters respiratory rhythm and minute ventilation to support increased oxygen demand[115]. Crucially, nasal respiration has been shown to entrain slow oscillations in human piriform cortex as well as higher frequency (delta, theta, and beta range) limbic oscillations in the amygdala and hippocampus, with affective and cognitive functions like fear discrimination and memory retrieval being enhanced during the nasal inspiratory phase[116].

Together, these findings point towards a complex multidirectional relationship between respiratory oscillatory patterns, allostatic regulation based on actual and predicted physiological states, and the stream of affective and cognitive events. In one direction, the occurrence, anticipation, or remembrance of a stimulus associated with an increased metabolic demand can trigger changes in respiratory rhythm and amplitude. In the other direction, respiratory dynamics entrain limbic oscillations and modulate affective and cognitive responses to fear-associated stimuli and memory retrieval. While the precise relationship between breathing, oscillatory brain dynamics, and memory is complex and a matter of ongoing research, the entrainment of nasal breathing and limbic regions via piriform cortex suggests that the breath holds a privileged mechanistic role in the encoding of memory and affect. A brief foray into the cognitive neuroscience of memory and affect will help to elucidate this.

Interoceptive Predictive Processing, Memory, and Affect

Interoceptive signals are the brain's representations of the body's internal visceral state, and because the stability of visceral function is a matter of survival, interoceptive signals are thought to have the highest a priori expected precision of any sensorimotor channel and to occupy the top of the predictive processing hierarchy as "first priors"[117]. This means that interoceptive prediction errors dominate the perceptual hierarchy, such that perceptual salience is computed relative to a stimulus's impact on visceral predictions rather than on exteroceptive evidence alone. In this view, cognition is fundamentally enslaved to embodiment rather than merely weighed by it, and any event that calibrates or alters interoceptive precision weights will have an outsized influence on the future behavior of the perceptual apparatus.

Predictive processing accounts treat affect as the consciously accessible consequence of the brain's interoceptive predictions about the physiological condition of the body, summarizing ongoing metabolic and autonomic regulation in terms of valence and arousal[51,118]. In this view, interoceptive sensations are limbic predictions about the body based on actual and predicted metabolic needs, which are experienced as lower dimensional feelings of affect[119]. Affective valence, experienced phenomenologically as positive or negative feelings, reflects whether incoming interoceptive signals reduce or increase prediction error relative to priors that encode long-term expectations about bodily and environmental states. Valence therefore tracks the success or failure of allostatic predictions (including self-predictions) across hierarchical timescales, linking emotion to the adaptive regulation of the body. For example, encountering an unexpected predator behind a bush will generate a large prediction error, trigger a large sympathetic response to provide the metabolic resources to fight or flee, and produce negatively valenced interoceptive sensations experienced as fear.

The memory of a salient and valenced experience is likely to encode allostatically useful information, i.e., information that can guide how the organism should behave and budget its metabolic resources in similar future instances. In our example, to avoid the large prediction errors associated with the unexpected predator in the future, the system will encode the affective, perceptual, and contextual features of the experience in memory and adjust its priors to include it, so that future encounters with the same or a similar bush will elicit the predator prediction, behaviorally and physiologically priming the system to respond to the threat. Memory, affect, and prediction are thus linked by the evolutionary imperative to encode associations between useful versus harmful stimuli and adaptive versus maladaptive behaviors.

Memory is embodied, enactive, and affective. Episodic memories are partially indexed by affective state[120] and reactivation of memories tends to co-activate representations of bodily arousal, valence, and motivational significance alongside perceptual and contextual details[121]. While declarative and procedural memory encode consciously accessible events/concepts and skills/motor actions, respectively, affective memory encodes the valence associated with past experiences, which contributes to guiding future behavior[122]. In predictive processing terms, generative models jointly encode expected sensory states and affect as low-dimensional representations of interoceptive predictions, with emotionally salient experiences training the model to associate a perceptual pattern with a specific interoceptive prediction. Put simply, memories have feelings attached to them, and when we remember something, we reexperience these feelings, which are encoded as valenced embodied sensations. Something that made you feel bad (or good) in the past is likely to make you feel bad (or good) in the future, with the associated feelings increasing the chances that you will avoid (or seek) the thing that triggered the feeling.

Electrophysiologically, during memory encoding, stronger gamma rhythms are thought to reflect the binding of perceptual and contextual features into episodic representations, while theta entrainment is believed to play a role in assigning sensory and contextual input to memories[123,124]. The retrieval of salient memories tends to evoke increased theta-band activity, particularly in frontal-midline and medial temporal areas, along with enhanced gamma-band power and cortico-hippocampal entrainment and phase-amplitude coupling[125]. At the same time, alpha and beta power decrease (event-related desynchronization), consistent with a release of inhibition that allows memory content to become consciously accessible[126].

Importantly, the magnitude of these oscillatory effects scales with emotional intensity, suggesting that emotional salience acts as a modulator of the memory system, primarily through amygdala-hippocampal interactions that boost the oscillatory response[127,128]. Specifically, hippocampal-amygdala theta entrainment, observed during fear learning and extinction, is thought to facilitate the encoding of emotional valence attached to memory[129]. Intracranial recordings show that successful aversive memory encoding depends on transient coupling between amygdala theta phase and hippocampal gamma activity[130] and that the amygdala modulates and temporally coordinates hippocampal gamma activity associated with correctly remembered aversive memories[128,131]. Amygdala-hippocampal theta entrainment therefore plays a key role in the encoding and retrieval of emotional memory. Since nasal breathing entrains theta oscillations in hippocampus and amygdala via piriform cortex, the finding that nasal breathing phase is correlated to successful memory retrieval places nasal breathing oscillations in a privileged position vis-à-vis allostatically relevant affectively charged memories. Of note, hippocampal representations go beyond simply encoding memory and have been shown to cover generalized predictive associations[132].

The Olfacto-Limbic Interoceptive Prior Recalibration (OLIPR) Mechanism

Following the early scientific accounts of FA meditation, most studies reduce FA to attentional regulation training and treat the breath as an incidental stimulus target, replaceable by any other. For a great many contemplative traditions, however, the breath is the doorway into the path of insight, spirit, and relief from suffering[107,108], with contemporary interpretations characterizing it as the bridge that connects the conscious to the unconscious mind[133]. Indeed, the

word for breath in Chinese (Qi, 氣), Sanskrit (Prana, प्राण), Latin (Spiritus), Greek (Pneuma, πνεῦμα), Hebrew (Ruach, רוּחַ, and Neshamah, נְשָׁמָה), and Polynesian (Mana/Ha) is the same as the word for spirit, showing that ancient peoples across cultures understood the breath as both physiological function and spiritual threshold.

In the Buddhist Pali Canon's Ānāpānasati Sutta, or Breath-Mindfulness Discourse, the Buddha describes awareness of the breath as the initial focus of meditation[134]. The discourse lays out a progression of contemplative practices split into four sections, beginning with contemplation of the body, beginning with the breath, and followed by contemplation of feeling, mind, and mental objects. Contemporary Buddhist traditions and others instruct practitioners to attend to the natural nasal breath by focusing attention on the airways or nasal passages while making no attempt to control the breath[135]. One such tradition teaches this style of meditation "to make [the mind] sensitive enough to feel the subtler realities within the framework of the body,"[135] by which is meant to help the practitioner experience how suffering arises from the connection between mental phenomena and embodied sensation, described as follows:

> The mental-physical phenomenon is like a coin with two sides. On one side are the thoughts and emotions arising in the mind, on the other side are the respiration and sensations in the body. Any thoughts or emotions, any mental impurities that arise, manifest themselves in the breath and the sensations of that moment. Thus, by observing the respiration or the sensations, we are in fact observing mental impurities [...] As a result, we discover that these impurities lose their strength; they no longer overpower us as they did in the past.[136]

These traditions treat the breath not only as an attentional target to improve concentration but also as a window into interoceptive sensation and its connection to affect and thought. According

to them, focused attention on the breath allows the practitioner to enter a state in which one can experience affective memories as interoceptive sensations without necessarily consciously associating them with declarative or episodic memories, so that nonjudgmental observation of the sensations can weaken their grip on the practitioner's mental state[136].

This contemplative tradition's description is strikingly amenable to predictive processing accounts of interoception and action. If we take affective memory encodings to include joint perceptual and interoceptive predictions associated to the remembered event, the subjective feeling accompanying memory retrieval would correspond to the reinstated interoceptive predictions and their precision (confidence), which determines how strongly affective content influences perception, thought, and action. Following this logic, a lived experience that recalls a similar, previously encoded salient experience, like approaching the bush behind which a predator once hid, would elicit an interoceptive prediction meant to mobilize behavior and prepare the body for a significant metabolic outlay. The interoceptive prediction would be experienced as interoceptive sensation and felt as fear. Moreover, its influence on the predictive system would be a product of the relative precision weight of the prior (or memory) vis-à-vis that of the sensory evidence. For example, a salient memory of an actual predatory attack–a very high precision prior–would cause the prediction to have a strong perceptual and affective impact on the system such that even dissimilar bushes might evoke the prediction. Put differently, a traumatic experience is much more likely to be re-elicited and to provoke strong feelings than a non-traumatic one.

That the behavior-eliciting and physiology-altering prediction is adaptive is predicated on the probability that a predator might be lurking behind this new bush and on the flexibility of the predictive system vis-à-vis the variance of the environment. The predictive system flexibly

adapts to a changing environment by estimating and updating not only the probabilities associated with events but also the volatility of the environment[137]. In other words, it continuously updates the precision of its priors, calibrating them to the changing statistics of the environment so that the correct predictions are elicited, at the correct magnitude, and at the appropriate time and place. For example, walking past a similar bush to the one behind which the predator hid, even if no predator appears, will initially trigger a strong interoceptive prediction and fear. However, each time that no predator is encountered, the precision assigned to the prediction of predatory danger vis-à-vis the sensory data of the bush will be downwardly revised, and if no predators are encountered for a long enough time (i.e., the statistics of the environment change), the prediction will stabilize at a lower precision and possibly become supplanted by other, more probable ones associated to the sensory data representing a bush. In this way, memory is constructive rather than reproductive, the act of remembering itself decoding and re-encoding memories, rendering the memory malleable and subject to modification before being re-instantiated[138].

Despite this adaptive flexibility in the predictive system, predictions are persistent, and negative predictions more so. Threat learning is asymmetrically fast, and threat predictions are asymmetrically resistant to updating[139–141], a phenomenon that likely follows from the fact that the potential cost of overpredicting a threat is lower than that of underpredicting one (e.g., missing a threat can be fatal, while missing an opportunity merely delays reward).

Importantly, when over-precise weights assigned to negative predictions (e.g., “I am helpless”) begin to suppress disconfirmatory prediction errors and selectively sample evidence that confirms these priors, the system can fall into a maladaptive self-fulfilling cycle that prevents the proper recalibration of precision, causing innocuous experiences to persistently

elicit negative affect[142]. Even without necessarily falling into such a pathological state, however, a high precision interoceptive prediction that evokes a predicted aversive bodily state can stay in place or be slow to change through avoidance, which acts as a precision-weighted policy selection that prevents the predicted aversive interoceptive state from being sampled[143]. In our example, this would correspond to avoiding any area with bushes after nearly being killed by the tiger that hid behind one. Avoiding the aversive state minimizes expected free energy in the short term, as no surprises are generated by any potential predators hiding behind bushes; and yet, by preventing the organism from entering the feared situation, no prediction error is generated, so the brain never receives evidence that the interoceptive prediction was overly precise vis-à-vis the environment (i.e., that the prevalence of tigers hidden behind bushes is actually quite low). Without model revision, the high-precision threat prediction is never tested or revised and continues to prescribe avoidance[144,145]. The result is a maladaptive stable attractor loop in which the high precision of aversive interoceptive predictions causes any experience that may elicit them to be avoided, while at the same time keeping in place the over-prediction of negative affect associated with them. Thus, even when the threat does not appear again, and even if the statistics of the environment change for the better, this is not enough to update beliefs (priors) and remove the suffering associated with negatively valenced interoceptive predictions. Indeed, one can think of suffering as negatively valenced interoceptive sensations, experienced as negative affect, and resistant to conscious efforts to dispel or avoid them because of their encoding as high-precision priors.

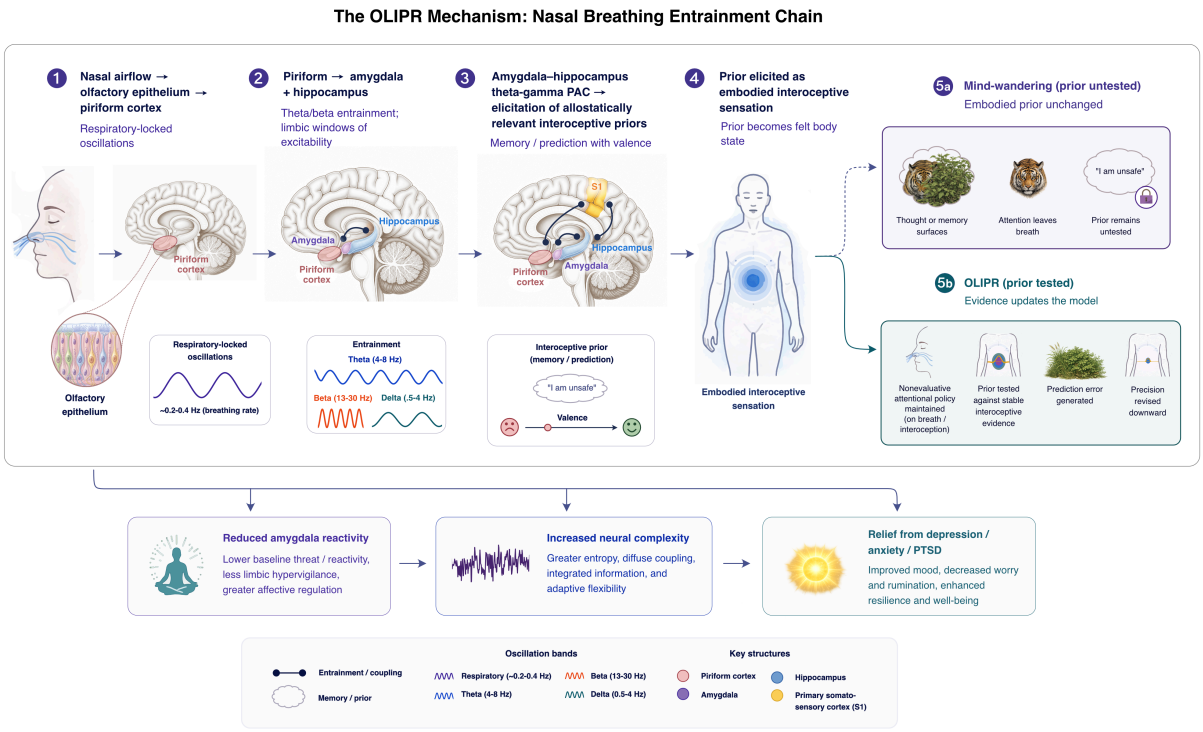


Figure 3.8: Olfacto-limbic interoceptive prior recalibration under focused attention meditation.

I propose that focused attention to the breath modulates the precision of interoceptive predictions by eliciting the interoceptive sensations associated with allostatically relevant interoceptive predictions (memories) (Figure 3.8). This allows the predictive system to test the predictions under a policy of non-reactivity and therefore against allostatically stable interoceptive sensory evidence, leading to the attenuation of these priors' high precision. Downwardly revised precision, in turn, loosens the grip of these priors on the predictive system, lowering the probability that they will be re-elicited and the felt salience of the interoceptive sensations when they are. I postulate that focused attention to the breath elicits interoceptive sensations associated with allostatically relevant interoceptive predictions to downregulate their precision by the following mechanism, which I call olfacto-limbic interoceptive prior recalibration (OLIPR).

Above, I established that nasal respiration entrains slow oscillations in piriform cortex and higher frequency delta, theta, and beta range limbic oscillations in the amygdala and hippocampus, with phase-dependent enhancement of memory retrieval and emotional discrimination. I also established that attention to a rhythmic stimulus entrains cortical delta and theta oscillations in primary sensory and motor cortices to the rhythmic characteristics of that stimulus. Finally, recall that hippocampal-amygdala theta entrainment facilitates the encoding of emotional valence attached to memory. Thus, when breathing becomes the stimulus on which attention is focused, a chain of entrainment becomes produced from the hippocampus and amygdala–medial temporal limbic regions that encode memory and affective valence–to the primary sensory regions that encode prediction error signals and are deeply embedded in prediction loops. Moreover, by creating windows of excitability that align to when signals arrive while excluding competing inputs during inhibitory phases, oscillatory entrainment between brain regions enhances information flow between them[146]. Entrainment differentiates conscious from unconscious processing and is believed to mediate access to conscious perception[147]. I therefore propose that nasal breathing closes an entrainment loop which allows allostatically relevant interoceptive priors (a.k.a. affectively charged memories that act as attractors on the predictive system) to ascend to cortical sensory circuits, elicit the associated embodied sensations and affective, cognitive, and perceptual conscious content, and either distract attention (as Lutz et al. describe) or be tested against low arousal interoceptive evidence. Put differently, sustained focused attention to nasal breathing entrains primary sensory oscillations to limbic oscillations, eliciting encoded predictions that produce either distraction or model updating, with a shift towards the latter as attentional regulation improves.

When the practitioner succeeds in maintaining attention focused on the breath and also opens attention to bodily sensations, as in many mindfulness practices, the affective priors are re-elicited as interoceptive sensation without the attached declarative memory, which would distract attention from the breath to the episodic remembrance of the memory associated with the interoceptive prediction. When the episodic component does become elicited and succeeds in distracting attention from the breath, we call this mind-wandering, and it does not produce a re-weighting of the elicited priors' precision. During mind wandering, like outside of the meditative state, recalling an episodic memory accompanied by negative affect–i.e., a high-precision prior that was originally encoded with an associated limbic prediction about the body that resulted in a large prediction error–will re-elicit the original interoceptive prediction, which will be experienced in the body as negatively valenced sensation. Remembering the predator behind the bush that almost killed us will trigger embodied feelings of fear and dread. Crucially, the most common responses to negative affect are avoidance and rumination: The mind avoids the negatively valenced feelings and sensations and quickly moves on from that memory, leaving the associated interoceptive predictions untested, or it falls into a train of associated negative memories that elicit more negatively valenced interoceptive sensations, sensory evidence that reinforces the original high-precision prior. In either case, the original interoceptive prior remains in place.

During meditation, however, the nonevaluative focused attention policy keeps attention focused on the breath alongside an accepting stance towards arising sensations, feelings, and thoughts. This allows affectively charged interoceptive predictions to be played out as interoceptive sensations without avoidance or rumination, such that the predictions can be felt and tested against sensory evidence coming from a body at rest. The resulting prediction error–

the difference between the prediction and the interoceptive evidence, which this time is the opposite of the prediction error responsible for the original encoding–reduces the prediction's precision, decreasing the probability that the prediction will be re-elicited and increasing the probability that a different prediction replaces it, thereby loosening its grip on the predictive system. In this way, focused attention on the breath not only regulates attention but also drives adaptive model updating via the relaxation of priors, not unlike serotoninergic psychedelics.

This proposed mechanism, which I call Olfacto-Limbic Interoceptive Prior Recalibration (OLIPR), parsimoniously accounts for empirical findings showing that FA meditation reduces habitual responding[1] and that, consistent with a progressive lowering of precision in affective priors, expert meditators show less activation in the amygdala than novices[148]. With time, by assigning greater relative precision to ascending sensory evidence and lower relative precision to priors, the system can break free from the priors that acted as attractors to operate in a more feedforward manner and inhabit a wider range of states. By the mechanisms described in sections 1 and 2, this would produce higher measures of signal complexity in the brain, accounting for yet another consistent empirical finding[149,150]. The revision of priors also accounts for how practices that include mindfulness of breathing, like meditation-based stress reduction (MBSR), tend to reduce symptoms of anxiety[151], pain[152], PTSD, and depression[153]–all conditions with a strong predictive component. Through the mechanism proposed, focused attention on nasal breathing literally "make[s the mind] sensitive enough to feel the subtler realities within the framework of the body"[135].

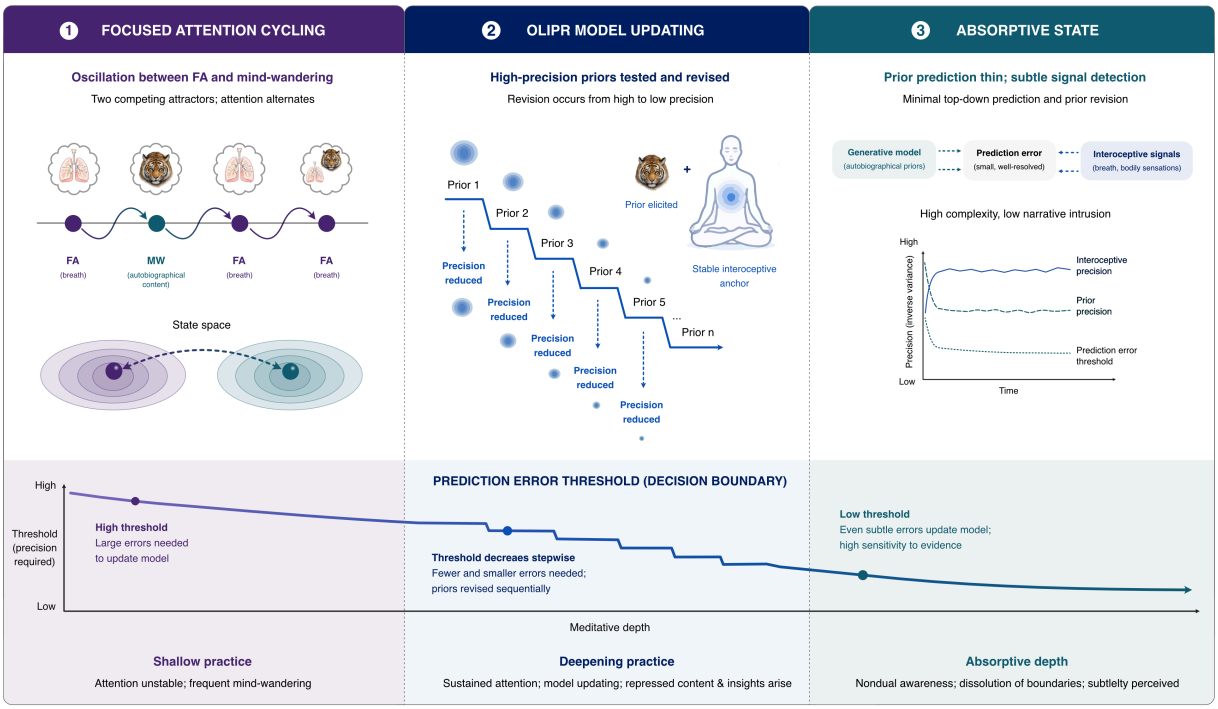


Figure 3.9: Three predictive regimes during FA meditation.

Multiple Predictive Regimes

I propose that there exist three different regimes depending on attentional policy success and predictive dynamics (Figure 3.9). So far, I have described two of these: The first covers the phase of iterative cycling between focused attention and mind wandering described by Lutz et al.[106] They argue that, as the breath becomes more predictable, precision shifts away from sensory prediction errors and up the predictive hierarchy towards higher-level autobiographical priors, then back to the breath to produce progressively earlier error detection. I propose that the shift away from breath-based sensory prediction errors towards autobiographical priors may not only follow from diminishing sensory prediction errors about the breath, but also from the mind's habitual tendency to avoid the unpleasant sensory experience of the high precision

interoceptive predictions elicited by the limbic-cortical sensory entrainment that focused attention on nasal breathing produces. Spending time in this regime shortens the time it takes for the system to detect the growing sensory prediction errors during mind wandering episodes, improving attentional regulation, strengthening the brain's capacity to selectively amplify signals, including unpleasant ones, over the habitual priors and spontaneous thought trajectories that ordinarily hijack attention.

Regime two is the state in which focused attention successfully remains on the breath with a nonevaluative and nonreactive stance while interoceptive predictions become evoked as embodied sensations, tested, and revised. As model updating relaxes high-precision priors, complexity increases, and progressively deeper priors become elicited and tested. The process samples priors descending through a gradient of salience, precision, and temporal depth, all the way through the organism’s embodied history. This explains why, as the meditative practice deepens, practitioners tend to experience the resurfacing of emotional memories and can experience spontaneous and profound emotional insights, including forgiveness and compassion. As interoceptive predictions are tested against sensory evidence and updated, the system stops over-predicting the priors that originated them, and the practitioner is no longer gripped by the emotions associated with them. This explains the trait changes and clinical benefits observed after mindfulness meditation (which combines FA and OM), including relief from the symptoms of depression, anxiety, stress, and post-traumatic stress.

The relaxation of predictive priors, here achieved endogenously, can be seen as largely equivalent to 5-HT_{2A}-based psychedelic modulation of predictive coding circuits (section 1). As interoceptive predictions are experienced as embodied sensations, the practitioner learns how to sustain focused attention simultaneously on the breath and on the elicited sensations without

becoming distracted by discursive mental content. This natural transition from FA meditation to open monitoring reinforces model updating through cortico-thalamic-cortical diffuse coupling and places FA and OM meditation on a continuum of mental practices with porous boundaries between them, rather than as discrete techniques separable by cognitive mechanism, as contemplative science has heretofore treated them.

Finally, regime three occurs when attention remains successfully focused on the breath but no longer elicits interoceptive or autobiographical predictions. This usually occurs after significant and intensive practice, once the most salient interoceptive predictions have been elicited, tested, and revised. The result is an absorptive state (Jhāna in Buddhism), which can go from focused concentration with thought and mental bliss, through increasingly refined stillness and equanimity, into formless states of infinite space, boundless consciousness, and nothingness. As the priors that structure perception (including self-perception) get recoded with low-enough precision, they release their grip on the predictive system, allowing conscious awareness to experience a version of reality that is less mediated by these hyper-priors. Interestingly, the subjective content of these states is not phenomenologically empty or devoid of valence, but rather a rich set of subtle states that are commonly attributed a numinous quality. Indeed, I propose that, as meditation advances through the three regimes, an additional process recalibrates prediction error thresholds and sensitizes the system from gross to progressively subtle sensory phenomena.

Importantly, regime three is not a perpetually stable state. Absorptive states may last minutes, hours, and in some rare occasions, days, until the sampling of a different set of priors returns the system to regime two. During long and intensive meditation retreats, the system can

cycle between regimes two and three multiple times, leading the practitioner into a subtly different absorptive state each time.

From Gross to Subtle: Re-calibration of Prediction Error Thresholds

Recall from hierarchical predictive coding that the threshold for a prediction error to be either explained away or sent up the prediction hierarchy when compared against a descending prediction is dynamic. For example, the precision or confidence of a specific prediction or prediction error, encoded in the gain of the deep or superficial L5p pyramidal cells and modulated by the 5-HT_{2A} receptor, determines the relative influence of a prediction vis-à-vis a prediction error. Recall as well that this threshold can vary based on the precision of a specific prediction or prediction error and can also vary globally, affecting the overall confidence of predictions versus prediction errors as it converges to a temporally stable level that matches the level of uncertainty the system is exposed to. This threshold, which determines the relative influence of predictions versus prediction errors, can be modulated by attention, uncertainty, and exogenous 5-HT_{2A} agonists, and is reflected in cortical excitation-to-inhibition (E/I) balance, which results from the competition between excitatory and inhibitory neuronal populations and sets the intrinsic excitability (gain) of the superficial pyramidal cells that encode prediction errors on hidden causes.

During OLIPR's regime one, attention strays from the breath due to habitual avoidance of high precision interoceptive priors recruited by entrainment between limbic and primary sensory regions. Attention gets refocused on autobiographical thoughts instead of on present-centered sensory flow, which would generate larger prediction errors and lead to model revision and

regime two. We can therefore think of this process as the system switching attention towards content that is known (low surprise) as opposed to experiencing the interoceptive consequences of untested high-precision predictions (potentially high surprise). Constrained by high precision predictions and a low level of surprise, this state would produce a low level of neural complexity.

In regime two, attention remains on the breath, high precision interoceptive priors get tested, and their precision gets reduced. Attentional focus on the sensory qualities of the breath keeps the precision of ascending sensory signals high, while the precision of individual predictions being tested gets revised down. This state is equivalent to navigating a high uncertainty environment in which it is more adaptive to trust novel sensory data than existing predictions. Prediction errors, produced by the mismatch between interoceptive sensory data and interoceptive predictions, drive model updating. In this process, the system will tend to test higher-precision predictions first, as they are the most likely to be elicited. As interoceptive predictions are updated, the prediction errors produced each time they are elicited get smaller.

At first, these prediction errors are not large enough to cross the error threshold, so fewer predictions get updated. During the normal waking state, the prediction error threshold varies within a range that is calibrated to the size distribution of prediction errors. Relatively stable statistics of the environment produce a relatively stable prediction error size distribution, which keeps the prediction error threshold within a metabolically adaptive range. During meditation, however, there is no or very limited exteroceptive sensory data, while model updating skews the size distribution of prediction errors towards smaller errors. As meditation changes the shape of the distribution, the prediction error threshold decreases and stabilizes at a lower level, so that smaller prediction errors, which before would not have triggered a model update, now do so. As a result, progressively subtler prediction error signals get sent up the predictive hierarchy to

update priors, finetuning the generative model. In free energy terms, the system begins to respond to smaller fluctuations, which before would have been treated as noise. In this way, intensive meditation practice sensitizes the perceptual apparatus, training and turning it to progressively subtler fluctuations (Figure 3.9).

During OLIPR's third regime, attention remains successfully focused on the breath and on interoceptive sensation, but predictions (including thoughts, memories, and interoceptive sensations) are no longer elicited or tested, allowing attention to enter an absorptive state and rest on awareness itself. In free energy terms, prediction has become so thin that ascending prediction errors no longer result in model updating. Interestingly, the resulting experience is often not experienced as devoid of content but rather as an entryway into a subtler, content-filled reality.

Among most mystical spiritual and religious traditions, including Hindu Yoga-Vedānta, Taoist internal alchemy, Vajrayāna Buddhism, Islamic Sufism, and Jewish Kabbalah, a convergent pedagogical principle holds that authentic spiritual training proceeds from coarser to more refined dimensions of perception. Whether articulated as the five *kośas* from the gross physical body to the bliss sheath, the Taoist refinement of *jīng* into *qì* into *shén* and finally into the formless *wújí*, the Tibetan tantric dissolution of gross mental activity into the subtle energy-winds and ultimately the "clear light" very-subtle mind, the Sufi sequential purification of the *nafs* through the *maqāmāt*, or the Kabbalistic ascent through *nefesh*, *ruach*, and *neshamah*, each tradition holds that subtler levels become accessible only once coarser ones have been experienced and transcended[154–156]. The progressive lowering of the prediction error threshold and the consequent sensitization of the predictive system to subtler fluctuations parsimoniously explains this progression from gross to subtle percepts. The epistemological and ontological implications of this are discussed in section 5. For now, suffice it to say that the parsimonious

mechanism of hierarchical predictive coding in regimes two and three is sufficient to account for this phenomenon.

Empirical Predictions and Evidence

Testable predictions for the OLIPR mechanism and the broader theoretical framework span five domains: nasal respiratory entrainment of limbic circuits, attentional regulation and its oscillatory correlates, interoceptive prior testing and model updating, signal complexity, and shifts between regimes. The existing evidence is substantially supportive of the oscillatory and affective components of the framework, while the breath-specific and regime-specific predictions remain the most important targets for future empirical work.

1. Respiratory Entrainment

The primary prediction concerns the privileged role of nasal breathing as a meditation target. If the OLIPR mechanism is correct, then focusing attention on nasal breathing, versus a structurally matched FA task using a non-respiratory target, should produce uniquely strong theta coherence between primary sensory oscillations and piriform cortex, amygdala, and hippocampus. Zelano et al.'s landmark intracranial EEG study in epilepsy patients, which found robust inspiratory-locked delta, theta, and beta power increases in limbic structures during nasal but not oral breathing, and demonstrated that breathing phase predicts performance on amygdala- and hippocampus-dependent cognitive tasks[116], provides strong support. However, the specific comparison between nasal-breath FA and non-respiratory FA has not yet been conducted in a

meditating population and represents an important empirical gap. Relatedly, I predict that switching meditators from nasal to oral breathing mid-session will attenuate limbic entrainment and increase mind-wandering.

OLIPR proposes that the nasal respiratory cycle creates windows of limbic excitability that facilitate the elicitation of affectively charged memories. If true, the nasal inspiratory cycle phase should predict the onset of mind-wandering episodes during FA meditation. The phase-dependent enhancement of memory retrieval and emotional processing during inspiration, documented by Zelano et al. and Herrero et al.[157], lends mechanistic plausibility to this claim. However, whether mind-wandering onset during meditation clusters around a specific respiratory phase has not been directly examined. Also untested is the prediction that individual differences in basal respiratory rate predict the cycle length of FA-to-mind-wandering episodes: if slower breathing entrains limbic circuits at lower frequency, practitioners with slower basal respiratory rates should produce longer windows between elicitations of competing priors and therefore exhibit longer on-task episodes before mind-wandering onset.

2. Attentional Regulation

The theory predicts that FA training progressively reduces the latency between mind-wandering onset and meta-aware detection of distraction, and that this improvement is indexed by increasing frontal midline theta power in the period just before the practitioner notices having wandered. Both components are independently supported. Brandmeyer and Delorme (2018) used an experience-sampling paradigm during one hour of concentration meditation and found that expert practitioners reported significantly less mind-wandering than novices, with increased

frontal midline theta and somatosensory alpha rhythms accompanying on-task states relative to mind-wandering[158]. Yoshida et al. (2020) confirmed the training-dose relationship between frontal midline theta and attentional depth, finding that frontal midline theta power increased after FA training in novice meditators and was positively associated with practice duration[159]. Finally, DeLosAngeles et al. (2016) showed that theta power correlated with both practice hours and self-reported depth of concentration in experienced practitioners[160]. The specific prediction that theta elevation temporally precedes and predicts the moment of distraction detection, rather than merely accompanying the meditative state, has not been isolated with sufficient temporal resolution but is consistent with the existing data.

The most diagnostically powerful untested prediction is that nasal-breath FA produces greater attenuation of conditioned fear responses than a structurally equivalent FA practice using a non-respiratory attentional target. This would directly distinguish whether the breath's therapeutic and insight-generating effects derive from OLIPR or from attentional regulation alone.

3. Interoceptive Prior Testing

The theory also predicts that FA meditation progressively reduces the precision of negative affect priors, manifesting as decreased amygdala reactivity to emotionally charged stimuli. Kral et al. (2018) provides dose-dependent support, finding that amygdala activation to negative images was specifically lower in long-term meditators with intensive retreat experience, while reductions to positive stimuli appeared with less practice[161]. This valence asymmetry is precisely what the OLIPR mechanism predicts, since high-precision negative priors should be

the most resistant to recalibration. Desbordes et al. (2012) provide complementary evidence, showing that eight weeks of FA meditation training produced a decrease in right amygdala activation to stimuli of all valences even when participants were not actively meditating, suggesting that prior-updating effects transfer to trait-level predictive processing changes[162].

The theory also predicts that intensive practice should lower interoceptive detection thresholds. Contradicting anecdotal accounts of meditators, multiple studies have found a negligible mean difference in heartbeat detection and respiratory interoceptive discrimination tasks between meditators and non-meditators[163,164], possibly reflecting the inadequacy of heartbeat and respiratory discrimination paradigms in assessing interoceptive accuracy.

4. Signal Complexity

The theory predicts that as high-precision priors are relaxed, the brain becomes able to access a wider range of states, yielding increased neural signal complexity. Most studies support this prediction[73–75,165], finding higher signature measures of entropy, complexity, or criticality during meditation versus rest, including a flatter aperiodic 1/f slope, consistent with a lowered prediction error threshold via higher excitation-to-inhibition balance. One study comparing six meditation styles against a mind-wandering control in skilled practitioners found the opposite effect[166], an apparent contradiction that might reflect the different baseline conditions used (resting state versus active mind-wandering).

5. FA-OM Meditation Continuum

The theory predicts that the transition from active prior-testing (regime two) to absorptive stillness (regime three) is marked by a collapse of hippocampal-amygdala theta-gamma phase-amplitude coupling and a subsequent shift toward broadband, low-amplitude, high-entropy signal. This remains untested.

Implications

The mechanistic framework developed in Section 2, spanning OM's diffuse thalamocortical coupling, FA's olfacto-limbic entrainment, and the progressive lowering of the prediction error threshold across three regimes, converges on a set of implications that extend beyond neurophysiology toward a deeper understanding of what meditation heals, how it heals it, and what happens once it does.

The Primacy of Embodied Memory

"Man is born free and everywhere he is in chains." – Jean-Jacques Rousseau

As much as we value freedom and like to think of ourselves as sovereign individuals, we are held and swayed by our emotions and embodied memories, which constrain our freedom to feel, act, and think as we would like. Since antiquity, the great dramas of the human experience have revolved around the fundamental inability to act in one’s best interest, even while knowing what it is. At the root of this are interoceptive predictions encoded with exceptionally high precision, the residues of large prediction error-generating events that demanded a durable

updating of the generative model to minimize future metabolic and survival risks. High precision ensures they are readily re-elicited and have an embodied (and disproportionately strong) constraining influence on perception, cognition, affect, and behavior – one that can outweigh or bypass volition, even as one is cognitively aware of it. Freedom is indeed rarer than we like to think and should be thought of within the context of the body.

Our embodied view of cognition[167] aligns with Antonio Damasio's somatic marker hypothesis[168], Lisa Feldman-Barrett's theory of constructed emotion[119], van der Kolk's theory of embodied trauma[169], and Allen and Tsakiris's predictive processing account of interoceptive priors[117], which takes cognition to be fundamentally enslaved to embodiment at the level of the generative model itself. At a basic level, this means that temporally deep processing is not only a cortical phenomenon but also a whole-body one. As meditative depth increases and hierarchically deep predictive processing falls away from more abstract and autobiographical priors down to affective and interoceptive ones (regime two), what the system encounters is not silence but memory–the embodied, allostatically encoded interoceptive predictions that constitute the body's archive of salient past experience.

The relaxation of priors follows the predictive hierarchical structure. Higher-level cognitive and autobiographical priors are the first to surface and be attenuated, as they depend on the deepest temporal models. After these fall away, what remains is not pure awareness but the embodied layer of visceral, somatosensory predictions, encoded with location, intensity, and valence, that represent allostatically relevant prior beliefs about bodily states. These predictions include those that were laid down earliest, reinforced most durably, and that carry the highest metabolic stakes. Their encoded precision reflects not just personal history but the body's running budget of expected metabolic costs and benefits. They are the last to be relinquished

because they are, in the hierarchy of the generative model, foundational. As such, they embed cognition, perception, emotion, and behavior. Nature, as it were, abhors a predictive vacuum. The progressive quieting of the mind does not initially reveal an empty channel but rather the foundational substrate on which the predictive architecture is built.

Mindfulness of Embodied Sensation as the Mechanism of Traumatic Resolution

Embodied priors and interoceptive prediction errors may dominate the perceptual hierarchy and influence action selection, operating at a level of the predictive hierarchy below conscious cognitive access, but cognition also constrains when and how these priors and prediction errors become expressed via suppression, avoidance, and rumination. Rumination, suppression, and avoidance preserve and reinforce high precision interoceptive priors by preventing the sampling of sensory evidence that would allow their precision to be revised. This is why, somewhat counter-intuitively, "consciously experiencing our primal pain loosens its hold on us,"[1701]–the clinical mechanism behind how exposure, psychedelic, and talk therapy reduce post-trauma symptoms.

What certain meditation techniques provide, and what my framework allows us to understand mechanistically, is an equanimous interoceptive context within which these high-precision predictions can be elicited and played out as embodied sensations without triggering the avoidance or rumination responses that ordinarily prevent their revision. The aversive interoceptive states are sampled (i.e., re-experienced in the body) within the container of

[1] Or, as put by the 19th Century mystics P.D. Ouspensky and G.I. Gurdjieff: "Work consists in subjecting oneself voluntarily to temporary suffering in order to be free from eternal suffering."[171]

equanimity provided by the nonevaluative and nonreactive attentional policy of mindfulness (FA + OM) meditation. Importantly, given meditation's attentional policy, this often occurs through sensation alone, without the explicit memory of the originally eliciting events coming to mind. The body lives through the prediction without the environment confirming it, so the resulting prediction error–the mismatch between the predicted aversive state and the comparatively stable interoceptive evidence from a body at rest–reduces the precision of the prior. Over repeated cycles, the prior's grip loosens, and the associated need for avoidance weakens. A weaker prior increases the degrees of freedom available to the system the next time it encounters a situation that would have elicited the prediction, a phenomenon experienced as embodied healing, forgiveness, and freedom from addiction, anxiety, and depression. In mechanistic terms, this is how mindfulness meditation heals trauma: not through cognitive reappraisal or narrative reconstruction, but through the direct interoceptive disconfirmation of high-precision embodied predictions in an allostatically stable context.

Dependent Origination and the Somatosensory Encoding of Prediction

A further implication concerns the representational format of predictions themselves. If the body is first prior, then a substantial proportion of predictions must be encoded not as abstract propositional structures but as somatosensory sensations, complete with location, intensity, and valence corresponding to those experienced during the original encoding event. This is precisely what predictive processing accounts of embodied emotion suggest, and what the OLIPR mechanism assumes: that when a prior is elicited, the somatosensory prediction it

encodes is reinstated as felt sensation, and that the behavioral response selected is responding to the embodied sensation rather than to an abstract propositional belief.

If behavior, or a large portion of it, is primarily a response to embodied interoceptive predictions rather than to deliberative propositional reasoning, then behavior modification and relief from suffering caused by unhealthy behavioral patterns require not a change of beliefs at the cognitive level but a change in the precision and valence of embodied predictions. And if those predictions are encoded and re-elicited through the limbic entrainment pathways described here, via nasal breathing, theta-gamma coupling, and amygdalo-hippocampal oscillatory dynamics, then focused attention on the breath is not just a concentration or attentional regulation exercise but a direct interface with the somatosensory substrate of feeling and decision-making itself.

This view resonates with classical Buddhist formulations of dependent origination (Paṭicca-samuppāda), in which craving and aversion, and the cycles of suffering they perpetuate, arise not from the external circumstances of the world but from contact with embodied sensation and conditioned responses to it[134]. Indeed, what the Buddha described as the chain of dependent arising, from contact through sensation to craving and clinging, describes the experiential equivalent of my theoretical framework's hierarchical predictive architecture: sensation or feeling-tone (vedanā) as the phenomenal aspect of interoceptive prediction, craving and aversion as precision-weighted behavioral policies, and liberation as the progressive recalibration of the generative model through the equanimous observation and reencoding of sensation.

Liberated Degrees of Freedom and Higher Metabolic Efficiency Underlie the Expansion of Psychological Possibility

If perceptual and value-based salience is computed relative to a stimulus's impact on visceral predictions, then the perceptual hierarchy's prediction errors, which are normally explained away by higher-level interoceptive priors, free themselves from the constraining influence of the priors as they become relaxed under regime two. New prediction errors may then ascend the predictive hierarchy and update the generative model, tightening its sensorimotor coupling with the environment and lowering the long-term average of surprise[37]. Importantly, once the layer of embodied memory has been sufficiently recalibrated, the revised generative model, now more congruent with the actual statistics of the environment, operates with lower expected free energy for the same sensory input. As a result of this, two things become liberated: computational degrees of freedom in the generative model, which were previously tied to hierarchically privileged interoceptive priors, and metabolic resources, which were previously dedicated to maintaining and explaining away high precision interoceptive predictions.

When a high-precision prior is revised downward, the metabolic and computational resources previously dedicated to maintaining it—generating its associated predictions, prescribing its associated behavioral policies, suppressing the prediction errors that would otherwise contest it—are no longer bound to that function. The system recovers degrees of freedom, which had been locked into the maintenance of a fixed predictive attractor, changing the topology of the accessible state space. Attractors that previously dominated the generative model and constrained the range of possible perceptual, affective, and behavioral states become weakened, increasing access to a broader range of stable configurations, a phenomenon reflected in the higher entropy and criticality signatures detected across various measures of neural activity under meditation. In free energy terms, the landscape flattens locally around the former

attractor, reducing the energetic cost of transitions away from it and enabling the system to explore regions of state space that were previously inaccessible or costly to reach.

This expansion of accessible state space has direct psychological consequences. High precision interoceptive priors constrain personality, relational style, cognitive flexibility, and the range of meanings and possibilities that the organism can entertain. A prior encoding such as "I am helpless" or "intimacy is dangerous" does not merely produce depression or attachment avoidance; it actively shapes perception, attention, and behavior across every domain of experience, systematically sampling evidence that confirms it and suppressing evidence that would disconfirm it. When such a prior is recalibrated, the freed degrees of freedom become available for new couplings with features of the internal and external environment that the prior had previously rendered invisible or inaccessible. New relational configurations become possible; new interpretations of past experience become available; new behavioral repertoires can be explored without the metabolic and attentional cost that the prior's maintenance had previously imposed.

Crucially, the new degrees of freedom are not coupled to the same material and metabolic constraints as the priors they replace. The released predictions had been encoded at high precision precisely because they were associated with large metabolic stakes–survival-relevant encodings that demanded durable, high-confidence behavioral policies. The new predictions that become accessible once these priors are recalibrated are less urgently tied to the frozen statistics of past threat and more flexibly coupled to features of the present environment. This is the mechanistic basis for the psychological possibilities that open up in this state and for the finding that both psychedelic-assisted therapy and intensive meditation practice increase trait openness–

the dispositional willingness to engage with novel experience–, one of the most robust predictors of positive long-term therapeutic outcome[172–174].

Clearing the Channel

"We don't see the world as it is, we see it as we are." – Anaïs Nin

The progressive lowering of the prediction error threshold that accompanies the meditation process sensitizes the system to smaller fluctuations. Once cleared of the high-amplitude signal of embodied memory, the system becomes equipped to detect and respond to subtler inputs, not because reality has changed but because the epistemic tension between the generative model and the environment has decreased. Lower-amplitude features, which before had been explained away as noise to respect the hierarchical primacy of interoceptive priors, can now be perceived. This progression from gross to subtle perception, described across contemplative traditions, follows the generative model's growing parsimony and sensitization to progressively finer scales. New degrees of freedom become available not by addition but by release: No longer coupled to the metabolic costs of maintaining high precision interoceptive predictions, they become available to encode the contents of more rarefied states of consciousness.

According to this view, just as the relaxed-beliefs state produced by psychedelics is not an absence of content but rather a content no longer constrained by the attractor basins of habitual prediction, the absorptive state, freed from the constraint of high-precision self- and body-related priors, encounters the world with a less top-heavy generative model and finds that

something is there which the prior constraints had previously excluded from awareness. The phenomenological richness reported at this stage is, by the present account, a real signal that was always present but beneath the detection threshold of the prediction-dominated system. The ascending hierarchy of subtle states is therefore a progressive disclosure of the world's lower-amplitude structure, made possible by the model's upward revision of its sensitivity and downward revision of its prior precision. At this point, insights tend to become transpersonal rather than personal and numinous rather than mundane, increasing the ineffability of the experience.

As the reader has surely grasped, the most radical implication of this mechanistic proposal is that the transpersonal or numinous content reported in deep meditative and psychedelic states may appear not as an arbitrary feature of altered consciousness or as an epiphenomenon of a dissolved self-model but as what becomes accessible once the high-precision layer of personal embodied memory has been sufficiently recalibrated: a veritable window into noumenal reality. From a free energy perspective, this state corresponds to one in which the cortico-thalamic-cortical system is operating at the knife’s edge of criticality, with conscious content informed by the ultra-low amplitude phenomena that only come into view in such a physical-computational state. Section 5 will examine this possibility in its computational, epistemological, and ontological dimensions.

Interim Summary

Section 2 developed a mechanistic framework that describes how meditation techniques produce neural, phenomenological, and therapeutic effects that converge with those of classic

psychedelics, through attentional practices and without requiring exogenous pharmacological agents. Two complementary biological mechanisms were proposed, one for open monitoring and one for focused attention, both grounded in the predictive processing architecture described in Section 1.

For open monitoring (OM) meditation, I proposed the Diffuse Coupling Theory, which holds that by sustaining broad, nonevaluative attention across the entire field of present-moment experience rather than selectively amplifying any single percept, OM meditation increases the ratio of diffuse matrix-type to targeted core-type thalamocortical connectivity. This shift toward matrix-dominant functional geometry, mediated by second-order thalamic nuclei including the pulvinar and mediodorsal nucleus, raises cortical excitation-to-inhibition balance, increases the gain of superficial pyramidal cells encoding prediction errors, and drives cortical dynamics toward a higher-entropy quasi-critical regime. Computationally, this is equivalent to a global reduction in the relative precision of descending predictions and a corresponding increase in the precision of ascending prediction errors, the same rebalancing of the predictive hierarchy proposed to underlie psychedelic 5-HT_{2A} agonism, here achieved endogenously through attentional modulation of thalamocortical functional geometry. The resulting state is characterized by higher neural entropy and complexity, attenuated DMN activity, reduced alpha power, and a loosening of the prediction-driven perceptual, affective, and cognitive categories that structure normal waking awareness. Empirical predictions concern the proportionality between diffuse thalamocortical functional connectivity, cortical entropy measures, and the subjective dissolution of time, space, and self.

For focused attention (FA) meditation, I proposed the Olfacto-Limbic Interoceptive Prior Recalibration (OLIPR) theory, which holds that sustained attention to nasal breathing entrains

cortical delta and theta oscillations in primary sensory cortices to the respiratory cycle via piriform cortex, which in turn entrains higher-frequency limbic oscillations in the amygdala and hippocampus–the regions responsible for encoding affective valence and allostatically relevant memory. Because hippocampal-amygdala theta-gamma phase-amplitude coupling is central to the encoding and retrieval of emotionally salient episodic and interoceptive memories, this entrainment chain creates windows of limbic excitability that allow allostatically relevant interoceptive predictions, encoded as embodied sensations with location, intensity, and valence, to ascend to cortical sensory circuits and become consciously accessible. Under the nonevaluative, nonreactive attentional policy of FA meditation, these predictions are tested against the stable low-arousal interoceptive evidence of the body at rest rather than avoided or elaborated through rumination, generating a prediction error that progressively reduces the precision of the elicited prior. Repeated recalibration relaxes the grip of high-precision interoceptive predictions on the generative model, producing trait-level reductions in amygdala reactivity, increased neural entropy and complexity, and relief from depression, anxiety, and PTSD, whose pathophysiology involves the over-precision of negatively valenced predictive priors.

Within this framework, FA and OM meditation were shown to exist on a continuum rather than as categorically distinct techniques. Three predictive regimes were identified: an initial cycling between focused attention and mind-wandering driven by habitual avoidance of high-precision interoceptive predictions; a model-updating regime in which the practitioner sustains attention through elicited interoceptive sensations, testing and revising priors and naturally transitioning into open monitoring; and an absorptive regime in which predictions are attenuated sufficiently for awareness to rest on progressively subtler signals. The progressive

lowering of the prediction error threshold across these regimes sensitizes the perceptual apparatus to smaller fluctuations, providing a mechanistic account of the convergent contemplative principle that contemplative practice proceeds from gross to subtle dimensions of experience.

The implications developed in the final subsection extend the framework in three directions. First, the body constitutes the first prior in the generative model hierarchy: as cognitively deep processing falls away, it is embodied interoceptive memory, not pure awareness, that initially fills the receding predictive space, and it is the equanimous re-experiencing and disconfirmation of these embodied predictions that constitutes the core mechanism of trauma resolution. Second, once this embodied layer has been sufficiently recalibrated, the degrees of freedom previously bound to high precision interoceptive prediction are released, lowering the metabolic cost of the generative model and clearing the channel for subtler conscious content, content that was always present as signal but previously fell beneath the system's detection threshold. Third, a substantial proportion of predictions are encoded as somatosensory sensation, such that eliciting a prior reinstates its associated embodied state and behavioral responses are responses to that reinstated sensation. This grounds classical formulations of Buddhist dependent origination directly in the architecture of embodied predictive coding, with the equanimous observation of sensation serving as the operative mechanism of liberation from conditioned behavioral cycles.

Together, the Diffuse Coupling and OLIPR theories provide empirically falsifiable, biologically grounded accounts of how self-regulated attentional practices can produce the neurophysiological signatures–increased entropy, criticality, and complexity; attenuated DMN and alpha activity; altered functional connectivity geometry–and the clinical and

phenomenological outcomes associated with FA and OM meditation, while additionally specifying the embodied and mnemonic substrate through which these effects confer lasting therapeutic benefit. Finally, they also account for the convergent phenomenology and therapeutic benefit of meditation and 5-HT_{2A} psychedelics.

Section 3: Caloric Restriction Produces Mystical Experience Through Metabolic Relaxation of Cortical Priors

Having provided a mechanistic theory for how FA and OM meditation can produce the neurophysiological signatures of altered states of consciousness shared with psychedelics, I now turn to the connection between these states and metabolism, as viewed through the lens of caloric restriction. Fasting has been recognized for millennia as a spiritually essential consciousness-altering practice conducive to mystical experiences, as well as an adjuvant to meditation and psychedelic-induced altered states of consciousness. While observational and anthropological evidence suggest that caloric restriction can reliably enhance meditative states and/or produce mystical states, the physiological reasons behind this and the broader physiological connection between metabolism and the altered states of consciousness produced by meditation, psychedelics, and fasting remain largely uncharacterized. Here, I review the existing literature and propose a novel, biologically grounded, and empirically falsifiable mechanistic theory for how caloric restriction may help to produce these states, both on its own and alongside psychedelics and meditation.

Fasting and Mystical States

Fasting is one of humanity's oldest and most widely distributed methods of accessing altered states of consciousness in general and mystical states in particular. The ancient Egyptians fasted before sacred rites, and Babylonian priests fasted before oracle consultations. Buddhist and Hindu traditions prescribe fasting as a form of ascetic discipline, and all three Abrahamic religions enshrine fasting as a form of purification and petition. Moses fasted for 40 days on Mount Sinai while receiving the Ten Commandments (Exodus 34:28); Jesus fasted for 40 days in the wilderness before beginning his ministry (Matthew 4:1-2); and the Prophet Muhammad fasted on Mondays and Thursdays, on days 13-15 of each lunar month, and annually on Ramadan (Sahih al-Bukhari 5134, Book 6). Intensive fasting combined with social isolation and prayer was a core practice of Christian mystics Catherine of Siena, Hildegard of Bingen, and John of the Cross, who first coined "The Dark Night of the Soul". Shamanic cultures across Siberia, the Americas, and Africa have reliably induced altered states of consciousness through fasting for centuries, and fasting plays a key role in the vision quests and initiatory rituals of many Native American cultures[175].

While the historical and anthropological record point to fasting as a technique for attaining mystical states in its own right, fasting and caloric restriction are also commonly practiced together with meditation and psychedelics to potentiate their consciousness-altering effects. Contemporary Buddhist practices prescribe ritual fasting and caloric restriction to facilitate entering and deepening meditative states[136,176], and a recent longitudinal study found fasting-induced increases in mindfulness and religious experience in Baha'i practitioners[177]. Similarly, widespread anecdotal reports claim a synergistic effect between fasting and serotoninergic psychedelics, with many recreational users reporting that limited fasting before

ingestion potentiates their effects and that larger doses are required to compensate for having recently eaten[178]. Ayahuasca ceremonial traditions, in which the N,N-DMT-containing brew is ingested, also emphasize drinking it on an empty stomach, while weeks or months-long Ayahuasca and plant medicine retreats in Amazonian cultures, originally designed as shamanic preparatory processes and now also used therapeutically, are known as "dietas" (diets) and involve strict dietary and caloric restrictions[170].

To examine how caloric restriction may induce mystical states and potentiate the effects of psychedelics and meditation described in sections 1 and 2, I begin by reviewing the metabolic physiology of the brain under caloric restriction.

Brain Metabolism

The brain accounts for 2% of total body weight yet uses 20-25% of the body's energy at rest, with neurons expending 70-80% of energy and glial cells the remaining 20-30%[179]. 50% of the brain's energy is used by the cortex, with the majority spent by neurons reversing the ion fluxes that produce electrical signaling via Na^+/K^+ ATPase[180,181]. Neurons are primarily oxidative, using glucose to fuel the TCA cycle to obtain ATP, while astrocytes are primarily glycolytic and provide lactate to neurons. Nonetheless, given that glycolysis is up to 100 times faster than oxidative phosphorylation at producing ATP and neurons' need to rapidly increase energy consumption to fire action potentials, neurons can shift to glycolysis to meet these demands[182,183]. Moreover, some brain regions have much higher rates of aerobic glycolysis than others, with the DMN being the most highly glycolytic and thus highly sensitive to glucose availability[184].

Despite high metabolic demands, the brain has negligible glycogen stores and relies on a continuous influx of substrates from the blood via the blood-brain barrier. In average-sized adults, glycogen stores normally become depleted after 10-14 hours at rest, limiting glucose availability and causing neurons to switch to ketone bodies β-hydroxybutyrate (BHB) and acetoacetate (AcAc) as their fuel source, known as the G-to-K switch[179]. Ketones deliver 30-70% of the brain's energy during development, a rate that drops significantly in adulthood but can increase dramatically during fasting, low carbohydrate/high fat diets, and prolonged exercise, during which the liver produces ketone bodies from the oxidation of fatty and amino acids[179].

Effects of Caloric Restriction

G-to-K switching has been shown to enhance cognitive performance, working memory, and strength and coordination; increase neuroplasticity, including neurogenesis and dendritic spine density; induce analgesia; and improve resistance to and recovery from ischemic injury, epilepsy, and neurodegenerative diseases[185,186]. In other words, subjecting the brain to a mild metabolic challenge improves its function (a phenomenon known as hormesis) through a process mediated through multiple molecular signaling pathways.

Effects of caloric restriction have been found on the following pathways: BHB ketones upregulate GABAergic tone[187], which reduces cortical excitation/inhibition balance to produce anticonvulsant effects. Enhanced BDNF expression[188,189], which enhances synaptogenesis, neurogenesis, mitochondrial biogenesis, and neuronal stress resistance while reducing neuroinflammation. Fasting upregulates fibroblast growth factor 2 (FGF2) expression, which stimulates neural stem cell proliferation, protects neurons against oxidative stress, and regulates

neurite outgrowth. Fasting inhibits the mechanistic target of rapamycin (mTOR) pathway, which drives cells to switch into a 'conserve energy' mode that stimulates autophagy. Fasting upregulates PGC1α, a transcriptional regulator of mitochondrial biogenesis that also enhances hippocampal synaptogenesis. Fasting upregulates Sirtuin 3 expression, which regulates fatty acid oxidation and ketogenesis and is neuroprotective. And fasting restructures gut microbiota implicated in cognitive function improvements[177,185].

Additional effects of fasting at the cellular level also merit attention. Short-term synapse plasticity (measured via paired-pulse facilitation) increases through fasting-mediated expression of NR2B-containing NMDA receptors[190]. Caloric restriction triggers astroglial remodeling, which reduces synaptic transmission noise[191]. BHB inhibits class I and II HDACs to promote histone acetylation and increase the transcription of genes involved in stress resistance, neuroplasticity, and antioxidant defense[185]. And long-term potentiation at hippocampal synapses is strengthened via upregulated BDNF, CREB, and Notch1, which may explain fasting-related memory and cognitive enhancements[192,193].

The G-to-K switch causes peripheral effects, including the release of ghrelin into the bloodstream, which stimulates the hypothalamus to induce hunger, alongside reductions in plasma levels of cytokines, insulin, and leptin, a hormone that signals energy status to influence appetite and satiety[185]. While these affect cellular physiology widely, none of them directly implicates brain changes consistent with producing mystical states, except reductions in circulating leptin levels, which is the key modulator of the theory of fasting-induced mystical states I will propose shortly.

Finally, while neuroimaging and EEG research into the effects of fasting and caloric restriction remains surprisingly scarce, the few available studies show a convergent

neurophysiological state to those evoked by psychedelics and meditation. González Henríquez Sr. and colleagues examined the impact of ketosis, a proxy for caloric restriction, on EEG activity and found a flatter 1/f aperiodic slope, consistent with a greater E/I balance, signal diversity, and neural entropy[194]. Orfanos and colleagues performed a double-blind fMRI study on the impact of overnight fasting on resting state functional connectivity and found that fasting diminished functional connectivity within the posterior DMN[195]. And indirect studies on insulin resistance in type 2 diabetes have also found reduced functional connectivity and deactivation in the DMN[196–198]. These studies support the notion that the convergent subjective phenomenology of states attained through fasting with those elicited through psychedelics and meditation may rest on equivalently convergent neurophysiological changes. I now address the lack of a biologically grounded, falsifiable theoretical model for how caloric restriction elicits these convergent neurophysiological changes and altered states of consciousness through the Metabolic Relaxation of Priors (MRCP) theory of fasting-induced mystical states.

The Metabolic Relaxation of Cortical Priors (MRCP) Theory of Fasting-Induced Mystical States

Cortical Neurons Reduce Coding Precision to Save Energy Under Caloric Restriction

The Metabolic Relaxation of Cortical Priors (MRCP) theory of how caloric restriction induces mystical states rests on the finding that the mammalian neocortex saves energy by reducing coding precision during food scarcity. A 2022 study by Padamsey et al.[199] used mice that were food-restricted to 85% of their baseline body weight (and were re-fed 1-3 hours before

experimental recordings to isolate the effects of acute hunger and stress from caloric restriction) and found that food restriction caused layer 2/3 (L2/3) excitatory neurons in primary visual cortex (V1) to reduce their excitatory synaptic currents and ATP use by 29% while preserving their spike rates and overall excitatory/inhibitory balance. To identify the cellular mechanism, ex vivo cortical slice recordings found that AMPA receptor (AMPAR) currents evoked by a stimulating electrode were reduced by 34% in food-restricted animals, with reductions driven by reduced AMPAR conductance.

Despite the 29% reduction in excitatory drive, spike rates were preserved through a 22% increase in input resistance (meaning that less current is needed to produce a given depolarization) and a 6-7 mV depolarization of the resting membrane potential (meaning less distance to the spike threshold without changing the threshold itself). Together, these two adjustments fully restored the relative excitability of neurons despite the reduced AMPAR drive. In other words, an energy-saving reduction in AMPAR conductance along with a compensatory increase in input resistance and a depolarization of the resting membrane potential allowed neurons to preserve their spiking rate while reducing ATP cost.

Higher input resistance and a more depolarized resting potential meant that small, noisy fluctuations in membrane voltage were more likely to cross the spike threshold, which resulted in a 62% higher trial-to-trial variability in subthreshold visually evoked responses. Two-photon calcium imaging of population responses to oriented grating stimuli showed a 32% broadening of orientation tuning curves in food-restricted animals, which translated into reduced discriminability of natural scene representations and impaired performance on a fine (but not gross) visual orientation discrimination task. In other words, food restriction resulted in reduced cortical coding precision and impaired fine visual discrimination.

Finally, the authors found that circulating leptin, which is secreted by adipocytes in proportion to fat mass and is reduced under caloric restriction, was lower in food restricted animals in a manner that correlated with the degree of broadened orientation tuning. Exogenous leptin supplementation in food restricted mice fully restored AMPAR conductance, orientation tuning, and behavioral performance on the discrimination task, establishing leptin as the afferent hormonal signal through which metabolic state regulates cortical coding precision.

In summary, this landmark study showed that mammalian sensory cortical neurons reduce their coding precision while maintaining their firing rates in response to caloric restriction, an ingenious way to preserve energy while privileging gross sensory abilities at the expense of finer ones, which are less likely to impact survival probabilities. This means that metabolic constraints affect information processing rather than activity per se, with effects on the circuits that process perceptual content. While Padamsey et al. established the effects of caloric restriction on L2/3 pyramidal neurons in V1, investigating the effects of caloric restriction on the rest of the brain and on the whole perceptual predictive coding hierarchy is the next logical step.

Lower AMPAR Conductance and Coding Precision Across the Predictive Hierarchy

In the active inference formulation of predictive coding, the influence of any signal on the posterior is determined by its precision weighing, which is the inverse of its variance. Signals with high precision (low variability) pull the posterior toward them, while signals with low precision (high variability) are downweighed and contribute less to updating beliefs. This applies to both bottom-up prediction error signals and to top-down prediction signals, such that the

posterior at all levels of the hierarchy is a precision-weighted average of top-down and bottom-up signals.

Since L2/3 V1 pyramidal neurons are the canonical carriers of precision-weighted prediction error signals ascending the visual hierarchy, the broadened orientation tuning of these pyramidal neurons caused by caloric restriction amounts to a reduction in the precision of the prediction error signal. At first sight, this would imply an increase in the variance of ascending prediction error signals, which would propagate up the cortical hierarchy. Receiving areas would assign lower precision to these prediction error signals and rely proportionally more on priors to generate posteriors. Posteriors would become more dominated by their generative models (priors) and less driven by sensory data–the opposite effect of psychedelics under the REBUS model (section 1) and of meditation under the diffuse coupling theory (section 2). Contrary to this surface-level prediction, however, caloric restriction, fasting, and sensory austerity are associated with REBUS and meditation-like states. This apparent contradiction can be solved by extrapolating the AMPAR conductance effects beyond L2/3 pyramidal cells and considering the density of leptin receptors (LepRs) and the effect of AMPAR currents across cortical predictive coding circuits, which reveals a more complex picture from which two plausible mechanisms of how caloric restriction may produce a loosening of prior-dominated perception emerge.

Metabolic Relaxation of Cortical Priors (MRCP) Mechanism 1: Somatostatin Versus Parvalbumin Expressing Interneurons and AMPAR-Mediated Excitation

While Padamsey et al. found that excitatory and inhibitory currents decreased proportionally to preserve the E/I ratio in L2/3 pyramidal cells, different interneuron subtypes

have very different functional roles, receptor expression profiles, and sensitivities to changes in circuit dynamics. In the hierarchical predictive coding laminar framework, somatostatin (SST) Martinotti interneurons in L2/3 and L5 implement the subtraction of top-down predictions from bottom-up input[200]. When a top-down prediction arrives, it activates SST interneurons, which suppress pyramidal cell output in proportion to how well the prediction matches the input, subtracting the prior from the likelihood to generate the error residual. These SST interneurons receive excitatory drive from local pyramidal cells and from top-down feedback axons arriving in L1 and upper L2/3, and project inhibitory output onto the distal apical dendrites of pyramidal cells, where top-down prediction signals are compared with bottom-up input[201].

Critically, synapses from pyramidal cells onto SST interneurons are facilitating: They increase in strength with each successive action potential, depending on repeated AMPAR-mediated activation to accumulate excitatory drive during sustained activity[202,203]. SST cells are therefore temporal integrators best recruited by sustained, reliable, temporally structured pyramidal firing and are specifically sensitive to variability in pyramidal output rather than to its mean rate. In contrast, parvalbumin (PV) interneurons perform perisomatic inhibition that sharpens spike timing precision, and pyramidal-to-PV synapses are depressing: They decrease in strength with repetitive stimulation[203]. PV cells therefore act as onset detectors, responding to the first spikes in a train and remaining relatively robust to variability in sustained firing.

The key anatomical constraint that shapes how caloric restriction should affect this circuit is that leptin receptors (LepRs) in the cortex are expressed predominantly on PV interneurons rather than on SST interneurons or pyramidal cells[204], making the PV population the primary cellular target of reduced leptin under caloric restriction. Impaired PV function, whether through reduced AMPAR conductance, altered intrinsic excitability, or other LepR-coupled signaling,

weakens the perisomatic inhibition that PV cells deliver to pyramidal cells. This has been shown to increase pyramidal response variability and reduce neural reliability: Optogenetic suppression of PV, but not SST, interneurons reduces response reliability in primary visual cortex, increases low firing rates while decreasing high firing rates, and reduces the signal-to-noise ratio of cortical representations[205]. PV inactivation also disrupts network synchrony and the response reliability and spatial extent of coactive neuronal ensembles[206].

Because SST cells need gradual, tonic, temporally sustained pyramidal activation to build up facilitation, and because the facilitating synapse starts weak and accumulates strength only with consistent repeated input, noisy, unreliable pyramidal firing fails to reliably recruit SST cells even when mean firing rate is preserved[202]. The facilitating synapse is a temporal integrator that rewards consistency, so that increased variability disrupts the temporal accumulation that makes it effective. A leptin-driven increase in pyramidal variability therefore specifically impairs SST interneurons through their dependence on the facilitating synapse. In contrast, PV cells, responding to transient onsets via their depressing pyramidal-to-PV synapses, are proportionally less affected by the same increase in variability.

Under normal conditions, SST cells act as a stabilizing force: When pyramidal neurons are firing reliably, SST cells become active and suppress PV cells, which keeps pyramidal firing reliable in the first place[207]. But once caloric restriction begins to undermine PV cells, making pyramidal responses noisier, SST cells will be recruited less, which will release PV cells from SST-mediated suppression. Disinhibited PV cells will then make pyramidal responses noisier still, which will recruit SST cells even less, creating a vicious cycle that drifts the system toward a state where pyramidal neurons fire erratically and SST cells are chronically underactive, impairing the subtraction of top-down predictions and bottom-up prediction errors.

With SST cells less active, the inhibitory subtraction of top-down predictions from pyramidal apical dendrites will fail because the local inhibitory circuit that implements the subtraction cannot be reliably recruited. As a result, the top-down prior would exert less suppressive influence over pyramidal cell responses, making prediction errors more influential and tilting the balance of perceptual inference toward bottom-up sensory evidence in a manner functionally analogous to REBUS and to diffuse coupling under OM meditation.

In summary, a direct leptin effect on PV cells would increase pyramidal response variability. Increased pyramidal variability would specifically impair SST recruitment via facilitating synapses, and the SST-PV relationship would create a second feedback loop, both of which would result in reduced dendritic inhibition of pyramidal apical dendrites and unsuccessful top-down prediction subtraction (Figure 3.10).

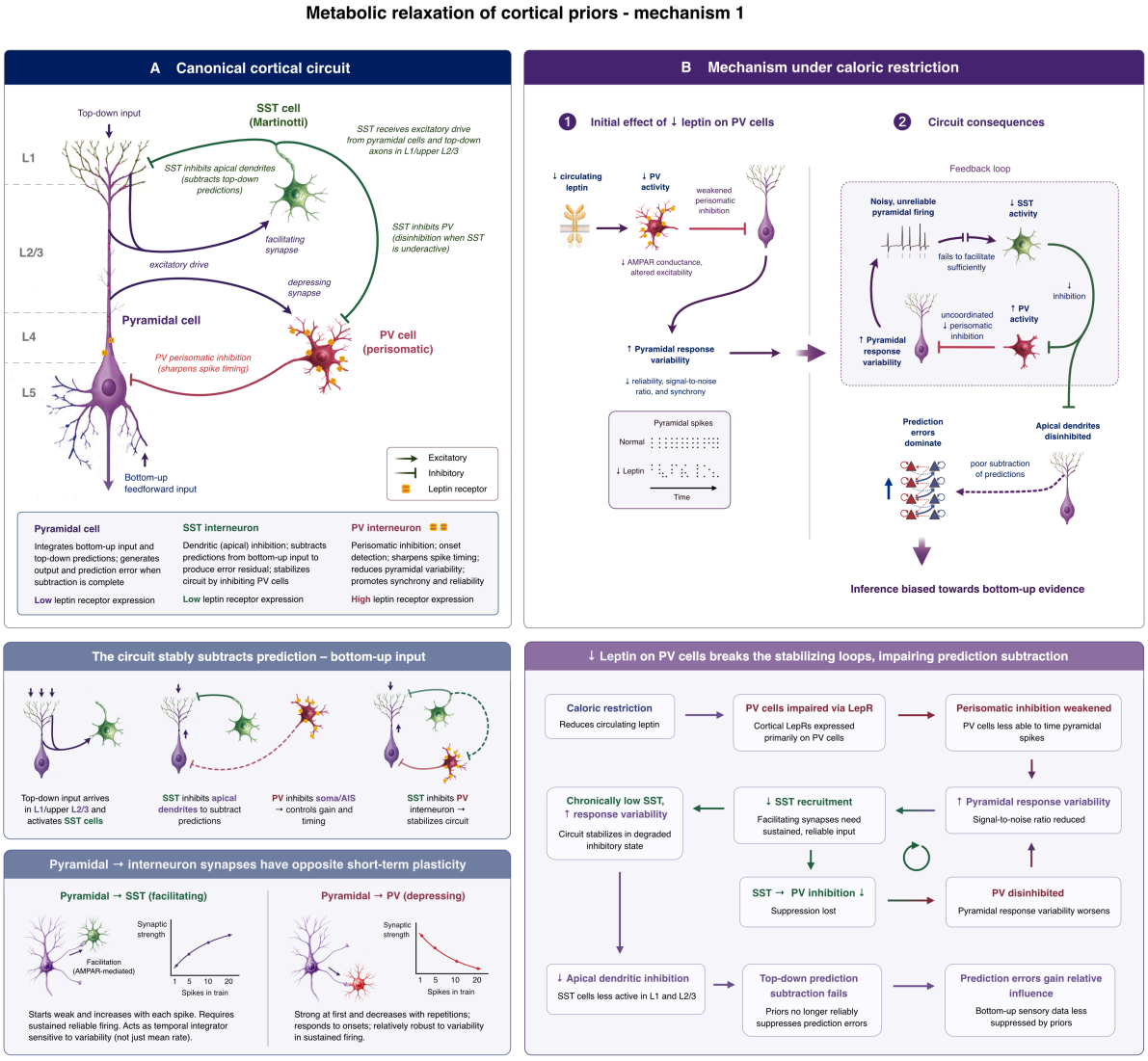


Figure 3.10: Metabolic relaxation of cortical priors (MRCP) mechanism 1, differential interneuron sensitivity to caloric restriction via leptin and synaptic plasticity.

Since the Padamsey et al. findings were limited to L2/3 excitatory neurons in V1 and have not been tested in interneuron subtypes or higher cortical areas, these are hypothetical extrapolations. Nonetheless, MRCP mechanism 1 parsimoniously rests on four empirically established facts: the predominant expression of leptin receptors on cortical PV interneurons[204]; the established consequence of PV impairment on pyramidal response variability[205,206]; the

facilitating property of pyramidal-to-SST synapses and the resulting SST sensitivity to variability over mean rate[202,203]; and the role of SST cells in gating top-down prediction signals onto pyramidal apical dendrites[201]. Empirically, if MRCP mechanism 1 is correct, PV interneuron activity should be reduced relative to pyramidal firing rates in a manner correlated with circulating leptin levels; pyramidal response reliability and trial-to-trial variability should be increased; SST firing rates should be secondarily reduced; and the gain of top-down feedback signals on pyramidal cell output should be attenuated, along with tonic dendritic inhibition of apical dendrites, all without a primary reduction in mean spike rate.

Metabolic Relaxation of Cortical Priors (MRCP) Mechanism 2: Differential Metabolic Vulnerability of Persistent Activity Across Cortical Levels

A second possible mechanism for how reduced coding precision triggered by lower leptin levels and AMPAR conductance could result in a less prior-heavy predictive cortical hierarchy depends on a fundamental difference in how primary sensory cortex and higher cortical areas maintain their activity (Figure 3.11). Primary sensory areas like V1 are driven by feedforward thalamic input, with neurons firing in response to arriving sensory signals and their responses persisting only as long as the thalamic drive continues, even with substantial recurrent excitation[208]. Upon silencing the thalamus, sensory-evoked activity in primary sensory cortex rapidly decays, with a time constant (~10 ms) close to a neuron's integration time window.

In contrast, higher cortical areas like the dorsolateral prefrontal cortex (dlPFC), anterior cingulate cortex (ACC), and DMN nodes such as the posterior cingulate cortex (PCC) and precuneus maintain representations across seconds-long delays through persistent recurrent

excitation among local pyramidal cell populations[209,210]. These self-sustaining activity states are the neural basis of the top-down priors sent down the predictive hierarchy. Their maintenance depends on long timescale recurrent excitation and on the stability of the recurrent attractor rather than on ongoing sensory drive. Spiking dynamics are maintained over timescales of seconds–longer than the time constant of individual neurons–, and activity is driven more by spikes from other neurons than by the cell's own recent spike history.

Within these recurrent circuits in higher cortical areas, AMPA and NMDA receptors help sustain persistent activity while playing distinct roles. NMDA receptors carry the information-specific component of persistent activity, while AMPARs contribute background depolarization. We know this from studies showing that recurrent excitation in primate dlPFC during a spatial working memory task was abolished by local NR2B NMDAR blockade or by systemic ketamine (NMDA antagonist) administration, while AMPARs provided tonic background depolarization to sustain network firing, as well as from how attractor dynamics maintain short-term memory in mouse frontal cortex[211,212].

This receptor-level difference means that if AMPAR conductance is globally reduced under caloric restriction, the consequences in primary sensory areas and higher cortical areas would differ: In primary sensory cortex, reduced AMPAR conductance would impair the amplification of ongoing thalamic drive, but the thalamic signal would continue to arrive, resetting and refreshing the cortical response. In the higher cortical areas that generate descending priors, reduced AMPAR background depolarization would reduce the sustained excitatory support needed for the recurrent attractor, increasing the likelihood that the network will revert to baseline. While both systems would become noisier, the influence of the noise on higher cortical areas would destabilize prior-encoding attractors, while primary sensory cortices

would merely lose fine discrimination abilities. Moreover, since NMDA receptors carry the information-specific component of persistent firing, the content of the prior would be partially preserved, while AMPAR-based changes would degrade the temporal stability of that representation, i.e., how strongly and consistently it suppresses incoming prediction errors.

Because NMDARs are primarily responsible for the information-specific component of persistent firing, reduced AMPAR conductance driven by caloric restriction would destabilize prior-encoding attractors without selectively destroying their tuning or content. An intermittently maintained prior would have a less reliable suppressive influence over ascending prediction errors than a stable one. The prior's precision would be reduced in a graded manner through lower temporal reliability, and less suppressed ascending prediction error signals would gain relative influence over the perceptual hierarchy. The result would be a gradual loosening of habitual categorical perception, consistent with the phenomenological reports associated with fasting and caloric restriction discussed earlier. This would be functionally equivalent to the relaxing of high-level priors under the REBUS mechanism, except that instead of a 5-HT_{2A}-mediated reduction of the descending signal's precision, high-level priors would loosen their grip on lower-level processing via decreased attractor instability, resulting in a gentle dissolution of prior-dominated content.

Finally, I note that these effects should be especially pronounced in the DMN, which has been shown to deactivate and lose functional integrity during psychedelic-induced mystical states and during meditation. The DMN is largely made up of the higher-order association cortices that MRCP 2 identifies as maximally vulnerable, regions at the top of the cortical hierarchy, farthest from primary thalamic drive, with long intrinsic timescales and heavy reliance on recurrent excitation to maintain self-sustaining activity. Moreover, the DMN's most

metabolically demanding nodes, the PCC, precuneus, and mPFC, are among the heaviest glucose-using regions in the brain at rest and therefore those in which energy saving adaptations would matter most[213,214]. MRCP 2 would therefore predict that the destabilization of prior-encoding attractors should be most evidenced in the DMN, where PCC, mPFC, and precuneus should show reduced temporal stability and reduced resting state functional connectivity under caloric restriction, especially as compared to sensory-driven regions like A1 and V1. Importantly, a double-blind fMRI BOLD study after overnight fasting shows precisely this[195]. Of note, all three techniques that induce mystical states–psychedelics, meditation, and caloric restriction–converge on DMN attenuation despite operating through different proximal mechanisms.

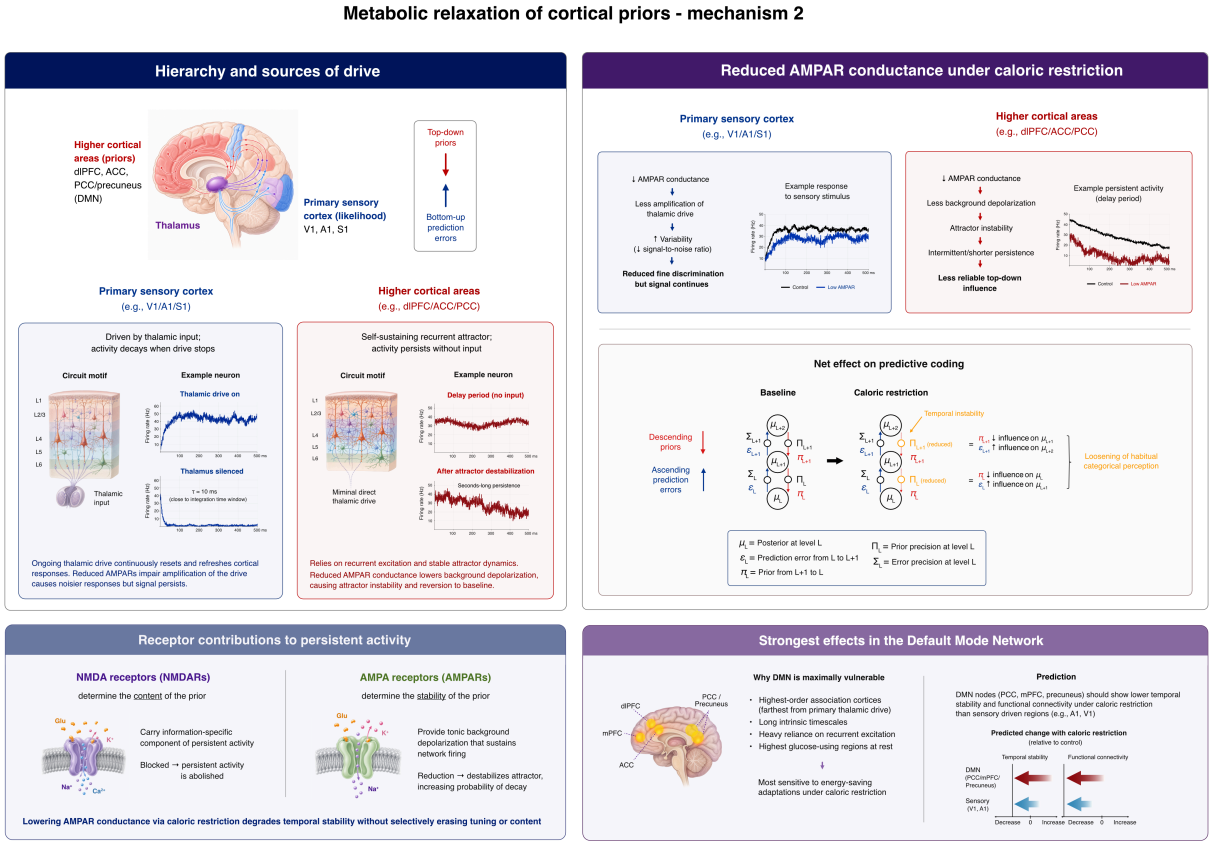


Figure 3.11: MRCP 2 - Differential metabolic vulnerability of persistent activity across cortical levels. Reduced AMPAR conductance under caloric restriction destabilizes recurrent attractors in higher cortex (priors) more than thalamocortical responses in primary sensory cortex.

In summary, higher cortical areas maintaining persistent prior-encoding activity are more vulnerable to AMPAR conductance reduction than primary sensory areas driven by thalamic input, with the difference between how AMPAR conductance acts on different cortical levels making high level prior-encoding representations disproportionately vulnerable to reduced AMPAR conductance, even if the reduction is uniform across the brain (Figure 3.11).

Importantly, MRCP mechanism 2 describes the consequences of a global reduction in AMPAR conductance, but whether the Padamsey et al. AMPAR conductance effect extends to

pyramidal cells in higher cortical areas remains untested. This is especially important given that cortical LepRs are located primarily on PV cells. If these effects do extend beyond V1 L2/3, MRCP mechanism 2 empirically predicts that caloric restriction should selectively destabilize persistent firing in higher cortical areas while leaving stimulus-driven responses in those same areas and in primary sensory cortices comparatively unperturbed. Effects on higher cortical areas should resemble an AMPAR blockade rather than a NMDAR one, with generally weakened sustained delay-period firing and lower overall stability of prior-encoding representations without selectively destroying their content or specificity. Behaviorally, this should manifest as lower performance in tasks requiring active maintenance of prior knowledge over a delay, with performance declining more steeply as delay duration increases, while rapid stimulus-driven discrimination remains comparatively preserved. At the network level, resting-state fMRI should show reduced within-network functional connectivity preferentially in high-level areas with long intrinsic timescales, like dlPFC, ACC, and PCC, relative to primary sensory areas. Finally, exogenous leptin administration should restore not only V1 orientation tuning but also dlPFC delay-period stability.

MRCP mechanisms implicitly assume that if the effects of caloric restriction on AMPAR conduction extend beyond V1 L2/3, they will not reduce the precision of descending priors as much as that of ascending prediction errors through their action on cortical pyramidal cells. This asymmetry, which favors preservation of the descending signal and degradation of the ascending one, is supported by studies showing that leptin receptors are primarily found in layer 6 non-pyramidal neurons that co-express parvalbumin and not on the deep-layer cortical pyramidal cells that generate descending predictions[204]. This raises the question of how leptin reduces AMPAR conductance on L2/3 pyramidal cells and suggests that it may involve an indirect

pathway possibly mediated through the L6 PV cells that do express LepRs. Furthermore, the L5p neurons that generate descending predictions do so by detecting coincidences between their basal dendrite input (carrying bottom-up sensory signals) and their apical tuft input (carrying top-down signals), a computation driven by NMDA and calcium spikes rather than by AMPAR-mediated currents[215,216]. Hence, a global reduction in AMPAR conductance would affect the basal dendritic compartment of L5p neurons (where the bottom-up signal arrives) and the membrane potential, but not NMDA/Ca^{2+}-based coincidence detection, leaving the precision of descending prediction signals relatively unperturbed. Together, these effects favor an asymmetric effect of AMPAR conductance reductions on bottom-up and top-down cortical traffic.

Finally, both mechanisms of metabolic relaxation of cortical priors would be additive, perturbing the predictive hierarchy at two distinct levels: MRCP 1 impairing the local inhibitory subtraction of predictions from incoming errors, while MRCP 2 independently reduces the temporal stability of the priors being subtracted. Additionally, these effects would be complementary to those of psychedelics and meditation: A less reliable subtraction of priors from prediction errors (MRCP 1) and a less temporally stable set of descending priors (MRCP 2) would enhance the effects of lower precision priors via 5-HT_{2A} agonism (psychedelics) and diffuse coupling (OM meditation). While caloric restriction could produce mystical states on its own via MRCP, it would also prime the system for psychedelics or meditation to more easily produce a mystical-type experience or profound altered state of consciousness, which matches the phenomenology.

Beyond the cellular and network-level predictions made above, MRCP makes joint predictions that follow from the additivity of mechanisms 1 and 2. The phenomenological consequence of both mechanisms operating together should be a subtle but measurable loosening

of categorical perception and a shift toward bottom-up sensory dominance during caloric restriction, detectable through increased binocular rivalry switching rate, slowed perceptual hysteresis, increased ambiguous figure flexibility, and increased mismatch negativity amplitude. Critically, the two-mechanism framework predicts that the magnitude of these effects should be greater than predicted by either MRCP 1 or MRCP 2 alone; that is, joint measures of impaired apical dendritic inhibition and reduced intrinsic timescale should predict phenomenological loosening better than either alone, distinguishing the MRCP framework from single-mechanism alternatives.

Table 3.1: Empirical Predictions, Evidence, and Tests for the MRCP Theory.

Empirical prediction	**Test / Supporting Evidence**
PV interneuron activity should be reduced relative to pyramidal firing rates in proportion to circulating leptin levels.	**Proposed design:** Cell-type-specific recordings (e.g., two-photon calcium imaging in PV-Cre or PV-GCaMP transgenic mice, or Neuropixels recordings with optotagging) in cortex of food-restricted vs. fed mice, with simultaneous plasma leptin assay. **Partial anchor:** Canepa et al. (2024)[204] established cortical LepR expression on PV cells; the firing-rate effect itself remains untested.
Pyramidal response reliability should decrease, and trial-to-trial variability should increase under caloric restriction.	**Partially supported:** Padamsey et al. (2022)[199] directly showed a 62% increase in trial-to-trial variability of subthreshold visually-evoked responses and a 32% broadening of orientation tuning in V1 L2/3 pyramidal cells of food-restricted mice. Extension to other cortical regions remains untested.
SST interneuron firing rates should be secondarily reduced under caloric restriction.	**Proposed design:** SST-Cre cell-type-specific recordings in cortex of food-restricted vs. fed mice, paired with simultaneous PV recordings to test the PV→variability→SST cascade. The mechanistic anchors[202,203] establish facilitating pyramidal→SST synapses; the consequence under caloric restriction has not been directly tested.
The gain of top-down feedback signals on pyramidal cell output should be attenuated, along with tonic dendritic inhibition of apical dendrites.	**Proposed design:** Two-photon imaging or whole-cell recordings of L2/3 or L5 pyramidal apical dendrites during top-down feedback activation (e.g., via long-range optogenetic stimulation of higher-area projections) in food-restricted vs. fed mice, with focal pharmacological silencing of SST cells as a control. Untested.
The above effects should occur without a primary reduction in mean pyramidal spike rate.	**Supported in V1 L2/3:** Padamsey et al. (2022)[199] found preserved spike rates despite reduced AMPAR drive. Generalization to other cortical areas remains untested.
Caloric restriction should selectively destabilize persistent firing in higher cortical areas while leaving stimulus-driven responses in primary sensory cortices relatively unperturbed; effects should resemble AMPAR rather than NMDAR blockade.	**Proposed design:** Single-unit or Neuropixels recordings in dlPFC or ACC during a delayed match-to-sample working memory task in food-restricted vs. fed primates or mice, with delay durations parametrically varied, and comparison to pharmacological AMPAR vs. NMDAR blockade. **Foundational anchors**: [211,212]. The caloric-restriction test is untested.

Table 3.1: Empirical Predictions, Evidence, and Tests for the MRCP Theory. (Continued)

Empirical prediction	**Test / Supporting Evidence**
Behaviorally, performance should decline more steeply with delay duration on tasks requiring active prior maintenance, while rapid stimulus-driven discrimination remains preserved.	**Proposed design**: Comparison of fasted vs. fed performance on delayed-response and working-memory tasks with parametric delay manipulation, alongside a coarse-discrimination control task. **Partial anchor**: Padamsey et al. (2022)[199] showed impaired fine but preserved coarse orientation discrimination, but did not test the working-memory delay dimension.
Resting-state fMRI should show reduced within-network functional connectivity preferentially in high-level areas with long intrinsic timescales (dlPFC, ACC, PCC) relative to primary sensory areas.	**Partially supported**: Fasting diminished functional connectivity selectively in posterior DMN[195]. **Proposed extension**: rsfMRI study comparing fasted vs. fed states with intrinsic-timescale parcellation to test the predicted gradient of vulnerability across the cortical hierarchy.
Exogenous leptin administration should restore not only V1 orientation tuning but also dlPFC delay-period firing stability.	**Supported for V1**: Padamsey et al. (2022) demonstrated full restoration of AMPAR conductance, orientation tuning, and discrimination behavior with exogenous leptin. **Proposed extension to dlPFC**: Combine systemic leptin administration with single-unit recordings in dlPFC of food-restricted primates or mice during working memory tasks to test if the Padamsey mechanism generalizes.
Caloric restriction should produce a measurable loosening of categorical perception and a shift toward bottom-up sensory dominance, detectable as increased binocular rivalry switching rate, slowed perceptual hysteresis, increased ambiguous figure flexibility, and increased mismatch negativity amplitude.	**Largely untested.** The closest available study[217] found reduced short-term ocular dominance plasticity during fasting, with the effect mediated by β-hydroxybutyrate, but tested plasticity rather than rivalry switching rate per se. **Proposed designs:** (a) within-subject binocular rivalry switching rate measured under matched fasted vs. fed conditions with neutral non-food stimuli; (b) Necker cube reversal-rate paradigm under matched conditions; (c) auditory oddball MMN paradigm comparing fasted vs. fed amplitudes; (d) gradual-transition perceptual hysteresis paradigm. None has been directly tested.
Joint measures of impaired apical dendritic inhibition (MRCP 1) and reduced intrinsic timescale (MRCP 2) should predict phenomenological loosening better than either alone.	**Proposed design:** Multimodal study combining cell-type-specific neural measures (e.g., proxies for apical dendritic inhibition such as alpha-power suppression or laminar EEG/MEG measures) with intrinsic-timescale estimates from resting-state fMRI, tested as joint predictors of behavioral loosening (rivalry switching, MMN amplitude) in fasted vs. fed states. **Untested:** Key prediction that distinguishes MRCP from any single-mechanism alternative.

Having presented the two core mechanisms behind MRCP, I now turn to additional specific synergies between caloric restriction, serotoninergic psychedelics, and meditation.

Serotoninergic Psychedelics, Metabolism, and Mystical States

In the case of psilocybin, the potentiating effect of pre-dose fasting may be at least partly explained by digestion slowing the dephosphorylation of orally ingested psilocybin into psilocin (its active metabolite) by alkaline phosphatases in the stomach, while for other orally ingested psychedelics, food digestion may slow their uptake into the bloodstream and across the blood-brain barrier, tempering their consciousness-altering effects. However, outside of digestion-mediated effects and caloric restriction, several neuroimaging studies have begun to elucidate the complex metabolic effects of psychedelics like psilocybin on the brain.

Neuroimaging studies point towards psilocybin inducing relative hypermetabolism in prefrontal cortical areas and relative hypometabolism in subcortical and occipital regions along with global decreases in absolute cerebral blood flow and BOLD signal. An arterial spin labeling (ASL) and blood oxygen level dependent (BOLD) fMRI study with intravenous psilocybin showed that changes in consciousness were exclusively accompanied by decreases in absolute cerebral blood flow (CBF) and in BOLD signal, which were highest in thalamus, ACC (anterior cingulate cortex), and PCC (posterior cingulate cortex) hub regions, with decreased ACC/mPFC activity specifically predicting the intensity of subjective effects[218]. At the same time, positron emission tomography (PET) studies have revealed absolute increases in cerebral glucose metabolism during psilocybin administration, with marked increases in frontomedial, frontolateral, anterior cingulate, and temporomedial cortices, smaller increases in sensorimotor

and occipital cortices, and decreases in the thalamus[219,220]. Similar hyperfrontal effects were found during administration of mescaline and of N,N-DMT-containing ayahuasca, including increased CBF in frontal and paralimbic areas, bilateral anterior insula, and right ACC/frontomedial cortex[221,222].

The apparent contradiction between lower CBF and BOLD signal with higher glucose metabolism becomes clearer when considering relative CBF changes, which indirectly capture local neuronal activity by adjusting for global brain perfusion. Relative CBF changes match glucose metabolism PET data showing frontal hypermetabolic activity during psilocybin administration. One study showed that psilocybin decreased absolute CBF in parietal, limbic, and frontal regions, while acutely increasing relative CBF in frontal and limbic regions and decreased it in parietal regions, with decreases in left postcentral gyrus and right superior temporal gyrus overlapping with psilocybin-induced increases in BOLD resting state connectivity in these same areas[223]. Interestingly, researchers also found that subjective psilocybin-induced effects, including disembodiment, were dependent on inter-individual differences at baseline relative CBF in the inferior frontal gyrus. A second study similarly showed psilocybin widely decreased absolute CBF while increasing relative CBF in right frontal and temporal regions and bilaterally in the anterior insula, while decreasing relative CBF in left parietal and temporal cortices and subcortical regions[224].

CBF perfusion and BOLD measures are indirect measures of neural activity, and serotonin and its agonists modulate vascular tone, confounding CBF-based inferences on neural and metabolic activity. As a result, rather than psychedelic-induced metabolic hyperfrontalism, I take the most consequential findings with metabolic implications to be that areas with psilocybin-induced relative CBF decreases had increases in BOLD resting state functional

connectivity and that subjective mystical-type effects were predicted by inter-individual differences in baseline relative CBF levels. Recall the robust finding that serotoninergic psychedelics disrupt the brain's normal hierarchical organization and functional geometry by inducing global functional hyperconnectivity, network disintegration and desegregation, and a high-entropy neural state, with consciousness altering effects scaling with these changes. If psychedelics modulate brain glucose metabolism in a spatially heterogeneous manner, and hypometabolic areas increase their functional connectivity, then at least part of the psychedelic-induced functional connectivity changes could be metabolically mediated. Indeed, I speculate that caloric restriction, with or without psychedelic administration, may selectively modulate functional connectivity synergistically with psychedelic-based functional reorganization. Specifically, I propose that through the MRCP 2 mechanism proposed above, caloric restriction potentiates subjective psychedelic effects, including mystical experience ratings, by diminishing baseline and/or acute DMN connectivity and reducing frontotemporal theta power.

DMN-Mediated Synergy Between Caloric Restriction and Psychedelics

Recall from section 1 that psychedelics consistently deactivate and functionally disintegrate DMN in a manner that scales with ego dissolution ratings[218,225,226]. Separately, multiple fMRI with fluorodeoxyglucose-PET studies have shown a positive correlation between glucose metabolism and the degree of functional connectivity in the DMN[227–229], and an fMRI BOLD study found that 15 hours of fasting resulted in diminished functional connectivity only within the posterior DMN[195]. Finally, if one considers that the brain accounts for approximately 25% of the body’s total glucose metabolism[230]; that the DMN is highly glycolytic, requiring 15-

16 times more glucose per ATP produced[231]; and that the medial posterior parts of DMN have the highest glucose consumption level of any cortical region in humans or other species[213,214], it follows that caloric restriction would preferentially affect the posterior DMN, destabilizing prior-encoding attractors via MRCP, diminishing intra-network functional connectivity, and releasing the functional geometry to increase global functional connectivity (Figure 3.12).

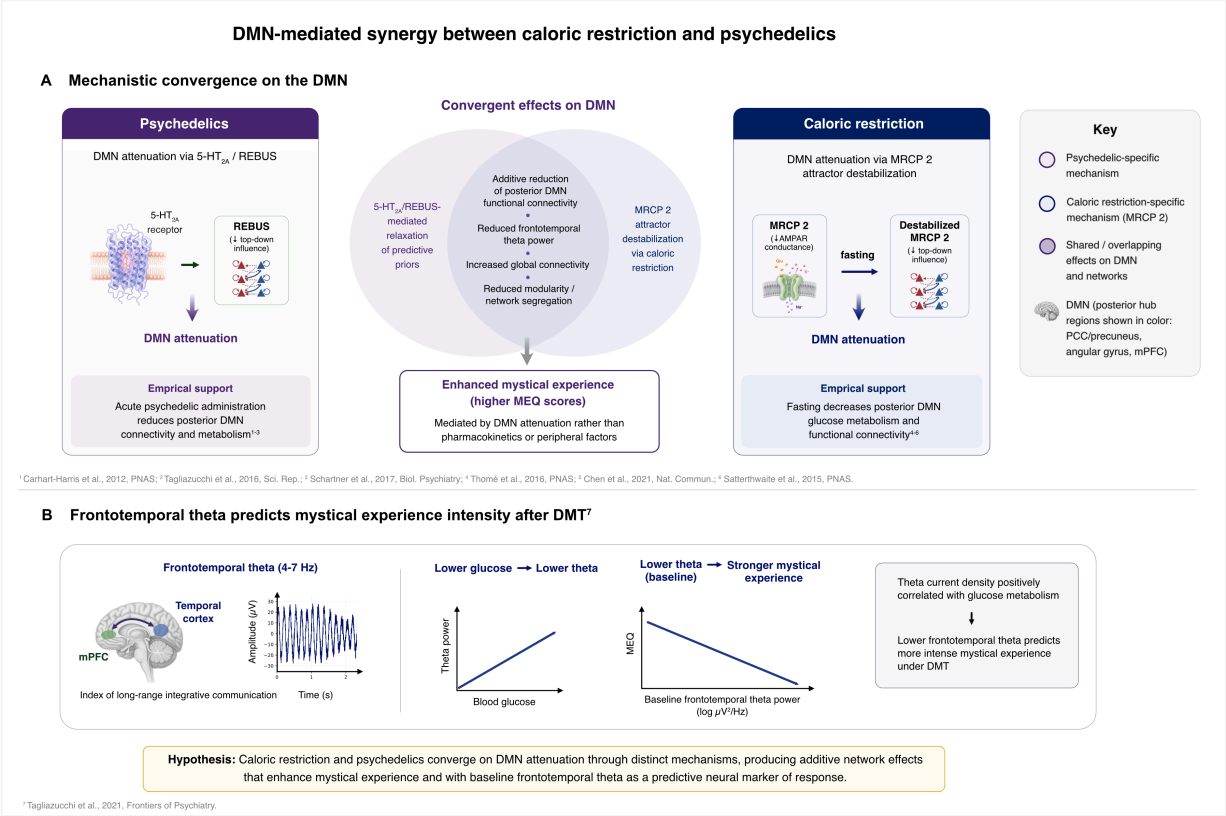


Figure 3.12: DMN-mediated synergy between caloric restriction and psychedelics.

Additional evidence suggests that caloric restriction may facilitate mystical states by increasing global functional connectivity, reducing functional modularity, and reducing theta power in frontotemporal areas, including parts of the DMN. A high resolution fMRI study of the impact of fasting on resting state networks in mice found that a 12 hour fast caused a global

increase in functional connectivity and a reduction in the modularity of functional networks in fasted but not on non-fasted mice[232]. Notably, both effects are hallmark markers of acute psychedelic states that scale with subjective effects, the latter being especially important in light of the mediating effect of mystical experiences in psychiatric clinical outcomes and in the absence of a classic dose response curve in serotoninergic psychedelics.

Moreover, I believe that the strength of these DMN-mediated effects may be encoded in the form of frontotemporal EEG theta power at baseline, based on the following two studies. A 2021 study by Tagliazucchi et al. showed that feelings of unity and transcendence, a core part of the mystical experience phenomenology, in human subjects who inhaled N,N-DMT were inversely correlated with frontotemporal EEG theta power at baseline[233], while a separate EEG/PET study found that, in the same frontotemporal region and in ACC (anterior cingulate cortex), theta current density was positively correlated with glucose metabolism[234]. Higher cerebral metabolism in the alert resting state was thus associated with greater EEG theta power in precisely the area of human cortex where greater EEG theta predicts a less profound mystical experienced attained via inhaled N,N-DMT. Of note, the DMN has significant frontotemporal coverage through the mPFC, the angular gyrus, and parts of the temporal parietal junction, implicating this as a potential ancillary mechanism to the one above.

Empirically, the DMN-mediated synergy hypothesis predicts that fasted psychedelic sessions should produce greater reductions in posterior DMN within-network functional connectivity than fed sessions for a matched dose, with the magnitude of this effect proportional to the duration of the pre-dose fast and to circulating leptin reduction. Mystical experience ratings, ego dissolution scores, and feelings of unity should be higher in fasted sessions, mediated by the additional DMN destabilization rather than by altered pharmacokinetics.

Baseline frontotemporal EEG theta power should predict mystical experience intensity inversely, both within fasted-versus-fed comparisons and across individuals, with caloric restriction reducing baseline theta in those regions in proportion to its potentiating effect on the experience. At the network level, fasting should preferentially reduce DMN modularity and preferentially increase global functional connectivity prior to dosing, priming the brain toward the high entropy, hyperconnected configuration psychedelics produce acutely. Phenomenologically, fasted sessions should produce subjectively distinct rather than merely more intense experiences, with greater attenuation of high-level priors (categorical perception, narrative self-model, conceptual structure) and partially attenuated bottom-up sensory amplification through the MRCP 1 noise-introduction mechanism. Clinically, in conditions characterized by rigid priors (depression, anxiety, OCD, addiction, chronic pain), combined caloric restriction and psychedelic-assisted therapy should produce greater symptom reduction than either alone, with clinical improvement mediated by measured neural markers of prior loosening rather than by mood, expectancy, or stress reduction.

Table 3.2: Empirical Predictions, Evidence, and Tests for DMN-Mediated Synergy Between Caloric Restriction and Psychedelics.

Empirical Prediction	**Test / Supporting Evidence**
Fasted psychedelic sessions should produce greater reductions in posterior DMN within-network functional connectivity than fed sessions for a matched dose, with the magnitude proportional to the duration of pre-dose fast and to circulating leptin reduction.	**Proposed design:** Within-subject fMRI study comparing acute psilocybin or LSD effects after a matched moderate fast vs. fed state, with pre-dose plasma leptin measurement and seed-based DMN connectivity analyses focused on PCC and precuneus. Anchored by independent findings of DMN attenuation by psychedelics[226] and by fasting-induced posterior DMN connectivity reduction[195]. The interaction effect is **untested**.
Mystical experience ratings, ego dissolution scores, and feelings of unity should be higher in fasted versus fed sessions, mediated by additional DMN destabilization rather than altered pharmacokinetics.	**Proposed design:** Same within-subject fasted-vs.-fed psychedelic dosing design, with the MEQ-30 and Ego Dissolution Inventory as outcomes, plasma psilocin pharmacokinetics measured to control for absorption differences, and DMN connectivity tested as a mediator. **Untested.**
Baseline frontotemporal EEG theta power should predict mystical experience intensity inversely, both within fasted-vs.-fed comparisons and across individuals; caloric restriction should reduce baseline theta in proportion to its potentiating effect.	**Partially supported**: Feelings of unity and transcendence after inhaled N,N-DMT were inversely correlated with baseline frontotemporal EEG theta[233], and frontotemporal and ACC theta current density correlates positively with glucose metabolism[234]. The combined fasted-meditation prediction has not been directly tested. **Proposed design**: Fasted vs. fed baseline EEG with subsequent psychedelic dosing and mystical experience scoring.
Fasting should preferentially reduce DMN modularity and increase global functional connectivity prior to psychedelic dosing, priming the brain toward the high entropy, hyperconnected configuration psychedelics produce acutely.	**Partially supported in animals**: 12-hour fasting in mice produced global increases in functional connectivity and reduced network modularity[232]. The human pre-psychedelic priming prediction has not been tested. **Proposed design**: Resting-state fMRI in healthy human volunteers in matched fasted and fed states with quantification of network modularity (e.g., Newman's Q) and global connectivity.

Table 3.2: Empirical Predictions, Evidence, and Tests for DMN-Mediated Synergy Between Caloric Restriction and Psychedelics. (Continued)

Empirical Prediction	**Test / Supporting Evidence**
Fasted psychedelic sessions should produce subjectively distinct rather than merely more intense experiences, with greater attenuation of high-level priors (categorical perception, narrative self-model, conceptual structure) and partially attenuated bottom-up sensory amplification.	**Proposed design**: Within-subject fasted-vs.-fed psychedelic dosing comparing detailed phenomenological scales separating high-level prior attenuation (e.g., Ego Dissolution Inventory, narrative self subscales) from sensory amplification (e.g., 11D ASC perceptual subscales). Behavioral measures of categorical perception (e.g., visual category boundaries, semantic categorization) and sensory acuity (e.g., contrast sensitivity, fine orientation discrimination) administered acutely under both conditions. **Untested**.
In conditions characterized by rigid priors (depression, anxiety, OCD, addiction, chronic pain), combined caloric restriction and psychedelic-assisted therapy should produce greater symptom reduction than either alone, with clinical improvement mediated by neural markers of prior loosening rather than by mood, expectancy, or stress reduction.	**Proposed design**: Randomized trial (psychedelic-assisted therapy with vs. without structured pre-session caloric restriction) in patients with treatment-resistant depression or another rigid-prior condition, with pre/post symptom scales as primary outcome and DMN connectivity, frontotemporal theta, and intrinsic timescale measures as candidate mediators. **Untested** in combined form.

Having proposed a novel, falsifiable, and biologically grounded set of mechanistic frameworks for metabolism-mediated effects of caloric restriction on the potency of psychedelic-induced mystical states, we now turn our attention to the connection between meditation and metabolism.

Meditation as a Hypometabolic State

There are no direct scientific studies testing whether caloric restriction improves meditation practice or helps facilitate absorptive or mystical states during meditation–a significant research gap. Nonetheless, traditional Buddhist monks tend to eat only one meal a

day, creating an ~20-hour daily fasting window, and purposefully limiting food intake to improve meditation quality, reduce drowsiness, and heighten clarity is widely reported in contemporary meditation communities despite being poorly documented scientifically. Of note, however, a recent longitudinal study found fasting-induced increases in mindfulness and religious experience in Baha'i practitioners[177].

Within contemplative science, meditation was proposed as a wakeful hypometabolic state of parasympathetic dominance distinct from ordinary relaxation, sleep, and hypnosis in the early 1970s by Wallace and colleagues, who identified a physiological signature of Transcendental meditation that included decreased oxygen consumption and CO_2 elimination, increases in galvanic skin resistance, decreased heart rate, decreased blood pressure, slow alpha-wave EEG activity, and decreased respiratory rate and minute ventilation without changes in respiratory quotient[235]. Further findings in support of the hypometabolic hypothesis include a drop in circulating catecholamines epinephrine and norepinephrine, decreased blood lactate, and decreased vascular resistance[236], all of which are consistent with a voluntary hypometabolic state of biological estivation that preserves energy while maintaining alertness[237]. This physiological pattern, interpreted as a reset of the resting metabolic level to a lower baseline, became known as the relaxation response and has been proposed as the physiological response to prayer, contemplation, and meditation generally[238].

Many of these findings have been documented among novice practitioners across other meditation practices, including Zen[239], yogic[240], and Buddhist[241] meditation styles. Advanced practitioners, in contrast, often have a different baseline physiology to novices and exhibit more complex changes during meditation, including increased metabolic activity (e.g. Tibetan

meditators raising body temperature)[242]. These differences underline that meditation is not a unitary physiological or neural state.

From existing studies, it is unclear what proportion of the physiological and hypometabolic effects of meditation are due to changes beyond the physical relaxation of the body during meditative practice–an important research gap. Nonetheless, the idea that the meditative state would lower the body's metabolic needs is consistent with attention being directed towards a present-centered stimulus like the breath or embodied sensation within a non-evaluative and non-reactive behavioral policy and therefore away from ATP-hungry DMN-mediated mind wandering. Indeed, similarly to psychedelics, FA, OM, and loving kindness meditation deactivate the main nodes of the DMN and increase functional connectivity between the PCC and regions outside the DMN, an effect that holds during meditation as well as at baseline in experienced meditators[243]. If the DMN is the source of allostatic predictions[51,244], which are experienced as mind wandering, and is also the most metabolically expensive set of regions within the most metabolically expensive organ, then an attentional policy that downregulates would significantly contribute to a drop in the body's overall metabolic rate. Moreover, the MRCP mechanism 2 would explain why caloric restriction would aid in the attainment of deeper meditation states, by temporally destabilizing the recurrent attractor activity of the DMN.

In addition to reducing the brain's metabolic rate by directly downregulating DMN activity, FA and OM meditation should further contribute to a hypometabolic state and trait by reducing the perceptual system's free energy via model updating, as explained by the OLIPR mechanism proposed in Section 2. Recall that the predictive hierarchy that performs allostasis is fundamentally motivated to manage metabolic resources by predicting energy outlays and thus

places the body at the top of the hierarchy as first prior. Predictions and the generative model that issues them therefore maximize adaptiveness over fidelity. Perceptual salience and valence are computed relative to the predicted impact of stimuli on visceral predictions, which encode the metabolic cost of allostatic action. As OLIPR's regime 2 drives model updating, with interoceptive predictions as embodied sensations being evoked, tested, and revised, the OLIPR framework predicts that new and more adaptive allostatic priors will replace older ones, which were less tightly coupled to the statistics of the body and the external environment, with more tightly coupled ones. As this process advances, the generative model will operate with progressively less expected free energy for the same sensory input, with metabolic resources and computational degrees of freedom previously dedicated to explaining away high precision interoceptive priors now liberated. Put differently, model updating leads to less tension between the model and the environment and therefore to less metabolic resources needed to explain away ascending prediction errors. Given that allostatic predictions are generated in higher level cortical areas generally and in DMN nodes specifically, this is consistent with deactivation and functional disintegration of DMN as both a state during meditation and a trait in experienced meditators, with associated lower metabolic rates.

Finally, the meditation-induced reduction of the prediction error threshold proposed in Section 2, under which the predictive system would operate closer to criticality and in a lower amplitude regime, would also predict a reduction in the resting metabolic rate. Subtler, lower amplitude perceptual computations produced during the meditative state are consistent with lower energy requirements and therefore with both a hypometabolic state and a synergistic relation to caloric restriction.

Empirically, the combination of fasting and meditation should produce additive DMN destabilization measurable through reduced within-network functional connectivity and shortened intrinsic timescales in PCC, precuneus, and mPFC, with the largest effects in the most metabolically demanding posterior DMN nodes. The hypometabolic signature of meditation should be enhanced by concurrent caloric restriction, with oxygen consumption, circulating catecholamines, blood lactate, and resting metabolic rate during fasted meditation dropping below the levels achieved by either intervention alone. Onset of meditative absorption should be faster and depth ratings higher in fasted versus fed sessions in matched practitioners, with effects scaling with the duration of the pre-session fast within a moderate range. Validated mystical experience scales (e.g., MEQ-30) should show higher scores in fasted meditation sessions compared to fed sessions, with the effect mediated by markers of DMN attenuation rather than by stress or dysphoria and disappearing or reversing under severe rather than moderate caloric restriction where stress and impaired attention dominate. The OLIPR-based prediction generates an additional, longer-timescale claim: Experienced meditators who incorporate sustained moderate caloric restriction should show greater progressive reductions in interoceptive prediction error magnitude and greater shifts toward critical, low-amplitude cortical dynamics than meditators without dietary restriction, indicating accelerated model updating rather than just an acute state effect. The framework would be weakened by failure of these synergies when stress and dysphoria are controlled for, by absence of mediation through DMN markers, or by failure of moderate fasting to lower the threshold for meditative absorption in experienced practitioners.

Table 3.3: Empirical Predictions, Evidence, and Tests for the Synergy Between Caloric Restriction and Meditation.

Empirical Prediction	**Test / Supporting Evidence**
The combination of fasting and meditation should produce additive DMN destabilization measurable through reduced within-network functional connectivity and shortened intrinsic timescales in PCC, precuneus, and mPFC, with the largest effects in posterior DMN nodes.	**Proposed design**: 2×2 factorial fMRI study (fasted vs. fed × meditating vs. resting) in experienced meditators, with within-network DMN functional connectivity and intrinsic timescale (autocorrelation decay) per condition, with interaction term tested for additivity. **Anchored** by independent findings of DMN attenuation by meditation[243] and by fasting[195]. The interaction is **untested**.
The hypometabolic signature of meditation should be enhanced by concurrent caloric restriction, with oxygen consumption, catecholamines, blood lactate, and resting metabolic rate during fasted meditation dropping below levels achieved by either intervention alone.	**Proposed design**: Same 2×2 factorial design with indirect calorimetry, plasma catecholamine assay, and blood lactate measurement during each session. Anchored by independent characterization of the meditation hypometabolic signature but interaction in human meditators is untested.
Onset of meditative absorption should be faster and depth ratings higher in fasted versus fed sessions in matched practitioners, with effects scaling with pre-session fast duration in a moderate range.	**Proposed design**: Within-subject fasted-vs.-fed comparison in experienced practitioners, with subjective absorption depth assessed via validated scales (e.g., Phenomenology of Consciousness Inventory) and onset latency measured against cued reference points within the session. Pre-session fast duration parametrically varied (e.g., 12, 18, 24 hours). **Untested**.
Mystical experience scale (MEQ-30) scores should be higher in fasted meditation sessions than fed sessions, with the effect mediated by DMN attenuation rather than stress/dysphoria and disappearing or reversing under severe rather than moderate caloric restriction.	**Partial anchor**: Fasting-induced increases in mindfulness and religious experience in Bahá'í practitioners[177]. **Proposed design**: Within-subject fasted-vs.-fed retreat-context meditation with MEQ-30 as the outcome, DMN connectivity as candidate mediator, and stress/cortisol/dysphoria measured as alternative explanatory variables. **Untested** in this controlled form.
Experienced meditators incorporating sustained moderate caloric restriction should show greater progressive reductions in interoceptive prediction error magnitude and greater shifts toward critical, low-amplitude cortical dynamics than meditators without dietary restriction, indicating accelerated model updating rather than just an acute state effect.	**Proposed design**: Longitudinal study comparing experienced meditators undertaking a sustained intermittent fasting regimen vs. matched controls maintaining ad libitum diet, with pre/post measures of interoceptive prediction error (heartbeat detection accuracy, respiratory load detection, EEG heartbeat-evoked potential amplitude) and cortical criticality measures (1/f slope of EEG/MEG power spectra). **Untested**.

In summary, although direct empirical work on caloric restriction as a facilitator of meditative depth remains scarce, multiple convergent mechanisms predict a synergistic relationship. The hypometabolic signature of meditation is consistent with an attentional policy that deactivates the DMN. The MRCP mechanism would compound this effect by destabilizing the recurrent attractor activity that sustains DMN priors, while the OLIPR framework predicts that progressive model updating during sustained practice liberates the metabolic resources previously dedicated to explaining away high precision interoceptive priors. The reduction of the prediction error threshold proposed earlier further predicts a lower-amplitude perceptual regime with correspondingly reduced energy demands. Together, these mechanisms position caloric restriction and meditation as mutually reinforcing routes to a shared hypometabolic, prior-loosened cortical state, explaining both the cross-cultural pairing of fasting with contemplative practice and the phenomenological convergence of their effects on the DMN and on perceptual experience.

Interim Summary

Across this section I have argued that caloric restriction is not merely a peripheral or anecdotal adjuvant to mystical states, but a mechanistically coherent route to producing them, both on its own and in combination with psychedelics and meditation. The Metabolic Relaxation of Cortical Priors (MRCP) framework anchors this argument in the empirical finding that the mammalian neocortex saves energy under food scarcity by reducing AMPAR conductance and coding precision, and proposes two complementary mechanisms by which this metabolic

adaptation could loosen prior-dominated perception: through cell-type-specific impairment of the inhibitory machinery that subtracts top-down predictions from bottom-up input (MRCP 1), and through the differential vulnerability of the recurrent attractors that sustain high-level priors in the DMN and other high-level cortices (MRCP 2). These mechanisms are additive, target the same regions that psychedelics and meditation independently attenuate, and predict that all three practices should converge on DMN destabilization through different routes. Caloric restriction's synergy with psychedelics is further specified through DMN connectivity, frontotemporal theta power, and global network reorganization, while caloric restriction's synergy with meditation is specified through shared hypometabolism, accelerated model updating under the OLIPR framework, and progression toward critical cortical dynamics. Together, these proposals position caloric restriction as a third pillar, alongside psychedelics and meditation, of a unified mechanistic theory of mystical states, in which a shared computational endpoint (the loosening of high-level priors and the attenuation of DMN-mediated narrative cognition) is reached through distinct but mutually reinforcing biological routes. With the three pillars now developed, I turn next to the shared computational endpoint itself and ask how the mystical state can be best conceptualized from a computational point of view. Having laid out a biologically grounded framework for how the three techniques converge on this territory of consciousness by modulating the circuits that produce conscious perception, we can take the theoretical framework and the empirical observations it is built on to explore the territory itself from a scientifically grounded perspective. Put simply, in Sections 1-3 I laid out three roads to Rome; now we ask what is Rome?

Section 4: Towards a Biologically Grounded Computational Understanding of Mystical-like States

"Our normal waking consciousness, rational consciousness as we call it, is but one special type of consciousness, whilst all about it, parted from it by the filmiest of screens, there lie potential forms of consciousness entirely different."

– William James, *The Varieties of Religious Experience* (1902)

So far, we have charted three separate routes toward a shared territory. The mystical-like states produced by psychedelics, meditation, and fasting share a consistent phenomenological structure across techniques and cultural contexts, first described by William James in 1902[245] and systematized by W.T. Stace[246] into what was later operationalized in the Mysticism Scale[247] and the Mystical Experiences Questionnaire (MEQ)[248]. Validated empirically across psychological, religious, and cultural backgrounds, the canonical features–unity, noetic quality, ineffability, transcendence of time and space, sacredness, deeply felt positive mood, paradoxicality, and transiency–are reliably reported by individuals who have accessed these states through any of the three routes.

Unity refers to the dissolution of the ordinary boundaries between self and world and the profound sense that all things are one. Noetic quality refers to a deeply felt sense that one has come into direct contact with reality at a deeper level than ordinary perception and cognition. Ineffability refers to the incapacity of language to describe the experience. Transcendence refers to feeling that the experience exists outside of time and physical distance. Sacredness or numinosity describe a quality of holiness that inspires awe and reverence. Deeply felt positive

mood describes overwhelming feelings of love, joy, peace, bliss, and gratitude, with intensities often exceeding those of any previous experience. Paradoxicality refers to the experience violating the logical principle of non-contradiction while retaining a sense of epistemological validity and ontological reality, such as experiencing things as simultaneously themselves and their opposites (e.g., self as both dissolved and present). Transiency refers to the experience feeling like a glimpse or temporary lifting of a veil and distinguishes it from neurologically or psychiatrically produced chronic altered states.

This consistent phenomenology of mystical-like states points toward a shared underlying neurophysiology. Despite differences between and within the states elicited by different techniques, shared neurophysiological features dominate and include deactivation or reduced within-network functional connectivity of the default mode network (DMN)[195,218,243]; increased neural signal complexity, entropy, and criticality[75,165,194,249]; increased global functional connectivity and reduced network modularity[232,250–252]; reduced alpha-band power (for psychedelics and meditation)[20,253,254]; altered aperiodic 1/f slope of EEG/MEG power spectrum[194,254,255]; and (for psychedelics and meditation) reduced anticorrelation between DMN and task-positive networks[82,243].

Sections 1-3 established the shared biological and computational substrate underlying these states within a predictive processing and active inference framework. Under such a framework, organisms perform allostasis by proactively predicting environmental demands to regulate internal states, with conscious perception being a product of this predictive regulation rather than a transparent readout of the body and the world. What we perceive, according to this framework, is the generative model's best precision-weighted estimate of the hidden causes of sensory input[27]. Interoceptive predictions about visceral state are the system's first priors, with

allostatic setpoints constraining perception, affect, and action, and affective valence indexing how interoceptive prediction errors track or violate these setpoints[51,117,119,143]. Perception is therefore a controlled hallucination optimized for adaptive utility over fidelity and an interface of evolutionarily useful affordances rather than a transparent representation[256,257]. Put simply, we see the world not as it is but as we are, and what we are, computationally, is a generative model whose priors encode the statistical and allostatic regularities that have proven adaptive.

Via the mechanisms proposed in Sections 1-3, all three routes alter the shapes of the descending prior and ascending prediction error distributions, with convergent effects on the posterior. Psychedelics broaden the variance of descending priors via 5-HT_{2A}-mediated sensitization of deep pyramidal neurons and disinhibition of higher-order thalamic relays that gate corticocortical precision (REBUS mechanism). OM meditation broadens descending-prior variance by shifting thalamocortical functional geometry toward diffuse matrix-type coupling. FA meditation narrows the variance of a single ascending interoceptive channel while simultaneously eliciting and updating the high precision interoceptive priors that act as attractors on the system (OLIPR mechanism). Caloric restriction destabilizes high-level priors through AMPAR-mediated reductions in the temporal reliability of persistent firing in association cortex and DMN (MRCP mechanism). In each case, the posterior becomes less dominated by the prior and more responsive to ascending evidence. Since high-level priors encode predictions over long timescales (including the autobiographical self, narrative continuity, counterfactual planning, and the projection of agency into past and future), the flattening of the predictive hierarchy impairs planning and self-referential processing. As temporal depth is reduced, the first priors of the body, normally buried under suppression, avoidance, and rumination policies that decouple awareness from interoceptive presence, surface into awareness. This is why these states are felt

as embodied insight, somatic release, emotional catharsis, and reconnection with feeling rather than as content-free quietude.

The thermodynamic logic of a system that is no longer bounding its internal entropy as tightly as during the normal wakeful state becomes reflected in these states' hallmark neurophysiological high entropy and subjective phenomenology: a transient dissolution of boundaries and a noetic sense of unity with all things, felt to be eminently real yet becoming ineffable as soon as the experience is over. This correspondence between the subjective experience produced by the dissolution of the computational boundaries that maintain the system's internal coherence and the neurophysiological biomarkers of such a state is the basis of the entropic brain hypothesis, which holds that the richness and quality of a conscious state is indexed by the entropy of its underlying neural dynamics[53,54]. Expanding on this correspondence to build a computational neurophenomenology of mystical states is the aim of this section. Rather than proposing empirically testable biological mechanisms, it treats the mechanisms in Sections 1-3 as perturbations to a system and examines what these perturbations reveal about the system itself.

The Experience is the Medicine: A Computational Pharmacology of Mystical-like States

Independently of the circuit-level pathway, the therapeutic mechanism is experience-dependent. The degree of mystical experience during a psychedelic session is the single strongest predictor of long-term therapeutic outcome across indications (depression, addiction, end-of-life anxiety, and PTSD)[258–262]. Crucially, this relationship holds independently of dose, which violates the classical pharmacological assumption that therapeutic effect is a monotonic function

of drug concentration at the target receptor. What predicts healing is not the amount of drug administered but the depth of the subjective state, indexed by brain entropy, that the drug occasions. Two individuals receiving identical doses in identical settings can have radically different therapeutic outcomes depending on whether the mystical state was reached. In classical pharmacology, the subjective experience of taking a drug is epiphenomenal to the molecular cascades that produce symptom reduction; here, the molecular cascades do not hold a privileged status over the experience. Moreover, a single dose has been shown to produce persistent clinical improvement, a unique occurrence in psychiatric pharmacology.

The mechanism of action of psychedelics involves a computational cascade that targets pathologies whose etiology is also partly computational, and tracing it requires an understanding of how these techniques modulate prediction-driven computational architectures in an experience-dependent manner. Specifically, the therapeutic action is not a direct pharmacological correction of a neurochemical deficit but the transient induction of a high-entropy quasi-critical state in which the system's highest-level priors are sufficiently relaxed that a large portion of the generative model can be reorganized. Crucially, the depth of prior relaxation required is not a simple function of 5-HT_{2A} occupancy; rather, it depends on the initial content and precision of the priors being recalibrated, the degree of diffuse thalamocortical coupling achieved, the quality of the attentional and interoceptive context, and the individual's baseline capacity for equanimous present-centered awareness–factors that vary greatly between individuals and determine whether any given dose will push the system across the threshold into the reorganizational state. When the mystical state is reached, the relaxation of the highest-level priors allows a reorganization of the generative model with new, more adaptive encodings

shaped by the experiential content of the state itself. When the mystical state is not reached, the therapeutic effect is attenuated regardless of the pharmacological dose received.

With meditation, the mystical state is approached gradually across the three regimes described in Section 2 rather than pharmacologically precipitated. The progressive lowering of the prediction error threshold, the recalibration of embodied priors through OLIPR, and the eventual dissolution of the temporally deep models that structure ordinary self-experience, collectively describe the same trajectory from a high-precision, prediction-dominated system toward a global reorganizational state. The destination, the computational mechanism of arrival, and the therapeutic logic of what happens once there are, on the present account, parallel ones.

Importantly, there is more to the experience-dependent nature of the mechanism than that priors must be retrieved and tested. The experience is both constituted and perturbable by agentic variables like volition, intention, and propositional beliefs. Unlike other therapeutics, the experience is a core part of the mechanism of action, and volitional agentic beliefs, attitudes, and intentions modulate the experience. Put differently, the mystical-like experience–the phenomenological index of the degree to which the generative model is relaxed–mediates the drug's therapeutic outcome, while at the same time, volitional agentic beliefs, attitudes, and actions modulate the experience.

Saying that a transient loosening of priors allows the system to escape maladaptive attractors accurately describes the mechanism from the outside, following a mean-field approach, but this is a process that simultaneously modulates consciousness and is modulated by it, with its trajectory subject to conscious intention. Existing theoretical descriptions of the computational pharmacology of mystical-like states have largely eschewed the role of conscious belief and

intention in their mechanism of action beyond mentioning that they exert an influence. To address this gap, I turn to the distinction between the content and the structure of beliefs (priors).

Prior Content, Prior Structure, and Circular Causation

Anecdotally, the importance of set and setting for psychedelic experiences has been known for decades. Recent studies have confirmed this empirically, for example, by emphasizing the link between being intentionally willing to surrender to the experience, holding a healing intention, and having positive clinical outcomes[262–266]. Moreover, a recent study showed that the intensity of the mystical experience, the key mediator of clinical outcome, is most significantly associated with spirituality and spiritual intention[266]. Rather than explaining away the fact that how one thinks and feels about reality is a major determinant of whether the mystical-like state will be attained and of its therapeutic potential, I take this as the starting point for understanding the mystical-like state's mechanism of action.

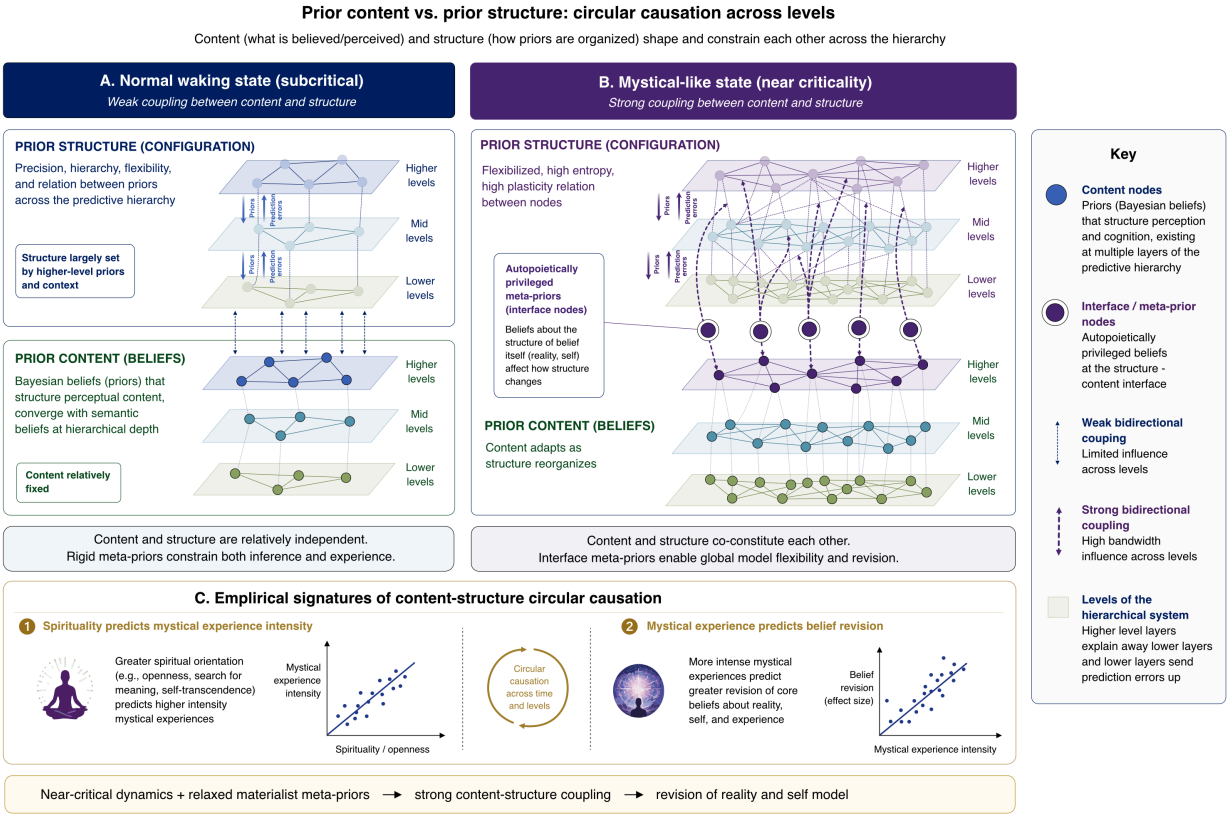


Figure 3.13: Prior content versus structure – circular causation across levels.

Specifically, there is a mechanistically meaningful connection between the computational *structure* of the system of priors (e.g., rigid or flexible; coupled with allostatically meaningful priors or not) and the *content* of the priors themselves (e.g., open to having a spiritual experience or not) (Figure 3.13). During the normal wakeful state, the relative impact of the content of priors on the structure of priors, and vice versa, is limited, whereas during the high-entropy mystical-like state, the relative influence of each level on the other would increase dramatically. In the case of an acute psychedelic session, it is not just that high-level priors become annealed and give way to a new possible configuration; the baseline *content* of the high-level priors will also impact the *extent* to which the configuration of priors will become loosened, and vice versa. For example, beliefs about the structure of reality, self, and world have a large determining effect

on the content, quality, and magnitude of the psychedelic-induced mystical state[263,265,266]. Holding a belief about reality that is open to the possibility of a spiritual experience will increase the chances that the compound will sensitize the system enough for high-level priors to become loosened and elicit a mystical-type experience, which will in turn update the content of priors. Conversely, the content, quality, and magnitude of mystical-type experiences changes beliefs about the structure of reality, self, and world, with metaphysical and self-related beliefs changing in predictable and durable ways toward panpsychist and spiritual beliefs in a manner correlated with clinical improvement[267–271]. In short, certain beliefs mediate the magnitude and quality of the mystical state, and the mystical state itself influences beliefs of the same class.

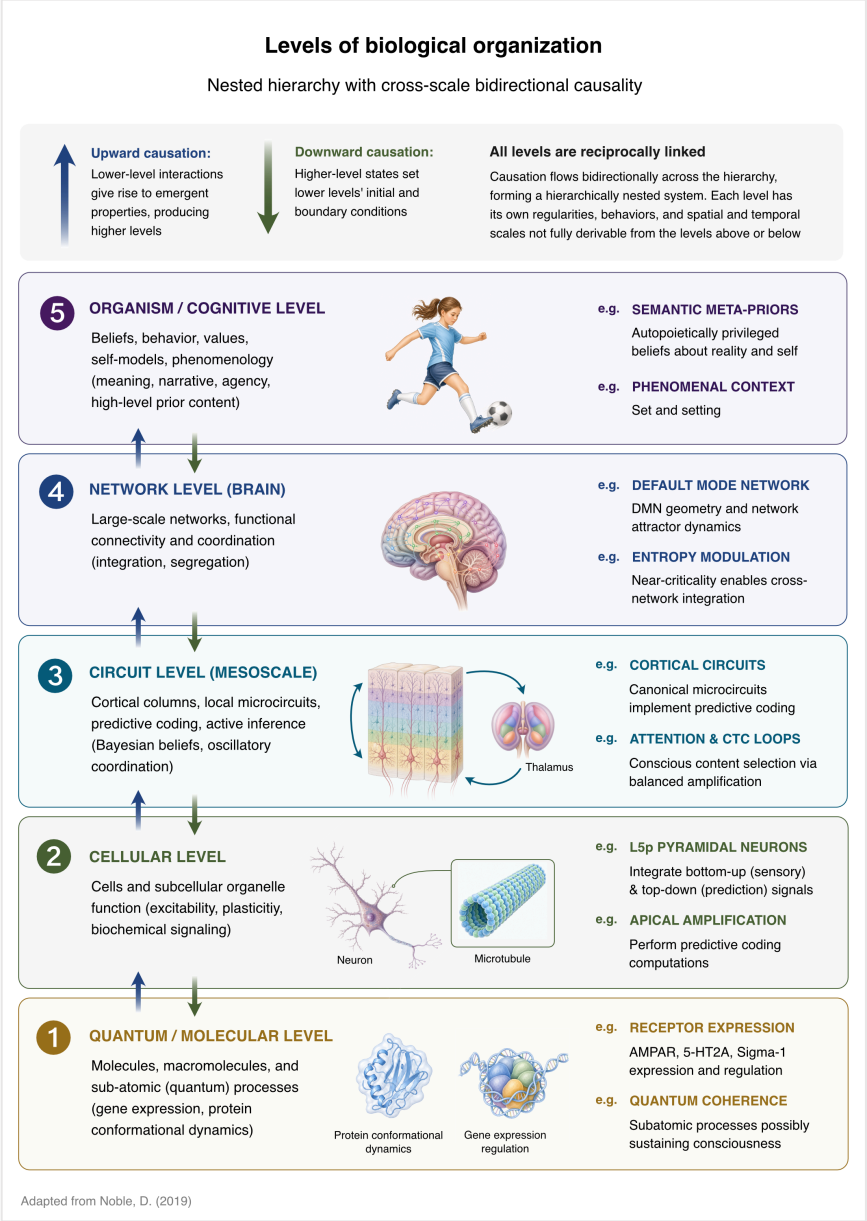


Figure 3.14: Levels of biological organization, adapted from Noble et al. (2019).

The border between the structure of the priors and their content is therefore porous, with causality running both ways. Back to our specific example, holding beliefs compatible with the possibility of a spiritual experience points to a more flexible set of perceptually relevant priors, and vice versa. That the content of a belief, operationalized as a prior, may be causally connected

to the structural flexibility of the configuration of priors that structures perception illustrates the autopoietic nature of the predictive processing system, with the autopoietic degree becoming enhanced in the mystical-like state. While there are boundaries between content and structure, there is also circular causality between them, mechanistically instantiated through precision-weighing and the hierarchical topology of the prior space, through which the structural position of a prior determines the influence it has on the rest of the system. For example, holding a belief in a spiritual realm and that healing may occur through it (prior content) conditions the predictive system (prior configuration) to be more sensitive to sensory signals consistent with this meta-prior, by modulating the relative precision of the class of perceptual priors and prediction-error signals hierarchically below it.

We can think of these two levels, prior content and configuration, as existing within a larger set of successive nested levels of biological organization, each with its own set of regularities and characteristic spatial and temporal scales not fully derivable from the level above or below, with downward causation setting the initial and boundary conditions of lower-level states while upward causation establishes how upper-level states are produced[272,273] (Figure 3.14).

Most priors describe domain-specific regularities–the persistence of objects, the symmetry of faces, the prevalence of light from above. However, a smaller subset occupies a structurally privileged position. They describe not the contents of perception but the meta-structure of perception itself, including how perception relates to action, to other minds, to time, and to reality as a whole. These priors are autopoietically privileged not because they are foundational in any metaphysical sense but because their content is structurally recursive: revising them rearranges the topology of the system through which all other priors are encoded

and updated. Beliefs about intentionality, about the boundary between self and world, about the ontological status of subjective experience, and about the meaningfulness of agency, fall into this class. Importantly, it is precisely these priors that mystical-like states most reliably revise[267,268], and it is the openness or closedness of these priors at baseline that most strongly predicts whether such a state will be attained at all.

Temporal Windows of Expanded and Exchanged Degrees of Freedom

This content-structure coupling can be framed more generally in terms of degrees of freedom and the information theoretical definition of a level boundary. The boundary between levels is an emergent, scale-dependent structure maintained by time and spatial scale separation, coupling strength ratios, and causal emergence. Time and spatial scale separation refers to the ratio of characteristic relaxation times within a level to that between levels, with the boundary emerging where there are relatively few degrees of freedom separating a cluster of fast (e.g., protein conformational dynamics occurring in pico/micro-seconds) and slow (e.g., gene expression dynamics occurring in minutes to hours) degrees of freedom[274]. A level boundary, also known as a Markov blanket, emerges by a large ratio of within-to-between-level coupling strengths, whereby DoFs at the same level have high mutual information with each other and lower mutual information with DoFs at adjacent levels[275]. Finally, a level is causally distinct from that below it when effective information (causal power) at the coarser scale exceeds that of the finer scale, which occurs when coarse-graining reduces noise and reveals a net gain in causal clarity[276,277].

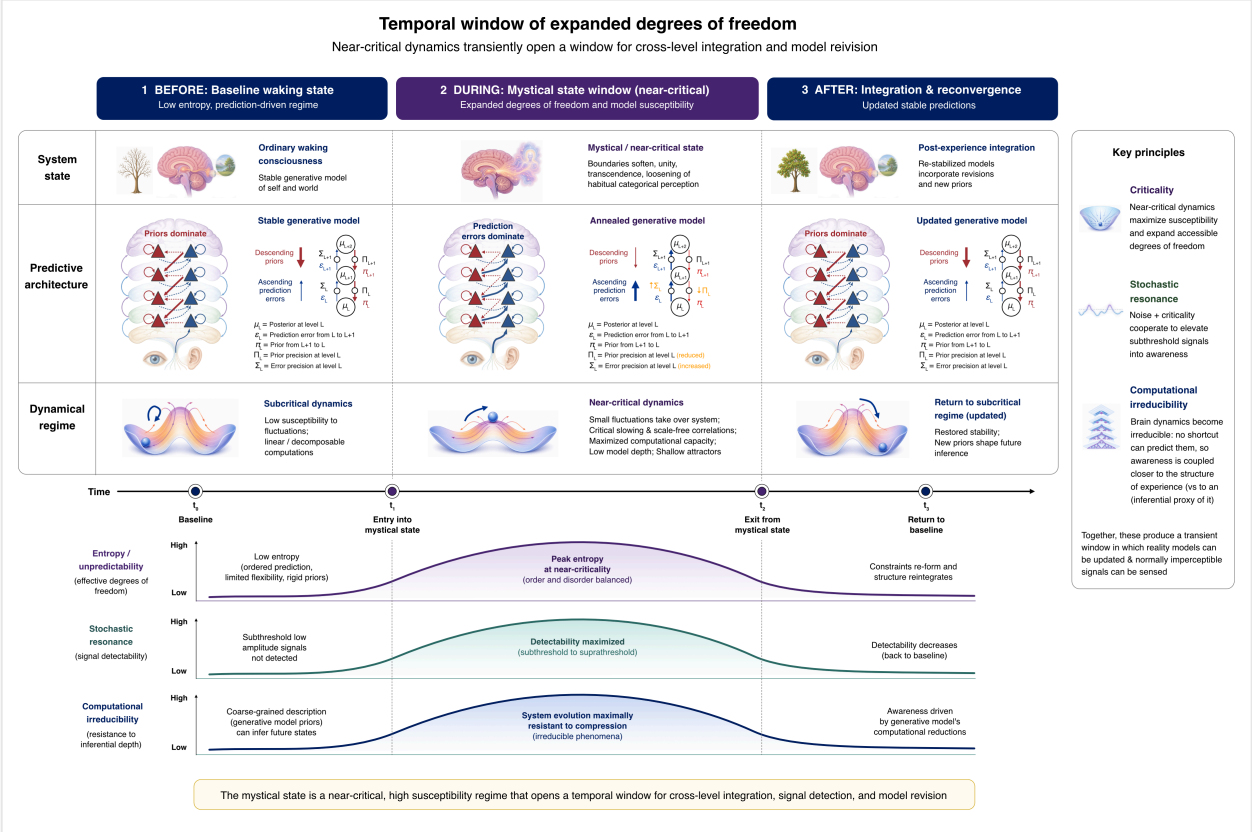


Figure 3.15: Mystical state as a temporal window of expanded and exchanged degrees of freedom.

Perceptual information processing is always occurring within-level (e.g., prior beliefs to other prior beliefs) and across-levels (e.g., 5-HT_{2A} modulation of cortical gain coupling the molecular level to the algorithmic). Under the brain's normal operating regime, within-level exchange is greater than between-level exchange. Were this not the case, the levels would not remain distinct, or one would be so strongly driven by the other that it would lose its own dynamics. The condition under which within-level exchange dominates makes the level structure useful, stable, and metabolically efficient. The ratio of within-to-between level exchange is dynamic, with cross-level causation occurring in both directions. Moreover, some degrees of freedom are structurally positioned at the level boundary, performing between-level exchange

and thus having a high degree of mutual information with adjacent levels. An example is autopoietically privileged priors, which are positioned at the boundary between prior content and configuration and thus have high leverage on the between-level coupling ratio.

Crucially, near criticality, the correlation length of fluctuations diverges (i.e., fluctuations that would have been damped within a level now propagate across levels); the fast and slow timescales between levels become less separated (i.e., the spectral gap narrows); the Markov blanket becomes thinner (i.e., internal and external states become less mutually insulated); and within-level effective information falls. Hence, near criticality, the coupling ratio reverses and cross-level information flows at a higher rate. I.e., criticality explores and tests the boundary conditions of the boundary.

I propose that the broadband desynchronization, increased complexity, and flattened 1/f slope observed during the high-entropy, near-critical mystical-like states index the increase of the between-to-within-level exchange ratio across multiple nested scales simultaneously (Figure 3.15). Put differently, mystical-like states correspond to a transient reduction in the spectral gaps, thinning of the Markov blankets, and decrease in local causal closure that normally maintains level separation. This, in turn, produces the phenomenological characteristics of dissolved boundaries, cross-modal integration, and the felt sense that normally segregated aspects of experience (thought/body, self/world, content/structure) become directly coupled.

Furthermore, autopoietically privileged meta-priors, such as spiritual or metaphysical beliefs about the nature of reality, are degrees of freedom whose Markov blanket spans multiple levels and whose mutual information with both adjacent levels is comparably high. They sit at the interface between prior content and prior structure, between the organism's model of the world and the organism's model of itself as a modeler. This is precisely why they are the

variables most capable of modulating the between-level coupling ratio when the system is near criticality: They are already positioned at the boundary, and under the high-entropy state, their influence propagates across it in both directions. Once the transient widening of between-level channels returns to baseline, there is a measurable and persistent change in the content of priors that are downstream from the meta-priors.

The dynamic nature of the coupling ratio is made apparent from the experience dependent changes in neural complexity during the mystical-like state. In the normal wakeful state, entropy is bounded by the coupling of available perceptual degrees of freedom to incoming sensory data. In the mystical-like state, the increased between-levels exchange increases the degrees of freedom available to the hierarchical system of perceptual priors. This is elegantly shown by a recent study, in which the entropy-enhancing effects of LSD diminished when participants opened their eyes or perceived external stimuli like video or music[278]. The study shows that the entropy of brain dynamics, which indexes the intensity of the mystical-like state, is modulated by the presence of stimuli. When stimuli appear, the perceptual apparatus must model them by coupling the available degrees of freedom to the statistics of the input. This reduces the degrees of freedom available for between-level exchange. Conversely, the absence of stimuli allows the available degrees of freedom to be free from coupling to bottom-up sensory input, freeing perception (i.e., the posterior) to reflect the internal structure and evolution of the predictive system itself under enhanced between-level exchange.

Since we can generate internal perceptual stimuli in the form of thoughts and imagined sensory percepts, their presence will likely reduce the entropy of neural dynamics in a parallel and content-sensitive manner to external sensory stimuli. Thoughts and intentions that relate to autopoietically privileged priors, whose content pertains to the structure of thought, perception,

reality, or the nature of the experience itself, are a special case of these. Through the mechanics explained above, they modulate the subjective experience closer or farther from the boundary-dissolving high-entropy state depending on their epistemological and ontological content.

The widened between-level coupling proposed above has two immediate computational consequences.

First, the system can explore regions of state space that are normally inaccessible because reaching them would require a monotonic traversal of paths constrained by within-level structure. When information can flow vertically through the hierarchy and be rearranged at a level where the required path through state space is shorter or topologically simpler, configurations become reachable that would otherwise demand an energetically prohibitive traversal of within-level attractors. The clinical-phenomenological correlate is the observation that, during the psychedelic state, intrusive thoughts can become felt as embodied sensations, somatic charges can resolve as cognitive insights, and emotional knots can reorganize as changes in propositional belief, transformations that would be effortful or impossible under ordinary cognition[279–281]. These cascades are consciously experienced and, to a degree, guided by intentionality.

Under the psychedelic state, the felt sense of a new thing being true regularly precedes its verbal articulation, consistent with the embodied and affective neighborhoods of the prior hierarchy being recalibrated first, with the conceptual layer settling into coherence with the recalibrated layers beneath. This temporal ordering, consistent with first-person accounts in psychedelic and contemplative phenomenology, is consistent with a topological flattening of the attractor landscape that proceeds non-uniformly through the prior space in specific, causally linked neighborhoods, rather than as the simultaneous mean-field event assumed by the REBUS

model. While I agree that the mechanism involves a topological flattening of the free energy landscape, the cascades of rearrangement are driven by intentionality and follow the structure of causally linked beliefs, propagating vertically up and down the hierarchy as well as horizontally between associated beliefs.

Second, expanded across-level coupling allows degrees of freedom from the body to become available to higher-level processing, akin to the proposed mechanism of entrainment patterns produced by attention to nasal breathing (Section 2's OLIPR). The interoceptive first priors that ordinarily exert downward influence on cognition through the narrow channels of affect, mood, and motivation become more directly available as consciously palpable content. Emotions become inspectable rather than merely behaviorally expressed; the felt sense of intention or aversion becomes examinable rather than acted upon; and the somatic record of the autobiographical body becomes amenable to perceptual sampling. This is the mechanistic basis of the embodied insight that characterizes these states, and it is what justifies framing the mystical-like state as more embodied rather than less.

In sum, the clinical action of serotonergic psychedelics resists a purely molecular reading. The mechanism of action straddles molecular, computational, and phenomenological levels: Psychedelics destabilize the predictive hierarchy, but the trajectory of that destabilization and the configuration the system settles into afterwards are shaped from the top down by the subject's intentions, beliefs, and conscious orientation as much as from the bottom up by 5-HT_{2A} receptor agonism. The content of certain autopoietically privileged priors is therefore not epiphenomenal to the structure of the predictive system but is causally coupled to it via circular causation across levels and may register as measurable variation in the entropy of neural dynamics.

The cost-benefit logic of these states is straightforward. The system gains high-dimensional reconfiguration capacity, access to a state space that is broader, more flexibly coupled across levels, and more sensitive to inputs from levels normally below detection, at the price of the temporally deep, level-segregated processing that supports planning, prediction, and stable selfhood. Because both cost and benefit are structural, these states must be transient: living systems require temporally deep prediction to perform allostasis. Mystical-like states are therefore best understood not as steady-state regimes but as temporally bounded windows of expanded and exchanged degrees of freedom, after which the system reconverges on a level-segregated regime, ideally with a re-encoded prior structure that minimizes long-term surprise more efficiently than before.

Empirical Predictions and Implications

My framework generates several testable predictions:

1. The intensity of mystical-like states should be inversely related to the bandwidth of exteroceptive input during the state. For example, eyes-closed, low-stimulation environments should produce higher MEQ scores at a given dose.
2. Baseline internally generated content of high structural relevance (intentions, ontologically open beliefs) should modulate neural entropy and MEQ scores more than baseline internally generated content of low structural relevance (task-relevant thoughts, narrative rumination), even when matched for arousal. This effect should be reversed during the acute phase, where internally generated content of high structural relevance should modulate neural entropy and MEQ scores less than baseline internally generated content of low structural relevance.

3. Across-level transfer events, moments at which cognitive content acquires a somatic representation, or vice versa, should cluster temporally and be accompanied by transient peaks in measures of cross-frequency or cross-scale coupling.
4. The cost of expanded across-level coupling should be measurable as a loss of within-level temporally deep processing: working memory, sequence planning, abstract reasoning, and counterfactual generation should be most degraded during moments of largest cross-level transfer, even as awareness itself is felt as expanded.

Several implications follow. First, the mechanism of action of these compounds cannot be characterized without reference to consciously held beliefs and intentions, making the patient's epistemic and spiritual stance a load-bearing pharmacological variable. Second, set and setting are constitutive. The meta-priors a subject brings are part of the active mechanism, not the context in which it acts. Third, and most important, the structure and content of the predictive system and the statistics of the internal and external environments to which the system's degrees of freedom are coupled all three exert mutual causality on one another. The mystical-type experience can therefore be conceived of as a transient widening of the channels of mutual causation between three normally segregated levels. Under the ordinary wakeful state, the structure of the system is relatively invariant on perceptual timescales, the content of priors is updated slowly, and the statistics of the environment are sampled through narrow attentional and behavioral apertures. Under the mystical-like state, the content of certain meta-priors becomes capable of modulating the system's structure, the structure becomes more sensitive to internal and external statistics it would otherwise dampen, and the statistics themselves are sampled across a broader sensory and interoceptive aperture.

Finally, one general question regards the impact of the mystical-like states on the organism's biology beyond the central nervous system and below the layer of brain-based cognitive architectures. Specifically, if mystical-like states are characterized by a temporal window of expanded and exchanged degrees of freedom between cognitively relevant layers of biological organization, does this window extend to the boundaries between biologically relevant layers across the organism? For example, does the ratio of within to between-level coupling strength amongst gene expression dynamics, protein conformational dynamics, and organism-level developmental dynamics also change during the mystical-like state? Emerging scientific work showing that non-neuronal cells have complex cognitive functions previously thought to only apply to neurons, along with anecdotal reports of non-psychiatric healing after psychedelic and non-psychedelic mystical-like experiences suggest this as a productive area for empirical inquiry.

The Physics of the Mystical State: Criticality, Computational Irreducibility, and Stochastic Noise

Criticality and the Computational Affordances of the Edge

The living organism bounds its entropy by compressing the statistically tractable correlations of its internal and external environments into lower-dimensional generative models. The free-energy principle formalizes this constraint by selecting the generative model to minimize variational free energy given sensory input, which is mathematically equivalent to maximizing model evidence while keeping complexity costs low. The resulting architecture

sacrifices full-dimensional sampling for compressive prediction, and this sacrifice is metabolically rational because the niche-relevant statistics of the world contain enough compressible regularity to sustain an evolutionarily accurate model. The optimal operating regime for such a system is neither rigidly ordered nor stochastically disordered but balanced near a critical point between the two, where the system maximizes its dynamic range, information transmission, and sensitivity to perturbations of arbitrary scale[282,283].

Empirical work over the past two decades has established that the cortex operates near such a critical point under normal wakeful conditions, with neuronal avalanches whose size distributions follow power laws, scale-free spatiotemporal organization, and long-range temporal correlations characteristic of self-organized critical (SOC) systems[284–286]. Anesthesia, deep NREM sleep, and disorders of consciousness shift the system in the subcritical direction, while psychedelics and certain forms of meditation move it closer to or beyond the critical point[43,75,249,287]. Two features of SOC systems are particularly consequential. First, as the system approaches criticality, the correlation length of fluctuations diverges, producing correlations between widely separated components that are absent in subcritical regimes[288]; small perturbations can therefore propagate across scales and exert global influence rather than being damped locally. Second, computational capacity, measured by entropy production, susceptibility, dynamic range, and the size of the accessible state space, is maximized at the critical point[282,283,289,290]. The neurophysiological signatures of mystical-like states–broadband desynchronization, flattened 1/f slope, increased Lempel-Ziv complexity, increased neural avalanche size and lifetime, and increased global functional connectivity–are the signatures of a system moving toward or across the critical point[249,291,292]. As correlations become scale-free, intention, belief, attention, and the content of autopoietically privileged priors become capable of

shaping the trajectory of the system in ways they could not at the subcritical baseline. The phenomenological observation that set, setting, and intention are load-bearing variables for the experience is therefore the result of the system moving into a regime where small inputs propagate across scales.

Living systems do not maintain themselves rigidly at the critical point. A system maximally susceptible to fluctuations is also maximally distracted by them, and the temporally deep, attractor-bound processing required for action selection and sequence planning is degraded in the same regime that maximizes synchronic computational capacity. There is therefore an optimal coarse-grained distance from criticality that depends on the statistics of the niche and the metabolic budget of the organism, within which the system oscillates. Closer to criticality, the system explores its own model: degrees of freedom are released, cross-scale couplings widen, and the generative model is exposed to inputs and rearrangements that update its structure. Farther from criticality, the system exploits: the model is consolidated, attractors are deepened, and behavior is executed against a stable representational background. This oscillation keeps the generative model simultaneously updated and parsimonious, and it operates on multiple nested timescales, from fast cortical fluctuations through circadian transitions to the longer scales at which generative models are reorganized through learning, sleep, and occasional mystical-like reorganization. Within this framework, mystical-like states are not anomalies but the deepest exploratory excursions of a system that ordinarily oscillates within a narrower range and occurring at moments of psychological impasse or therapeutic intervention when the current attractor structure no longer adequately tracks the statistics of the body or the environment.

Because critical systems have no characteristic scale, as the system approaches criticality, the smallest fluctuation it can detect and propagate decreases: every perturbation, however small,

can in principle propagate through the system[293,294]. The progressive lowering of the prediction-error threshold described in Section 2, which produces successive recalibration from gross to subtle priors, is therefore the perceptual signature of the system being tuned closer to a regime in which it is sensitive to lower-amplitude signal across all scales. The phenomenological richness reported in deep meditative, psychedelic, and fasting-induced states, and the progressive move from mundane to numinous perceptual content described across contemplative traditions, is, on this account, a signal that becomes detectable as the system enters the regime in which low-amplitude correlations propagate across scales.

Mystical-like States and Computational Irreducibility

A second formal lens, complementary to criticality, is Wolfram's principle of computational equivalence and its corollary, computational irreducibility[295,296]. A process is computationally irreducible if there is no shortcut to its future state shorter than simulating the process step by step. Most non-trivial dynamical systems, including many cellular automata, fluid turbulence, and many biological processes, are computationally irreducible. A small but evolutionarily indispensable subset of processes, however, are computationally reducible: their future states can be predicted by a generative model that compresses the dynamics into a lower-dimensional representation. I propose thinking of predictive processing as precisely the exploitation of computational reducibility for adaptive purposes. The brain succeeds as an inference machine because the niche-relevant statistics of the world contain enough compressible regularity to be modeled with metabolic efficiency. The corollary is that the brain's perceptual interface is biased toward computationally reducible features of the world, and the ordinary

wakeful state systematically excludes from awareness the computationally irreducible structure of the world, including most of the dynamics of the system itself.

As the system approaches criticality, it loses the capacity to compress its own dynamics into low-dimensional, attractor-bound representations. Scale-free correlations and divergent susceptibility mean that the system's own evolution becomes increasingly computationally irreducible. At the same time, the perceptual interface is tuned toward dynamics it can no longer shortcut, so what becomes accessible to awareness is precisely the computationally irreducible structure of the body, the environment, and the system itself. The phenomenological characteristics of the mystical-like state follow naturally from this shift. Ineffability follows because language is a tool for transmitting computationally reducible content. Paradoxicality follows because irreducible dynamics admit no consistent categorical decomposition. Noetic quality follows because the experience is a direct sampling of structure rather than its compressed inferential proxy. Higher dimensionality follows as well: as correlations become scale-free and within-level constraints relax, the effective dimensionality of accessible neural states increases, manifesting phenomenologically as an expanded consciousness with more available perceptual, affective, and cognitive degrees of freedom per unit of time, a finding that recent topological and manifold-based analyses of neural dynamics under psychedelics and meditation have begun to document empirically[44,73,297].

This view yields a candidate computational definition of the mystical-like state as a transient state in which the system's distance from criticality is sufficiently reduced that the dynamics under awareness become predominantly computationally irreducible rather than computationally reducible. By extension, meditation can be reframed not behaviorally, as the self-regulation of attention on a present-moment object, but computationally, as a self-directed

practice that tunes attention toward computationally irreducible phenomena. Awareness of breath, of bodily sensation, of feeling, and of the arising of thought itself are all computationally irreducible. Their next state cannot be compressed by an external model, only sampled in real time. In contrast, discursive thought about these phenomena is computationally reducible, as it is the system attempting to model the irreducible by inferential proxy, which is exactly what falls away as meditation or mystical-like states deepen[298,299]. This reframing makes the convergence of psychedelics, meditation, and fasting computationally precise. All three are routes by which the system is tuned toward the computational irreducibility horizon, with different distal mechanisms but a shared proximal target. It predicts that neural signatures of criticality should track behavioral measures of meditative depth and psychedelic experience intensity; that the practices should generalize to any sustained attentional engagement with computationally irreducible content (e.g., flow states, devotional absorption, improvisational artistic engagement) with neurophysiological signatures tracking the criticality axis rather than the practice label; and that the human capacity to accumulate information across timescales should be optimized not by maximizing reducibility or irreducibility but by oscillating between them, with exposure to computationally irreducible regimes followed by consolidation periods in which the generative model is restructured around the new content.

Entropy, Randomness, and Stochastic Noise

A third formal lens involves stochastic noise and its relation to randomness and entropy. Entropy, in the information-theoretic sense, measures the uncertainty or incompressibility of a process or signal. A high-entropy signal is less describable by a generative description than a low

entropy one, which makes entropy an information-theoretic relative of computational irreducibility. A second consequence of higher entropy in nonlinear physical systems is captured by stochastic resonance. Under appropriate conditions, the addition of noise to a nonlinear system increases its sensitivity to weak signals that would otherwise lie below detection thresholds[300–302]. Counterintuitively, adding noise to a system sensitizes it to weak signals. This occurs as random fluctuations occasionally summate with subthreshold inputs to push the system across its detection threshold, increasing its responsiveness to inputs whose amplitude is too small to drive it unassisted. Stochastic resonance has been documented across physical, sensory, and neural systems, with neural variants demonstrated in mechanoreceptors, auditory and visual cortex, and large-scale brain dynamics[303,304].

The increased entropy that characterizes mystical-like states could therefore be reframed as an increase in functionally useful neural noise that brings ordinarily undetectable signals across the threshold of awareness. This is consistent with the criticality framework, where the detection threshold decreases as the system approaches the critical point, but it adds a distinct mechanism: Even within a fixed distance from criticality, an increase in the variance of subthreshold dynamics can render previously imperceptible structure perceivable. The two mechanisms likely operate together. Closer to criticality, small fluctuations propagate. With higher entropy and stochastic variance, they are also more likely to be generated in the first place. The system is not malfunctioning when its dynamics become more variable. Rather, it is harnessing stochasticity as a computational resource, exactly in the manner described by multi-scale accounts of biological computation in which noise is treated as an exploited rather than tolerated feature[304,305].

Across all four lenses–increased incompressibility (entropy), increased proximity to criticality (scale-free correlation), increased computational irreducibility (resistance to shortcut prediction), and increased exploitation of stochastic variability (noise-mediated subthreshold detection)–biology temporarily cultivates randomness in a controlled and transient manner to maximize the long-term adaptiveness of the organism's generative model. This is not a failure of inference but a phase within an adaptive oscillatory dynamic that is likely to be present in free energy minimizing systems beyond the human brain. That biology would cultivate randomness is unsurprising when one considers that randomized algorithms are more efficient than nonrandom deterministic ones at a large class of computational problems, such as determining if a number is prime, even though the structure that the randomness reveals is composed of a nonrandom pattern[306].

At this point, I have proposed a model of the mystical-like state as a temporal window of expanded and exchanged degrees of freedom in which criticality, computational irreducibility, and stochastic noise converge to reveal a correspondence between its computational, phenomenological, and physical properties. I have established its adaptive role in the context of a generative model that must remain predictively accurate and metabolically and computationally efficient. Rather than eschewing the influence of beliefs on the magnitude, content, and quality of the mystical-like state, and vice-versa, as tangential or epiphenomenal to its mechanism of action, I have presented a framework for how beliefs, intentionality, and agency interact with the biologically grounded computational architecture to produce therapeutic effects. In doing so, I have traced the outlines of the computational pharmacology necessary to understand these mechanisms of action. However, while I have described the role of consciously mediated beliefs and intentions in the therapeutic mechanism, I have so far ignored the specific perceptual

phenomenology of the mystical-like state. If the experience is the medicine, then what conclusions can or should be drawn from the experience itself?

Interim Summary

This section treated the mystical-like state as a perturbation of a multi-scale architecture and examined it through four complementary lenses: a computational pharmacology in which mystical experience rather than dose mediates clinical outcome; a phenomenology of set and setting in which the content and structure of priors are coupled by circular causation across levels; a physics of criticality and computational irreducibility in which the state corresponds to the system's dynamics becoming scale-free and resistant to shortcut prediction; and an information-theoretic lens in which the same state corresponds to an increase in functionally exploited stochastic variability. Across these lenses, a common characterization emerges: The mystical-like state is a transient, temporally bounded window in which the boundaries between nested levels of the predictive architecture become more permeable; degrees of freedom within and between levels expand and are exchanged; the system is tuned closer to a critical regime where small perturbations acquire scale-free reach; awareness is recoupled to the computationally irreducible structure of body and environment; and the resulting reorganization of the generative model is shaped by the autopoietically privileged content of the priors the subject brings into the state.

This characterization is empirically tractable and biologically grounded. It does not require any commitment to the metaphysical status of what is encountered in such states. Whether the noetic, numinous, and unitive content that subjects consistently report is best

understood as a real disclosure of structure ordinarily below the system's detection threshold, as the phenomenal signature of a dissolved self-model encountering its own substrate, or as the projection of meaning by a high-entropy generative model onto its own dynamics, is a question the computational framework alone cannot decide. Section 5 takes up these questions through the lens of field theories of consciousness. I carry forward three claims: (1) that the entropy of neural dynamics indexes a real computational property of the system, and the correspondence between this property and the phenomenology of expanded states is mechanistically grounded rather than coincidental; (2) that the structure and content of the predictive system, and the statistics of the internal and external environments to which it is coupled, exert mutual causality on one another, such that consciously held meta-priors are load-bearing variables of the system's dynamics; and (3) that the convergent target of psychedelics, meditation, and fasting is a regime in which the system maximizes access to computationally irreducible, low-amplitude, scale-free structure. With these three claims in hand, Section 5 turns to what it means for the system to inhabit such a state.

Section 5: Beyond the Computational Horizon: Numinous Phenomenology and the Ontological Question

"The time has come to realize that an interpretation of the universe, even a positivist one, remains unsatisfying unless it covers the interior as well as the exterior of things; mind as well as matter. The true physics is that which will, one day, achieve the inclusion of man in his wholeness in a coherent picture of the world."

– Pierre Teilhard de Chardin, *The Phenomenon of Man* (1955)

Section 4 provided a biologically grounded computational and physical characterization of the mystical-like state. This section asks what it means to inhabit such a regime. A substantial portion of the mystical state's phenomenology and therapeutic mechanism of action is well-accounted for by the existing neuroscientific literature and by the theoretical machinery of Sections 1-4, but the consistently numinous and noetic quality of the experience resists that accounting in ways that are both scientifically significant and clinically relevant.

The portion of the phenomenology that is computationally and algorithmically tractable revolves around emotional reprocessing, resolution and relief of emotional and physical pain, and epiphanic insight and content. Across psychedelic, meditative, and other mystical-like states, the resurfacing and felt resolution of affectively charged biographical content can be said to follow the computational cascade driven by the relaxation of high-level priors. Under ordinary conditions, the allostatic self-model governs salience, determining which interoceptive signals reach consciousness and which are filtered as irrelevant to current policy selection[307,308]. When high-level priors lose precision, they become amenable to revision by the bottom-up evidence they had been suppressing, such that previously suppressed content, including affectively charged memories and sidelined embodied knowledge, can become reexperienced and reencoded[37].

Relief from physical and emotional pain can be attributed to the attenuation of the predictive component of pain by the flattening of the predictive hierarchy, the reencoding of pain-predicting priors and embodied memories, peripheral anti-inflammatory action (in the case of psychedelics)[309], and endogenous opioidergic modulation[251,310]. Finally, epiphanic content can be understood as the product of fact free learning through Bayesian model reduction, a

refinement of the generative model whereby complexity is eliminated to reveal a more parsimonious model from priors alone and perceived as insight[86,311]. Moreover, with high-level priors relaxed, incoming percepts arrive with near-zero prior probability and high epistemic gain, which becomes registered as positive valence and revelatory insight[312,313].

Together, these mechanisms account for what the clinical literature identifies as the primary active components of psychedelic therapy and of many contemplative practices: adaptive reprocessing of maladaptive psychological material, revision of entrenched allostatic priors, and the felt acquisition of insight that reorganizes the affordance landscape. What scientific theoretical frameworks do not explain, and what the empirical literature has largely failed to account for, is a class of content that is among the most robustly reported, therapeutically significant, and epistemically challenging features of the mystical state: numinous encounters with seemingly conscious, autonomous, and intelligent non-human entities.

The Numinous Noetic Content and the Entity Encounter

Numinosity, the felt encounter with something of ultimate significance that is irreducible to any ordinary category[245], is operationalized in the MEQ-30 as sacredness and in the M-Scale as the experience of the holy[247,248]. Across the psychedelic clinical literature, these two dimensions are the strongest predictors of lasting therapeutic benefit, indicating that they are not phenomenological epiphenomena but mechanistically active components of therapeutic change. Their noetic quality–the felt sense of having direct contact with reality at a deeper level than ordinary perception and cognition–reliably produces lasting ontological belief revision[281,314,315], with a single transformative experience shifting metaphysical commitments toward panpsychism

and animism in proportion to the depth of the mystical experience and persisting in time[267]. A large-scale survey of 4,285 psychedelic- or non-psychedelic-induced encounters with what individuals termed "God" or "ultimate reality" found that more than two-thirds of participants who identified as atheist before the experienced ceased to do so afterwards[316]. This amounts to a revision of the highest-level priors in the generative model hierarchy, and their persistence indicates that the noetic numinous experience is consistently registered as carrying maximal epistemic authority.

Within the rubric of numinous noetic experiences, encounters with beings or entities felt to be unmistakably conscious, autonomous, intelligent, typically benevolent, and existing at a level of reality that exceeds ordinary waking life are some of the most common, impactful, and challenging to understand. In one survey of 3,778 experiences with inhaled N,N-DMT, 45.5% involved entity encounters and interactions[317]. In another survey of 2,561 people reporting inhaled N,N-DMT entity encounters, 96% described the entity as conscious, 96% as intelligent, 78% as benevolent, 58% as more real than baseline reality, and 69% received what they interpreted as a communicated message[318]. Entity experiences have also been consistently reported during intravenous N,N-DMT sessions[319], LSD sessions[320], ayahuasca sessions[321], and other psychedelics[322]. Most of these encounters are associated with N,N-DMT, the endogenous psychedelic, and while most are reported to be positive, a survey of ayahuasca users found that 14.9% reported feeling a harmful connection with a "spirit world"[323].

The entities reported fall into a consistent typology that includes beings of light, guides, geometric intelligences, alien-like presences, and deceased relatives that are described with a culturally encoded surface vocabulary. For example, the ayahuasca practitioner meets luminous serpentine spirits and plant intelligences[321], while the recreational N,N-DMT user reports

machine elves, interdimensional ambassadors, or presences that transmit information directly and wordlessly[317]. Yet beneath this variation, there are transculturally stable perceptual and relational forms, which are centered around an autonomous being with attributed consciousness, intelligence, and benevolent communicativeness, and who can take the form of an autonomous and intentional agent, animal spirit, ancestor spirit, or deity[324]. In short, entity encounters are simultaneously stable in their deep structure across individuals, cultures, and time periods and modulated in their surface form by cultural priors.

Neuroscientifically, entity encounters are among the best documented and least mechanistically explained features of the psychedelic state. The clinical literature has largely treated them as peripheral to the mystical experience despite accumulating evidence that they independently mediate therapeutic outcomes through meaning-making, confrontation of mortality, and the felt receipt of unconditional care from a benevolent other[325]. Clinically, their therapeutic utility appears to depend on interpreting the encounter as genuine, which raises what has been termed the Comforting Delusion Problem: If the therapeutically useful interpretation is factually unwarranted, then psychedelic-assisted therapy would be in the uncomfortable position of deploying a mechanism whose efficacy is predicated on a false belief[326].

Most arguments have responded to the problem by attempting to decouple the therapeutic benefit from ontological commitment, while scientific attempts at accounting for entity phenomenology have centered around subjects' cognitive and neural processes, with phenomenological consistency proposed to emerge from innate cognitive modules that are part of evolved human neural architectures or from a destabilized predictive processing generative model. Crucially, neither of these successfully accounts for the phenomenology while solving the Comforting Delusion Problem.

Existing Scientific Accounts of Numinous Entity Phenomenology

Existing accounts of entity encounters span a spectrum from the fully naturalistic to the conditionally ontologically open, with most decoupling the therapeutic benefit from ontological commitment. At the naturalistic pole, hyperactive agent detection (HADD) and neurognostic accounts grounded in evolutionary psychology propose an evolved tendency to detect intentional agents in ambiguous stimuli that is amplified under psychedelics, generating apparent encounters with agents in the absence of real external ones[324,327,328]. These accounts argue that thalamic and lower-brain mechanisms containing innate cognitive templates that evolved for social cognition become released from the top-down control of prefrontal cortex and DMN during psychedelic or meditative states, allowing the modules to attribute agency to nonexistent percepts while shaping visionary experience[327]. Similar accounts, like the interactive religious experience model, argue that a general pre-existing belief in supernatural agents leads people to seek situations that confirm agency-intuitions, which enable them to create personal beliefs[329].

Accounts grounded in predictive processing offer more computationally specific and neuroscientifically robust theories. For example, Deane (2020)[308] argues that psychedelic hallucinations occur when precision shifts to sensory evidence over predictions and illusory patterns emerge due to overlearning (i.e., overfitting), while Buck et al. (forthcoming)[330] argue that entity experiences are best explained as high level predictive inferences recruited under conditions of psychedelic destabilization. In their account, psychedelics increase neural entropy and alter precision weighting, weakening the high-level models that organize perception around a stable self, body, and world. When incoming sensory, interoceptive, emotional,

autobiographical, and agency-related signals no longer fit the normal model of self and world, the predictive system searches for an alternative model able to reduce uncertainty and lands on supernatural-agent inferences, which can coherently explain otherwise anomalous experiences, such as voices, presences, bodily takeover, revelations, healing sensations, uncanny intelligence, altered worlds, and communications that feel external or transpersonal. Since these experiences function as integrative attractors, once an entity agent model is recruited, perception, attention, affect, and meaning making become reorganized around it.

Buck et al.'s predictive processing-based account proposes that when the allostatic self-model collapses through the flattening of the temporally thick model that sustains it, the social-cognitive generative model continues running without its self-anchoring function, attributing consciousness, intentionality, communication, and other outputs to exogenous entities. The entities, in their model, are neither delusions nor real external beings but rather reorganizations of the same generative machinery that normally produces the phenomenal self, with surface-level characteristics of the entity encounter shaped by contextual priors and the invariant core reflecting the neural architecture of the predicted self-model. Importantly, Buck et al. construct their argument around the case that computational agentive modeling continues while the free energy minimization processes that sustain phenomenal, embodied selfhood become weakened; i.e., they argue that agency modeling is more general and resilient than self-modeling under 5-HT_{2A} receptor agonism. Specifically, they posit that "supernatural agent inferences are the next-best inference on the consequences of endogenously caused actions under absence of attributions of these actions to the self, given that these sensory consequences will bear all the ear-marks of agency,"[330] and they buttress their claim that agentive inferences persist despite attenuated self modeling by arguing, with McNamara, that efference copies of motor commands are left

unattenuated by psychedelic 5-HT_{2A} receptor agonism and must be explained[331]. Thus, once the self-model ceases to infer selfhood but the system still needs to explain agency-like structure in experience (intentionality, communication, control, goal-directedness, presence), a supernatural agent model becomes the better-fitting inference, becoming a perceptual hypothesis that the generative model accesses as mid-level priors to generate the entity perception.

While computationally rigorous, these accounts to fail to account for crucial parts of the entity phenomenology and make several doubtful assumptions. The interactive religious experience model, for example, fails to explain why most atheists, whose beliefs tend to be deeply held and are fundamentally incompatible with numinous entity experiences, still reliably have such encounters and experience them as so real as to cause most of them to abandon their atheism. Despite lacking a pre-existing belief in supernatural agents that would lead them to seek situations that confirm agency-intuitions, these experiences are felt to be legitimate enough to justify changing their core beliefs. Accepting the premise of the interactive religious experience model alongside the empirical data therefore amounts to a contradiction.

The neurognostic and predictive processing-based accounts avoid this issue by accounting for why the entity experience might be felt as eminently real–by virtue of it being generated as an inference by the same machinery that regularly generates the sense of self. Yet they cannot account for the noetic quality of the experience–the felt sense that it is *more* real than normal waking reality–or for experiences in which entities are not only passively sensed but are perceived to be responsive to coherent intentionality and communication coming from an experiencer that is able to differentiate between self and other. Crucially, the latter phenomenology implies that self-modeling is not necessarily lost or significantly attenuated during the entity encounter, unlike during the experience of ego dissolution. Indeed, reported

entity experiences commonly involve the experience of two-way communication, entity responsiveness to intentionality, and performance of actions by entities on the felt body and psyche of the experiencing person. The assumption that self-modeling becomes attenuated before agency modeling is thus inconsistent with the phenomenology of entities that respond to and act on the body and mind, the felt sense of which requires the functioning self-model that Buck et al. presume to have been dissolved.

Buck et al. mistakenly conflate the phenomenology of ego dissolution, in which the sense of self becomes dissolved, with that of entity experiences, which preserve a felt sense of a self that can intend, communicate, give, and receive. While both experiences occur during acute, high-dose psychedelic sessions and are linked to positive therapeutic outcomes, ego dissolution is commonly reported during psilocybin assisted therapy sessions, while entity experiences are a hallmark of the N,N-DMT phenomenology, and while they can co-occur, they tend not to do so simultaneously. A careful look at entity encounters reveals that they do not preclude the phenomenology produced by a self-model nor do they necessitate a phenomenal destabilization of it to occur. Indeed, while reports include passive phenomenal experiences (for e.g., visual) of autonomous entities, they emphasize active, self-agentive, intentional, and bidirectional interactions with them in which the integrity and continuity of the phenomenal self are preserved. Besides assuming that self-related inferences are less persistent than agency-attributing ones–an empirically tenuous assumption given that many motor-control processes use efference copy signals for correction, stabilization, and coordination without explicit self-attribution–, their account fails under the common situation where a phenomenal, inferred self is preserved during entity experiences.

Hence, despite these attempts to explain the entity phenomenon through perceptual biases and destabilized neural and cognitive architectures, entity encounters remain scientifically unexplained. Moreover, by implying that patients who receive therapeutic benefit from psychedelics may be doing so via false beliefs induced by chemically compromised cognition, they tacitly declare the Comforting Delusion Problem to be insoluble–a stance which I find to be scientifically and clinically unsatisfactory.

The Suspension of the Ontological Question and the Case for Ontological Openness

Faced with the Comforting Delusion Problem, most philosophical and clinical treatments choose to suspend or eschew the ontological question. Some, like Yaden et al.[332], posit that the therapeutic value of the mystical state does not require the truth of any supernatural claim. The "mystical experience" umbrella, they argue, is too coarse to identify therapeutic mechanisms, and specific acute subjective effects like awe, emotional breakthrough, insightfulness, oceanic boundlessness, connectedness, and disembodiment, differentially predict specific therapeutic outcomes. This has direct implications for understanding entity encounters, for the relational and communicative dimensions of encounters (feeling loved, receiving healing information, meeting a guide) are distinct from the unitive/oceanic dimension of mystical experience and may predict different therapeutic outcomes. Similarly suspending the ontological question, Letheby[326] argues that the Comforting Delusion Objection is not decisive because many therapeutically effective insights (e.g., reduced ego rigidity, increased sense of connection, diminished death anxiety) are defensible without requiring commitment to supernaturalism. Others, including Gładziejewski[333], Van Eyghen[334], and Lutkajtis[335], suspend the question by arguing it may not necessarily be

incompatible with naturalism or by emphasizing therapeutic value via post-acute therapeutic integration within a naturalist epistemology.

Rather than suspending the question, others have made the case for ontological openness. Meyer[336], for example, argued that the reality hypothesis–that entities represent genuine contact with non-human others–cannot be ruled out by the available evidence, and that the behavioral consistency, apparent autonomy, and information content of entity communications exceed what standard models of hallucination predict, an argument that has been largely set aside rather than being formally refuted in the three decades since.

Others making the case for ontological openness have observed that foreclosing the ontological question by materialist assumption is no more epistemically justified than affirming it by credulous assumption, with both being premature closures[337]. A systematic empirical argument in favor of openness by David Luke argues that the N,N-DMT entity encounter overlaps substantially with near-death experience (NDE) phenomenology–entity encounters and interactions with non-human intelligences and a subsequent transformation of death attitudes–, an overlap independently documented in clinical NDE research with DMT-naïve populations[338]. He also emphasizes the indigenous ethnobotanical context of N,N-DMT, which is explicitly framed around death, dying, and communication with the deceased[339,340]. Arguing for a principled agnostic realism, Luke claims that the empirical data do not rule out genuine entity-based information transfer and thus that the responsible scholarly position is to hold the question open rather than foreclose it with materialist assumptions.

I agree that the scientific discomfort of genuine ontological openness is more appropriate than attempts at foreclosing it, especially when these have so far failed to comprehensively and parsimoniously account for the phenomenology, therapeutic role, and biological mechanistic

basis of these largely ubiquitous and meaningful encounters. Before proposing a biologically and physically grounded mechanistic possibility to account for them, I emphasize three points.

The first, grounded in the indigenous anthropological record, is that the full range of cultures that have sustained systematic entheogenic inquiry, from the Mixtec curanderas of Oaxaca for whom the entheogen literally speaks[341], to the greatly diverse Amazonian ayahuasca traditions[170,321,342], has consistently reached the conclusion that entity encounters represent genuine contact with non-human others possessing healing intent and access to information unavailable through ordinary channels. These traditions represent long-term, internally rigorous empirical programs operating under conditions that systematically relax the materialist hyper-prior. Their convergent conclusion deserves epistemic respect that a reflexive dismissal of the non-Western cannot provide.

The second is the observation that the materialist prior is not a conclusion of physics, but rather an assumption maintained by the dominant cultural model of contemporary biomedical research. Within that context, it has been assigned high precision not because of direct evidence against field-level consciousness but because such content falls outside the dominant scientific paradigm[343]. Its cultural specificity is evident from its absence in virtually every other tradition that has practiced systematic entheogenic investigation. This does not establish that the materialist prior is correct or incorrect; rather, it suggests that treating it as epistemically necessary rather than historically contingent is a category error that would contradict a committedly empirical and honestly scientific stance.

The third and last observation is that the phenomenological pattern of entity encounters, with their invariant core and culturally shaped surface, is unique in that it is not predicted by either a constructivist account, which would predict greater variation in core features, nor by a

purely realist one, which would predict less variation in surface form. Rather, the actual pattern is precisely what would be expected if the experience is produced by a real substrate filtered through a culturally specific generative model.

The Field-Theoretic Possibility: Criticality, Stochastic Resonance, and the Perceptibility of Entities Inhabiting Field Consciousness

I propose that the framework of Sections 1-4 provides the precise physical, biological, and computational conditions under which a field-theoretic or quantum-level substrate of consciousness would become phenomenally accessible, with this accessibility being a direct consequence of the altered state's dynamics. The argument proceeds in two steps. The first concerns the ontology of consciousness itself and the second brings this into contact with the near-critical dynamics of Sections 1-4.

Field Theories of Consciousness

A family of scientifically serious proposals converges on the claim that phenomenal experience is not generated by neural computation per se but is rather underwritten by structured physical fields operating at scales the predictive processing hierarchy does not ordinarily model. Known as field theories of consciousness, they propose that the substrate of conscious experience is a continuous, multidimensional field rather than computation emerging from discrete, localized neural firings[344–346]. The most conservative of these locate consciousness in the brain's classic electromagnetic field. For example, McFadden's Conscious Electromagnetic

Information (CEMI) theory holds that synchronously firing neurons collectively generate an endogenous electromagnetic (EM) field that integrates distributed activity into a unified experience and feeds back to influence firing probabilities across the cortex, with the locus of consciousness being the field rather than the computations that produce it[347,348]. Similarly, Pockett's electromagnetic field theory of consciousness proposes that specific spatiotemporal EM field patterns constitute conscious states, such that altering the field geometry alters or eliminates experience[349].

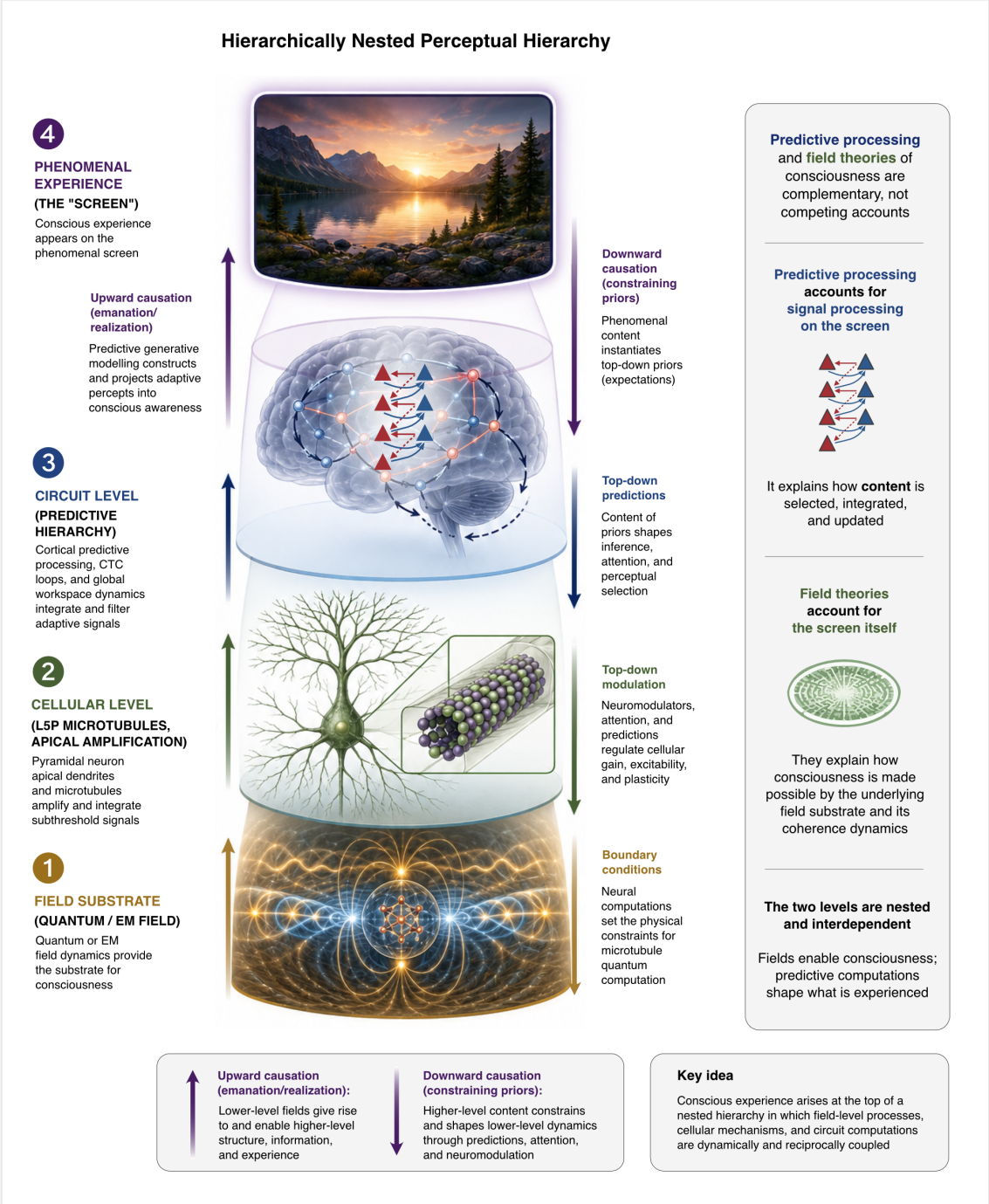


Figure 3.16: Hierarchically nested levels of the perceptual hierarchy.

Other noteworthy proposals depart from classical mechanics. Freeman and Vitiello[350], for example, show that large-scale cortical dynamics exhibit phase transitions and amplitude

modulation better described by dissipative quantum field theory than by classical nonlinear oscillation. Hameroff and Penrose's Orchestrated Objective Reduction (Orch OR) theory proposes quantum gravity events in the tubulin dimers of microtubules within the dendrites and soma of cortical layer 5 pyramidal (L5p) neurons–the same cells implicated in the circuits described in Sections 1 and 2–as the physical substrate of each moment of experience[351,352]. At the most fundamental pole of the field spectrum, Federico Faggin argues from the physics of information that consciousness is not a property that neurons generate but the intrinsic experiential dimension of quantum fields as such and thus a fundamental, irreducible, constitutive property of the universe[353]. In both Orch OR and in Faggin's theory of consciousness, the body functions as a quantum-classical bridge that translates quantum events into classically physical ones. Finally, bridging scales, Hunt and Schooler's Resonance Theory of Consciousness proposes that the richness of experience reflects the depth of resonant coupling across nested levels of oscillatory activity, such that broader cross-scale resonance corresponds to richer phenomenology[354].

These accounts diverge in mechanism, in the spatial scale of the relevant substrate, and in the degree to which quantum rather than classical field dynamics are involved. What they share, which is decisive for the present argument, is the implication that the predictive processing hierarchy is a macroscopic structure built upon a substrate with its own phenomenal properties. In other words, the computational and field or quantum levels of description are nested rather than competitive. Neuronal computations via predictive processing and free energy minimization may successfully describe experience in terms of prediction, precision, and free energy at a macro level, while leaving open the field-level or quantum-level properties of the substrate on which those computations run (Figure 3.16). Put differently, within most field theories of

consciousness, neural computations are a valid but incomplete description of the substrate generating phenomenal experience.

As an illustrative example of how this may be biologically instantiated in the case of Penrose and Hameroff's Orch OR theory, recall the role of layer 5 pyramidal (L5p) neurons presented in Sections 1 and 2 as encoding higher-level priors and issuing predictions downward to lower levels of the hierarchy. L5p neurons were introduced as the cells thought to hold and broadcast the brain's predictive model, with their basal dendrites receiving bottom-up sensory signals, their apical dendrites receiving top-down predictive and modulatory signals, and firing occurring when both inputs arrive simultaneously (apical amplification). Recall that apical amplification, which correlates with stimulus awareness thresholds, is blocked by GABAergic anesthetics. Moreover, L5p neurons innervate higher-order thalamic nuclei, which integrate convergent L5p prediction signals from many cortical areas, computes a context-informed posterior, and broadcasts it back to update sensory expectations by modulating the gain of superficial pyramidal cells.

Importantly, L5p cell bodies and dendrites also have the largest collection of mixed polarity microtubule networks, which the Orch OR theory takes to be the key to interference and scale-invariant processes involved in consciousness[355]. In short, the Orch OR theory proposes that qubits, made up of delocalized electrons in tubulin rings, form a unified, coherent quantum state across the neuron's microtubule network, with the quantum state being modulated by classical synaptic inputs, membrane potentials, and microtubule-associated proteins. When the accumulated quantum-gravitational threshold is reached, as per objective reduction, the quantum wave function collapses, producing a moment of conscious experience and altering the structural and electrostatic properties of the microtubule lattice, plus directly influencing classical synaptic

functions, including apical amplification and oscillatory rhythms[356]. Importantly, Hameroff proposes that the anti-parallel mixed polarity microtubules in L5p neurons oscillate at slightly different frequences to generate bottom-up interference patterns via reverse resonance that modulate the transition from dendritic-somatic integration to axonal firing[355].

While a comprehensive view integrating predictive processing with Orch OR is beyond the scope of this account, the underlying neurophysiology implicated by both theories coincides in L5p neurons at two complementary scales: Under Orch OR, consciousness emerges from the quantum collapse produced in the microtubule networks of the L5p cells that hold the organism's predictive generative model, which under predictive processing, is precisely what we consciously perceive. This convergence places L5p neurons at the locus of both the quantum-classical bridge and the bridge between the phenomenal emergence of conscious moments and their content. Under this model, the predictive apparatus, made up of the hierarchical, free energy minimizing generative model, sits on top of the intracellular quantum-biological substrate of conscious awareness, such that the single interconnected macroscopic quantum state formed by microtubules across the brain flows up from the quantum to the classical to produce conscious experience via an objective reduction collapse of the quantum wave function, while the contents of such a moment under normal conditions is set by the circuit-level classical predictive generative model.

While I remain consciousness theory agnostic, I take the general principle that the *substrate* of consciousness that the theories account for interacts with and incorporates the *contents* of consciousness from the hierarchical predictive processing architecture that lies hierarchically atop it. In other words, predictive processing, active inference, and free energy minimization do not amount to a theory of consciousness but rather account for the perceptual

architecture that processes afferent and intrinsic signals to generate the content of consciousness, which becomes available through perception. Drawing a simplified analogy, if consciousness describes a screen, predictive processing describes the signal processing that projects onto it (Figure 5.1).

Independently of how different theories might account for the emergence of consciousness, the mechanics of this emergence remain transparent to perception because they operate through processes or at scales that the predictive processing hierarchy does not ordinarily model. Under field theories of consciousness, quantum or EM field phenomena may underlie consciousness itself, yet we do not regularly perceive such field phenomena, firstly, because the predictive processing perceptual apparatus is optimized to encode the statistical and allostatic regularities that have proven adaptive rather than to provide a phenomenal readout of the world, and, secondly, because subtle quantum or EM-field phenomena would produce neural signals below the ordinary perceptual threshold unless they involved strong external stimulation, coherent ephaptic coupling, or a specialized receptor and amplification mechanism. The perceptual transparency to field phenomena (or lack thereof) therefore rests on the perceptual apparatus being calibrated on the allostatically relevant range of signals.

Next, this architecture is brought into contact with the near-critical physical and computational dynamics of Sections 1-4 to account for how numinous, noetic content, including entity experiences, may emerge when the predictive processing system becomes poised closer to the critical edge.

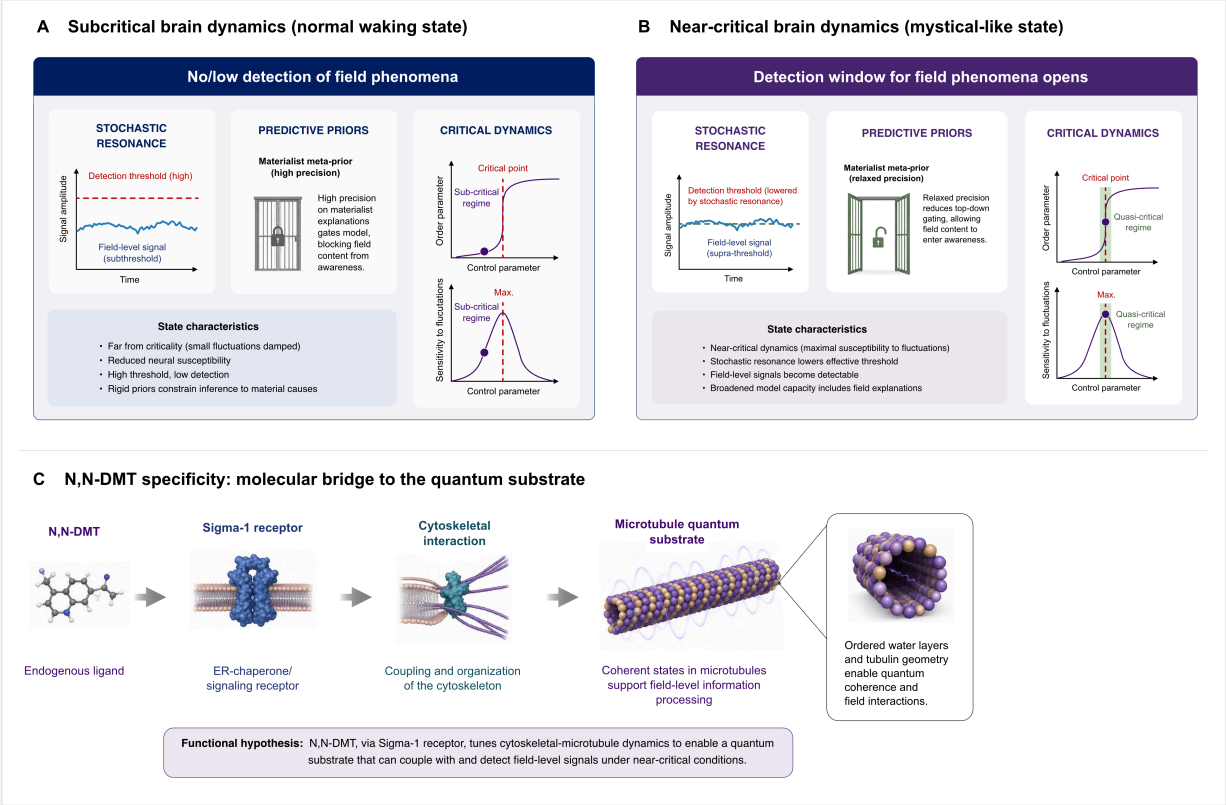


Figure 3.17: Field phenomena under subcritical (A) and near-critical (B) brain dynamics.

Field Phenomena Under Criticality and Stochastic Resonance

Recall that perception flows from a generative model that hierarchically subtracts precision-weighted descending priors and ascending prediction errors, and that a dynamic threshold, established by the relative precision weights of ascending and descending signals, determines whether the difference between them is large enough to justify sending the prediction error to the layer above or small enough for the descending prior to be accepted as adequately explaining away sense data and sent to the next stage of processing. From Sections 1-2, recall as well that this gain-modulated precision-weight-based threshold, which determines the relative influence of prediction versus prediction errors, covaries with the precision of specific

predictions or prediction errors and globally through the competition between excitatory and inhibitory neuronal populations modulated by attention, uncertainty, and exogenous 5-HT_{2A} agonists. Under the regime described in Section 4, whether because of 5-HT_{2A}-mediated L5p gain modulation, thalamocortical diffuse coupling, or metabolically mediated AMPAR conductance, the predictive hierarchy lowers its tolerance for prediction errors. The precision of priors vis-à-vis that of prediction errors decreases (prior relaxation), and prediction errors that ordinarily would have been explained away by descending priors now ascend the perceptual hierarchy and shape the posterior with higher probability. Such a system explains away a lower proportion of ascending sensory content and is more sensitized to ascending sensory signals. Whether this results in noisier perception devoid of meaning or in the ability to perceive subtle signals that would ordinarily have been explained away depends on whether meaningful subthreshold signals are there to begin with and on how a system in the near-critical regime can amplify and perceive them.

In the near-critical regime, marked by maximal stochastic resonance, collapsed prior precision, and peak susceptibility to low-amplitude scale-free signals, two conditions directly relevant to field-level detection are simultaneously realized (Figure 3.17A-B). First, stochastic resonance amplifies signals that ordinarily fall below the detection threshold of the predictive model. If the substrate of consciousness is carried by electromagnetic or quantum-level dynamics that constitute a real physical signal, the near-critical state is precisely the regime in which that signal would cross into the detectable range, a direct application of the formal result that criticality maximizes signal sensitivity across frequency bands[282,357]. Second, the relaxation of high-level prior precision simultaneously relaxes the meta-prior that there is nothing at this level to detect. Under normal waking conditions, the materialist meta-prior functions as a high-

precision constraint, assigning effectively zero model capacity to field-level perceptual content and fully explaining away any subtle signals consistent with it before they can propagate upward through the hierarchy. In the quasi-critical state, this meta-prior loses precision along with all others, and the detection window opens.

The argument is conditional yet parsimonious: If any of the field or quantum theories of consciousness is correct, and if consciousness has a substrate operating at scales below the predictive hierarchy, then the quasi-critical state describes not merely a high-entropy computational regime but a window onto a subtle stratum of physical reality that the predictive architecture normally occludes. This is not the claim that all entity encounters represent genuine contact with external conscious fields or disembodied autonomous entities; rather, it is the more defensible claim that the theoretical conditions for such contact are precisely those instantiated by the mystical state and that the null hypothesis, that field-level signals are absent or exactly zero, is not necessarily the more parsimonious explanation. Put simply, were subtle, immaterial, subthreshold field signals of autonomous entities present in a quantum or EM field constitutive of or accessible via consciousness, they would be filtered out by a sober-state perceptual system trained on higher amplitude signals, material reality percepts, and operating under a materialist meta-prior. A quasi-critical state maximally sensitive to small fluctuations and with relaxed prior precision, however, would parsimoniously account for their persistent, consistent, cross-cultural appearance during such states, for their phenomenologically invariant core and culturally shaped surface, and for the noetic quality of such encounters.

Suggestive molecular evidence extends this conditional to the pharmacological level (Figure 5.2C). Unlike psilocin, N,N-DMT is an endogenous sigma-1 receptor ligand[358], and sigma-1 receptors, located at mitochondria-associated membranes and endoplasmic reticulum-

mitochondria contact sites, interact directly with cytoskeletal proteins, modulating the intraneuronal architecture implicated by quantum consciousness accounts[359,360]. Separately, 5-HT_{2A} receptors form multi-receptor complexes at specific dendritic compartments with complex intracellular trafficking dynamics[361], and proteomic analyses show that DMT-containing compounds modulate cytoskeletal protein networks in ways extending well beyond synaptic pharmacology[359]. While not directly claiming that 5-HT_{2A} agonism directly modulates microtubule quantum coherence (the decoherence timescale objection to warm biological quantum processes remains a serious challenge[362]), I note that the pharmacological footprint of DMT reaches into the cytoskeletal domain that quantum theories identify as the relevant substrate, a footprint warranting dedicated experimental attention, and one that stands in striking complementarity to the consciousness-eliminating pharmacology of volatile anesthetics, which achieve their effect in part by binding tubulin at clinical concentrations[363]. I also draw attention to recent empirical work showing that microtubule stabilizer epothilone B delays volatile anesthetic-induced unconsciousness[364], supporting the notion that consciousness is a property of a neural microtubule quantum state. To my knowledge, this also constitutes the only existing explanation for why entity encounters are a hallmark of N,N-DMT and 5-MeO-DMT experiences and are significantly rarer under psilocybin and non-DMT psychedelics.

Complementary Theories of DMT Entities

My argument is complementary to Gómez-Emilsson's phenomenologically-grounded proposal that DMT increases the brain's ability to detect and maintain higher-order symmetries, causing phenomenal space to transition from approximately Euclidean to hyperbolic geometry, a

state in which relational structures that cannot be embedded in ordinary 3D space, including autonomous entities, can be experienced[365]. It is also complementary to Gallimore, Hermansson, and Hoffman's philosophically-grounded proposal that DMT transiently perturbs our perceptual interface by expanding the accessible experience space to allow normally imperceptible conscious agents to leave traces of themselves within the experience[366]. While Gómez-Emilsson's hyperbolic geometry describes the geometry of the altered experiential manifold, Gallimore, Hermansson, and Hoffman use conscious realism–the theory that consciousness, rather than physical matter, is fundamental, and that perception is an evolutionarily adapted interface and not reality itself–to argue for the possibility that real autonomous entities might interact outside of our sober perceptual interface. They provide crucial descriptions of the perceptual state induced by DMT and a principled theory for why perception might miss the entities to begin with, respectively, but they do not provide a biologically plausible mechanism for how psychedelics perturb the perceptual interface to make hyperbolic geometry and traces of higher-dimensional agents visible. The framework proposed here explicitly links the known pharmacologically induced neurophysiological changes under psychedelics to the specific perceptual state or interface in which the processes described by Gómez-Emilsson and Gallimore et al. occur.

Noumenal Content and the Challenge of Categorization

The framework advanced here generates one central implication–that at least some content of the mystical state may constitute genuinely noumenal input as opposed to hallucinatory content. While not directly claiming this to be the case, I draw attention to the

tenuous theoretical and empirical grounding of existing accounts of the entity phenomenon as compared to the parsimony of the account I present and the consistency of the phenomenological reports. The combination of a possible field theoretical substrate of consciousness with a quasi-critical perceptual apparatus presents the possibility of phenomenal experience whose true cause is not endogenous generative modeling but real physical structure at a level the predictive hierarchy does not ordinarily access. This is not the claim that all entity encounters represent such contact. The phenomenology is heterogeneous, with some encounters bearing clear marks of culturally specific symbolic elaboration, emotion-congruent content, and biographical resonance. Yet others bear what Meyer called the "reality signature": surprise, apparent autonomy, information content exceeding plausible endogenous generation, and convergence on the universal structural core (consciousness, intelligence, benevolence) that persists across cultural contexts[336]. We do not currently possess reliable methods for distinguishing these categories in individual reports, nor methods to verify (or disconfirm) field theories of consciousness. What the framework of Section 5 provides is the principled claim that the possibility is scientifically meaningful and empirically tractable under the right experimental conditions, and that treating it as inherently untractable is a choice, not a finding.

The history of cartography offers an appropriate analogy. Early modern maps populated ocean regions with sea monsters and fantastical creatures on exactly the same evidential footing as genuinely real but rarely observed animals. Massive whales and giant squid, creatures whose scale would have seemed no less implausible to observers whose prior experience included neither, were assumed to populate the oceans along with mermaids, aquatic unicorns, and ichthyocentaurs. The scientific resolution of those maps did not proceed by refusing to navigate the unmapped regions. It proceeded by developing methods capable of distinguishing which of

their contents were real and which were projections of the cartographer's imagination. Some of the fantastical creatures turned out to be real; most did not. If the conditions I lay out above turn out to be correct, then the entity encounter literature stands precisely in that position: A genuinely uncharted region populated by contents, some of which may prove to be endogenous projections of the cultural generative model and some of which may not. The theoretical framework of Section 5 does not resolve which is which. It specifies, with some precision, why this region exists, when it becomes accessible, and what physical and computational conditions would allow some of its contents to be real.

Interim Summary

This section distinguished the portions of mystical phenomenology that existing scientific frameworks successfully account for and those it does not. Emotional reprocessing, relief from physical and psychological pain, and epiphanic insight can all be attributed to the prior relaxation cascade, the primary active ingredients of psychedelic-assisted therapy as identified by the clinical literature. However, the numinous, noetic, and entity-encountering phenomenology that constitutes some of the most robustly reported and therapeutically significant features of these states are not well accounted for. Entity encounters are present in roughly half of inhaled N,N-DMT experiences, with entities described as conscious, intelligent, and benevolent by over ninety percent of respondents and as more real than ordinary reality by a majority. Entities exhibit a transcultural invariant deep structure with surface features shaped by cultural priors. Critically, numinous and noetic dimensions are the strongest predictors of lasting therapeutic benefit, making them mechanistically central rather than incidental.

Existing scientific explanations, including hyperactive agent-detection and neurognostic accounts, cannot explain why committed atheists have such experiences and find them credible enough to revise core metaphysical commitments. The most developed predictive processing account (Buck et al.) attributes entity encounters to supernatural-agent inferences recruited when the self-model collapses but agentive modeling persists, yet this misidentifies the phenomenology and fails to account for the N,N-DMT specificity: Entity encounters typically preserve a functioning self capable of intentional, bidirectional interaction with the entity, requiring exactly the self-model the account presumes dissolved. None of these accounts resolves the Comforting Delusion Problem, the clinical predicament that therapeutic efficacy may depend on a false belief.

Prefaced by the observation that the materialist prior is a historically contingent cultural assumption rather than a conclusion of physics, a field-theoretic explanation for the entity phenomenon is developed in two steps. First, several field theories of consciousness converge on the claim that phenomenal experience is underwritten by physical fields operating below the resolution of the predictive hierarchy, with computational-level descriptions nested within field-level ones. In the case of Orch OR specifically, L5p neurons, the primary locus of prior precision identified in Sections 1 and 2, also contain the mixed-polarity microtubule networks implicated as the quantum substrate of consciousness. Second, in the near-critical regime, stochastic resonance maximizes sensitivity to low-amplitude signals ordinarily below the detection threshold, while simultaneous relaxation of the materialist meta-prior opens model capacity to field-level content. If any field theory of consciousness is correct, the mystical state is precisely the regime in which its substrate would become phenomenally accessible. N,N-DMT's unique activity as a sigma-1 receptor ligand, a system interacting directly with cytoskeletal architecture,

offers additional molecular specificity, providing a principled explanation for why entity encounters are a specific hallmark of N,N-DMT phenomenology.

Conclusion

This paper began with the observation that three physiologically unrelated interventions, a serotonergic psychedelic, a self-directed attentional practice, and caloric restriction, reliably converge on the same richly structured and therapeutically potent state of consciousness. That convergence is not merely phenomenologically interesting. It is the kind of evidence that, in any other domain of biology, would be taken as decisive indication of a shared underlying mechanism. The principal contribution of Sections 1-4 has been to identify or propose that mechanism at multiple levels of description simultaneously: molecular (5-HT_{2A}-mediated sensitization of L5p cortical pyramidal neurons and disinhibition of higher-order thalamic relay nuclei), circuit (attentional modulation of core-to-matrix thalamocortical functional geometry and olfacto-limbic entrainment of interoceptive prior recalibration), metabolic (leptin-mediated AMPAR conductance reduction and differential destabilization of recurrent attractors in higher cortical areas), computational (precision-weighted relaxation of the predictive hierarchy and progressive recalibration of interoceptive priors), and physical (movement toward the edge-of-chaos critical regime where stochastic resonance, scale-free correlations, and computational irreducibility converge). The shared endpoint of all three routes is a transient window of expanded degrees of freedom in which the brain's generative model is sufficiently annealed for large-scale reorganization to occur. That window produces the experience known as the mystical-like state.

The most clinically significant finding encoded in this framework is that the experience is the mechanism. Across indications and compounds, it is the depth of the mystical state and not the drug dose, the number of meditation sessions, or the duration of the fast, that is the strongest predictor of lasting therapeutic benefit. This means that what heals is not a molecular correction of a neurochemical deficit but a structural reorganization of the generative model that is constituted by, and inseparable from, a subjective state. The therapeutic agent, properly understood, is not psilocybin, breathwork, or caloric restriction. It is the temporarily widened channel between levels of biological organization that all three elicit and the quality of what flows through it. Consciousness, intentionality, and belief are not epiphenomenal to this process. They are load-bearing variables of the mechanism itself, as empirically consequential as receptor occupancy or thalamocortical coupling geometry.

This has direct implications for the science of these interventions. The field has made rapid progress in characterizing the efficacy of psychedelic-assisted therapy and mindfulness-based interventions, and that progress is not to be minimized. But efficacy studies answer the narrowest of the available scientific questions. The theoretical frameworks developed here–diffuse coupling, OLIPR, MRCP, and their convergence on a shared near-critical computational endpoint–generate dozens of specific, falsifiable predictions at the molecular, circuit, network, behavioral, and phenomenological levels, the great majority of which remain untested. The experimental infrastructure now exists to test them: cell-type-specific calcium imaging, Neuropixels recordings with optotagging across cortical layers, high-resolution laminar EEG, MEG, and fMRI, intracranial recordings in clinical populations, within-subject pharmacological fasting-psychedelic crossing designs, longitudinal neuroimaging across meditation regimes. The

empirical program required to verify or falsify the mechanisms proposed here is demanding but tractable.

The field is also ready, I believe, for a bolder set of scientific questions that has so far been treated as peripheral or premature. If the experience is the medicine, then the question of what that experience actually is, and what it may be contacting, cannot be indefinitely deferred on grounds of scientific discomfort. Section 5 argued that field-theoretic proposals for the physical substrate of consciousness are not inconsistent with the framework developed here, and that the near-critical state instantiated by psychedelics, meditation, and fasting is precisely the state in which, if any such substrate exists, it would become perceptible. The numinous, noetic, and entity-encountering phenomenology that constitutes the most therapeutically active and least mechanistically explained feature of these states is not a curiosity to be set aside pending a more tractable research question. It *is* the research question. The convergent report, across thousands of individuals and dozens of cultures, of contact with something felt to be more real than ordinary waking reality and to possess healing intent is a datum that demands a scientific account commensurate with its consistency and its clinical consequences.

There is, moreover, a category of therapeutic outcome that may not be fully reducible to molecular or computational mechanism. Some of what heals in the psychedelic or contemplative encounter appears to involve a transformation in the patient's relationship to meaning, finitude, and the felt reality of connection–transformations that are phenomenologically and clinically real, and for which pharmacology does not have, and may not develop, an adequate account. This does not place such transformations outside science; it places them inside a science that takes seriously the mutually constitutive relationship between biology, computation, and experience. Understanding that relationship–not merely characterizing it at the level of correlates

but resolving it at the level of mechanism–is the larger scientific project toward which the present paper is a contribution.

The science of mystical states is at an inflection point analogous to the one at which the science of the unconscious stood in the early twentieth century: a large, consistent, and clinically significant body of phenomenological observation, insufficiently explained by existing mechanistic frameworks, pointing toward dimensions of biological organization that current scientific tools are only beginning to reach. The present paper has attempted to build a bridge between the molecular and the phenomenological, between the computational and the experiential, and between the clinical and the ontological. That bridge is not complete, and many of its spans remain empirically unsupported, but it is oriented toward a science that takes seriously the possibility that what the brain encounters in its deepest exploratory states is not merely a noise-amplified reflection of its own architecture, but something that was always there to be found.

Acknowledgments

Chapter 3 contains unpublished material and is currently being prepared for submission for publication of the material. The dissertation author was the sole author of this material.

REFERENCES

1. Halberstadt AL, Geyer MA. Multiple receptors contribute to the behavioral effects of indoleamine hallucinogens. Neuropharmacology. 2011;Serotonin: The New Wave61:364–81. doi:10.1016/j.neuropharm.2011.01.017

2. Madsen MK, Fisher PM, Burmester D, Dyssegaard A, Stenbæk DS, Kristiansen S, Johansen SS, Lehel S, Linnet K, Svarer C, Erritzoe D, Ozenne B, Knudsen GM. Psychedelic effects of psilocybin correlate with serotonin 2A receptor occupancy and plasma psilocin levels. Neuropsychopharmacology. 2019;44:1328–34. doi:10.1038/s41386-019-0324-9

3. López-Giménez JF, González-Maeso J. Hallucinogens and Serotonin 5-HT2A Receptor-Mediated Signaling Pathways. In: Halberstadt AL, Vollenweider FX, Nichols DE, editors. Behavioral Neurobiology of Psychedelic Drugs [Internet]. Berlin, Heidelberg: Springer; 2018 [cited 2025 Jul 4]. p. 45–73. Available from: https://doi.org/10.1007/7854_2017_478 doi:10.1007/7854_2017_478

4. Nichols DE. Psychedelics. Pharmacol Rev. 2016;68:264–355. doi:10.1124/pr.115.011478

5. Roth BL. 5-HT2A SEROTONIN RECEPTOR BIOLOGY: Interacting proteins, kinases and paradoxical regulation. Neuropharmacology. 2011;61:348–54. doi:10.1016/j.neuropharm.2011.01.012 PubMed PMID: 21288474; PubMed Central PMCID: PMC3110590.

6. Aghajanian GK, Marek GJ. Serotonin Induces Excitatory Postsynaptic Potentials in Apical Dendrites of Neocortical Pyramidal Cells. Neuropharmacology. 1997;36:589–99. doi:10.1016/S0028-3908(97)00051-8

7. Schmitz GP, Chiu YT, König GM, Kostenis E, Roth BL, Herman MA. Psychedelic compounds directly excite 5-HT2A Layer 5 Pyramidal Neurons in the Prefrontal Cortex through a 5-HT2A Gq -mediated activation mechanism [Internet]. bioRxiv; 2022 [cited 2025 Jul 14]. p. 2022.11.15.516655. Available from: https://www.biorxiv.org/content/10.1101/2022.11.15.516655v1 doi:10.1101/2022.11.15.516655

8. Kłodzinska A, Bijak M, Tokarski K, Pilc A. Group II mGlu receptor agonists inhibit behavioural and electrophysiological effects of DOI in mice. Pharmacol Biochem Behav. 2002;73:327–32. doi:10.1016/s0091-3057(02)00845-6 PubMed PMID: 12117586.

9. Riga MS, Soria G, Tudela R, Artigas F, Celada P. The natural hallucinogen 5-MeO-DMT, component of Ayahuasca, disrupts cortical function in rats: reversal by antipsychotic drugs. Int J Neuropsychopharmacol. 2014;17:1269–82. doi:10.1017/S1461145714000261

10. Marvan T, Polák M, Bachmann T, Phillips WA. Apical amplification-a cellular mechanism of conscious perception? Neurosci Conscious. 2021;2021:niab036. doi:10.1093/nc/niab036 PubMed PMID: 34650815; PubMed Central PMCID: PMC8511476.

11. Takahashi N, Ebner C, Sigl-Glöckner J, Moberg S, Nierwetberg S, Larkum ME. Active dendritic currents gate descending cortical outputs in perception. Nat Neurosci. 2020;23:1277–85. doi:10.1038/s41593-020-0677-8 PubMed PMID: 32747790.

12. Aru J, Suzuki M, Larkum ME. Cellular Mechanisms of Conscious Processing. Trends Cogn Sci. 2020;24:814–25. doi:10.1016/j.tics.2020.07.006 PubMed PMID: 32855048.

13. Aru J, Suzuki M, Rutiku R, Larkum ME, Bachmann T. Coupling the State and Contents of Consciousness. Front Syst Neurosci. 2019;13:43. doi:10.3389/fnsys.2019.00043 PubMed PMID: 31543762; PubMed Central PMCID: PMC6729974.

14. Harris KD, Mrsic-Flogel TD. Cortical connectivity and sensory coding. Nature. 2013;503:51–8. doi:10.1038/nature12654

15. Harris KD, Shepherd GMG. The neocortical circuit: themes and variations. Nat Neurosci. 2015;18:170–81. doi:10.1038/nn.3917

16. Marshel JH, Kim YS, Machado TA, Quirin S, Benson B, Kadmon J, Raja C, Chibukhchyan A, Ramakrishnan C, Inoue M, Shane JC, McKnight DJ, Yoshizawa S, Kato HE, Ganguli S, Deisseroth K. Cortical layer-specific critical dynamics triggering perception. Science. 2019;365:eaaw5202. doi:10.1126/science.aaw5202 PubMed PMID: 31320556; PubMed Central PMCID: PMC6711485.

17. Claar LD, Rembado I, Kuyat JR, Russo S, Marks LC, Olsen SR, Koch C. Cortico-thalamo-cortical interactions modulate electrically evoked EEG responses in mice. eLife. 2023;12:RP84630. doi:10.7554/eLife.84630 PubMed PMID: 37358562; PubMed Central PMCID: PMC10328504.

18. Whyte CJ, Redinbaugh MJ, Shine JM, Saalmann YB. Thalamic Contributions to the State and Contents of Consciousness. Neuron. 2024;112:1611–25. doi:10.1016/j.neuron.2024.04.019 PubMed PMID: 38754373; PubMed Central PMCID: PMC11537458.

19. Suzuki M, Larkum ME. General Anesthesia Decouples Cortical Pyramidal Neurons. Cell. 2020;180:666-676.e13. doi:10.1016/j.cell.2020.01.024 PubMed PMID: 32084339.

20. Muthukumaraswamy SD, Carhart-Harris RL, Moran RJ, Brookes MJ, Williams TM, Errtizoe D, Sessa B, Papadopoulos A, Bolstridge M, Singh KD, Feilding A, Friston KJ, Nutt DJ. Broadband Cortical Desynchronization Underlies the Human Psychedelic State. J Neurosci. 2013;33:15171–83. doi:10.1523/JNEUROSCI.2063-13.2013 PubMed PMID: 24048847.

21. Carhart-Harris RL, Muthukumaraswamy S, Roseman L, Kaelen M, Droog W, Murphy K, Tagliazucchi E, Schenberg EE, Nest T, Orban C, Leech R, Williams LT, Williams TM, Bolstridge M, Sessa B, McGonigle J, Sereno MI, Nichols D, Hellyer PJ, Hobden P, Evans J, Singh KD, Wise RG, Curran HV, Feilding A, Nutt DJ. Neural correlates of the LSD experience revealed by multimodal neuroimaging. Proc Natl Acad Sci. 2016;113:4853–8. doi:10.1073/pnas.1518377113

22. Celada P, Puig MV, Díaz-Mataix L, Artigas F. The hallucinogen DOI reduces low-frequency oscillations in rat prefrontal cortex: reversal by antipsychotic drugs. Biol Psychiatry. 2008;64:392–400. doi:10.1016/j.biopsych.2008.03.013 PubMed PMID: 18436196.

23. Mayer A, Schwiedrzik CM, Wibral M, Singer W, Melloni L. Expecting to See a Letter: Alpha Oscillations as Carriers of Top-Down Sensory Predictions. Cereb Cortex N Y N 1991. 2016;26:3146–60. doi:10.1093/cercor/bhv146 PubMed PMID: 26142463.

24. Fries P. Rhythms for Cognition: Communication through Coherence. Neuron. 2015;88:220–35. doi:10.1016/j.neuron.2015.09.034 PubMed PMID: 26447583.

25. Mantini D, Perrucci MG, Del Gratta C, Romani GL, Corbetta M. Electrophysiological signatures of resting state networks in the human brain. Proc Natl Acad Sci U S A. 2007;104:13170–5. doi:10.1073/pnas.0700668104 PubMed PMID: 17670949; PubMed Central PMCID: PMC1941820.

26. Iemi L, Gwilliams L, Samaha J, Auksztulewicz R, Cycowicz YM, King JR, Nikulin VV, Thesen T, Doyle W, Devinsky O, Schroeder CE, Melloni L, Haegens S. Ongoing neural oscillations influence behavior and sensory representations by suppressing neuronal excitability. NeuroImage. 2022;247:118746. doi:10.1016/j.neuroimage.2021.118746

27. Friston K. The free-energy principle: a unified brain theory? Nat Rev Neurosci. 2010;11:127–38. doi:10.1038/nrn2787

28. Clark A. A nice surprise? Predictive processing and the active pursuit of novelty. Phenomenol Cogn Sci. 2018;17:521–34. doi:10.1007/s11097-017-9525-z

29. Bastos AM, Usrey WM, Adams RA, Mangun GR, Fries P, Friston KJ. Canonical microcircuits for predictive coding. Neuron. 2012;76:695–711. doi:10.1016/j.neuron.2012.10.038 PubMed PMID: 23177956; PubMed Central PMCID: PMC3777738.

30. Rikhye RV, Wimmer RD, Halassa MM. Toward an Integrative Theory of Thalamic Function. Annu Rev Neurosci. 2018;41:163–83. doi:10.1146/annurev-neuro-080317-062144 PubMed PMID: 29618284.

31. Kanai R, Komura Y, Shipp S, Friston K. Cerebral hierarchies: predictive processing, precision and the pulvinar. Philos Trans R Soc B Biol Sci. 2015;370:20140169. doi:10.1098/rstb.2014.0169

32. Luu P, Tucker DM, Friston K. From active affordance to active inference: vertical integration of cognition in the cerebral cortex through dual subcortical control systems. Cereb Cortex N Y N 1991. 2024;34:bhad458. doi:10.1093/cercor/bhad458 PubMed PMID: 38044461.

33. Jiang J, Summerfield C, Egner T. Attention sharpens the distinction between expected and unexpected percepts in the visual brain. J Neurosci Off J Soc Neurosci. 2013;33:18438–47. doi:10.1523/JNEUROSCI.3308-13.2013 PubMed PMID: 24259568; PubMed Central PMCID: PMC3834051.

34. Matias S, Lottem E, Dugué GP, Mainen ZF. Activity patterns of serotonin neurons underlying cognitive flexibility. Gold JI, editor. eLife. 2017;6:e20552. doi:10.7554/eLife.20552

35. Feldman H, Friston KJ. Attention, uncertainty, and free-energy. Front Hum Neurosci. 2010;4:215. doi:10.3389/fnhum.2010.00215 PubMed PMID: 21160551; PubMed Central PMCID: PMC3001758.

36. Kosciessa JQ, Lindenberger U, Garrett DD. Thalamocortical excitability modulation guides human perception under uncertainty. Nat Commun. 2021;12:2430. doi:10.1038/s41467-021-22511-7

37. Carhart-Harris RL, Friston KJ. REBUS and the Anarchic Brain: Toward a Unified Model of the Brain Action of Psychedelics. Pharmacol Rev. 2019;71:316–44. doi:10.1124/pr.118.017160 PubMed PMID: 31221820.

38. Monckton JE, McCormick DA. Neuromodulatory Role of Serotonin in the Ferret Thalamus. J Neurophysiol. 2002;87:2124–36. doi:10.1152/jn.00650.2001

39. Wai MSM, Lorke DE, Kwong WH, Zhang L, Yew DT. Profiles of serotonin receptors in the developing human thalamus. Psychiatry Res. 2011;185:238–42. doi:10.1016/j.psychres.2010.05.003

40. Gaddis A, Lidstone DE, Nebel MB, Griffiths RR, Mostofsky SH, Mejia AF, Barrett FS. Psilocybin induces spatially constrained alterations in thalamic functional organizaton and connectivity. NeuroImage. 2022;260:119434. doi:10.1016/j.neuroimage.2022.119434

41. Inserra A, De Gregorio D, Rezai T, Lopez-Canul MG, Comai S, Gobbi G. Lysergic acid diethylamide differentially modulates the reticular thalamus, mediodorsal thalamus, and infralimbic prefrontal cortex: An in vivo electrophysiology study in male mice. J Psychopharmacol (Oxf). 2021;35:469–82. doi:10.1177/0269881121991569

42. Shine JM. Neuromodulatory control of complex adaptive dynamics in the brain. Interface Focus. 2023;13:20220079. doi:10.1098/rsfs.2022.0079

43. Toker D, Pappas I, Lendner JD, Frohlich J, Mateos DM, Muthukumaraswamy S, Carhart-Harris R, Paff M, Vespa PM, Monti MM, Sommer FT, Knight RT, D'Esposito M. Consciousness is supported by near-critical slow cortical electrodynamics. Proc Natl Acad Sci. 2022;119. doi:10.1073/pnas.2024455119 PubMed PMID: 35145021.

44. Atasoy S, Roseman L, Kaelen M, Kringelbach ML, Deco G, Carhart-Harris RL. Connectome-harmonic decomposition of human brain activity reveals dynamical repertoire re-organization under LSD. Nat Sci Rep. 2017;7:1–18. doi:10.1038/s41598-017-17546-0

45. Viol A, Palhano-Fontes F, Onias H, de Araujo DB, Viswanathan GM. Shannon entropy of brain functional complex networks under the influence of the psychedelic Ayahuasca. Sci Rep. 2017;7:1. doi:10.1038/s41598-017-06854-0

46. Buzsaki G. Rhythms of the Brain. Oxford University Press; 2006. 465 p.

47. Tognoli E, Kelso JAS. The Metastable Brain. Neuron. 2014;81:35–48. doi:10.1016/j.neuron.2013.12.022 PubMed PMID: 24411730; PubMed Central PMCID: PMC3997258.

48. Shew WL, Yang H, Yu S, Roy R, Plenz D. Information capacity and transmission are maximized in balanced cortical networks with neuronal avalanches. J Neurosci Off J Soc Neurosci. 2011;31:55–63. doi:10.1523/JNEUROSCI.4637-10.2011 PubMed PMID: 21209189; PubMed Central PMCID: PMC3082868.

49. Li M, Han Y, Aburn MJ, Breakspear M, Poldrack RA, Shine JM, Lizier JT. Transitions in information processing dynamics at the whole-brain network level are driven by alterations in neural gain. PLOS Comput Biol. 2019;15:e1006957. doi:10.1371/journal.pcbi.1006957

50. Carhart-Harris RL, Erritzoe D, Williams T, Stone JM, Reed LJ, Colasanti A, Tyacke RJ, Leech R, Malizia AL, Murphy K, Hobden P, Evans J, Feilding A, Wise RG, Nutt DJ. Neural correlates of the psychedelic state as determined by fMRI studies with psilocybin. Proc Natl Acad Sci. 2012;109:2138–43. doi:10.1073/pnas.1119598109

51. Barrett LF, Simmons WK. Interoceptive predictions in the brain. Nat Rev Neurosci. 2015;16:419–29. doi:10.1038/nrn3950 PubMed PMID: 26016744; PubMed Central PMCID: PMC4731102.

52. Kleckner IR, Zhang J, Touroutoglou A, Chanes L, Xia C, Simmons WK, Quigley KS, Dickerson BC, Barrett LF. Evidence for a Large-Scale Brain System Supporting Allostasis and Interoception in Humans. Nat Hum Behav. 2017;1:0069. doi:10.1038/s41562-017-0069 PubMed PMID: 28983518; PubMed Central PMCID: PMC5624222.

53. Carhart-Harris RL, Leech R, Hellyer PJ, Shanahan M, Feilding A, Tagliazucchi E, Chialvo DR, Nutt D. The entropic brain: a theory of conscious states informed by neuroimaging research with psychedelic drugs. Front Hum Neurosci. 2014;8. doi:10.3389/fnhum.2014.00020

54. Carhart-Harris RL. The entropic brain - revisited. Neuropharmacology. 2018;Psychedelics: New Doors, Altered Perceptions142:167–78. doi:10.1016/j.neuropharm.2018.03.010

55. Shao LX, Liao C, Gregg I, Davoudian PA, Savalia NK, Delagarza K, Kwan AC. Psilocybin induces rapid and persistent growth of dendritic spines in frontal cortex in vivo. Neuron. 2021;109:2535-2544.e4. doi:10.1016/j.neuron.2021.06.008 PubMed PMID: 34228959; PubMed Central PMCID: PMC8376772.

56. Ly C, Greb AC, Cameron LP, Wong JM, Barragan EV, Wilson PC, Burbach KF, Soltanzadeh Zarandi S, Sood A, Paddy MR, Duim WC, Dennis MY, McAllister AK, Ori-McKenney KM, Gray JA, Olson DE. Psychedelics Promote Structural and Functional Neural Plasticity. Cell Rep. 2018;23:3170–82. doi:10.1016/j.celrep.2018.05.022 PubMed PMID: 29898390; PubMed Central PMCID: PMC6082376.

57. Moliner R, Girych M, Brunello CA, Kovaleva V, Biojone C, Enkavi G, Antenucci L, Kot EF, Goncharuk SA, Kaurinkoski K, Kuutti M, Fred SM, Elsilä LV, Sakson S, Cannarozzo C, Diniz CRAF, Seiffert N, Rubiolo A, Haapaniemi H, Meshi E, Nagaeva E, Öhman T, Róg T, Kankuri E, Vilar M, Varjosalo M, Korpi ER, Permi P, Mineev KS, Saarma M, Vattulainen I, Casarotto PC, Castrén E. Psychedelics promote plasticity by directly binding to BDNF receptor TrkB. Nat Neurosci. 2023;26:1032–41. doi:10.1038/s41593-023-01316-5

58. Hatzipantelis CJ, Olson DE. The Effects of Psychedelics on Neuronal Physiology. Annu Rev Physiol. 2024;86:27–47. doi:10.1146/annurev-physiol-042022-020923

59. Vargas MV, Dunlap LE, Dong C, Carter SJ, Tombari RJ, Jami SA, Cameron LP, Patel SD, Hennessey JJ, Saeger HN, McCorvy JD, Gray JA, Tian L, Olson DE. Psychedelics promote neuroplasticity through the activation of intracellular 5-HT2A receptors. Science. 2023;379:700–6. doi:10.1126/science.adf0435

60. Kato K, Kleinhenz JM, Shin YJ, Coarfa C, Zarrabi AJ, Hecker L. Psilocybin treatment extends cellular lifespan and improves survival of aged mice. Npj Aging. 2025;11:55. doi:10.1038/s41514-025-00244-x

61. Tang YY, Hölzel BK, Posner MI. The neuroscience of mindfulness meditation. Nat Rev Neurosci. 2015;16:213–25. doi:10.1038/nrn3916 PubMed PMID: 25783612.

62. Dahl CJ, Lutz A, Davidson RJ. Reconstructing and deconstructing the self: Cognitive mechanisms in meditation practice. Trends Cogn Sci. 2015;19:515–23.

doi:10.1016/j.tics.2015.07.001 PubMed PMID: 26231761; PubMed Central PMCID: PMC4595910.

63. Greenwell B. Energies of Transformation: A Guide to the Kundalini Process. Motilal Banarsidass Publishe; 2002. 354 p.

64. Krishna G. Kundalini: The Evolutionary Energy in Man. Shambhala Publications; 2018. 308 p.

65. Millière R, Carhart-Harris RL, Roseman L, Trautwein FM, Berkovich-Ohana A. Psychedelics, Meditation, and Self-Consciousness. Front Psychol. 2018;9. doi:10.3389/fpsyg.2018.01475

66. Eliade M. Shamanism: Archaic Techniques of Ecstasy. Princeton University Press; 2020. 643 p.

67. Escohotado A. Historia general de las drogas: completada por el apéndice fenomenología de las drogas. Espasa; 1999. 1544 p.

68. Grof S, Grof C. Holotropic Breathwork, Second Edition: A New Approach to Self-Exploration and Therapy [Internet]. State University of New York Press; 2023 [cited 2025 Dec 23]. Available from: https://www.jstor.org/stable/jj.18253967 doi:10.2307/jj.18253967

69. Millière R, Carhart-Harris RL, Roseman L, Trautwein FM, Berkovich-Ohana A. Psychedelics, Meditation, and Self-Consciousness. Front Psychol. 2018;9:1475. doi:10.3389/fpsyg.2018.01475 PubMed PMID: 30245648; PubMed Central PMCID: PMC6137697.

70. Egger K, Meling D, Polat F, Seifritz E, Avram M, Scheidegger M. Meditation, psychedelics, and brain connectivity: A randomized controlled resting-state fMRI study of N,N-dimethyltryptamine and harmine in a meditation retreat. Imaging Neurosci. 2025;3:IMAG.a.907. doi:10.1162/IMAG.a.907

71. Singer B, Meling D, Hirsch-Hoffmann M, Michels L, Kometer M, Smigielski L, Dornbierer D, Seifritz E, Vollenweider FX, Scheidegger M. Psilocybin enhances insightfulness in meditation: a perspective on the global topology of brain imaging during meditation. Sci Rep. 2024;14:7211. doi:10.1038/s41598-024-55726-x

72. Atad DA, Mediano PAM, Rosas FE, Berkovich-Ohana A. Meditation and complexity: a review and synthesis of evidence. Neurosci Conscious. 2025;2025:niaf013. doi:10.1093/nc/niaf013

73. Atasoy S, Escrichs A, Stark E, Terry KGM, Camara E, Sanjuan A, Chandaria S, Deco G, Kringelbach ML. The meditative brain: State and trait changes in harmonic complexity for long-term mindfulness meditators [Internet]. bioRxiv; 2023 [cited 2025 Sep 25]. p.

2023.11.16.567347. Available from: https://www.biorxiv.org/content/10.1101/2023.11.16.567347v1 doi:10.1101/2023.11.16.567347

74. Kakumanu RJ, Nair AK, Venugopal R, Sasidharan A, Ghosh PK, John JP, Mehrotra S, Panth R, Kutty BM. Dissociating meditation proficiency and experience dependent EEG changes during traditional Vipassana meditation practice. Biol Psychol. 2018;135:65–75. doi:10.1016/j.biopsycho.2018.03.004

75. Martínez Vivot R, Pallavicini C, Zamberlan F, Vigo D, Tagliazucchi E. Meditation Increases the Entropy of Brain Oscillatory Activity. Neuroscience. 2020;431:40–51. doi:10.1016/j.neuroscience.2020.01.033 PubMed PMID: 32032666.

76. Kumar GP, Sharma K, Ramakrishnan AG, Adarsh A. Increased Entropy of Gamma Oscillations in the Frontal Region during Meditation. Annu Int Conf IEEE Eng Med Biol Soc IEEE Eng Med Biol Soc Annu Int Conf. 2021;2021:787–90. doi:10.1109/EMBC46164.2021.9629633 PubMed PMID: 34891408.

77. Pascarella A, Thölke P, Meunier D, O'Byrne J, Lajnef T, Raffone A, Guidotti R, Pizzella V, Marzetti L, Jerbi K. Meditation induces shifts in neural oscillations, brain complexity, and critical dynamics: novel insights from MEG. Neurosci Conscious. 2025;2025:niaf047. doi:10.1093/nc/niaf047 PubMed PMID: 41287816; PubMed Central PMCID: PMC12640546.

78. Cahn BR, Goodman MS, Peterson CT, Maturi R, Mills PJ. Yoga, Meditation and Mind-Body Health: Increased BDNF, Cortisol Awakening Response, and Altered Inflammatory Marker Expression after a 3-Month Yoga and Meditation Retreat. Front Hum Neurosci. 2017;11:315. doi:10.3389/fnhum.2017.00315 PubMed PMID: 28694775; PubMed Central PMCID: PMC5483482.

79. Garrison KA, Zeffiro TA, Scheinost D, Constable RT, Brewer JA. Meditation leads to reduced default mode network activity beyond an active task. Cogn Affect Behav Neurosci. 2015;15:712–20. doi:10.3758/s13415-015-0358-3 PubMed PMID: 25904238; PubMed Central PMCID: PMC4529365.

80. Garrison K, Santoyo J, Davis J, Thornhill T, Kerr C, Brewer J. Effortless awareness: using real time neurofeedback to investigate correlates of posterior cingulate cortex activity in meditators' self-report. Front Hum Neurosci. 2013;7. doi:10.3389/fnhum.2013.00440

81. Carhart-Harris RL, Erritzoe D, Williams T, Stone JM, Reed LJ, Colasanti A, Tyacke RJ, Leech R, Malizia AL, Murphy K, Hobden P, Evans J, Feilding A, Wise RG, Nutt DJ. Neural correlates of the psychedelic state as determined by fMRI studies with psilocybin. Proc Natl Acad Sci U S A. 2012;109:2138–43. doi:10.1073/pnas.1119598109 PubMed PMID: 22308440; PubMed Central PMCID: PMC3277566.

82. Carhart-Harris RL, Leech R, Erritzoe D, Williams TM, Stone JM, Evans J, Sharp DJ, Feilding A, Wise RG, Nutt DJ. Functional connectivity measures after psilocybin inform a novel hypothesis of early psychosis. Schizophr Bull. 2013;39:1343–51. doi:10.1093/schbul/sbs117 PubMed PMID: 23044373; PubMed Central PMCID: PMC3796071.

83. Josipovic Z. Neural correlates of nondual awareness in meditation. Ann N Y Acad Sci. 2014;1307:9–18. doi:10.1111/nyas.12261

84. Duda AT, Clarke AR, Barry RJ, De Blasio FM. Mindfulness meditation alters alpha amplitude without affecting arousal. Int J Psychophysiol Off J Int Organ Psychophysiol. 2025;214:113197. doi:10.1016/j.ijpsycho.2025.113197 PubMed PMID: 40523405.

85. Corcoran AW, Pezzulo G, Hohwy J. From allostatic agents to counterfactual cognisers: active inference, biological regulation, and the origins of cognition. Biol Philos. 2020;35:32. doi:10.1007/s10539-020-09746-2

86. Laukkonen RE, Slagter HA. From many to (n)one: Meditation and the plasticity of the predictive mind. Neurosci Biobehav Rev. 2021;128:199–217. doi:10.1016/j.neubiorev.2021.06.021

87. Mukherjee A, Lam NH, Wimmer RD, Halassa MM. Thalamic circuits for independent control of prefrontal signal and noise. Nature. 2021;1–5. doi:10.1038/s41586-021-04056-3

88. Wimmer RD, Schmitt LI, Davidson TJ, Nakajima M, Deisseroth K, Halassa MM. Thalamic control of sensory selection in divided attention. Nature. 2015;526:705–9. doi:10.1038/nature15398

89. Jones EG. Thalamic circuitry and thalamocortical synchrony. Philos Trans R Soc Lond B Biol Sci. 2002;357:1659–73. Located at: PubMed; 12626002. doi:10.1098/rstb.2002.1168

90. Fischer J, Whitney D. Attention gates visual coding in the human pulvinar. Nat Commun. 2012;3:1051. doi:10.1038/ncomms2054

91. Komura Y, Nikkuni A, Hirashima N, Uetake T, Miyamoto A. Responses of pulvinar neurons reflect a subject's confidence in visual categorization. Nat Neurosci. 2013;16:749–55. doi:10.1038/nn.3393 PubMed PMID: 23666179.

92. Shipp S. The brain circuitry of attention. Trends Cogn Sci. 2004;8:223–30. doi:10.1016/j.tics.2004.03.004 PubMed PMID: 15120681.

93. Saalmann YB, Pinsk MA, Wang L, Li X, Kastner S. The pulvinar regulates information transmission between cortical areas based on attention demands. Science. 2012;337:753–6. doi:10.1126/science.1223082 PubMed PMID: 22879517; PubMed Central PMCID: PMC3714098.

94. Saalmann YB, Kastner S. Gain control in the visual thalamus during perception and cognition. Curr Opin Neurobiol. 2009;19:408–14. doi:10.1016/j.conb.2009.05.007 PubMed PMID: 19556121; PubMed Central PMCID: PMC3140205.

95. Lam NH, Mukherjee A, Wimmer RD, Nassar MR, Chen ZS, Halassa MM. Prefrontal transthalamic uncertainty processing drives flexible switching. Nature. 2025;637:127–36. doi:10.1038/s41586-024-08180-8

96. Gao R, Peterson EJ, Voytek B. Inferring synaptic excitation/inhibition balance from field potentials. NeuroImage. 2017;158:70–8. doi:10.1016/j.neuroimage.2017.06.078 PubMed PMID: 28676297.

97. Buzsaki G. Rhythms of the Brain. Oxford University Press; 2006. 466 p.

98. Müller EJ, Munn BR, Shine JM. Diffuse neural coupling mediates complex network dynamics through the formation of quasi-critical brain states. Nat Commun. 2020;11:6337. doi:10.1038/s41467-020-19716-7

99. Feldman H, Friston K. Attention, Uncertainty, and Free-Energy. Front Hum Neurosci. 2010;4. doi:10.3389/fnhum.2010.00215

100. Mateos DM, Guevara Erra R, Wennberg R, Perez Velazquez JL. Measures of entropy and complexity in altered states of consciousness. Cogn Neurodyn. 2018;12:73–84. doi:10.1007/s11571-017-9459-8

101. Fuentes N, Garcia A, Guevara R, Orofino R, Mateos DM. Complexity of Brain Dynamics as a Correlate of Consciousness in Anaesthetized Monkeys. Neuroinformatics. 2022;20:1041–54. doi:10.1007/s12021-022-09586-3

102. Aru J, Suzuki M, Larkum ME. Cellular Mechanisms of Conscious Processing. Trends Cogn Sci. 2020;24:814–25. doi:10.1016/j.tics.2020.07.006 PubMed PMID: 32855048.

103. Huang Z, Mashour GA, Hudetz AG. Propofol disrupts the functional core-matrix architecture of the thalamus in humans. Nat Commun. 2024;15:7496. doi:10.1038/s41467-024-51837-1

104. Bishop SR, Lau M, Shapiro S, Carlson L, Anderson ND, Carmody J, Segal ZV, Abbey S, Speca M, Velting D, Devins G. Mindfulness: A proposed operational definition. Clin Psychol Sci Pract. 2004;11:230–41. doi:10.1093/clipsy.bph077

105. Lutz A, Slagter HA, Dunne JD, Davidson RJ. Attention regulation and monitoring in meditation. Trends Cogn Sci. 2008;12:163–9. doi:10.1016/j.tics.2008.01.005 PubMed PMID: 18329323; PubMed Central PMCID: PMC2693206.

106. Lutz A, Mattout J, Pagnoni G. The epistemic and pragmatic value of non-action: a predictive coding perspective on meditation. Curr Opin Psychol. 2019;Mindfulness28:166–71. doi:10.1016/j.copsyc.2018.12.019

107. Analayo, Kabat-Zinn J. Mindfulness of Breathing: A Practice Guide and Translations. Windhorse Publications. 288 p.

108. Bodhi B. What Does Mindfulness Really Mean? A Canonical Perspective. Contemp Buddhism. 2011;12:19–39. doi:10.1080/14639947.2011.564813

109. Calderone DJ, Lakatos P, Butler PD, Castellanos FX. Entrainment of neural oscillations as a modifiable substrate of attention. Trends Cogn Sci. 2014;18:300–9. doi:10.1016/j.tics.2014.02.005 PubMed PMID: 24630166; PubMed Central PMCID: PMC4037370.

110. Besle J, Schevon CA, Mehta AD, Lakatos P, Goodman RR, McKhann GM, Emerson RG, Schroeder CE. Tuning of the Human Neocortex to the Temporal Dynamics of Attended Events. J Neurosci. 2011;31:3176–85. doi:10.1523/JNEUROSCI.4518-10.2011 PubMed PMID: 21368029.

111. Lakatos P, Karmos G, Mehta AD, Ulbert I, Schroeder CE. Entrainment of Neuronal Oscillations as a Mechanism of Attentional Selection. Science. 2008;320:110–3. doi:10.1126/science.1154735

112. Graaf TA de, Gross J, Paterson G, Rusch T, Sack AT, Thut G. Alpha-Band Rhythms in Visual Task Performance: Phase-Locking by Rhythmic Sensory Stimulation. PLOS ONE. 2013;8:e60035. doi:10.1371/journal.pone.0060035

113. Bauer M, Stenner MP, Friston KJ, Dolan RJ. Attentional Modulation of Alpha/Beta and Gamma Oscillations Reflect Functionally Distinct Processes. J Neurosci. 2014;34:16117–25. doi:10.1523/JNEUROSCI.3474-13.2014 PubMed PMID: 25429152.

114. Boiten FA. The effects of emotional behaviour on components of the respiratory cycle. Biol Psychol. 1998;49:29–51. doi:10.1016/S0301-0511(98)00025-8

115. Miyamoto T, Sotobayashi D, Ito G, Kawai E, Nakahara H, Ueda S, Toyama T, Saku K, Nakanishi Y, Kinoshita H. Physiological role of anticipatory cardiorespiratory responses to exercise. Physiol Rep. 2022;10:e15210. doi:10.14814/phy2.15210 PubMed PMID: 35246949; PubMed Central PMCID: PMC8897741.

116. Zelano C, Jiang H, Zhou G, Arora N, Schuele S, Rosenow J, Gottfried JA. Nasal Respiration Entrains Human Limbic Oscillations and Modulates Cognitive Function. J Neurosci. 2016;36:12448–67. doi:10.1523/JNEUROSCI.2586-16.2016 PubMed PMID: 27927961.

117. Allen M, Tsakiris M. The body as first prior: Interoceptive predictive processing and the primacy of self-models. In: Tsakiris M, De Preester H, editors. The Interoceptive Mind: From Homeostasis to Awareness [Internet]. Oxford University Press; 2018 [cited 2026 Apr 3]. p. 0. Available from: https://doi.org/10.1093/oso/9780198811930.003.0002 doi:10.1093/oso/9780198811930.003.0002

118. Seth AK, Critchley HD. Extending predictive processing to the body: Emotion as interoceptive inference. Behav Brain Sci. 2013;36:227–8. doi:10.1017/S0140525X12002270

119. Barrett LF. The theory of constructed emotion: an active inference account of interoception and categorization. Soc Cogn Affect Neurosci. 2017;12:1–23. doi:10.1093/scan/nsw154

120. McClay M, Sachs ME, Clewett D. Dynamic emotional states shape the episodic structure of memory. Nat Commun. 2023;14:6533. doi:10.1038/s41467-023-42241-2 PubMed PMID: 37848429; PubMed Central PMCID: PMC10582075.

121. Poppa T, Bechara A. The somatic marker hypothesis: revisiting the role of the 'body-loop' in decision-making. Curr Opin Behav Sci. 2018;Emotion-cognition interactions19:61–6. doi:10.1016/j.cobeha.2017.10.007

122. Kensinger EA, Fields E. Affective Memory. In: Kahana MJ, Wagner AD, editors. The Oxford Handbook of Human Memory, Two Volume Pack: Foundations and Applications [Internet]. Oxford University Press; 2024 [cited 2026 Feb 13]. p. 0. Available from: https://doi.org/10.1093/oxfordhb/9780190917982.013.20 doi:10.1093/oxfordhb/9780190917982.013.20

123. Sirota A, Montgomery S, Fujisawa S, Isomura Y, Zugaro M, Buzsáki G. Entrainment of neocortical neurons and gamma oscillations by the hippocampal theta rhythm. Neuron. 2008;60:683–97. doi:10.1016/j.neuron.2008.09.014 PubMed PMID: 19038224; PubMed Central PMCID: PMC2640228.

124. Gattas S, Larson MS, Mnatsakanyan L, Sen-Gupta I, Vadera S, Swindlehurst AL, Rapp PE, Lin JJ, Yassa MA. Theta mediated dynamics of human hippocampal-neocortical learning systems in memory formation and retrieval. Nat Commun. 2023;14:8505. doi:10.1038/s41467-023-44011-6

125. Roehri N, Bréchet L, Seeber M, Pascual-Leone A, Michel CM. Phase-Amplitude Coupling and Phase Synchronization Between Medial Temporal, Frontal and Posterior Brain Regions Support Episodic Autobiographical Memory Recall. Brain Topogr. 2022;35:191–206. doi:10.1007/s10548-022-00890-4 PubMed PMID: 35080692; PubMed Central PMCID: PMC8860804.

126. Hanslmayr S, Staudigl T, Fellner MC. Oscillatory power decreases and long-term memory: the information via desynchronization hypothesis. Front Hum Neurosci.

2012;6:74. doi:10.3389/fnhum.2012.00074 PubMed PMID: 22514527; PubMed Central PMCID: PMC3322486.

127. Heinbockel H, Quaedflieg CWEM, Schneider TR, Engel AK, Schwabe L. Stress enhances emotional memory-related theta oscillations in the medial temporal lobe. Neurobiol Stress. 2021;15:100383. doi:10.1016/j.ynstr.2021.100383 PubMed PMID: 34504907; PubMed Central PMCID: PMC8414174.

128. Costa M, Pacheco-Estefan D, Gil-Nagel A, Toledano R, Imbach L, Sarnthein J, Strange BA. Human hippocampal reactivation of amygdala encoding-related gamma patterns during aversive memory retrieval. Nat Commun. 2025;16:6820. doi:10.1038/s41467-025-61928-2

129. Zheng J, Stevenson RF, Mander BA, Mnatsakanyan L, Hsu FPK, Vadera S, Knight RT, Yassa MA, Lin JJ. Multiplexing of Theta and Alpha Rhythms in the Amygdala-Hippocampal Circuit Supports Pattern Separation of Emotional Information. Neuron. 2019;102:887-898.e5. doi:10.1016/j.neuron.2019.03.025

130. Costa M, Lozano-Soldevilla D, Gil-Nagel A, Toledano R, Oehrn CR, Kunz L, Yebra M, Mendez-Bertolo C, Stieglitz L, Sarnthein J, Axmacher N, Moratti S, Strange BA. Aversive memory formation in humans involves an amygdala-hippocampus phase code. Nat Commun. 2022;13:6403. doi:10.1038/s41467-022-33828-2

131. Mackiewicz KL, Sarinopoulos I, Cleven KL, Nitschke JB. The effect of anticipation and the specificity of sex differences for amygdala and hippocampus function in emotional memory. Proc Natl Acad Sci. 2006;103:14200–5. doi:10.1073/pnas.0601648103

132. Aitken F, Kok P. Hippocampal representations switch from errors to predictions during acquisition of predictive associations. Nat Commun. 2022;13:3294. doi:10.1038/s41467-022-31040-w PubMed PMID: 35676285; PubMed Central PMCID: PMC9178037.

133. Epstein M, Lama TD. Thoughts Without A Thinker: Psychotherapy From A Buddhist Perspective. Basic Books. 256 p.

134. Bodhi. In the Buddha's Words: An Anthology of Discourses from the Pali Canon. Simon and Schuster; 2005. 512 p.

135. Hart W. The Art of Living: Vipassana Meditation: As Taught by S. N. Goenka. Harper Collins; 1987. 178 p.

136. Goenka SN. Discourse Summaries. Pariyatti Publishing; 2012. 124 p.

137. Behrens TEJ, Woolrich MW, Walton ME, Rushworth MFS. Learning the value of information in an uncertain world. Nat Neurosci. 2007;10:1214–21. doi:10.1038/nn1954

138. Nader K, Schafe GE, Le Doux JE. Fear memories require protein synthesis in the amygdala for reconsolidation after retrieval. Nature. 2000;406:722–6. doi:10.1038/35021052

139. Baumeister RF, Bratslavsky E, Finkenauer C, Vohs KD. Bad is Stronger than Good. Rev Gen Psychol. 2001;5:323–70. doi:10.1037/1089-2680.5.4.323

140. Ohman A, Eriksson A, Olofsson C. One-trial learning and superior resistance to extinction of autonomic responses conditioned to potentially phobic stimuli. J Comp Physiol Psychol. 1975;88:619–27. doi:10.1037/h0078388 PubMed PMID: 1171119.

141. Maren S, Holmes A. Stress and Fear Extinction. Neuropsychopharmacology. 2016;41:58–79. doi:10.1038/npp.2015.180 PubMed PMID: 26105142; PubMed Central PMCID: PMC4677122.

142. Kube T, Schwarting R, Rozenkrantz L, Glombiewski JA, Rief W. Distorted Cognitive Processes in Major Depression: A Predictive Processing Perspective. Biol Psychiatry. 2020;87:388–98. doi:10.1016/j.biopsych.2019.07.017 PubMed PMID: 31515055.

143. Seth AK, Friston KJ. Active interoceptive inference and the emotional brain. Philos Trans R Soc Lond B Biol Sci. 2016;371:20160007. doi:10.1098/rstb.2016.0007 PubMed PMID: 28080966; PubMed Central PMCID: PMC5062097.

144. Lovibond PF, Mitchell CJ, Minard E, Brady A, Menzies RG. Safety behaviours preserve threat beliefs: Protection from extinction of human fear conditioning by an avoidance response. Behav Res Ther. 2009;47:716–20. doi:10.1016/j.brat.2009.04.013 PubMed PMID: 19457472.

145. Salinas-Hernández XI, Vogel P, Betz S, Kalisch R, Sigurdsson T, Duvarci S. Dopamine neurons drive fear extinction learning by signaling the omission of expected aversive outcomes. eLife. 2018;7:e38818. doi:10.7554/eLife.38818 PubMed PMID: 30421719; PubMed Central PMCID: PMC6257816.

146. Fries P. Rhythms for Cognition: Communication through Coherence. Neuron. 2015;88:220–35. doi:10.1016/j.neuron.2015.09.034 PubMed PMID: 26447583; PubMed Central PMCID: PMC4605134.

147. Melloni L, Molina C, Pena M, Torres D, Singer W, Rodriguez E. Synchronization of neural activity across cortical areas correlates with conscious perception. J Neurosci Off J Soc Neurosci. 2007;27:2858–65. doi:10.1523/JNEUROSCI.4623-06.2007 PubMed PMID: 17360907; PubMed Central PMCID: PMC6672558.

148. Brefczynski-Lewis JA, Lutz A, Schaefer HS, Levinson DB, Davidson RJ. Neural correlates of attentional expertise in long-term meditation practitioners. Proc Natl Acad Sci U S A. 2007;104:11483–8. doi:10.1073/pnas.0606552104 PubMed PMID: 17596341; PubMed Central PMCID: PMC1903340.

149. Lieberman JM, McConnell PA, Estarellas M, Sacchet MD. Neurophysiological mechanisms of focused attention meditation: A scoping systematic review. Imaging Neurosci. 2025;3:IMAG.a.14. doi:10.1162/IMAG.a.14 PubMed PMID: 40800838; PubMed Central PMCID: PMC12327082.

150. Pascarella A, Thölke P, Meunier D, O'Byrne J, Lajnef T, Raffone A, Guidotti R, Pizzella V, Marzetti L, Jerbi K. Meditation induces shifts in neural oscillations, brain complexity, and critical dynamics: novel insights from MEG. Neurosci Conscious. 2025;2025:niaf047. doi:10.1093/nc/niaf047 PubMed PMID: 41287816; PubMed Central PMCID: PMC12640546.

151. Khoury B, Sharma M, Rush SE, Fournier C. Mindfulness-based stress reduction for healthy individuals: A meta-analysis. J Psychosom Res. 2015;78:519–28. doi:10.1016/j.jpsychores.2015.03.009

152. Hilton L, Hempel S, Ewing BA, Apaydin E, Xenakis L, Newberry S, Colaiaco B, Maher AR, Shanman RM, Sorbero ME, Maglione MA. Mindfulness Meditation for Chronic Pain: Systematic Review and Meta-analysis. Ann Behav Med. 2017;51:199–213. doi:10.1007/s12160-016-9844-2

153. Li WW, Nannestad J, Leow T, Heward C. The effectiveness of mindfulness-based stress reduction (MBSR) on depression, PTSD, and mindfulness among military veterans: A systematic review and meta-analysis. Health Psychol Open. 2024;11:20551029241302969. doi:10.1177/20551029241302969

154. Scholem G. Major Trends in Jewish Mysticism. New York: Schocken; 1995. 496 p.

155. Feuerstein G. The Yoga Tradition: Its History, Literature, Philosophy and Practice. Chino Valley, Arizona: Hohm Press; 2008. 552 p.

156. Pregadio F. Great Clarity: Daoism and Alchemy in Early Medieval China. Stanford, Calif: Stanford University Press; 2006. 385 p.

157. Herrero JL, Khuvis S, Yeagle E, Cerf M, Mehta AD. Breathing above the brain stem: volitional control and attentional modulation in humans. J Neurophysiol. 2018;119:145–59. doi:10.1152/jn.00551.2017 PubMed PMID: 28954895; PubMed Central PMCID: PMC5866472.

158. Brandmeyer T, Delorme A. Reduced mind wandering in experienced meditators and associated EEG correlates. Exp Brain Res. 2018;236:2519–28. doi:10.1007/s00221-016-4811-5

159. Yoshida K, Takeda K, Kasai T, Makinae S, Murakami Y, Hasegawa A, Sakai S. Focused attention meditation training modifies neural activity and attention: longitudinal EEG data in non-meditators. Soc Cogn Affect Neurosci. 2020;15:215–24. doi:10.1093/scan/nsaa020

160. DeLosAngeles D, Williams G, Burston J, Fitzgibbon SP, Lewis TW, Grummett TS, Clark CR, Pope KJ, Willoughby JO. Electroencephalographic correlates of states of concentrative meditation. Int J Psychophysiol. 2016;110:27–39. doi:10.1016/j.ijpsycho.2016.09.020

161. Kral TRA, Schuyler BS, Mumford JA, Rosenkranz MA, Lutz A, Davidson RJ. Impact of short- and long-term mindfulness meditation training on amygdala reactivity to emotional stimuli. NeuroImage. 2018;181:301–13. doi:10.1016/j.neuroimage.2018.07.013

162. Desbordes G, Negi LT, Pace TWW, Wallace BA, Raison CL, Schwartz EL. Effects of mindful-attention and compassion meditation training on amygdala response to emotional stimuli in an ordinary, non-meditative state. Front Hum Neurosci. 2012;6. doi:10.3389/fnhum.2012.00292

163. Khalsa SS, Rudrauf D, Hassanpour MS, Davidson RJ, Tranel D. The practice of meditation is not associated with improved interoceptive awareness of the heartbeat. Psychophysiology. 2020;57:e13479. doi:10.1111/psyp.13479

164. Daubenmier J, Sze J, Kerr CE, Kemeny ME, Mehling W. Follow your breath: respiratory interoceptive accuracy in experienced meditators. Psychophysiology. 2013;50:777–89. doi:10.1111/psyp.12057 PubMed PMID: 23692525; PubMed Central PMCID: PMC3951998.

165. Pascarella A, Thölke P, Meunier D, O'Byrne J, Lajnef T, Raffone A, Guidotti R, Pizzella V, Marzetti L, Jerbi K. Meditation induces shifts in neural oscillations, brain complexity, and critical dynamics: novel insights from MEG. Neurosci Conscious. 2025;2025:niaf047. doi:10.1093/nc/niaf047

166. Young JH, Arterberry ME, Martin JP. Contrasting Electroencephalography-Derived Entropy and Neural Oscillations With Highly Skilled Meditators. Front Hum Neurosci. 2021;15. doi:10.3389/fnhum.2021.628417

167. Christov-Moore L, Jinich-Diamant A, Safron A, Lynch C, Reggente N. Cognitive Science Below the Neck: Toward an Integrative Account of Consciousness in the Body. Cogn Sci. 2023;47:e13264. doi:10.1111/cogs.13264

168. Damasio AR. Descartes' Error. HarperCollins; 1994. 340 p.

169. van der Kolk B. The Body Keeps the Score: Brain, Mind, and Body in the Healing of Trauma. Penguin Publishing Group; 2015. 464 p.

170. Tafur J, Maté G. The Fellowship of the River: A Medical Doctor's Exploration into Traditional Amazonian Plant Medicine. Espiritu Books and Joseph Tafur. 290 p.

171. Ouspensky PD. In Search of the Miraculous. Rare Treasure Editions; 2021. 741 p.

172. Crescentini C, Capurso V. Mindfulness meditation and explicit and implicit indicators of personality and self-concept changes. Front Psychol. 2015;6. doi:10.3389/fpsyg.2015.00044

173. Bucher MA, Suzuki T, Samuel DB. A meta-analytic review of personality traits and their associations with mental health treatment outcomes. Clin Psychol Rev. 2019;70:51–63. doi:10.1016/j.cpr.2019.04.002 PubMed PMID: 30981042.

174. MacLean KA, Johnson MW, Griffiths RR. Mystical Experiences Occasioned by the Hallucinogen Psilocybin Lead to Increases in the Personality Domain of Openness. J Psychopharmacol Oxf Engl. 2011;25:1453–61. doi:10.1177/0269881111420188 PubMed PMID: 21956378; PubMed Central PMCID: PMC3537171.

175. Altering Consciousness: Multidisciplinary Perspectives : History, Culture, and the Humanities. Biological and psychological perspectives. Praeger; 2011. 401 p.

176. Fitriani T, Seelananda P. Beyond Religions: The Serenity of Fasting in Buddhism and its Impact on Mental Well-being. Subhasita J Buddh Relig Stud. 2023;1:75–86. doi:10.53417/jsb.102

177. Demmrich S, Koppold-Liebscher D, Klatte C, Steckhan N, Ring RM. Effects of religious intermittent dry fasting on religious experience and mindfulness: A longitudinal study among Baha'is. Psychol Relig Spiritual. 2023;15:459–70. doi:10.1037/rel0000423

178. Shroomery Message Board - The Psychedelic Experience [Internet]. [cited 2026 Apr 27]. Fasting Before Consuming Mushrooms. Available from: https://www.shroomery.org/forums/showflat.php/Number/15602568

179. Camandola S, Mattson MP. Brain metabolism in health, aging, and neurodegeneration. EMBO J. 2017;36:1474–92. doi:10.15252/embj.201695810

180. Herculano-Houzel S. Scaling of brain metabolism with a fixed energy budget per neuron: implications for neuronal activity, plasticity and evolution. PloS One. 2011;6:e17514. doi:10.1371/journal.pone.0017514 PubMed PMID: 21390261; PubMed Central PMCID: PMC3046985.

181. Attwell D, Laughlin SB. An energy budget for signaling in the grey matter of the brain. J Cereb Blood Flow Metab Off J Int Soc Cereb Blood Flow Metab. 2001;21:1133–45. doi:10.1097/00004647-200110000-00001 PubMed PMID: 11598490.

182. Melkonian EA, Schury MP. Biochemistry, Anaerobic Glycolysis. In: StatPearls [Internet]. Treasure Island (FL): StatPearls Publishing; 2026 [cited 2026 Apr 30]. Available from: http://www.ncbi.nlm.nih.gov/books/NBK546695/ PubMed PMID: 31536301.

183. Turner DA, Adamson DC. Neuronal-Astrocyte Metabolic Interactions: Understanding the Transition into Abnormal Astrocytoma Metabolism. J Neuropathol Exp Neurol.

2011;70:167–76. doi:10.1097/NEN.0b013e31820e1152 PubMed PMID: 21293295; PubMed Central PMCID: PMC3045672.

184. Vaishnavi SN, Vlassenko AG, Rundle MM, Snyder AZ, Mintun MA, Raichle ME. Regional aerobic glycolysis in the human brain. Proc Natl Acad Sci. 2010;107:17757–62. doi:10.1073/pnas.1010459107

185. Mattson MP, Moehl K, Ghena N, Schmaedick M, Cheng A. Intermittent metabolic switching, neuroplasticity and brain health. Nat Rev Neurosci. 2018;19:63–80. doi:10.1038/nrn.2017.156 PubMed PMID: 29321682; PubMed Central PMCID: PMC5913738.

186. Fontán-Lozano Á, López-Lluch G, Delgado-García JM, Navas P, Carrión ÁM. Molecular Bases of Caloric Restriction Regulation of Neuronal Synaptic Plasticity. Mol Neurobiol. 2008;38:167–77. doi:10.1007/s12035-008-8040-1

187. Rogawski MA, Löscher W, Rho JM. Mechanisms of Action of Antiseizure Drugs and the Ketogenic Diet. Cold Spring Harb Perspect Med. 2016;6:a022780. doi:10.1101/cshperspect.a022780 PubMed PMID: 26801895; PubMed Central PMCID: PMC4852797.

188. Sleiman SF, Henry J, Al-Haddad R, El Hayek L, Abou Haidar E, Stringer T, Ulja D, Karuppagounder SS, Holson EB, Ratan RR, Ninan I, Chao MV. Exercise promotes the expression of brain derived neurotrophic factor (BDNF) through the action of the ketone body β-hydroxybutyrate. Elmquist JK, editor. eLife. 2016;5:e15092. doi:10.7554/eLife.15092

189. Marosi K, Kim SW, Moehl K, Scheibye-Knudsen M, Cheng A, Cutler R, Camandola S, Mattson MP. 3-Hydroxybutyrate regulates energy metabolism and induces BDNF expression in cerebral cortical neurons. J Neurochem. 2016;139:769–81. doi:10.1111/jnc.13868 PubMed PMID: 27739595; PubMed Central PMCID: PMC5123937.

190. Fontán-Lozano Á, Sáez-Cassanelli JL, Inda MC, de los Santos-Arteaga M, Sierra-Domínguez SA, López-Lluch G, Delgado-García JM, Carrión ÁM. Caloric Restriction Increases Learning Consolidation and Facilitates Synaptic Plasticity through Mechanisms Dependent on NR2B Subunits of the NMDA Receptor. J Neurosci. 2007;27:10185–95. doi:10.1523/JNEUROSCI.2757-07.2007 PubMed PMID: 17881524; PubMed Central PMCID: PMC6672666.

191. Popov A, Denisov P, Bychkov M, Brazhe A, Lyukmanova E, Shenkarev Z, Lazareva N, Verkhratsky A, Semyanov A. Caloric restriction triggers morphofunctional remodeling of astrocytes and enhances synaptic plasticity in the mouse hippocampus. Cell Death Dis. 2020;11:208. doi:10.1038/s41419-020-2406-3

192. Zhang L, Xu H, Ding N, Li X, Chen X, Chen Z. Beneficial Effects on Brain Micro-Environment by Caloric Restriction in Alleviating Neurodegenerative Diseases and Brain Aging. Front Physiol. 2021;12. doi:10.3389/fphys.2021.715443

193. Beveridge J, Montgomery A, Grossberg G. Intermittent fasting and neurocognitive disorders: What the evidence shows. J Nutr Health Aging. 2025;29:100480. doi:10.1016/j.jnha.2025.100480

194. Henríquez FIG, Medel V, O'Byrne DF. Impact of ketosis on neuronal activity: a characterization of the functional role of ketone bodies using non-invasive encephalography in humans. Alzheimers Dement. 2025;21:e103513. doi:10.1002/alz70856_103513 PubMed PMID: null; PubMed Central PMCID: PMC12742683.

195. Orfanos S, Toygar T, Berthold-Losleben M, Chechko N, Durst A, Laoutidis ZG, Vocke S, Weidenfeld C, Schneider F, Karges W, Beckmann CF, Habel U, Kohn N. Investigating the impact of overnight fasting on intrinsic functional connectivity: a double-blind fMRI study. Brain Imaging Behav. 2018;12:1150–9. doi:10.1007/s11682-017-9777-9 PubMed PMID: 29071464; PubMed Central PMCID: PMC6063348.

196. Bolo NR, Musen G, Jacobson AM, Weinger K, McCartney RL, Flores V, Renshaw PF, Simonson DC. Brain activation during working memory is altered in patients with type 1 diabetes during hypoglycemia. Diabetes. 2011;60:3256–64. doi:10.2337/db11-0506 PubMed PMID: 21984582; PubMed Central PMCID: PMC3219930.

197. Marder TJ, Flores VL, Bolo NR, Hoogenboom WS, Simonson DC, Jacobson AM, Foote SE, Shenton ME, Sperling RA, Musen G. Task-induced brain activity patterns in type 2 diabetes: a potential biomarker for cognitive decline. Diabetes. 2014;63:3112–9. doi:10.2337/db13-1783 PubMed PMID: 24705405; PubMed Central PMCID: PMC4141362.

198. Musen G, Jacobson AM, Bolo NR, Simonson DC, Shenton ME, McCartney RL, Flores VL, Hoogenboom WS. Resting-state brain functional connectivity is altered in type 2 diabetes. Diabetes. 2012;61:2375–9. doi:10.2337/db11-1669 PubMed PMID: 22664957; PubMed Central PMCID: PMC3425418.

199. Padamsey Z, Katsanevaki D, Dupuy N, Rochefort NL. Neocortex saves energy by reducing coding precision during food scarcity. Neuron. 2022;110:280-296.e10. doi:10.1016/j.neuron.2021.10.024 PubMed PMID: 34741806.

200. Jordan R, Keller GB. Opposing Influence of Top-down and Bottom-up Input on Excitatory Layer 2/3 Neurons in Mouse Primary Visual Cortex. Neuron. 2020;108:1194-1206.e5. doi:10.1016/j.neuron.2020.09.024

201. Naka A, Veit J, Shababo B, Chance RK, Risso D, Stafford D, Snyder B, Egladyous A, Chu D, Sridharan S, Mossing DP, Paninski L, Ngai J, Adesnik H. Complementary

networks of cortical somatostatin interneurons enforce layer specific control. eLife. 8:e43696. doi:10.7554/eLife.43696 PubMed PMID: 30883329; PubMed Central PMCID: PMC6422636.

202. Fanselow EE, Richardson KA, Connors BW. Selective, State-Dependent Activation of Somatostatin-Expressing Inhibitory Interneurons in Mouse Neocortex. J Neurophysiol. 2008;100:2640–52. doi:10.1152/jn.90691.2008 PubMed PMID: 18799598; PubMed Central PMCID: PMC2585405.

203. Reyes A, Lujan R, Rozov A, Burnashev N, Somogyi P, Sakmann B. Target-cell-specific facilitation and depression in neocortical circuits. Nat Neurosci. 1998;1:279–85. doi:10.1038/1092

204. Canepa CR, Kara JA, Lee CC. Cell-Type-Specific Expression of Leptin Receptors in the Mouse Forebrain. Int J Mol Sci. 2024;25:9854. doi:10.3390/ijms25189854 PubMed PMID: 39337341; PubMed Central PMCID: PMC11432612.

205. Zhu Y, Qiao W, Liu K, Zhong H, Yao H. Control of response reliability by parvalbumin-expressing interneurons in visual cortex. Nat Commun. 2015;6:6802. doi:10.1038/ncomms7802 PubMed PMID: 25869033.

206. Agetsuma M, Hamm JP, Tao K, Fujisawa S, Yuste R. Parvalbumin-Positive Interneurons Regulate Neuronal Ensembles in Visual Cortex. Cereb Cortex. 2018;28:1831–45. doi:10.1093/cercor/bhx169

207. Rikhye RV, Yildirim M, Hu M, Breton-Provencher V, Sur M. Reliable Sensory Processing in Mouse Visual Cortex through Cooperative Interactions between Somatostatin and Parvalbumin Interneurons. J Neurosci. 2021;41:8761–78. doi:10.1523/JNEUROSCI.3176-20.2021 PubMed PMID: 34493543.

208. Reinhold K, Lien AD, Scanziani M. Distinct recurrent versus afferent dynamics in cortical visual processing. Nat Neurosci. 2015;18:1789–97. doi:10.1038/nn.4153 PubMed PMID: 26502263.

209. Inagaki HK, Fontolan L, Romani S, Svoboda K. Discrete attractor dynamics underlies persistent activity in the frontal cortex. Nature. 2019;566:212–7. doi:10.1038/s41586-019-0919-7

210. Hart E, Huk AC. Recurrent circuit dynamics underlie persistent activity in the macaque frontoparietal network. Salinas E, Behrens TE, Salinas E, Compte A, editors. eLife. 2020;9:e52460. doi:10.7554/eLife.52460

211. Wang M, Yang Y, Wang CJ, Gamo NJ, Jin LE, Mazer JA, Morrison JH, Wang XJ, Arnsten AFT. NMDA Receptors Subserve Persistent Neuronal Firing during Working Memory in Dorsolateral Prefrontal Cortex. Neuron. 2013;77:736–49. doi:10.1016/j.neuron.2012.12.032 PubMed PMID: 23439125.

212. Vugt B van, Kerkoerle T van, Vartak D, Roelfsema PR. The Contribution of AMPA and NMDA Receptors to Persistent Firing in the Dorsolateral Prefrontal Cortex in Working Memory. J Neurosci. 2020;40:2458–70. doi:10.1523/JNEUROSCI.2121-19.2020 PubMed PMID: 32051326.

213. Gusnard DA, Raichle ME, Raichle ME. Searching for a baseline: functional imaging and the resting human brain. Nat Rev Neurosci. 2001;2:685–94. doi:10.1038/35094500 PubMed PMID: 11584306.

214. Vogt BA, Laureys S. Posterior cingulate, precuneal and retrosplenial cortices: cytology and components of the neural network correlates of consciousness. Prog Brain Res. 2005;150:205–17. doi:10.1016/S0079-6123(05)50015-3 PubMed PMID: 16186025; PubMed Central PMCID: PMC2679949.

215. Larkum ME, Nevian T, Sandler M, Polsky A, Schiller J. Synaptic integration in tuft dendrites of layer 5 pyramidal neurons: a new unifying principle. Science. 2009;325:756–60. doi:10.1126/science.1171958 PubMed PMID: 19661433.

216. Shai AS, Anastassiou CA, Larkum ME, Koch C. Physiology of Layer 5 Pyramidal Neurons in Mouse Primary Visual Cortex: Coincidence Detection through Bursting. PLoS Comput Biol. 2015;11:e1004090. doi:10.1371/journal.pcbi.1004090 PubMed PMID: 25768881; PubMed Central PMCID: PMC4358988.

217. Animali S, Steinwurzel C, Dardano A, Sancho-Bornez V, Del Prato S, Morrone MC, Daniele G, Binda P. Effect of fasting on short-term visual plasticity in adult humans. Eur J Neurosci. 2023;57:148–62. doi:10.1111/ejn.15873 PubMed PMID: 36437778; PubMed Central PMCID: PMC10108283.

218. Carhart-Harris RL, Erritzoe D, Williams T, Stone JM, Reed LJ, Colasanti A, Tyacke RJ, Leech R, Malizia AL, Murphy K, Hobden P, Evans J, Feilding A, Wise RG, Nutt DJ. Neural correlates of the psychedelic state as determined by fMRI studies with psilocybin. Proc Natl Acad Sci U S A. 2012;109:2138–43. doi:10.1073/pnas.1119598109 PubMed PMID: 22308440; PubMed Central PMCID: PMC3277566.

219. Vollenweider FX, Leenders KL, Scharfetter C, Maguire P, Stadelmann O, Angst J. Positron emission tomography and fluorodeoxyglucose studies of metabolic hyperfrontality and psychopathology in the psilocybin model of psychosis. Neuropsychopharmacol Off Publ Am Coll Neuropsychopharmacol. 1997;16:357–72. doi:10.1016/S0893-133X(96)00246-1 PubMed PMID: 9109107.

220. Gouzoulis-Mayfrank E, Schreckenberger M, Sabri O, Arning C, Thelen B, Spitzer M, Kovar KA, Hermle L, Büll U, Sass H. Neurometabolic effects of psilocybin, 3,4-methylenedioxyethylamphetamine (MDE) and d-methamphetamine in healthy volunteers. A double-blind, placebo-controlled PET study with [18F]FDG. Neuropsychopharmacol Off Publ Am Coll Neuropsychopharmacol. 1999;20:565–81. doi:10.1016/S0893-133X(98)00089-X PubMed PMID: 10327426.

221. Riba J, Romero S, Grasa E, Mena E, Carrió I, Barbanoj MJ. Increased frontal and paralimbic activation following ayahuasca, the pan-amazonian inebriant. Psychopharmacology (Berl). 2006;186:93–8. doi:10.1007/s00213-006-0358-7

222. Hermle L, Fünfgeld M, Oepen G, Botsch H, Borchardt D, Gouzoulis E, Fehrenbach RA, Spitzer M. Mescaline-induced psychopathological, neuropsychological, and neurometabolic effects in normal subjects: Experimental psychosis as a tool for psychiatric research. Biol Psychiatry. 1992;32:976–91. doi:10.1016/0006-3223(92)90059-9

223. Rieser NM, Gubser LP, Moujaes F, Duerler P, Lewis CR, Michels L, Vollenweider FX, Preller KH. Psilocybin-induced changes in cerebral blood flow are associated with acute and baseline inter-individual differences. Sci Rep. 2023;13:17475. doi:10.1038/s41598-023-44153-z

224. Lewis CR, Preller KH, Kraehenmann R, Michels L, Staempfli P, Vollenweider FX. Two dose investigation of the 5-HT-agonist psilocybin on relative and global cerebral blood flow. NeuroImage. 2017;159:70–8. doi:10.1016/j.neuroimage.2017.07.020

225. Palhano-Fontes F, Andrade KC, Tofoli LF, Santos AC, Crippa JAS, Hallak JEC, Ribeiro S, Araujo DB de. The Psychedelic State Induced by Ayahuasca Modulates the Activity and Connectivity of the Default Mode Network. PLOS ONE. 2015;10:e0118143. doi:10.1371/journal.pone.0118143

226. Gattuso JJ, Perkins D, Ruffell S, Lawrence AJ, Hoyer D, Jacobson LH, Timmermann C, Castle D, Rossell SL, Downey LA, Pagni BA, Galvão-Coelho NL, Nutt D, Sarris J. Default Mode Network Modulation by Psychedelics: A Systematic Review. Int J Neuropsychopharmacol. 2022;26:155–88. doi:10.1093/ijnp/pyac074 PubMed PMID: 36272145; PubMed Central PMCID: PMC10032309.

227. Tomasi D, Wang GJ, Volkow ND. Energetic cost of brain functional connectivity. Proc Natl Acad Sci U S A. 2013;110:13642–7. doi:10.1073/pnas.1303346110 PubMed PMID: 23898179; PubMed Central PMCID: PMC3746878.

228. Passow S, Specht K, Adamsen TC, Biermann M, Brekke N, Craven AR, Ersland L, Grüner R, Kleven-Madsen N, Kvernenes OH, Schwarzlmüller T, Olesen RA, Hugdahl K. Default-mode network functional connectivity is closely related to metabolic activity. Hum Brain Mapp. 2015;36:2027–38. doi:10.1002/hbm.22753 PubMed PMID: 25644693; PubMed Central PMCID: PMC5006878.

229. Aiello M, Salvatore E, Cachia A, Pappatà S, Cavaliere C, Prinster A, Nicolai E, Salvatore M, Baron JC, Quarantelli M. Relationship between simultaneously acquired resting-state regional cerebral glucose metabolism and functional MRI: a PET/MR hybrid scanner study. NeuroImage. 2015;113:111–21. doi:10.1016/j.neuroimage.2015.03.017 PubMed PMID: 25791784.

230. Magistretti PJ, Allaman I. Brain Energy Metabolism. In: Neuroscience in the 21st Century [Internet]. Springer, New York, NY; 2013 [cited 2026 Apr 28]. p. 1591–620. Available from: https://link.springer.com/rwe/10.1007/978-1-4614-1997-6_56 doi:10.1007/978-1-4614-1997-6_56

231. Blazey T, Snyder AZ, Su Y, Goyal MS, Lee JJ, Vlassenko AG, Arbeláez AM, Raichle ME. Quantitative positron emission tomography reveals regional differences in aerobic glycolysis within the human brain. J Cereb Blood Flow Metab. 2019;39:2096–102. doi:10.1177/0271678X18767005

232. Tsurugizawa T, Djemai B, Zalesky A. The impact of fasting on resting state brain networks in mice. Sci Rep. 2019;9:2976. doi:10.1038/s41598-019-39851-6

233. Tagliazucchi E, Zamberlan F, Cavanna F, de la Fuente L, Romero C, Sanz Perl Y, Pallavicini C. Baseline Power of Theta Oscillations Predicts Mystical-Type Experiences Induced by DMT in a Natural Setting. Front Psychiatry. 2021;12:720066. doi:10.3389/fpsyt.2021.720066 PubMed PMID: 34803754; PubMed Central PMCID: PMC8602571.

234. Pizzagalli DA, Oakes TR, Davidson RJ. Coupling of theta activity and glucose metabolism in the human rostral anterior cingulate cortex: An EEG/PET study of normal and depressed subjects. Psychophysiology. 2003;40:939–49. doi:10.1111/1469-8986.00112

235. Wallace RK. Physiological Effects of Transcendental Meditation. Science. 1970;167:1751–4. doi:10.1126/science.167.3926.1751

236. Jevning R, Wallace RK, Beidebach M. The physiology of meditation: A review. A wakeful hypometabolic integrated response. Neurosci Biobehav Rev. 1992;16:415–24. doi:10.1016/S0149-7634(05)80210-6

237. Young JDE, Taylor E. Meditation as a Voluntary Hypometabolic State of Biological Estivation. News Physiol Sci Int J Physiol Prod Jointly Int Union Physiol Sci Am Physiol Soc. 1998;13:149–53. doi:10.1152/physiologyonline.1998.13.3.149 PubMed PMID: 11390779.

238. Wallace RK, Benson H, Wilson AF. A wakeful hypometabolic physiologic state. Am J Physiol. 1971;221:795–9. doi:10.1152/ajplegacy.1971.221.3.795 PubMed PMID: 5570336.

239. Chiesa A. Zen Meditation: An Integration of Current Evidence. J Altern Complement Med. 2009;15:585–92. doi:10.1089/acm.2008.0416

240. Balaji PA, Varne SR, Ali SS. Physiological Effects of Yogic Practices and Transcendental Meditation in Health and Disease. North Am J Med Sci. 2012;4:442–8. doi:10.4103/1947-2714.101980 PubMed PMID: 23112963; PubMed Central PMCID: PMC3482773.

241. Sudsuang R, Chentanez V, Veluvan K. Effect of buddhist meditation on serum cortisol and total protein levels, blood pressure, pulse rate, lung volume and reaction time. Physiol Behav. 1991;50:543–8. doi:10.1016/0031-9384(91)90543-W

242. Kozhevnikov M, Elliott J, Shephard J, Gramann K. Neurocognitive and Somatic Components of Temperature Increases during g-Tummo Meditation: Legend and Reality. PLOS ONE. 2013;8:e58244. doi:10.1371/journal.pone.0058244

243. Brewer JA, Worhunsky PD, Gray JR, Tang YY, Weber J, Kober H. Meditation experience is associated with differences in default mode network activity and connectivity. Proc Natl Acad Sci U S A. 2011;108:20254–9. doi:10.1073/pnas.1112029108 PubMed PMID: 22114193; PubMed Central PMCID: PMC3250176.

244. Kleckner IR, Zhang J, Touroutoglou A, Chanes L, Xia C, Simmons WK, Quigley KS, Dickerson BC, Barrett LF. Evidence for a Large-Scale Brain System Supporting Allostasis and Interoception in Humans. Nat Hum Behav. 2017;1:0069. doi:10.1038/s41562-017-0069 PubMed PMID: 28983518; PubMed Central PMCID: PMC5624222.

245. James W. The Varieties of Religious Experience: A Study in Human Nature. Random House Publishing Group; 1999. 641 p.

246. Stace WT. Mysticism and Philosophy. Lippincott; 1960. 384 p.

247. Hood RW. The Construction and Preliminary Validation of a Measure of Reported Mystical Experience. J Sci Study Relig. 1975;14:29–41. doi:10.2307/1384454

248. Barrett FS, Johnson MW, Griffiths RR. Validation of the revised Mystical Experience Questionnaire in experimental sessions with psilocybin. J Psychopharmacol Oxf Engl. 2015;29:1182–90. doi:10.1177/0269881115609019 PubMed PMID: 26442957; PubMed Central PMCID: PMC5203697.

249. Schartner MM, Carhart-Harris RL, Barrett AB, Seth AK, Muthukumaraswamy SD. Increased spontaneous MEG signal diversity for psychoactive doses of ketamine, LSD and psilocybin. Sci Rep. 2017;7:46421. doi:10.1038/srep46421 PubMed PMID: 28422113; PubMed Central PMCID: PMC5396066.

250. Tagliazucchi E, Roseman L, Kaelen M, Orban C, Muthukumaraswamy SD, Murphy K, Laufs H, Leech R, McGonigle J, Crossley N, Bullmore E, Williams T, Bolstridge M, Feilding A, Nutt DJ, Carhart-Harris R. Increased Global Functional Connectivity Correlates with LSD-Induced Ego Dissolution. Curr Biol CB. 2016;26:1043–50. doi:10.1016/j.cub.2016.02.010 PubMed PMID: 27085214.

251. Jinich-Diamant A, Simpson S, Zuniga-Hertz JP, Chitteti R, Schilling JM, Bonds JA, Case L, Chernov AV, Dispenza J, Maree J, Amkie Stahl NE, Licamele M, Fazlalipour N, Devulapalli S, Christov-Moore L, Reggente N, Poirier MA, Moeller-Bertram T, Patel HH. Neural and molecular changes during a mind-body reconceptualization, meditation, and

open label placebo healing intervention. Commun Biol. 2025;8:1525. doi:10.1038/s42003-025-09088-3

252. Lutz A, Greischar LL, Rawlings NB, Ricard M, Davidson RJ. Long-term meditators self-induce high-amplitude gamma synchrony during mental practice. Proc Natl Acad Sci. 2004;101:16369–73. doi:10.1073/pnas.0407401101

253. Godfrey K, Luan LX, Timmermann C. Effects of psychedelics on human oscillatory brain activity. Int Rev Neurobiol. 2025;181:171–202. doi:10.1016/bs.irn.2025.04.012 PubMed PMID: 40541309.

254. Rodriguez-Larios J, Bracho Montes de Oca EA, Alaerts K. The EEG spectral properties of meditation and mind wandering differ between experienced meditators and novices. NeuroImage. 2021;245:118669. doi:10.1016/j.neuroimage.2021.118669 PubMed PMID: 34688899.

255. Muthukumaraswamy SD, Liley DTJ. 1/f electrophysiological spectra in resting and drug-induced states can be explained by the dynamics of multiple oscillatory relaxation processes. NeuroImage. 2018;179:582–95. doi:10.1016/j.neuroimage.2018.06.068

256. Seth A. Being You: A New Science of Consciousness. Penguin; 2021. 353 p.

257. Hoffman D. The Case Against Reality: Why Evolution Hid the Truth from Our Eyes. National Geographic Books; 2022. 272 p.

258. Brudner RM, Kaczmarek E, Blainey MG, Schulz-Quach C, Meshkat S, Doyle Z, Lipsitz O, Offman H, Sethi R, Weiglein G, McIntyre RS, Rosenblat JD. Examining mystical experiences as a predictor of psilocybin-assisted psychotherapy for treatment-resistant depression. J Psychopharmacol Oxf Engl. 2025;39:950–6. doi:10.1177/02698811251346697 PubMed PMID: 40590216; PubMed Central PMCID: PMC12371138.

259. Yaden DB, Griffiths RR. The Subjective Effects of Psychedelics Are Necessary for Their Enduring Therapeutic Effects. ACS Pharmacol Transl Sci. 2020;4:568–72. doi:10.1021/acsptsci.0c00194 PubMed PMID: 33861219; PubMed Central PMCID: PMC8033615.

260. Ko K, Knight G, Rucker JJ, Cleare AJ. Psychedelics, Mystical Experience, and Therapeutic Efficacy: A Systematic Review. Front Psychiatry. 2022;13:917199. doi:10.3389/fpsyt.2022.917199 PubMed PMID: 35923458; PubMed Central PMCID: PMC9340494.

261. Romeo B, Kervadec E, Fauvel B, Strika-Bruneau L, Amirouche A, Bezo A, Piolino P, Benyamina A. The intensity of the psychedelic experience is reliably associated with clinical improvements: A systematic review and meta-analysis. Neurosci Biobehav Rev. 2025;172:106086. doi:10.1016/j.neubiorev.2025.106086

262. Viljoen G, Walter H, Bendau A, Koslowski M, Betzler F. Predictors of therapeutic response to psychedelic-assisted therapy: A systematic review. J Psychopharmacol (Oxf). 2025;02698811251389581. doi:10.1177/02698811251389581

263. Aday JS, Davis AK, Mitzkovitz CM, Bloesch EK, Davoli CC. Predicting Reactions to Psychedelic Drugs: A Systematic Review of States and Traits Related to Acute Drug Effects. ACS Pharmacol Transl Sci. 2021;4:424–35. doi:10.1021/acsptsci.1c00014

264. Russ SL, Carhart-Harris RL, Maruyama G, Elliott MS. Replication and extension of a model predicting response to psilocybin. Psychopharmacology (Berl). 2019;236:3221–30. doi:10.1007/s00213-019-05279-z PubMed PMID: 31203401.

265. Haijen ECHM, Kaelen M, Roseman L, Timmermann C, Kettner H, Russ S, Nutt D, Daws RE, Hampshire ADG, Lorenz R, Carhart-Harris RL. Predicting Responses to Psychedelics: A Prospective Study. Front Pharmacol. 2018;9. doi:10.3389/fphar.2018.00897

266. Laird KT, Siddarth P, Ramos A, Rich R, Youssef B, Schwartz GM, Sergi K, Linton M, Schwartzberg L, Kelly DF, Heinzerling KG. Intentions, Spirituality, Set, and Setting Are Associated with Mystical Experiences in Psilocybin-Assisted Therapy. Psychedelic Med. 2026;28314425251413425. doi:10.1177/28314425251413425

267. Timmermann C, Kettner H, Letheby C, Roseman L, Rosas FE, Carhart-Harris RL. Psychedelics alter metaphysical beliefs. Sci Rep. 2021;11:22166. doi:10.1038/s41598-021-01209-2

268. Nayak SM, Singh M, Yaden DB, Griffiths RR. Belief changes associated with psychedelic use. J Psychopharmacol (Oxf). 2023;37:80–92. doi:10.1177/02698811221131989

269. MacLean KA, Johnson MW, Griffiths RR. Mystical experiences occasioned by the hallucinogen psilocybin lead to increases in the personality domain of openness. J Psychopharmacol (Oxf). 2011;25:1453–61. doi:10.1177/0269881111420188

270. Griffiths RR, Hurwitz ES, Davis AK, Johnson MW, Jesse R. Survey of subjective "God encounter experiences": Comparisons among naturally occurring experiences and those occasioned by the classic psychedelics psilocybin, LSD, ayahuasca, or DMT. PLOS ONE. 2019;14:e0214377. doi:10.1371/journal.pone.0214377

271. Lyons T, Carhart-Harris RL. Increased nature relatedness and decreased authoritarian political views after psilocybin for treatment-resistant depression. J Psychopharmacol (Oxf). 2018;32:811–9. doi:10.1177/0269881117748902

272. Noble R, Tasaki K, Noble PJ, Noble D. Biological Relativity Requires Circular Causality but Not Symmetry of Causation: So, Where, What and When Are the Boundaries? Front Physiol. 2019;10. doi:10.3389/fphys.2019.00827

273. Noble D. A theory of biological relativity: no privileged level of causation. Interface Focus. 2011;2:55–64. doi:10.1098/rsfs.2011.0067

274. Haken H. Synergetics: An Introduction. Springer Science & Business Media; 2013. 395 p.

275. Friston K. Life as we know it. J R Soc Interface. 2013;10:20130475. doi:10.1098/rsif.2013.0475 PubMed PMID: 23825119; PubMed Central PMCID: PMC3730701.

276. Hoel EP, Albantakis L, Tononi G. Quantifying causal emergence shows that macro can beat micro. Proc Natl Acad Sci U S A. 2013;110:19790–5. doi:10.1073/pnas.1314922110 PubMed PMID: 24248356; PubMed Central PMCID: PMC3856819.

277. Hoel EP. When the Map Is Better Than the Territory. Entropy. 2017;19:188. doi:10.3390/e19050188

278. Mediano PAM, Rosas FE, Timmermann C, Roseman L, Nutt DJ, Feilding A, Kaelen M, Kringelbach ML, Barrett AB, Seth AK, Muthukumaraswamy S, Bor D, Carhart-Harris RL. Effects of External Stimulation on Psychedelic State Neurodynamics. ACS Chem Neurosci. 2024;15:462–71. doi:10.1021/acschemneuro.3c00289 PubMed PMID: 38214686; PubMed Central PMCID: PMC10853937.

279. Watts R, Day C, Krzanowski J, Nutt D, Carhart-Harris R. Patients' Accounts of Increased "Connectedness" and "Acceptance" After Psilocybin for Treatment-Resistant Depression. J Humanist Psychol. 2017;57:520–64. doi:10.1177/0022167817709585

280. Belser AB, Agin-Liebes G, Swift TC, Terrana S, Devenot N, Friedman HL, Guss J, Bossis A, Ross S. Patient Experiences of Psilocybin-Assisted Psychotherapy: An Interpretative Phenomenological Analysis. J Humanist Psychol. 2017;57:354–88. doi:10.1177/0022167817706884

281. Roseman L, Nutt DJ, Carhart-Harris RL. Quality of Acute Psychedelic Experience Predicts Therapeutic Efficacy of Psilocybin for Treatment-Resistant Depression. Front Pharmacol. 2017;8:974. doi:10.3389/fphar.2017.00974 PubMed PMID: 29387009; PubMed Central PMCID: PMC5776504.

282. Shew WL, Plenz D. The Functional Benefits of Criticality in the Cortex. The Neuroscientist. 2013;19:88–100. doi:10.1177/1073858412445487

283. Beggs JM, Plenz D. Neuronal Avalanches in Neocortical Circuits. J Neurosci. 2003;23:11167–77. doi:10.1523/JNEUROSCI.23-35-11167.2003 PubMed PMID: 14657176.

284. Chialvo DR. Emergent complex neural dynamics. Nat Phys. 2010;6:744–50. doi:10.1038/nphys1803

285. Cocchi L, Gollo LL, Zalesky A, Breakspear M. Criticality in the brain: A synthesis of neurobiology, models and cognition. Prog Neurobiol. 2017;158:132–52. doi:10.1016/j.pneurobio.2017.07.002 PubMed PMID: 28734836.

286. Linkenkaer-Hansen K, Nikouline VV, Palva JM, Ilmoniemi RJ. Long-range temporal correlations and scaling behavior in human brain oscillations. J Neurosci Off J Soc Neurosci. 2001;21:1370–7. doi:10.1523/JNEUROSCI.21-04-01370.2001 PubMed PMID: 11160408; PubMed Central PMCID: PMC6762238.

287. Tagliazucchi E, Carhart-Harris R, Leech R, Nutt D, Chialvo DR. Enhanced repertoire of brain dynamical states during the psychedelic experience. Hum Brain Mapp. 2014;35:5442–56. doi:https://doi.org/10.1002/hbm.22562

288. Bak P, Tang C, Wiesenfeld K. Self-organized criticality. Phys Rev Gen Phys. 1988;38:364–74. doi:10.1103/physreva.38.364 PubMed PMID: 9900174.

289. Shew WL, Yang H, Yu S, Roy R, Plenz D. Information Capacity and Transmission Are Maximized in Balanced Cortical Networks with Neuronal Avalanches. J Neurosci. 2011;31:55–63. doi:10.1523/JNEUROSCI.4637-10.2011 PubMed PMID: 21209189; PubMed Central PMCID: PMC3082868.

290. Hengen KB, Shew WL. Is criticality a unified setpoint of brain function? Neuron. 2025;113:2582-2598.e2. doi:10.1016/j.neuron.2025.05.020

291. Timmermann C, Roseman L, Schartner M, Milliere R, Williams LTJ, Erritzoe D, Muthukumaraswamy S, Ashton M, Bendrioua A, Kaur O, Turton S, Nour MM, Day CM, Leech R, Nutt DJ, Carhart-Harris RL. Neural correlates of the DMT experience assessed with multivariate EEG. Sci Rep. 2019;9:1. doi:10.1038/s41598-019-51974-4

292. Beggs JM. The criticality hypothesis: how local cortical networks might optimize information processing. Philos Transact A Math Phys Eng Sci. 2008;366:329–43. doi:10.1098/rsta.2007.2092 PubMed PMID: 17673410.

293. Tognoli E, Kelso JAS. The metastable brain. Neuron. 2014;81:35–48. doi:10.1016/j.neuron.2013.12.022 PubMed PMID: 24411730; PubMed Central PMCID: PMC3997258.

294. Varley TF, Carhart-Harris R, Roseman L, Menon DK, Stamatakis EA. Serotonergic psychedelics LSD & psilocybin increase the fractal dimension of cortical brain activity in spatial and temporal domains. NeuroImage. 2020;220:117049. doi:10.1016/j.neuroimage.2020.117049 PubMed PMID: 32619708.

295. Wolfram S. Undecidability and intractability in theoretical physics. Phys Rev Lett. 1985;54:735–8. doi:10.1103/PhysRevLett.54.735 PubMed PMID: 10031602.

296. Wolfram S. A New Kind of Science. Wolfram Media, Inc.; 2016. 1280 p.

297. Singleton SP, Luppi AI, Carhart-Harris RL, Cruzat J, Roseman L, Nutt DJ, Deco G, Kringelbach ML, Stamatakis EA, Kuceyeski A. Receptor-informed network control theory links LSD and psilocybin to a flattening of the brain's control energy landscape. Nat Commun. 2022;13:5812. doi:10.1038/s41467-022-33578-1 PubMed PMID: 36192411; PubMed Central PMCID: PMC9530221.

298. Manuello J, Vercelli U, Nani A, Costa T, Cauda F. Mindfulness meditation and consciousness: An integrative neuroscientific perspective. Conscious Cogn. 2016;40:67–78. doi:10.1016/j.concog.2015.12.005 PubMed PMID: 26752605.

299. Berkovich-Ohana A, Glicksohn J, Goldstein A. Mindfulness-induced changes in gamma band activity - implications for the default mode network, self-reference and attention. Clin Neurophysiol Off J Int Fed Clin Neurophysiol. 2012;123:700–10. doi:10.1016/j.clinph.2011.07.048 PubMed PMID: 21940201.

300. Wiesenfeld K, Moss F. Stochastic resonance and the benefits of noise: from ice ages to crayfish and SQUIDs. Nature. 1995;373:33–6. doi:10.1038/373033a0 PubMed PMID: 7800036.

301. Gammaitoni L, Hänggi P, Jung P, Marchesoni F. Stochastic resonance. Rev Mod Phys. 1998;70:223.

302. McDonnell MD, Abbott D. What is stochastic resonance? Definitions, misconceptions, debates, and its relevance to biology. PLoS Comput Biol. 2009;5:e1000348. doi:10.1371/journal.pcbi.1000348 PubMed PMID: 19562010; PubMed Central PMCID: PMC2660436.

303. McDonnell MD, Ward LM. The benefits of noise in neural systems: bridging theory and experiment. Nat Rev Neurosci. 2011;12:415–26. doi:10.1038/nrn3061 PubMed PMID: 21685932.

304. Faisal AA, Selen LPJ, Wolpert DM. Noise in the nervous system. Nat Rev Neurosci. 2008;9:292–303. doi:10.1038/nrn2258 PubMed PMID: 18319728; PubMed Central PMCID: PMC2631351.

305. Noble R, Noble D. Harnessing stochasticity: How do organisms make choices? Chaos. 2018;28:106309. doi:10.1063/1.5039668 PubMed PMID: 30384641.

306. Solovay R, Strassen V. A Fast Monte-Carlo Test for Primality. SIAM J Comput. 1977;6:84–5. doi:10.1137/0206006

307. Seth AK, Tsakiris M. Being a Beast Machine: The Somatic Basis of Selfhood. Trends Cogn Sci. 2018;22:969–81. doi:10.1016/j.tics.2018.08.008 PubMed PMID: 30224233.

308. Deane G. Dissolving the self: Active inference, psychedelics, and ego-dissolution. Philos Mind Sci. 2020;1:1–27.

309. Nichols CD. Psychedelics as potent anti-inflammatory therapeutics. Neuropharmacology. 2022;219:109232. doi:10.1016/j.neuropharm.2022.109232

310. Sharon H, Maron-Katz A, Simon EB, Flusser Y, Hendler T, Tarrasch R, Brill S. Mindfulness Meditation Modulates Pain Through Endogenous Opioids. Am J Med. 2016;129:755–8. doi:10.1016/j.amjmed.2016.03.002

311. Friston KJ, Lin M, Frith CD, Pezzulo G, Hobson JA, Ondobaka S. Active Inference, Curiosity and Insight. Neural Comput. 2017;29:2633–83. doi:10.1162/neco_a_00999

312. Deane G, Miller M, Wilkinson S. Losing Ourselves: Active Inference, Depersonalization, and Meditation. Front Psychol. 2020;11. doi:10.3389/fpsyg.2020.539726

313. Miller M, Kiverstein J, Rietveld E. The Predictive Dynamics of Happiness and Well-Being. Emot Rev. 2022;14:15–30. doi:10.1177/17540739211063851

314. Griffiths RR, Richards WA, McCann U, Jesse R. Psilocybin can occasion mystical-type experiences having substantial and sustained personal meaning and spiritual significance. Psychopharmacology (Berl). 2006;187:268–83; discussion 284-292. doi:10.1007/s00213-006-0457-5 PubMed PMID: 16826400.

315. Griffiths RR, Johnson MW, Carducci MA, Umbricht A, Richards WA, Richards BD, Cosimano MP, Klinedinst MA. Psilocybin produces substantial and sustained decreases in depression and anxiety in patients with life-threatening cancer: A randomized double-blind trial. J Psychopharmacol (Oxf). 2016;30:1181–97. doi:10.1177/0269881116675513 PubMed PMID: 27909165; PubMed Central PMCID: PMC5367557.

316. Griffiths RR, Hurwitz ES, Davis AK, Johnson MW, Jesse R. Survey of subjective "God encounter experiences": Comparisons among naturally occurring experiences and those occasioned by the classic psychedelics psilocybin, LSD, ayahuasca, or DMT. PloS One. 2019;14:e0214377. doi:10.1371/journal.pone.0214377 PubMed PMID: 31013281; PubMed Central PMCID: PMC6478303.

317. Lawrence DW, Carhart-Harris R, Griffiths R, Timmermann C. Phenomenology and content of the inhaled N, N-dimethyltryptamine (N, N-DMT) experience. Sci Rep. 2022;12:8562. doi:10.1038/s41598-022-11999-8 PubMed PMID: 35610230; PubMed Central PMCID: PMC9130218.

318. Davis AK, Clifton JM, Weaver EG, Hurwitz ES, Johnson MW, Griffiths RR. Survey of entity encounter experiences occasioned by inhaled N,N-dimethyltryptamine: Phenomenology, interpretation, and enduring effects. J Psychopharmacol (Oxf). 2020;34:1008–20. doi:10.1177/0269881120916143 PubMed PMID: 32345112.

319. Strassman R. DMT: The Spirit Molecule: A Doctor's Revolutionary Research into the Biology of Near-Death and Mystical Experiences. Simon and Schuster; 2000. 338 p.

320. Grof S. Varieties of transpersonal experiences: Observations from LSD psychotherapy. J Transpers Psychol. 1972;4:45. Located at: Periodicals Index Online; 1312136713

321. Shanon B. The Antipodes of the Mind: Charting the Phenomenology of the Ayahuasca Experience. Oxford University Press; 2002. 498 p.

322. Luke DP, Kittenis M. A preliminary survey of paranormal experiences with psychoactive drugs. J Parapsychol. 2005;69:305.

323. Bouso JC, Andión Ó, Sarris JJ, Scheidegger M, Tófoli LF, Opaleye ES, Schubert V, Perkins D. Adverse effects of ayahuasca: Results from the Global Ayahuasca Survey. PLOS Glob Public Health. 2022;2:e0000438. doi:10.1371/journal.pgph.0000438

324. Winkelman MJ. The supernatural as innate cognitive operators. In: The Supernatural After the Neuro-Turn. Routledge; 2019.

325. Lutkajtis A. Entity encounters and the therapeutic effect of the psychedelic mystical experience. J Psychedelic Stud. 2021. doi:10.1556/2054.2020.00143

326. Letheby C. Philosophy of Psychedelics. Oxford, New York: Oxford University Press; 2021. 272 p. (International Perspectives in Philosophy and Psychiatry).

327. Winkelman MJ. The Mechanisms of Psychedelic Visionary Experiences: Hypotheses from Evolutionary Psychology. Front Neurosci. 2017;11:539. doi:10.3389/fnins.2017.00539 PubMed PMID: 29033783; PubMed Central PMCID: PMC5625021.

328. Barrett JL. Exploring the natural foundations of religion. Trends Cogn Sci. 2000;4:29–34. doi:10.1016/S1364-6613(99)01419-9 PubMed PMID: 10637620.

329. Van Leeuwen N, van Elk M. Seeking the supernatural: the Interactive Religious Experience Model. Relig Brain Behav. 2019;9:221–51. doi:10.1080/2153599X.2018.1453529

330. Buck Z, Vervaeke J, Miller M. Supernatural Agent Experiences on Psychedelics: A Predictive Account [Internet]. 2026 [cited 2026 May 24]. Available from: https://osf.io/atx45_v1

331. McNamara P. The Cognitive Neuroscience of Religious Experience: Decentering and the Self [Internet]. 2nd ed. Cambridge: Cambridge University Press; 2022 [cited 2026 May 26]. Available from: https://www.cambridge.org/core/books/cognitive-neuroscience-of-religious-experience/DBF2E9E8F3B0F8BAF99412251F725167 doi:10.1017/9781108973496

332. Yaden DB, Goldy SP, Weiss B, Griffiths RR. Clinically relevant acute subjective effects of psychedelics beyond mystical experience. Nat Rev Psychol. 2024;3:606–21. doi:10.1038/s44159-024-00345-6

333. Gładziejewski P. From Altered States to Metaphysics: The Epistemic Status of Psychedelic-induced Metaphysical Beliefs. Rev Philos Psychol. 2025;16:175–97. doi:10.1007/s13164-023-00709-6

334. Van Eyghen H. Psychedelics and the Entropic Brain Beyond the Self. Int J Psychol Relig. 2023;33:277–93. doi:10.1080/10508619.2023.2192078

335. Lutkajtis A. Entity encounters and the therapeutic effect of the psychedelic mystical experience. J Psychedelic Stud. 2020;4:171–8. doi:10.1556/2054.2020.00143

336. Meyer P. Apparent communication with discarnate entities induced by dimethyltryptamine (DMT). Psychedelics. 1994;161–203.

337. Rodriguez MA. A Methodology for Studying Various Interpretations of the N,N-dimethyltryptamine-Induced Alternate Reality. J Sci Explor. 2007;21.

338. van Lommel P, van Wees R, Meyers V, Elfferich I. Near-death experience in survivors of cardiac arrest: a prospective study in the Netherlands. The Lancet. 2001;358:2039–45. doi:10.1016/S0140-6736(01)07100-8

339. Luke D. Discarnate entities and dimethyltryptamine (DMT): Psychopharmacology, phenomenology and ontology. J Soc Psych Res. 2011;75.

340. Luke D. Anomalous psychedelic experiences: at the neurochemical juncture of the humanistic and parapsychological. J Humanist Psychol. 2022;62:257–97.

341. Fagetti A. Cuando" habla" la semilla: adivinación y curación con enteógenos en la Mixteca oaxaqueña. Cuicuilco. 2012;19:229–55.

342. Narby J. The Cosmic Serpent. Penguin; 1999. 273 p.

343. Kuhn TS. The Structure of Scientific Revolutions [Internet]. University of Chicago Press; 1996. (ISSR collection). Available from: https://books.google.com/books?id=Lafvo9ghqBsC

344. Gassab L, Pusuluk O, Cattaneo M, Müstecaplıoğlu ÖE. Quantum Models of Consciousness from a Quantum Information Science Perspective. Entropy. 2025;27:243. doi:10.3390/e27030243 PubMed PMID: 40149167; PubMed Central PMCID: PMC11941443.

345. Kuhn RL. A landscape of consciousness: Toward a taxonomy of explanations and implications. Prog Biophys Mol Biol. 2024;190:28–169. doi:10.1016/j.pbiomolbio.2023.12.003 PubMed PMID: 38281544.

346. Hunt T, Jones M, McFadden J, Delorme A, Hales CG, Ericson M, Schooler J. Editorial: Electromagnetic field theories of consciousness: opportunities and obstacles. Front Hum Neurosci. 2023;17:1342634. doi:10.3389/fnhum.2023.1342634 PubMed PMID: 38495476; PubMed Central PMCID: PMC10941648.

347. McFadden J. Synchronous Firing and its Influence on the Brain's Electromagnetic Field: Evidence for an Electromagnetic Field Theory of Consciousness. J Conscious Stud. 2002;9:23–50.

348. McFadden J. Integrating information in the brain's EM field: the cemi field theory of consciousness. Neurosci Conscious. 2020;2020:niaa016. doi:10.1093/nc/niaa016 PubMed PMID: 32995043; PubMed Central PMCID: PMC7507405.

349. Pockett S. The Electromagnetic Field Theory of Consciousness. J Conscious Stud. 2012;19:191–223.

350. Freeman WJ, Vitiello G. Nonlinear brain dynamics as macroscopic manifestation of underlying many-body field dynamics. Phys Life Rev. 2006;3:93–118. doi:10.1016/j.plrev.2006.02.001

351. Hameroff S, Penrose R. Consciousness in the universe: a review of the "Orch OR" theory. Phys Life Rev. 2014;11:39–78. doi:10.1016/j.plrev.2013.08.002 PubMed PMID: 24070914.

352. Hameroff S. "Orch OR" is the most complete, and most easily falsifiable theory of consciousness. Cogn Neurosci. 2021;12:74–6. doi:10.1080/17588928.2020.1839037 PubMed PMID: 33232193.

353. Faggin F. Irreducible: Consciousness, Life, Computers, and Human Nature. Essentia Books; 2024. 336 p.

354. Hunt T, Schooler JW. The Easy Part of the Hard Problem: A Resonance Theory of Consciousness. Front Hum Neurosci. 2019;13:378. doi:10.3389/fnhum.2019.00378 PubMed PMID: 31736728; PubMed Central PMCID: PMC6834646.

355. Hameroff S. Consciousness, Cognition and the Neuronal Cytoskeleton – A New Paradigm Needed in Neuroscience. Front Mol Neurosci. 2022;15. doi:10.3389/fnmol.2022.869935

356. Sergi A, Messina A, Martino G, Caccamo MT, Magazù S, Ruffini G, Kuo MF, Nitsche MA. The quantum-classical complexity of consciousness and orchestrated objective reduction. Front Hum Neurosci. 2025;19:1630906. doi:10.3389/fnhum.2025.1630906 PubMed PMID: 40977855; PubMed Central PMCID: PMC12447588.

357. Beggs JM, Plenz D. Neuronal Avalanches in Neocortical Circuits. J Neurosci. 2003;23:11167–77. doi:10.1523/JNEUROSCI.23-35-11167.2003 PubMed PMID: 14657176.

358. Fontanilla D, Johannessen M, Hajipour AR, Cozzi NV, Jackson MB, Ruoho AE. The hallucinogen N,N-dimethyltryptamine (DMT) is an endogenous sigma-1 receptor regulator. Science. 2009;323:934–7. doi:10.1126/science.1166127 PubMed PMID: 19213917; PubMed Central PMCID: PMC2947205.

359. Dakic V, Minardi Nascimento J, Costa Sartore R, Maciel R de M, de Araujo DB, Ribeiro S, Martins-de-Souza D, Rehen SK. Short term changes in the proteome of human cerebral organoids induced by 5-MeO-DMT. Sci Rep. 2017;7:12863. doi:10.1038/s41598-017-12779-5 PubMed PMID: 28993683; PubMed Central PMCID: PMC5634411.

360. Frecska E, Bokor P, Winkelman M. The Therapeutic Potentials of Ayahuasca: Possible Effects against Various Diseases of Civilization. Front Pharmacol. 2016;7:35. doi:10.3389/fphar.2016.00035 PubMed PMID: 26973523; PubMed Central PMCID: PMC4773875.

361. González-Maeso J, Ang RL, Yuen T, Chan P, Weisstaub NV, López-Giménez JF, Zhou M, Okawa Y, Callado LF, Milligan G, Gingrich JA, Filizola M, Meana JJ, Sealfon SC. Identification of a serotonin/glutamate receptor complex implicated in psychosis. Nature. 2008;452:93–7. doi:10.1038/nature06612 PubMed PMID: 18297054; PubMed Central PMCID: PMC2743172.

362. Tegmark M. Importance of quantum decoherence in brain processes. Phys Rev E Stat Phys Plasmas Fluids Relat Interdiscip Top. 2000;61:4194–206. doi:10.1103/physreve.61.4194 PubMed PMID: 11088215.

363. Craddock TJA, St. George M, Freedman H, Barakat KH, Damaraju S, Hameroff S, Tuszynski JA. Computational Predictions of Volatile Anesthetic Interactions with the Microtubule Cytoskeleton: Implications for Side Effects of General Anesthesia. PLoS ONE. 2012;7:e37251. doi:10.1371/journal.pone.0037251 PubMed PMID: 22761654; PubMed Central PMCID: PMC3382613.

364. Khan S, Huang Y, Timuçin D, Bailey S, Lee S, Lopes J, Gaunce E, Mosberger J, Zhan M, Abdelrahman B, Zeng X, Wiest MC. Microtubule-Stabilizer Epothilone B Delays Anesthetic-Induced Unconsciousness in Rats. eNeuro. 2024;11. doi:10.1523/ENEURO.0291-24.2024 PubMed PMID: 39147581.

365. Gómez-Emilsson A. The Hyperbolic Geometry of DMT Experiences: Symmetries, Sheets, and Saddled Scenes [Internet]. 2016 [cited 2026 Jul 7]. Available from: https://www.qri.org/blog/hyperbolic-geometry-DMT

366. Gallimore A, Hermansson N, Hoffman D. Traces of the Other – Are DMT Entities Real? DMT Phenomenology in the Framework of Conscious Realism [Internet]. 2026 [cited 2026 Jul 7]. Available from: https://osf.io/8qvgy_v2

CONCLUSION

This dissertation set out to test whether the brain's predictive hierarchy is a productive level of analysis for understanding mind-body interventions, and whether ecologically and pharmacologically diverse techniques can be brought under a common biologically grounded computational account. The three studies address that question at progressively wider scope, and they converge on a coherent answer.

Chapter 1 demonstrated, in a randomized controlled setting, that four days of mindfulness training reduce experimentally induced pain by approximately one-third, and that this reduction is predicted within meditators by a meditation-induced rise in the Shannon entropy of cortical functional connectivity networks. The finding is the first to directly link entropy of cortical network organization to mindfulness-based pain relief. Computationally, it is consistent with the proposal that meditation flattens the prediction-driven attractor landscape that ordinarily sustains the percept of pain, providing an empirical anchor for the broader claim that mind-body practice modulates the precision of predictive inference.

Chapter 2 extended that anchor to a far broader physiological system. A seven-day retreat combining Kundalini-style meditation, didactic reconceptualization, and open-label placebo healing produced lower whole-brain modularity and reduced default mode and salience network connectivity during meditation, alongside coordinated plasma changes encompassing elevated BDNF, endogenous opioid signaling, enhanced glycolytic metabolism, and modulation of exosomal transcripts implicated in neurotransmission. Downstream assays confirmed that this signaling environment promoted neurite outgrowth and shifted cellular metabolism. Interpreted under predictive processing, this constitutes a coordinated reorganization of the brain-body system across all three levels of the hierarchy the intervention targets: high-level priors

(reconceptualization), present-moment precision (meditation), and ritual-driven gating of healing response (open label placebo).

Chapter 3 placed these empirical results within a broader theoretical landscape. By tracing the physiologically distinct routes through which serotonergic psychedelics, contemplative practice, and caloric restriction converge on a common computational endpoint–a transient near-critical regime characterized by relaxed priors, scale-free cortical dynamics, and expanded between-level coupling–it offered a unifying account of mystical-like states and argued that the depth of the resulting subjective experience is the proper unit of therapeutic mechanism. This is a non-trivial reframing. It places experience itself, not the pharmacological or behavioral occasion of experience, at the causal center of mind-body therapeutic action, and it suggests that progress in this field will depend on the ability to characterize, manipulate, and predict the phenomenology of the state, and its associated computational cascades, with the same scientific seriousness that has been applied to its molecular precipitants.

Taken together, the three studies make three contributions. First, they offer empirical evidence, at the level of cortical dynamics (Chapter 1) and brain-body multi-omic signaling (Chapter 2), that mind-body practice produces measurable, mechanistically interpretable reorganization of the predictive hierarchy. Second, they show that this reorganization is not technique-specific in the narrow sense: distinct interventions acting on different levels of the hierarchy produce, when composed, a coordinated brain-body response that resembles the response produced by pharmacologically and metabolically unrelated interventions reported across human cultures to occasion transformative states. Third, they articulate, in Chapter 3, a computationally explicit and biologically grounded framework within which these convergent observations cohere and from which falsifiable predictions can be derived.

Several directions follow. Empirically, the cortical entropy findings of Chapter 1 should be replicated with continuous, non-binarized entropy measures, in clinical pain populations, and across longer training timescales. The brain-body coupling demonstrated in Chapter 2 invites controlled designs that dissect the contributions of meditation, reconceptualization, and placebo ritual individually and in factorial combination, and that adjudicate the contribution of expectations, diet, social context, and other retreat-specific covariates. Chapter 3's framework generates a large set of specific predictions, about the relationship between exteroceptive bandwidth and mystical-experience intensity, about the structural role of meta-priors in shaping outcome, and about the cross-modal substitutability of the proposed routes, each of which is testable with available tools. Translationally, this dissertation suggests that combinations of mind-body techniques targeting different levels of the predictive hierarchy, rather than competing alternative therapies, may be the most efficient route to durable clinical reorganization, and that the design of such combinations should be guided by an explicit model of which level each component is meant to engage.

More broadly, the line of work undertaken here suggests that the science of mind-body interventions is ready to move past the demonstration of efficacy to the articulation of mechanism, and that this articulation has the most traction when it crosses the conventional boundaries between cortical dynamics, peripheral physiology, computational architecture, and conscious phenomenology. The brain is not only a predictive organ; it is a predictive organ embedded in, regulated by, and partly constituted by a body that participates in its inference. The most powerful interventions on its function are the ones that operate at the seam between these levels. Contributing to the science that lives at that seam has been the main task of this

dissertation, done in the hope of furthering its capacity to increase human understanding and to alleviate human suffering.